12-2009

Application of Different Bioanalytical Workflows for Proteomics of Prostate Cancer

Li Chen
University of Tennessee Health Science Center

Application of Different Bioanalytical Workflows for Proteomics of Prostate Cancer

DOI
10.21007/etd.cghs.2009.0050

APPLICATION OF DIFFERENT BIOANALYTICAL WORKFLOWS FOR PROTEOMICS OF PROSTATE CANCER

A Dissertation
Presented for
The Graduate Studies Council
The University of Tennessee
Health Science Center

In Partial Fulfillment
Of the Requirements for the Degree
Doctor of Philosophy
From The University of Tennessee

By
Li Chen
December 2009

DEDICATION

To my husband and son, who remind me daily of the joys of life;
and to my parents and my brother for their everlasting love and support.

ACKNOWLEDGEMENTS

First and foremost, I would like to express my deepest and most sincere appreciation to my advisor and mentor, Dr. Sarka Beranova-Giorgianni, for the training I received in her lab. Thanks for her supervision, advice and encouragement for the research projects. I also thank her for the time she spent guiding me writing, editing and revising the manuscripts.

I would also like to thank the other members of my committee, Dr. Duane D. Miller, Dr. Ivan C. Gerling, Dr. Dominic Desiderio, and Dr. Wei Li for their invaluable suggestions, guidance, and assistance.

I would like to especially acknowledge Dr. Jeffrey R. Gingrich and Ms. Tina Barrett for generously providing me with the human prostate cancer samples and LNCaP cell lines without which a major portion of this research would not have been possible. I must also thank Dr. Ram I. Mahato and Mr. Michael Danquah for establishing the cooperation research work and providing the mouse prostate tumor samples for comparative proteomic study. I am especially grateful to Dr. Nataliya I. Lenchik in Dr. Gerling's group for her training and assistance in the gel image analysis package and Ingenuity software. I would also like to thank Ms. Margaret M. Jefferson for her help with gel imaging equipment.

I especially thank all former and current members in Dr. Beranova-Giorgianni's Lab, Dr. Francesco Giorgianni, Dr. Amira Wohabrebbi, Dr. Yingxin Zhao, Dr. Bin Fang and Ms. Dina Mohamed Fallog, for technical help, discussions and suggestions.

My thanks are extended to the staff in the Departments of Pharmaceutical Sciences, including Brenda Thornton for her administrative help in committee meeting; and Faith B. Barcroft for her help in reagent purchasing and administrative work.

Tremendous thanks to my husband, my parents, my brother and my son. Without their incredible love and support, I would not accomplish my graduate training.

.

ABSTRACT

In the current dissertation, we focused on the development and application of multiple mass spectrometry-based bioanalytical platforms for phosphoproteomic characterization in cell culture and clinical specimens of prostate cancer; and on the application of optimized methods to analysis of differential protein expression to reveal molecular mechanism of drug action in animal model of prostate cancer.

Characterization of the phosphoproteome in prostate cancer

Our study in phosphoprotein signatures on a large scale in prostate cancer focused on the LNCaP human prostate cancer cell line, and on human prostate cancer tissue.

For the LNCaP prostate cancer cell line, we applied a combination of analytical platforms: (1) a novel in-gel isoelectric focusing (IEF) LC-MS/MS analytical platform; (2) a 2-DE based platform combined with phospho-specific staining.

The in-gel IEF LC-MS/MS analytical methodology used in the study included separation of the LNCaP proteins by in-gel isoelectric focusing; digestion of the proteins with trypsin; enrichment of the digests for phosphopeptides with immobilized metal ion affinity chromatography (IMAC); analysis of the enriched digests by LC-MS/MS; and identification of the phosphorylated peptides/proteins through searches of the Swiss-Prot protein sequence database. With in-gel IEF based analytical platform, we have characterized over 600 different phosphorylation sites in 296 phosphoproteins in the LNCaP prostate cancer cell line. This panel of the LNCaP phosphoproteins was 3-fold larger than the panel obtained in our previous work, and is the largest phosphoprotein panel in prostate cancer reported to date. The phosphoproteins identified in this study belonged to various locations within the cell and were involved in various processes including cell differentiation, transcription regulation, and intercellular signal transduction.

We also developed a 2-DE based platform, in combination with multiplexed staining and LC-MS/MS, for the identification of LNCaP phosphoproteins. In this study, we applied 2-DE as separation technique, Pro-Q^{TM} Diamond stain as phosphoprotein detection method, LC-MS/MS and database searches for protein identification to investigate the phosphoproteins in the LNCaP prostate cancer cell line. Proteins identified from spots of interest were shown to be highly relevant to prostate cancer. We demonstrated the feasibility of using 2-DE with phospho-specific stain and mass spectrometry to investigate the phosphoproteins in the LNCaP cell line. This methodology complements the in-gel IEF LC-MS/MS platform that we used for phosphoproteomics study; it will be of particular value for future comparative studies of phosphoproteins in various physiological states.

For prostate cancer tissue, a gel-free approach was performed to analyze five prostate cancer tissue specimens to obtain phosphoproteomic signature of prostate cancer

for biomarker discovery. Proteins were extracted with Trizol reagent, and then in-solution digested with trypsin. Phosphopeptides were enriched with IMAC, and analyzed the phosphorylated peptides/proteins by LC-MS/MS with identification through searches of the Swiss-Prot protein sequence database. The panels obtained for prostate cancer tissue contain 15-24 phosphoproteins. Some of the characterized phosphoproteins were present in all five specimens; in addition, each specimen also produced a unique set of phosphoproteins. The findings provided a direct glimpse into the phosphoprotein machinery operating within the human prostate cancer tissue. This pilot study focused on a small set of specimens. The phosphoprotein panels that were obtained contained a number of proteins that were unique to a particular specimen.

Comparative proteomics study of drug effects in prostate cancer

We carried out the first comparative proteomics study for the examination of the effects of bicalutamide/embelin combination treatment on prostate tumors by characterizing the alterations in protein expression that was induced upon treatment of mice bearing prostate tumors with anticancer combination therapy.

A comparative proteomic strategy based on 2-DE coupled with LC-MS/MS was performed on mouse prostate tumor tissue. Proteins from the mouse prostate tumors were extracted with Trizol, and the protein mixtures were separated by 2-DE. Differences in the protein profiles for the different treatment groups were evaluated by computer-assisted analysis of SYPRO Ruby stained 2-DE gels. LC-MS/MS and database searches were used to identify differentially expressed proteins. Pathway analysis was carried out on the dataset of identified proteins with the Ingenuity bioinformatics tool. Out of the 33 differentially expressed protein spots, 30 protein spots were identified and grouped into various functional classes. The major protein categories were metabolism (52%), stress response (12%), protein biosynthesis (13%) and apoptosis (11%), suggesting that alterations in these processes may be involved in the mechanism of drug action. Proteins associated with oxidative stress were up-regulated, which indicated that treatment with bicalutamide/embelin may affect the redox balance within the prostate tumor, and this effect may contribute to tumor suppression.

TABLE OF CONTENTS

CHAPTER 1. INTRODUCTION 1

1.1 Prostate Cancer 1

1.2 Why Apply Proteomic Technologies for Biomarker Discovery in Prostate Cancer? 2

1.3 Elements of Proteomics-based Approach 3

1.3.1 Sample Preparation 3

1.3.2 Protein Separation 3

1.3.2.1 Two-dimensional Polyacrylamide Gel Electrophoresis (2-DE) 3

1.3.2.2 Other Approaches 7

1.3.3 Mass Spectrometry 7

1.3.4 Database Searches and Other Bioinformatics Analyses 10

1.4 Selected Proteomic Technologies Applied in Prostate Cancer Research 12

1.4.1 In-gel-based Platform 12

1.4.2 Gel-free Platform 16

1.5 Phosphoproteomics Studies of Prostate Cancer 17

1.5.1 Classical Approaches to Phosphoprotein Analysis 18

1.5.1.1 $^{32}P/^{33}P$ Radioactive Labeling 18

1.5.1.2 Immunodetection 18

1.5.1.3 Phosphospecific Staining 19

1.5.2 Mass Spectrometry-based Approaches 19

1.5.2.1 Sample Preparation 19

1.5.2.2 Enrichment of Phosphorylated Species 20

1.5.2.3 Phosphopeptide Sequencing by Tandem Mass Spectrometry 22

1.5.2.4 Bioinformatics Resources for Phosphoproteomics 22

1.6 Summary and Research Aims 24

CHAPTER 2. CHARACTERIZATION OF THE PHOSPHOPROTEOME IN LNCAP PROSTATE CANCER CELLS BY IN-GEL ISOELECTRIC FOCUSING AND TANDEM MASS SPECTROMETRY 27

2.1 Introduction 27

2.2 Materials and Methods 29

2.2.1 Protein Extraction from LNCaP Cells 29

2.2.2 In-gel IEF 30

2.2.3 In-gel Digestion 30

2.2.4 Enrichment of Phosphopeptides with IMAC 30

2.2.5 LC-MS/MS Analysis 31

2.2.6 Database Searches 31

2.3 Results and Discussion 32

2.3.1 In-gel IEF LC-MS/MS Approach 32

2.3.2 Characteristics of Identified Phosphoproteins/phosphopeptides 34

2.3.3 Classifications of Identified Phosphoproteins 37

2.3.4 Selected Examples of Identified Phosphoproteins 37

2.4 Conclusions 40

CHAPTER 3. INVESTIGATION OF PHOSPHOPROTEIN SIGNATURES IN ARCHIVED HUMAN PROSTATE CANCER TISSUES VIA PROTEOMIC ANALYSIS 41
3.1 Introduction 41
3.2 Materials and Methods 43
3.2.1 Characteristics of Clinical Samples 43
3.2.2 Protein Extraction 43
3.2.3 In-solution Digestion of Proteins 43
3.2.4 Enrichment of Phosphopeptides with IMAC 44
3.2.5 LC-MS/MS 44
3.2.6 Database Searches 44
3.2.7 Additional Bioinformatics Analysis 45
3.3 Results 45
3.4 Discussion 46
3.5 Conclusions 57

CHAPTER 4. IDENTIFICATION OF PHOSPHOPROTEINS IN THE LNCAP HUMAN PROSTATE CANCER CELL LINE BY A 2-DE AND PHOSPHO-SPECIFIC STAINING-BASED PROTEOMICS PLATFORM 59
4.1 Introduction 59
4.2 Materials and Methods 61
4.2.1 Protein Extraction from LNCaP Cells 61
4.2.2 Sample Preparation 61
4.2.2.1 Standard Rehydration Buffer 61
4.2.2.2 Destreak Rehydration Buffer 61
4.2.3 First Dimension: Isoelectric Focusing 62
4.2.3.1 IEF with Multiphor Unit 62
4.2.3.2 IEF with IPGphor Unit 62
4.2.4 Second Dimension: SDS-PAGE 62
4.2.4.1 Gel Casting 62
4.2.4.2 SDS-PAGE with Dodeca Cell Unit 63
4.2.5 Gel Staining 63
4.2.5.1 Pro-Q™ Diamond Staining 63
4.2.5.2 SYPRO Ruby Staining 63
4.2.6 Gel Imaging 63
4.2.7 Spot Excision 64
4.2.8 In-gel Tryptic Digestion 64
4.2.9 Peptide Processing 64
4.2.10 LC-MS/MS Analysis 64
4.2.11 Database Searches 65
4.2.12 Inspection of Protein Information 65
4.3 Results 65

4.3.1 Application of Different Rehydration Buffers: Standard vs. Destreak 65
4.3.2 IPGphor vs. Multiphor 66
4.3.3 Detection of Proteins by Sequential Staining 66
4.3.4 Protein Identification 70
4.3.5. Additional Examination of the Phosphoprotein Panel 70
4.4 Discussion 80
4.5 Conclusions 83

CHAPTER 5. PROTEOMIC ANALYSIS OF PROTEIN ALTERATIONS IN MOUSE PROSTATE CANCER TISSUE INDUCED BY BICALUTAMIDE/EMBELIN COMBINATION TREATMENT 84
5.1 Introduction 84
5.2 Materials and Methods 85
5.2.1 In Vivo Studies 85
5.2.2 Protein Preparation 85
5.2.3 2-DE 87
5.2.4 Gel Staining and Imaging 87
5.2.5 In-gel Tryptic Digestion 88
5.2.6 LC-MS/MS Analysis 88
5.2.7 Database Searches 88
5.2.8 Bioinformatics and Network Analysis 89
5.3 Results 89
5.3.1 Profile of Mouse Prostate Tumor Specimens 90
5.3.2 Proteomic Patterns of Bicalutamide/embelin Combination Treatment 90
5.3.3 Identification of Candidate Protein Spots from 2-DE Gels 93
5.3.4 Classification of Identified Proteins 93
5.3.5 Pathway Analysis of Proteins Modulated in Bicalutamide/embelin Treatment 100
5.4 Discussion 100
5.5 Conclusions 106

CHAPTER 6. SUMMARY 107
6.1 Discussion of Selected Analytical Aspects 107
6.2 Summary 108
6.2.1 Characterization of the Phosphoproteome in Prostate Cancer 108
6.2.2 Comparative Proteomics Study of Drug Effects in Prostate Cancer 110

LIST OF REFERENCES 111

APPENDIX……..... 130

VITA……..... 225

LIST OF TABLES

Table 1-1 Summary of main proteomics methods used in prostate cancer studies 13

Table 1-2 A list of major websites for phosphoproteomics. 25

Table 2-1 Summary of the LNCaP phosphoproteome characterization results: in-gel IEF LC-MS/MS vs. gel-free methodology 34

Table 3-1 Characteristics of prostate cancer specimens used in the study 43

Table 3-2 Summary of results for the analyses of the phosphoproteome in human prostate cancer tissue 48

Table 3-3 Phosphoproteins characterized in the prostate cancer specimens 49

Table 4-1 Protein identification results for Pro-Q^{TM} Diamond-stained spots from pH 3-10 gel 73

Table 4-2 Protein identification results for Pro-Q^{TM} Diamond-stained spots from pH 4-7 gel. 76

Table 4-3 Example of cancer relevant phosphorproteins identified in LNCaP 82

Table 5-1 Proportion of the matched spots among the different ranges of the CV of the normalized volume..... 91

Table 5-2 List of identified protein spots down-regulated by bicalutamide/embelin treatment 94

Table 5-3 List of identified protein spots up-regulated by bicalutamide/embelin treatment 96

Table 5-4 Protein categories by Gene Ontology..... 100

Table 5-5 Representative networks associated with identified proteins by IPA software..... 101

Table A-1 Full list of phosphopeptides and phosphoproteins characterized in LNCaP cells.....130

Table A-2 Phosphorylation sites assigned by product ions in MS/MS spectrum..... 167

Table A-3 Subcellular locations and functional categories of the characterized phosphoproteins. 196

Table A-4 Details of characterized phosphoproteins..... 219

Table A-5 Scansite results for the characterized phosphorylation sites 224

LIST OF FIGURES

Figure 1-1 Elements of proteomics-based study 4

Figure 1-2 Peptide fragmentation series 10

Figure 1-3 An example of tandem MS/MS under data-dependent acquisition 11

Figure 1-4 A representative MS/MS spectrum of a phosphopeptide 23

Figure 2-1 Outline of the in-gel IEF LC-MS/MS strategy 28

Figure 2-2 A representative MS/MS spectrum obtained in the LC-MS/MS analysis of IMAC-enriched digest from gel section 4 33

Figure 2-3 Distribution of phosphoproteins/phosphopeptides in the IPG strip sections 35

Figure 2-4 Distribution of singly, doubly, and triply phosphorylated peptides 36

Figure 2-5 Summary of the sub-cellular locations of the LNCaP phosphoproteins characterized by in-gel IEF LC-MS/MS 38

Figure 2-6 Classification of the characterized LNCaP phosphoproteins based on their involvement in cellular processes 39

Figure 3-1 Outline of the gel-free analytical methodology 42

Figure 3-2 An example of MS/MS spectrum of GQLpSDDEKFLFVDK 47

Figure 3-3 Distribution of identified phosphopeptides in five prostate tissues analyzed 53

Figure 3-4 Classification of identified phosphoproteins by molecular function according to GO annotation at the level 2. 54

Figure 4-1 Schematic of 2-DE and phospho-specific staining based proteomics platform 60

Figure 4-2 2-DE gels of LNCaP proteins with pH 3-10NL using different rehydration buffers (a) Standard rehydration buffer (b) Destreak rehydration solution 67

Figure 4-3 2-DE gels of LNCaP using different IEF units (a) Multiphor II (b) IPGphor 68

Figure 4-4 2-DE gels of LNCaP proteins detected with multiplexed staining (a) Pro-Q^{TM} Diamond Phosphoprotein staining (b) SYPRO Ruby staining. 69

Figure 4-5 16 protein spots selected from 2-DE gel with pH 4-7 71

Figure 4-6 14 protein spots selected from 2-DE gel with pH 3-10 72

Figure 5-1 Outline of 2-DE based comparative proteomics platform 86

Figure 5-2 Representative 2-DE gels of mouse prostate cancer proteome (a) Control (b) Free bicalutamide/embelin treatment. 92
Figure 5-3 Classification of biological processes of identified proteins according to GO annotations 98
Figure 5-4 Classification of molecular functions of identified proteins according to GO annotations 99
Figure 5-5 Network of small molecule biochemistry associated with modulated proteins identified in bicalutamide/embelin treatment in mouse prostate tumor tissue. 102

LIST OF ABBREVIATIONS

µg	micro gram
AcOH	acetic acid
ACN	acetonitrile
ANOVA	analysis of variance
AR	androgen receptor
BPH	benign prostatic hypertrophy
CID	collision induced dissociation
cm	centimeter
CV	coefficient of variation
°C	degrees Celsius
Da	dalton
DHB	2,5-dihydroxybenzoic acid
DRE	digital rectal examination
ECD	electron capture dissociation
ESI	electrospray ionization
ETD	electron transfer dissociation
FA	formic acid
GO	gene ontology
IDA	iminodiacetic acid
iTRAQ	isobaric tags for relative and absolute quantitation
IEF	isoelectric focusing
IMAC	immobilized metal ion affinity chromatography
IPA	ingenuity pathway analysis
IPG	immobilized pH gradient
HPLC	high performance liquid chromatography
LC-MS	liquid chromatography – mass spectrometry
mA	milliamp
MALDI-TOF	matrix assisted laser desorption ionization – time of flight
MeOH	methanol
mL	milli liter
mm	milli meter
MS/MS	tandem mass spectrometry
MudPIT	multidimensional protein identification technology
MW	molecular weight
NTA	nitrilotriacetic acid
pI	isoelectric point
PMF	peptide mass fingerprint
ppm	parts per million
PSA	prostate specific antigen
PTM	post translational modification
Rm	relative migration
RP	reverse phase
SDS-PAGE	sodium dodecyl sulfate – polyacrylamide gel electrophoresis

SPE	solid phase extraction
TCA	trichloroacetic acid
TFA	trifluoroacetic acid
2-DE	two dimensional – polyacrylamide gel electrophoresis
2D-DIGE	two dimensional difference gel electrophoresis

CHAPTER 1. INTRODUCTION

1.1 Prostate Cancer

Prostate cancer is the most frequently diagnosed cancer and the second leading cause of cancer death among men in the United States (Ann. Intern. Med., 2008). According to Cancer Facts & Figures 2008 from American Cancer Society, an estimated 186,320 American males will be diagnosed with prostate cancer and 28,660 deaths will result from prostate cancer in the US during 2008. Prostate cancer continues to represent a major health concern.

Clinically, prostate cancer is diagnosed as local or advanced (Miller et al., 2003). During the initial period of prostate cancer, the tumor is dependent on androgen for growth, and therefore responses to therapies of surgical and/or pharmacological depletion of circulating androgens, such as radical local treatment or androgen-deprivation (androgen ablation) treatment. However, the success of the therapies is temporary; most tumors relapse within 2 years as a metastatic and androgen-independent state. Whereas surgery is curative for local prostate cancer, there are not effective treatments for androgen-independent prostate cancer.

Therefore, understanding molecular mechanisms and biological activities of cancer development and progression is the key objective to improve the diagnosis and develop novel prostate cancer therapeutics. Currently, the main tools used for prostate cancer diagnosis include digital rectal examination (DRE), serum prostate specific antigen (PSA) screening and biopsy (Smith et al., 2009).

In the late 1980s, serum PSA was introduced into clinical practice and became the most widely used biomarker for screening and early detection of prostate cancer (Farwell et al., 2007; Rao et al., 2008). The application of serum PSA measurement in clinical practice has dramatically changed detection and treatment of prostate cancer. The incidence of this tumor has increased whereas the impact on mortality rates is less evident. Over diagnosis leading to unnecessary treatment and associated adverse effects have been strongly implicated to occur (Lin et al., 2008).

Using current recommended guidelines, the PSA test suffers from both poor specificity and low sensitivity (Ross et al., 2004). Although higher PSA levels are associated with the risk of cancer, PSA levels can change for many reasons other than cancer, such as enlargement of the prostate (benign prostatic hypertrophy (BPH)) and infection of the prostate (prostatitis). PSA level above 4.0 ng/ml is the traditional cutoff value for diagnosis of prostate cancer (Welch et al., 2005). However, a single PSA cutoff point lacks specificity and sensitivity needed for an accurate diagnosis of prostate cancer; in men with PSA below 4.0 ng/ml the risk of cancer is approximately 15% and 15% these patients have high grade disease. Conversely for PSA levels above 4.0 ng/ml, cancer is found on biopsy in only 25% to 30% of the men evaluated (Parekh et al., 2007; Thompson et al., 2004).

Several modifications of PSA measurement have been investigated, including PSA velocity, PSA density, PSA glycosylation and PSA doubling time (Carter et al., 1992; Catalona et al., 1994; Fang et al., 2002; Meany et al., 2009). However, none of these modifications are superior to PSA in clinical practice, and since they are more difficult to measure than PSA, they are unlikely to replace PSA for prostate cancer screening and have not been found wide application in clinical practice.

Therefore, new investigation into more accurate diagnostic and prognostic biomarkers to complement PSA is critical to assist in early detection and prognosis, monitor therapeutic response, and to determine the best course of therapy for cancer patients to improve the clinical outcomes. To date, with the advances in biotechnology such as immunohistochemical staining, proteomics, tissue microarray, DNA microarray, many promising biomarkers, such as human kallikrein, hepsin, have been identified and are under investigation and validation.

1.2 Why Apply Proteomic Technologies for Biomarker Discovery in Prostate Cancer?

Current biology research efforts often focus on describing the detailed complexity of particular aspects of the total system of cancer development and progression. It is of help to consider systems study, describing multitude of pathways and interactions that regulate biological processes. To capture all interactions and get a complete picture of what is really happening during pathogenesis and disease progression, conventional tools to study single protein or pathway are inadequate and large-scale, high throughput approaches are required to provide complementary information.

Advances in new high throughput technologies, such as genomics, transcriptomics and proteomics, lead to the accelerating growth of information and the improved molecular tools for cancer diagnosis, prognosis and treatment. However, gene expression analysis can not accurately predict protein expression and post-translational modifications (such as phosphorylation) (Blackstock and Weir, 1999). Transcriptome represents a set of messenger RNA (mRNA) produced by a given cell and can reflect the gene expression under a specific condition. But transcriptome neither can completely reflect the underlying biology due to alternative splicing and post-translational modifications in response to changes of external conditions. As the ultimate products for gene expression, proteins are directly responsible for the molecular functions to mediate most changes at the cellular level in cancer. Therefore, protein-directed studies using advanced technologies are of significant interest and significance.

Proteomics is the simultaneous study of multiple proteins on a large scale by high throughput analyses of body fluids, cells and tissues (Anderson and Anderson, 1998). The expansion of the field of proteomics has been enabled by concurrent developments: completion of the human genome project, advances in separation techniques, major improvements in mass spectrometry technologies, and progress in bioinformatics.

The speed, selectivity and sensitivity of mass spectrometry (MS) make MS-based proteomic methodologies a powerful alternative to traditional biological methods for analyses of proteins in complex biological systems (Feng et al., 2008). The distinct advantage of proteomics and the advances in proteomic technologies have created tremendous opportunities for biomarker discovery and for biological studies of cancer.

Proteomics-based approaches have the potential to provide novel, systems-level insight into the underlying molecular mechanisms of prostate cancer, and also hold great promise for biomarker discovery in prostate cancer.

1.3 Elements of Proteomics-based Approach

The bioanalytical strategy of a proteomics-based study involves the incorporation of a number of technologies and knowledge of biochemistry, molecular biology, bioinformatics and bioanalytical chemistry (Patton, 1999). Although a number of options exist within each stage of the proteomic analysis, a typical approach includes the following components: sample preparation, protein separation, protein identification, and data mining (Figure 1-1).

1.3.1 Sample Preparation

The first, critically important step of a proteomics-based study is sample preparation. Proteins are isolated from biological samples and then solubilized for separation. The task of sample preparation is to maximally solubilize sample proteins under conditions compatible with subsequent method of analysis, without introducing artefactual modifications. There have been a number of reviews that discussed various approaches to sample preparation and solubilization of proteins for 2-DE (Rabilloud, 1996; Rabilloud, 2009). The use of a protease and/or phosphatase inhibitor cocktail is often included to inhibit protein degradation and/or dephosphorylation. In addition, the application of various combinations of reducing agents, chaotropic agents and detergents is used to disrupt intra- and inter-protein interactions and maximize protein solubilization (Rabilloud et al., 1997).

1.3.2 Protein Separation

1.3.2.1 Two-dimensional Polyacrylamide Gel Electrophoresis (2-DE)

2-DE is the most commonly applied technique for the separation of proteins in complex mixtures because of its efficiency and high resolution (Gorg et al., 2004). The technique combines isoelectric focusing (IEF) in the first dimension, and sodium dodecyl sulfate-polyacrylamide gel electrophoresis (SDS-PAGE) in the second dimension. The superior separation power of 2-DE stems from the fact that proteins are separated based on two different physicochemical properties. Proteins are separated based on their

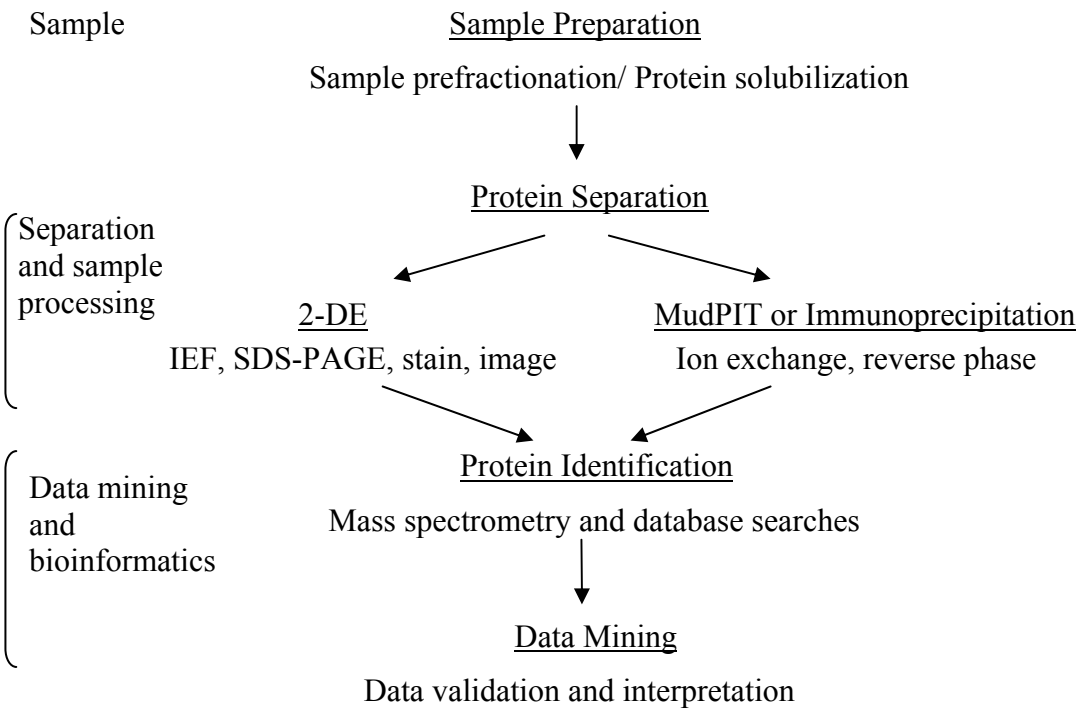

Figure 1-1 Elements of proteomics-based study.

different isoelectric points in the first dimension, and based on molecular weight in the second dimension. Then proteins are visualized with various staining methods, such as Coomassie Blue, silver staining, or fluorescent stains. Protein profiles can be quantitatively analyzed through 2-DE gel imaging software (Dunn, 1987). Mass spectrometry has been intensively used for identification of proteins of interest in 2-DE-based proteomics studies.

First dimension**:** Isoelectric focusing (IEF) is a technique for separating proteins by their electric charge differences. Proteins are amphoteric molecules with acidic and basic groups. A protein carries a charge depending on the pH of its surroundings. This characteristic is used for IEF in pH gradients. A protein will have positive net charge in a pH region below its isoelectric point (pI), and in an electric field it will migrate towards the cathode. During protein migration in a pH gradient, the charge will decrease until the protein reaches the pH region that corresponds to its pI. At this point it has no net charge and the migration stops. Analogously, negatively charged protein molecules will migrate towards the anode to the protein pI. As a result, the protein is focused into a sharp stationary band at its specific pI in the pH gradient.

The great improvement of IEF is the introduction of the immobilized pH gradient (IPG) strips for the first dimension separation (Bjellqvist et al., 1982). IPG strips are composed of acidic and basic buffering groups covalently linked to large-pore polyacrylamide gel matrix. The polyacrylamide gel is cast onto a plastic backing that allows easy manipulation of the IPG strip. Compared with carrier ampholyte-based IEF, IPG-based IEF has a very high resolution, permits large amount of proteins loading, and presents more reproducible results (Gianazza and Righetti, 2009; Gorg et al., 2000). Moreover, there are pre-cast IPG strips with various lengths and pH ranges commercially available from several vendors. The development and commercialization of the IPG technology has contributed to the expansion of 2-DE from a handful of highly specialized laboratories to many laboratories in diverse fields of life sciences.

In terms of equipment, several different configurations are used to perform IEF separations. These configurations differ mainly in the procedure for strip rehydration, and in the maximum voltage that can be applied.

Second dimension: Sodium dodecyl sulfate polyacrylamide gel electrophoresis (SDS-PAGE) is used to separate proteins according to their molecular weight. Unlike IEF, SDS-PAGE itself is a widely used, standard analytical technique for protein separation. SDS is used to denature proteins by disrupting hydrogen bonds, blocking hydrophobic interactions and unfolding the proteins to eliminate protein tertiary and secondary structures. Reducing agent (such as DTT) is added to disrupt the disulphide bond between polypeptides and unfold proteins into flexible polypeptides. Then SDS masks the charge of the polypeptides and forms anionic SDS-protein complexes with a constant net negative charge per unit mass. The separation principle of SDS-PAGE involves differential migration of SDS-protein complexes through a restrictive polyacrylamide gel with a define pore size. Under the influence of an electric field, the SDS-protein complexes with a constant charge-to-mass ratio migrate towards the anode.

Smaller proteins experience less restriction in their movement through gel pores and hence travel the farthest; large proteins are impeded and hence travel the least distance. Thus proteins in a mixture become separated according to their molecular weight (Ibel et al., 1990).

Depending on the specific application, the characteristics of the gel such as size, thickness and percentage of acrylamide should be taken into account. In addition, SDS-PAGE systems are available in both horizontal and vertical configurations. Horizontal units are convenient for use with single gels. Vertical units allow simultaneous separations of multiple samples and are often performed for higher throughput analyses minimizing run-to-run variations (Gorg et al., 2004).

Protein detection: After gel electrophoresis, proteins in 2-DE gels are visualized with various staining methods, such as Coomassie Blue, silver staining, or fluorescent stains. Each method has its advantages and disadvantages. Staining with Coomassie Blue dye is simple and provides good linearity; however, the stain is not very sensitive. Silver staining provides much higher detection limits but suffers from reproducibility and linearity issues. Recently, fluorescent stains become an attractive alternative to other staining methods for protein detection. Fluorescent stains (such as SYPRO stains) non-covalently bind to proteins in 2-DE. Compared with Coomassie and silver stains, fluorescent stains offer a number of advantages, including wide dynamic range, high sensitivity, and simplicity of procedure. The SYPRO stains are fully compatible with mass spectrometry analyses, which is an important consideration (Patton, 2000). The shortcomings associated with fluorescent stains are high cost for the requirement of specialized imaging equipment.

Protein imaging: Image analyses are performed with an imaging system that is able to acquire, analyze and store the 2-DE images. In general, image analysis includes spot detection, protein spots matching in different gels, and normalization for protein quantification. A number of computer-based software packages are commercially available for the analysis of 2D gel images, such as PDQuest (Bio-Rad, Hercules, CA), Progenesis (Nonlinear USA Inc, Durham, NC), Z3 2DE analysis system (Compugen, NJ). Although image analysis is a semi-automated procedure, several issues (such as gel distortions, variation in sample loading, staining intensities) require manual intervention.

Recent development in 2-DE: Classical 2-DE, while powerful, suffers from limitations. The main issues include partial proteome coverage, and run-to-run variability. To address some of the issues, improvements of the 2-DE platform have been made. A significant new advancement is the introduction of two-dimensional difference gel electrophoresis (2D-DIGE). 2D-DIGE incorporates differential labeling of different sample populations through the use of fluorescent molecules (CyDyes) (Unlu et al., 1997). Up to three different protein samples can be covalently labeled with fluorescent dyes (Cy3, Cy5, and Cy2), combined and subjected to 2-DE. The differential labeling allows separation of multiple proteomes on a single gel, reducing the gel-to-gel variations. After the gel electrophoresis, images of the gel at different excitation/emission wavelengths (specific for each CyDye) are generated. Images can be overlaid directly by the

DeCyder™ software (GE Healthcare) to locate proteins that are differentially expressed between the samples. Advanced data analysis such as hierarchical clustering can be performed (Minden et al., 2009).

1.3.2.2 Other Approaches

In addition to 2-DE based approaches, a number of different separation methodologies have been developed since the advent of proteomics. In general, these methodologies fall within two categories: 1D-gel-based, and gel-free. Furthermore, various methods aimed at reduction of the proteome complexity prior to analysis have been introduced.

One-dimensional gel-based proteomics strategies use a single dimension of electrophoretic separation at the protein level, combined with advanced LC-MS/MS for protein identification. A combination of SDS-PAGE and LC-MS/MS, termed geLC-MS/MS, has been developed and used for numerous applications. Our group has developed a method that combines in-gel IEF at the protein level with LC-MS/MS. This 1D-gel strategy, named in-gel IEF LC-MS/MS, has been applied to analyses of the proteome in the human pituitary (Zhao et al., 2005) and human prostate tissue.

A well-known example of a gel-free proteomics strategy is the Multidimensional protein identification technology (MudPIT). The technique is also known as shotgun proteomics. MudPIT involves multidimensional chromatographic separation of complex mixtures at the peptide level. In brief, a whole protein mixture is digested directly and the resulting peptides are separated by two different types of liquid chromatography (ion exchange and reversed-phase LC), coupled to tandem mass spectrometry. Compared with 2-DE, MudPIT method is unbiased, meaning that proteins that are normally under-represented in 2D gels (low-abundance proteins, proteins with extremes in pI and MW, and membrane proteins) can be probed with MudPIT (Washburn et al., 2001).

Immunoprecipitation is an example of a strategy that aims at reducing the complexity of the mixture to be analyzed. Instead of aiming to probe all proteins in a proteome, immunoprecipitation studies focus on targeted analyses of specific proteins or protein groups. Immunoprecipitation methods use an antibody that specifically isolates and concentrates a particular protein or group of proteins from a complex proteome sample. For example, such strategy can be applied to study the composition of protein complexes, or to investigate post-translationally modified proteins.

1.3.3 Mass Spectrometry

Mass spectrometry (MS) is a powerful technology for the identification and characterization of peptides, proteins, and other biomolecules. The development of advanced mass spectrometry instrumentation that allowed high-sensitivity, high-throughput protein identification has been one of the enabling events underlying the expansion of proteomics (Yates, III, 2000). New and improved instruments are being

continuously developed, thus pushing the power of mass spectrometry to higher and higher levels.

MS is an analytical technique that measures the molecular weight of molecules according to their mass-to-charge ratio. A mass spectrometer is composed of three key components: ion source, mass analyzer and detector. Analytes are converted into gas-phase ions within an ion source. The ions are then sorted and separated according to their mass-to-charge (m/z) ratio in a mass analyzer, and the signal is detected by a suitable device such as an electron multiplier. The resulting MS spectra are represented as ion intensity vs. the m/z values (Corthals et al., 2000). There are a number of different types of mass spectrometers that include different combination of ion sources and mass analyzers (Patterson and Aebersold, 1995; Yates et al., 2009).

In general, protein identification by mass spectrometry involves cleaving the protein of interest into a set of peptides, which are then subjected to MS analysis. Production of gas-phase ions from peptides is therefore a critical step in mass spectrometry analysis. There are two broadly used ionization methods in proteomics research, namely matrix-assisted laser desorption ionization (MALDI), and electrospray ionization (ESI) (Gevaert and Vandekerckhove 2000). MALDI sources are usually coupled to time-of-flight (TOF) mass analyzers while ESI sources are commonly linked to ion traps or quadrupole mass analyzers (Corthals et al., 2000).

Ionization of analytes by MALDI involves the use of a UV-absorbing matrix. A sample is co-crystallized with the matrix in a well on a samples plate; inside the ion source, the sample-matrix mixture is irradiated with a laser beam. This process results in vaporization of the matrix and analyte molecules are brought into a dense phase (plume) above the sample surface, where they are ionized by proton transfer reactions. Peptides generally ionize through addition of a proton, forming a singly charged molecular ion, $[M+H]^+$(Henzel et al., 1993).

ESI can directly generate gas-phase ionized molecules from a liquid solution. This feature is of great benefit because it enables on-line coupling of ESI-based mass spectrometers with HPLC. During ESI ionization, the LC eluent is sprayed from a tip of a needle held at a high voltage; through this process, a mist of highly charges droplets is created. Gas and/or heat applied to the droplets causes evaporation of the solvent in the droplets. As the size of droplets decreases, the charge density in the droplets increases. That leads to increase in the surface tension, the droplets dissociate into smaller ones and eventually gas-phase analyte ions are produced. Peptides ionized with ESI usually form multi-protonated molecular ions, $[M+nH]^{n+}$, n = 2 or 3 depending on the number of basic sites in the peptide sequence. The fact that multi-protonated ions are formed upon ESI has important implications for the ability to measure larger peptides, and for gas-phase dissociations of peptide ions (Fenn et al., 1989).

The LTQ two-dimensional linear ion trap mass analyzer is one of commonly used mass analyzers, which is comprised of four parallel hyperbolic shaped rods, segmented in three secions. Ions are trapped radially in a radio frequency (RF) electric field and axially

in a static electric field using DC voltages. Through the application of appropriate voltages to all three segments, the trapped ions with specific m/z ratio are ejected in the radial direction through the two parallel slots in the center section of the linear ion trap. Two highly efficient detectors are placed on either side of the trap to maximize sensitivity. The unique configuration of this device improves the ion storage capacity, trapping efficiency and detection efficiency (Schwartz et al., 2002).

Mass spectrometry measurements can be carried out in two general ways: as single-stage mass spectrometry (MS), or as tandem mass spectrometry (MS/MS). An MS experiment includes ionization of the analytes, and measurement of the m/z ratios for the source-generated ions. For peptide ions such as singly-protonated ions produced upon MALDI, information about peptide MWs can be derived easily. This aspect, as it applies to protein identification, is discussed in more detail in the following paragraph. An MS/MS experiment is more complex than MS and includes additional steps. The steps in an MS/MS experiment are: ionization of the analyte molecules and formation of molecular ions; selection of one of the source-generated ions as the so-called precursor ion; activation of the mass selected precursor ion through collisions with a target gas followed by dissociation of the activated precursor ion into a series of structure-determining product ions; mass analysis of the product ions and recording of the signal. In MS/MS, protonated peptide ions dissociate predominantly via cleavages along the peptide backbone, theoretically forming several different product ion series. Under the conditions used in my research, two major ion series arise from cleavage of the peptide bond: the N-terminal ion series (b-ion series) and the C-terminal ion series (y-ion series) (Figure 1-2). As shown in the figure, the m/z of the product ions can be used to derive amino acid sequence information for the peptide under analysis.

Protein identification in proteomics studies may be achieved with MS. The MS-based identification strategy is termed peptide mass fingerprinting (PMF) and it is commonly performed with a MALDI-TOF mass spectrometer. The method includes: cleavage of protein of interest into peptides with a specific enzyme (such as trypsin, which cleaves at the C-terminus of lysine and arginine); measurement of the m/z ratios of the peptide ions with MALDI-TOF; comparison of the observed peptide mass fingerprint to the theoretical mass fingerprints of proteins in a protein sequence database; generation of a list of possible candidate proteins based on peptide matching scores. The PMF identification strategy is simple and provides high throughput. It has been applied widely for identification of proteins in 2D gel spots. It should be noted that PMF is based on measurements of peptide masses, and that it is therefore applicable only to single proteins or simple protein mixtures.

Protein identification may also be accomplished with MS/MS, commonly in conjunction with LC separation (LC-MS/MS). As with PMF, the protein of interest is first cleaved into peptides, usually with trypsin. The tryptic peptides are separated by LC, and the eluting peptides are analyzed by MS/MS. The LC-MS/MS measurements on unknown peptide mixtures are performed using data-dependent acquisition (DDA). During DDA, the instrument cycles through MS and MS/MS (Spahr et al., 2000). This principle is illustrated in Figure 1-3 for a cycle performed for ions eluting with the LC

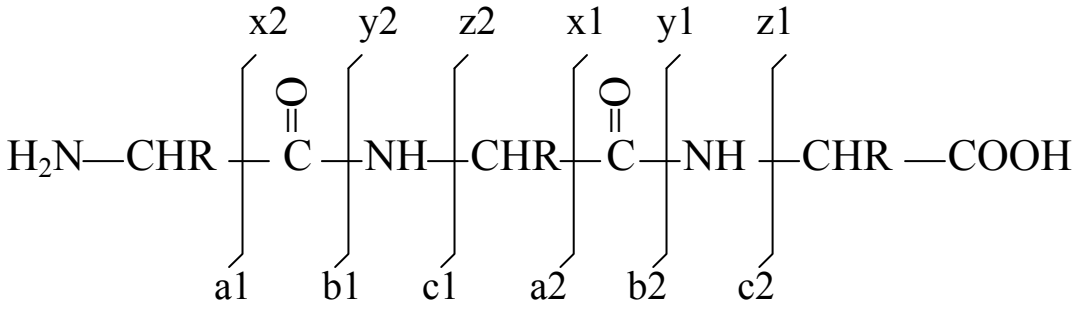

Figure 1-2 Peptide fragmentation series.

retention time around 58.26 min. The instrument acquired an MS spectrum that surveyed the analytes eluting at that particular time. Based on the information from this MS spectrum, subsequent MS/MS measurements were performed on the precursor ions detected in the MS spectrum. One of these MS/MS spectra, acquired for the precursor ion with m/z 942. The product ion m/z 893 is shown in the bottom section of the Figure 1-3. During a single LC-MS/MS analysis, the instrument cycles through many of such MS-MS/MS sequences. The entire MS/MS dataset is used to search a protein sequence database to identify the protein(s) of interest (Yates, III et al., 1995). It is important to point out that, in contrast to PMF that only measures peptide masses, sequence-diagnostic MS/MS data are obtained for each peptide being analyzed. Based on LC-MS/MS data, proteins in 2D gel spots as well as in highly complex protein mixtures can be identified. Therefore, LC-MS/MS is an integral part of 1D-gel and gel-free bioanalytical platforms.

1.3.4 Database Searches and Other Bioinformatics Analyses

Identification of proteins of interest based on MS or MS/MS has been enabled by the creation of protein sequence databases that are being continuously updated, and on the development of database search software programs.

In all my projects, sequence information derived from MS/MS was used for database searches with the SEQUEST search engine in the Swiss-Prot protein sequence database. Swiss-Prot is a curated protein sequence database that provides a high level of annotations (such as protein function, protein sequence, post-translational modifications, variants, etc.), minimizes the redundancy and integrates with other databases. Now the Swiss-Prot database has been merged into the UniProt database. SEQUEST is one of the two most widely used searching algorithms (Yates, III et al., 1995). With SEQUEST, proteins in the database are cleaved in silico into peptides, and theoretical product-ion patterns are generated for these peptides. These theoretical patterns are compared to the experimental MS/MS patterns; when a match is retrieved, it is evaluated with a scoring system. Thus, the output of the database search is a list of proteins whose peptide sequences were matched based on MS/MS data.

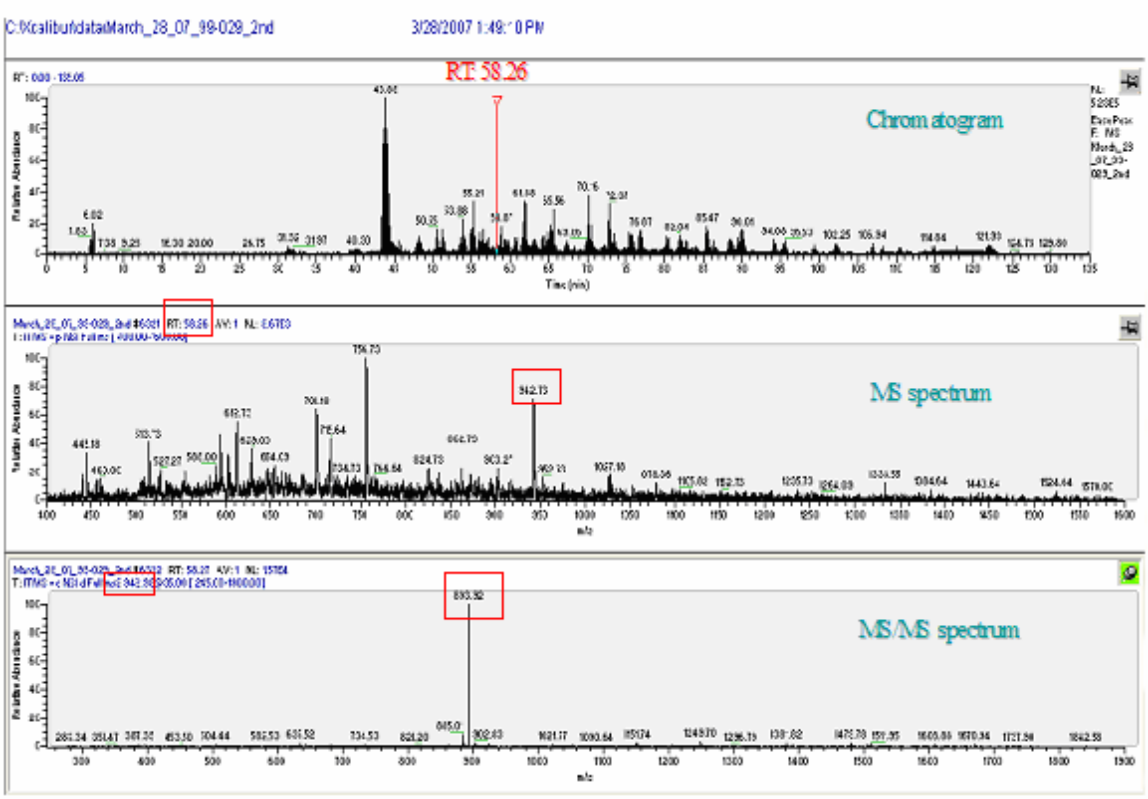

Figure 1-3 An example of tandem MS/MS under data-dependent acquisition.

The top section of the Figure1-3 is chromatogram of LC. The instrument acquired an MS spectrum that surveyed the analytes eluting at the LC retention time around 58.26 min. Based on the information from the MS spectrum, subsequent MS/MS measurements were performed on one of the precursor ions with m/z 942 detected in the MS spectrum. The product ion m/z 893 is shown in the MS/MS spectrum in the bottom section of the Figure 1-3.

One of the important components of any proteomics research study is to integrate the information about both protein identifications and their corresponding functional characteristics. Gene ontology (GO) is a collection of controlled vocabularies describing the biology of a gene product in any organism (Khatri and Draghici, 2005). GO (http://bioinfo.vanderbilt.edu/webgestalt/) is performed to classify identified proteins according to molecular function, biological process, and molecular component (subcellular location).

Ingenuity Pathway Analysis (IPA) is a powerful curated database and analysis system for understanding how proteins work together to effect cellular changes. It builds hypothetical networks from identified proteins and other proteins, based on published literature; these networks involve interactions between genes, proteins and other biological molecules (Hoorn et al., 2005; Raponi et al., 2004).

1.4 Selected Proteomic Technologies Applied in Prostate Cancer Research

Recently, intense efforts have been involved in the application of various proteomics technologies to the study of prostate cancer (Table 1-1). Proteomic studies have generated numerous datasets of potential diagnostic, prognostic, and therapeutic significance for prostate cancer.

1.4.1 In-gel-based Platform

Gel-based protein separation is an extensively used proteomics methodology. Generally, proteins are separated with one-dimensional (IEF or SDS-PAGE) or two-dimensional (2-DE or 2D-DIGE) gels prior to mass spectrometry identification. The platforms are easily adapted to research projects in various labs and have been widely used.

Malik et al. employed a combination of chemical pre-fractionation, SDS-PAGE, LC-MS/MS and SELDI-based immunoassay to identify discriminatory expression proteins of Dunning rat prostate tumor cell lines of varying metastatic potential (Malik et al., 2007).

Liu et al. identified the alterations in protein expression patterns of LNCaP after incubation with Somatostatin/ Somatostatin derivative using 2-DE in combination with mass spectrometry, and found that Sms/smsdx triggered up-regulation of catalytic mitochondrial proteins and seemed to affect apoptosis-related proteins (Liu et al., 2007).

Wu et al. identified key regulatory molecules involved in prostate cancer metastasis in two human androgen-independent Prostate cancer cell lines, highly metastatic 1E8-H and lowly metastatic 2B4-L cells through 2-DE and MS analyses, and demonstrated that up-regulation of vimentin expression positively correlates with the invasion and metastasis of androgen-independent prostate cancer (Wu et al., 2007).

Table 1-1 Summary of main proteomics methods used in prostate cancer studies.

Platform	Method	Sample	Reference
In-gel-based platform			
Sodium dodecyl sulfate polyacrylamide gel electrophoresis (SDS-PAGE)	SDS-PAGE, LC-MS/MS and SELDI-based immunoassay	Dunning rat prostate tumor cell line	Malik et al., 2007
Two-dimensional polyacrylamide gel electrophoresis (2-DE)	2-DE in combination with MS	LNCaP after incubation with Somatostatin/ Somatostatin derivative	Liu et al., 2007
	2-DE in combination with MS	Two human androgen-independent prostate cancer cell lines, highly metastatic 1E8-H and lowly metastatic 2B4-L cells	Wu et al. 2007
	2-DE coupled with MS	Conditioned medium from LNCaP, C4-2, and C4-2B cell	Pang et al., 2009
	2-DE followed by matrix-assisted laser desorption/time of flight mass spectrometry (MALDI-TOF-MS)	The highly metastatic human prostate epithelial cell line PC-3M-1E8 (1E8-H) and the low metastatic line PC-3M-2B4 (2B4-L)	Wei et al, 2008
	2-DE and MALDI-TOF-MS/MS	Needle biopsy specimens from patients with prostate cancer or benign prostatic hyperplasia	Lin et al., 2007
	2-DE coupled with MS	Biopsy samples from benign prostate hyperplasia and prostate cancer	Ummanni et al., 2008
Two dimension difference gel electrophoresis (2D-DIGE)	2D-DIGE technology coupled with LC-MS/MS	LNCaP human prostate cancer cell line	Rowland et al., 2007
	2D-DIGE technology coupled with MS	Human prostate cancer cells treated with enzymatically active free-PSA	Bindukumar et al., 2008

Table 1-1 (continued).

Platform	Method	Sample	Reference
	2D-DIGE technology coupled with MS	Three radioresistant prostate cancer cell lines	Skvortsova et al., 2008
	Immunoaffinity depletion and 2D-DIGE followed by LC-MS/MS	Serum samples of patients with prostate cancer	Byrne et al., 2009
Gel-free-based platform			
Multidimensional protein identification technology (MudPIT)	2DLC-MS/MS	Conditioned medium from prostate cancer cell line PC3(AR)(6)	Sardana et al., 2007
	iTRAQ followed by 2DLC-MS/MS	The poorly metastatic LNCaP cell line and its highly metastatic variant LNCaP-LN3 cell line	Glen et al., 2008
	Offline SCX followed by capillary RPLC-MS/MS	Conditioned media of three prostate cancer cell lines: PC3, LNCaP, and 22Rv1	Sardana et al., 2008
	iTRAQ coupled with 2DLC-MS/MS	Tissue specimens from patients with benign prostatic hyperplasia and with prostate cancer	Garbis et al., 2008
Immunoprecipitation	Immunoprecipitation coupled with microLC-ESI-MS/MS.	C4-2 prostate cancer cells	Dall'Era et al., 2007

Pang et al. analyzed conditioned medium (CM) from LNCaP, C4-2, and C4-2B cells using 2-DE coupled with mass spectrometry, and found that higher levels of ubiquitous mitochondrial creatine kinase (uMtCK) in the CM of androgen independent prostate cancer than that of androgen dependent prostate cancer cells (Pang et al., 2009).

Wei et al. performed comparative proteomic analysis of the highly metastatic human prostate epithelial cell line PC-3M-1E8 (1E8-H) and the low metastatic line PC-3M-2B4 (2B4-L) by 2-DE, followed by MALDI-TOF-MS. Highly expressed vimentin was detected in highly metastatic cell line compared to low metastatic cells (Wei et al., 2008).

Lin et al. defined the proteomic features of prostate needle biopsy specimens from patients with prostate cancer or benign prostatic hyperplasia to identify candidate biomarkers for prostate cancer. Using 2-DE, 52 protein spots were exhibited statistically significantly changes among prostate cancer and benign prostatic hyperplasia groups and identified by MALDI-TOF-MS/MS (Lin et al., 2007).

Ummenni et al. investigated biopsy samples from benign prostate hyperplasia and prostate cancer patients by 2-DE and mass spectrometry to identify potential biomarkers which might distinguish the two clinical situations. Eighty eight protein spots were differentially expressed with statistical significance. Prohibitin was significantly up-regulated in prostate cancer compared to benign prostatic hyperplasia (Ummanni et al., 2008).

Rowland et al. investigated the effect of androgen (R1881) and anti-androgen (bicalutamide) on the androgen-responsive prostate cancer LNCaP cell line using 2D-DIGE proteomic approach. Out of 197 differentially expressed spots, 165 spots have been successfully identified corresponding to 125 distinct proteins. Identified proteins were involved in diverse processes including the stress response and intracellular signaling (Rowland et al., 2007).

Bindukumar et al. identified proteins modulated in human prostate tumor cells treated with enzymatically active free-PSA by 2D-DIGE technology coupled with LC-MS/MS. Several proteins involved in tumor progression had been shown to down-regulate by the treatment of PSA (Bindukumar et al., 2008).

Skvortsova et al. determined differences in the proteome profiles in three radioresistant human prostate carcinoma cell lines compared to parental cells using 2D-DIGE followed by MS, to define the mechanism involved in the radioresistance development (Skvortsova et al., 2008).

Byrne et al. subjected serum samples to immunoaffinity depletion and analyzed protein expression using 2D-DIGE. Out of 63 differential expression spots between the Gleason score 5 and 7 cohorts ($p < 0.05$), 13 spots were identified using LC-MS/MS. Pigment epithelium-derived factor (PEDF) has been validated in serum and tissue

samples from the original cohort and also from a larger independent cohort of patients, indicating to be a predictor of early stage prostate cancer (Byrne et al., 2009).

1.4.2 Gel-free Platform

Although in-gel-based approaches are the mainstays for prostate cancer analysis, gel-free methodologies including Multidimensional Protein Identification Technology (MudPIT), and immunoprecipitation are emerging as alternative proteomic technologies for prostate cancer studies.

Using strong anion-exchange chromatography, Sardana et al. fractionated the conditioned medium from the prostate cancer cell line PC3(AR)(6), and then further fractionated tryptic fractions by reversed-phase C-18 chromatography before being subjected to ESI-MS/MS, and identified a novel candidate biomarker Mac-2BP (Sardana et al., 2007).

Using the poorly metastatic LNCaP cell line and its highly metastatic variant LNCaP-LN3 cell line as a model, Glen et al. employed a proteomic approach of isobaric tags for relative and absolute quantitation (iTRAQ), followed by strong cation exchange (SCX) chromatography coupled with capillary C-18 reversed-phase liquid chromatography-tandem mass spectrometry (RPLC-MS/MS). Out of the total 280 unique proteins identified, the relative expression data for 176 proteins was obtained. This was the first application of iTRAQ technology for the global proteomic profiling of prostate cancer cells (Glen et al., 2008).

Sardana et al. performed a proteomic analysis of the conditioned media of three prostate cancer cell lines (PC3, LNCaP, and 22Rv1) for discovering novel prostate cancer biomarkers. From the analysis, 2124 proteins were identified by using a bottom-up approach, consisting of offline SCX chromatography followed by RPLC-MS/MS (Sardana et al., 2008b).

Garbis et al. analyzed prostate tissue specimens from patients with benign prostatic hyperplasia and with prostate cancer by isobaric stable isotope labeling (iTRAQ) and two-dimensional liquid chromatography-tandem mass spectrometry (2DLC-MS/MS) approaches (Garbis et al., 2008).

Dall'Era et al. isolated CD10-protein complexes from C4-2 prostate cancer cells by immunoprecipitation using anti-CD10 monoclonal antibodies. Eluted fractions were combined, trypsinized, and the resulting peptides were analyzed by LC-ESI-MS/MS. HSP27 and HSP70 were found to interact with CD10 in C4-2 prostate cancer cells (Dall'Era et al., 2007).

1.5 Phosphoproteomics Studies of Prostate Cancer

Application of DNA microarray and proteomics to profile gene and protein expression shows a big promise in the discovery of prostate cancer markers. However, protein or gene expression does not necessarily reflect protein activity, which is often regulated by post-translational modifications.

Protein phosphorylation is one of the most prominent prost-translational modifications and plays a critical role in the regulation of major cellular processes like proliferation, differentiation or apoptosis through signaling pathways. Phosphorylation of serine, threonine and tyrosine residue is the most common in mammalian cells. Researchers estimate that as many as 30-50% of proteins are phosphorylated at any given time (Kalume et al., 2003). Covalent attachment of phosphate group to amino acid changes the charge in the region of a protein and results in a conformation change of the whole protein, which affects both the folding and function of proteins.

Disruptions of phosphorylation-mediated cell signaling are associated with various diseases, including cancer (Benzeno et al., 2006; Iakoucheva et al., 2004; Stephens et al., 2005). Furthermore, distinct phosphotyrosine proteome of the breast and liver tumors were found (Lim et al., 2004; Lim, 2005; Meng et al., 2004). The evidence for the existence of tumor-specific phosphoproteome shows promising to mine the tumor phosphoproteome as potential prostate cancer biomarkers in cancer diagnosis and therapeutics.

The phosphorylation status of proteins is regulated by a complex interplay between protein kinases and protein phosphatases. Protein kinases are the targets of several new cancer drugs and drug candidates. However, the functions of these protein kinases drugs are not fully understood. There is an urgent need to understand and monitor kinase signalling pathways (Ashman and Lopez, 2009).

Thus, the analysis of protein phosphorylation in prostate cancer is of paramount importance. The long-term goal of studying of the phosphorylation status of proteins in prostate cancer with phosphoproteomics methods is to provide large phosphorylation databases for prostate cancer tissues and cell lines, aid in furthering our knowledge of phosphorylation-dependent events associated with prostate cancer, and lead to the identification of new target proteins for clinical research.

Phosphoproteomics is the subdiscipline of proteomics that is focused on the comprehensive study of the extent and dynamics of protein phosphorylation. Its tasks include identification of the phosphoproteins, determination of the phosphorylation sites on the proteins, quantification of the phosphorylation under different conditions, prediction of protein kinases responsible for phosphorylation, and discovery of specific drug targets.

Compared with proteomics, phosphoproteomics faces more technical challenges due to the nature of the biomolecules being studied. Protein phosphorylation is a highly

dynamic, reversible process, and the ratio of phosphorylated to nonphosphorylated proteins is rather low in vivo. Therefore, phosphoproteomic approaches generally require additional enrichment steps to achieve sufficient sensitivity.

In fact, most phosphoproteomics studies to date have two features in common: protein or peptide fractionation and phosphospecific enrichment. Reduction of the sample complexity is a major step necessary for an effective analysis of low-abundance phosphoproteins; this reduction can be achieved by various fractionation techniques. Furthermore, considerable amount of effort has been devoted to development of methods for phosphospecific enrichment, compatible with mass spectrometry. The objective of this enrichment is isolation of phosphoproteins and/or phosphopeptides.

As the field of phosphoproteomics continues to develop, there have been a number of recent advances in phosphoproteomics technologies, including sample preparation, phospho-specific enrichment, characterization of phosphorylation sites by MS/MS, and bioinformatics analyses of protein phosphorylation. The following subchapters offer a detailed review of protein phosphorylation analysis, emphasizing advancements in MS-based phosphoproteomics platforms.

1.5.1 Classical Approaches to Phosphoprotein Analysis

There are several traditional approaches for detecting phosphoproteins. In general, protein samples are separated by one-dimensional or two-dimensional polyacrylamide gel electrophoresis (1-DE or 2-DE) depending on the complexity of the protein sample, and then phosphorylated species are visualized by radiolabeling, immunodetection or phosphospecific staining.

1.5.1.1 $^{32}P/^{33}P$ Radioactive Labeling

Radioactive labeling is the most sensitive method for phosphoprotein detection, and it is possible to be used both in vivo and in vitro. Phosphoproteins can be radioactively labeled with $^{32}P/^{33}P$ and visualized by autoradiography. Several studies have been performed based on radiolabeling (Chen et al., 2004; Czupalla et al., 2003). However, the methodology is not widely used in current proteomics research due to the toxicity of ^{32}P and the possibility of artificially triggered phosphorylation by exposure to $^{32/33}P$-orthophosphate.

1.5.1.2 Immunodetection

Phosphoproteins can be detected by Western blotting using antibodies against phosphoamino acids. This antibody-based approach is widely used in biochemical studies and it is compatible with MS-based phosphoproteome analysis, provided that issues with protein amounts needed for Western blotting vs. those needed for MS are considered and addressed. However, the efficiency and specificity of the immunodetection method strongly depend on the quality of the applied antibody. While antibodies available for

phosphotyrosine (pTyr) show high selectivity and therefore can be used to specifically detect phosphotyrosine-containing proteins (Ide et al., 2002), antibodies against phosphoserine (pSer) and phosphothreonine (pThr) lack both selectivity and sensitivity, and are not routinely used (Kaufmann et al., 2001).

1.5.1.3 Phosphospecific Staining

Fluorescence-based protein detection methods have recently shown excellent promise in terms of quantitative accuracy, detection sensitivity, and compatibility with mass spectrometry. Pro-Q™ Diamond dye has been developed to detect phosphoproteins directly in polyacrylamide gels or on nitrocellulose membranes after electrophoretic separation. In comparison with radiolabeling and immunodetection approaches, phosphospecific staining offers significant advantages, such as avoidance of radioactivity, no need for expensive antibodies, and direct detection of phosphorylated proteins obtained from cells, tissue, or body fluids. The stain noncovalently binds to phosphoproteins and it is fully compatible with mass spectrometry or Edman sequencing. Commonly, the phosphospecific staining is combined with generic protein staining in a multiplexed fashion – that is, Pro-Q™ Diamond stain is applied to a gel to specifically detect phosphorylated proteins, and this staining is followed by detection of all proteins by Sypro Ruby fluorescent stain. Goodman et al detected phosphoproteins on nitrocellulose membranes using the Pro-Q™ Diamond staining (Goodman et al., 2004). Stasyk et al. combined a standard 2D-DIGE protocol with subsequent post-staining of gels with phosphospecific fluorescent Pro-Q™ Diamond dye for quantitative detection of phosphoproteins in 2-DE gels in mammary epithelial cells (Stasyk et al., 2005). Hopper et al. characterized the phosphoproteome of porcine heart mitochondria, as detected by Pro-Q™ Diamond stain using 2-DE and ^{32}P radioisotopic analysis as well as perform an initial screen for mitochondrial kinases and phosphatases associated with these protein phosphorylations (Hopper et al., 2006). Wu et al. devised a sequential protein staining procedure to visualize proteins separated by 2-DE, using Pro-Q™ Diamond (phosphoprotein), followed by Pro-Q™ Emerald 488 (glycoprotein), followed by SYPRO Ruby stain (general protein stain), and finally silver stain for total protein profile in spleen leukocytes (Wu et al., 2005).

1.5.2 Mass Spectrometry-based Approaches

Phosphoproteomics requires proper sample preparation of proteins from biological samples, efficient enrichment of phosphorylated proteins or peptides, and the application of sensitive MS to the identification of phosphorylated proteins and characterization of exact phosphorylation sites.

1.5.2.1 Sample Preparation

In addition to the general concerns discussed previously in the context of protein sample preparation, minimizing phosphatase activities is an important point that needs to be considered for phosphoprotein sample preparation. Performing all sample preparation

at low temperature will reduce the activities of phosphatases; furthermore, adding phosphatase inhibitors to buffers in the initial step of sample solubilization will inhibit phosphatase action and thus preserve original phosphorylation patterns (Zahedi et al., 2006).

1.5.2.2 Enrichment of Phosphorylated Species

MS approaches are site-specific analyses of protein phosphorylation, requiring that phosphoproteins first be cleaved by site-specific proteases in order to produce phosphopeptides that are amenable to MS analysis. However, digestion of a protein mixture will generate phosphorylated as well as non-phosphorylated peptides. The phosphopeptides will comprise only a small portion of the digest. Furthermore, phosphopeptides are not easy to analyze by MS because of lower ionization efficiency of phosphopeptides in the presence of high-abundance nonphosphorylated peptides. To account for these drawbacks, phosphoproteins and/or phosphopeptides must be specifically enriched prior to MS in order to reduce background and thereby increase sensitivity and improve characterization effectiveness. There are a number of phosphospecific enrichment strategies currently available. Here I will discuss two widely used enrichment methods: immobilized metal ion affinity chromatography (IMAC) and titanium dioxide chromatography (TiO_2).

Immobilized metal ion affinity chromatography (IMAC): To date, IMAC is an extensively used affinity technique for the isolation of phosphopeptides from peptide mixtures prior to MS analysis (Albuquerque et al., 2008; Gioeli et al., 2002; Hoffmann et al., 2005; Moser and White, 2006; Posewitz and Tempst, 1999). The technique is based on the electrostatic interaction between negatively charged phosphopeptides at low pH and positively charged metal ions (Fe^{3+},Ga^{3+}, Al^{3+}, Zr^{4+}), which are chelated to nitrilotriacetic acid (NTA) or iminodiacetic acid (IDA) immobilized onto a solid support. Typically, a peptide digest is applied to an IMAC column and the phosphopeptides contained in this digest will bind, while other peptides will wash through. Elution with a suitable buffer will release the bound phosphopeptides. However, IMAC often suffers from limitations, most importantly issues related to specificity, and to recovery of phosphopeptides carrying multiple phosphate groups.

Nonspecific binding of peptides containing acidic amino acid residues to the IMAC columns is one of the main drawbacks associated with the IMAC technique. Peptides containing multiple acidic amino acid residues are often co-purified with the phosphopeptides, thereby reducing the selectivity of the method. To diminish nonspecific binding of acidic peptides, Ficarro and co-workers derivatized the carboxylic groups on acidic amino acid residues in peptides by O-methyl esterification and thereby improved phosphopeptide enrichment (Ficarro et al., 2002). Salomon et al. developed an effective method for the large-scale determination of sites of tyrosine phosphorylation, applying the strategy of phosphotyrosine immunoprecipitation combined with methyl esterification and IMAC of tryptic peptides, and MS identification (Salomon et al., 2003). Kim et al. provided a list of protein phosphorylation sites identified from HT-29 human colon adenocarcinoma cell line by methyl esterification of carboxyl groups on the tryptic

peptides prior to IMAC enrichment combined with LC-MS/MS analysis (Kim et al., 2005). However, it is argued that reaction conditions of esterification procedure have to be optimized to avoid introducing byproducts and increasing sample complexity.

Furthermore, IMAC is generally biased against multiply phosphorylated peptides due to the strong binding of multiple phosphorylated peptides to IMAC resins, resulting in the reduction of elution efficiency. Optimization of binding, washing and elution conditions of IMAC could improve the efficiency of phosphopeptide enrichment (Dubrovska and Souchelnytskyi, 2005; Hart et al., 2002; Ndassa et al., 2006; Tsai et al., 2008).

Titanium dioxide (TiO_2) chromatography: Recently, TiO_2 chromatography has been introduced as a promising alternative to IMAC. Originally, TiO_2 was utilized in bioelectrochemical studies of protein functions using the adsorption of proteins to TiO_2 films (Topoglidis et al., 2000) and enrichment of phospholipids (Csucs and Ramsden, 1998), which phosphate groups build self-assembling monolayers on TiO_2 surface. The approach is based on the selective interaction of phosphates with porous titanium dioxide microspheres. Phosphopeptides are captured in a TiO_2 precolumn under acidic conditions and released under basic conditions. Selective interaction with phosphate and the chemical stability make TiO_2 a promising enrichment for phosphopeptides. Pinkse et al. presented an online 2D LC-MS/MS strategy for phosphopeptide analysis on the femtomole level, using titanium dioxide precolumn as the first dimension for phosphopeptides enrichment and reverse phase column as the second dimension (Pinkse et al., 2004).

To reduce co-purified acidic peptides, Larsen et al. reported the improvement of the selectivity of TiO_2 to phosphopeptide by adding 2,5-dihydroxybenzoic acid (DHB) to the loading buffer. DHB seems to efficiently reduce the binding of nonphosphorylated peptides to TiO_2 while keeping its high binding affinity for phosphorylated peptides (Larsen et al., 2005; Thingholm et al., 2006). Yu et al. improved TiO_2 enrichment of phosphopeptides from HeLa cells by the use of NH_4Glu for a TiO_2 column wash, which significantly increased the efficiency of TiO_2 phosphopeptide enrichment (Yu et al., 2007a).

The utility of zirconium dioxide microtips for phosphopeptide isolation prior to mass spectrometric analysis has been reported. These microtips display similar overall performance as TiO_2 microtips. But a slight difference was shown in the selectivity; compared to ZrO2, TiO_2 preferentially enriched multiply phosphorylated peptides (Kweon and Hakansson, 2006).

Although metal oxides are still not as widespread as IMAC in proteome research, high efficiency for enrichment of phosphopeptides and chemical stability of TiO_2 chromatography make the method a potential alternative to IMAC for phosphoproteomic research (Kweon and Hakansson, 2008; Li et al., 2008; Marcantonio et al., 2008).

1.5.2.3 Phosphopeptide Sequencing by Tandem Mass Spectrometry

Today most phosphopeptides are identified by MS/MS combined with database searches; analysis is performed to obtain MS/MS data diagnostic of the phosphopeptide sequences and to the location of the phosphorylated residues.

Phosphate group-specific dissociation in MS/MS can serve as supporting evidence for the presence of phosphopeptides. When peptide is phosphorylated, the amino acid residue (such as serine, threonine or tyrosine) will have a mass shift owing to the gain of a phosphate group (80 Da). Detection of phosphopeptides by ion trap MS in the positive mode can be achieved on the basis of their tendency to lose the elements of phosphoric acid under low energy dissociation conditions. Under these conditions, MS/MS spectrum of peptides containing phosphoserine or phosphothreonine presents a predominant neutral loss of 98 Da (owing to H_3PO_4 loss) during fragmentation by low energy collisions, while peptides bearing phosphotyrosine rarely exhibit a loss of 98 Da in their MS/MS spectra (Figure 1-4) (Tholey et al., 1999). The evidence of the loss of 98 Da can be used as a signature for phosphopeptides and peptide sequence information can be used for determination of phosphorylation site in an ion trap (DeGnore and Qin, 1998).

Low energy CID is widely used to achieve gas-phase dissociation of peptide backbone and to produce ions for sequence analysis and identification of phosphorylation sites. However, the CID process often leads to elimination of phosphoric acid as the major dissociation channel for phospho-serine and phospho-threonine-containing peptides, without sufficient dissociation of the amide bonds along the peptide backbone. This low dissociation extent may result in lack of sequence information in MS/MS spectra. Leitner et al. have recently reported to improve the dissociation efficiency of poorly fragmenting peptides and phosphopeptides during CID by malondialdehyde modification of arginine residues (Leitner et al., 2007). Despite significant technological advancements in peptide sequencing by mass spectrometry, poor fragmentation upon CID remains a challenge for analyzing phosphopeptides.

Electron transfer dissociation (ETD) and Electron capture dissociation (ECD) have been recently introduced as alternatives to CID. These alternative ion activation methods provide a more comprehensive coverage of phosphopeptide sequences (Chi et al., 2007; Molina et al., 2007; Sweet et al., 2006).

1.5.2.4 Bioinformatics Resources for Phosphoproteomics

Identification of phosphopeptides and proteins based on MS/MS data is accomplished using the same principles that were discussed in section 1.3.4. MS/MS datasets are submitted for searches of a protein sequence database; these searches are performed with a suitable search engine such as SEQUEST. For phosphorylation analysis, database search conditions are set to include modifications of Ser, Thr, and/or Tyr residues. Because not all such amino acid residues are modified, phosphorylation is considered as either/or “dynamic” modification.

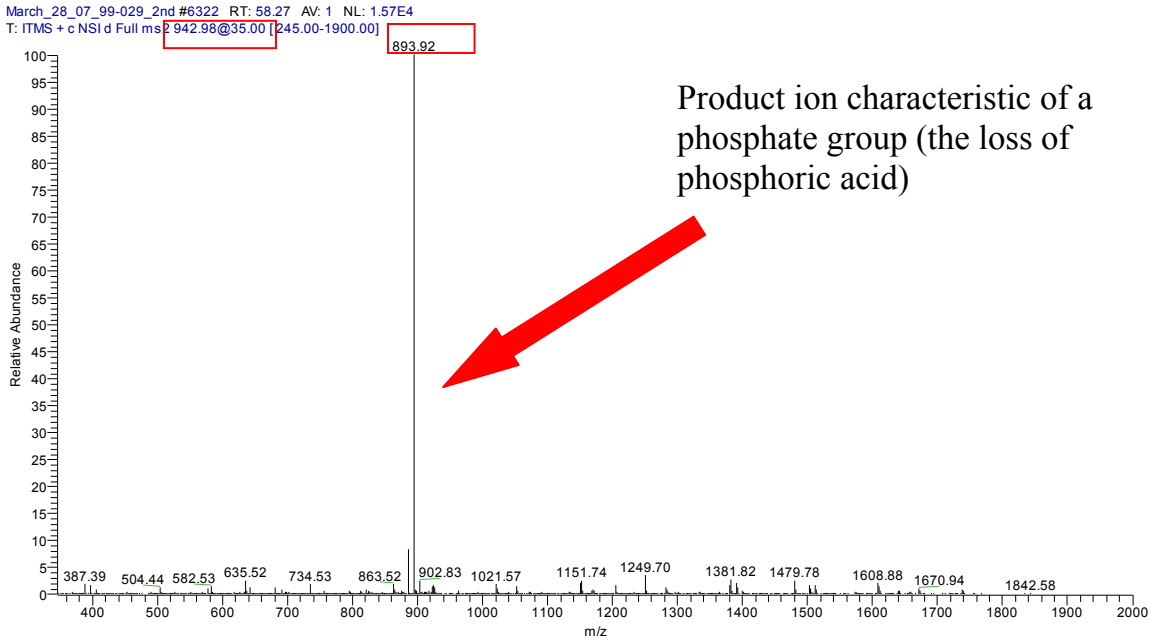

Figure 1-4 A representative MS/MS spectrum of a phosphopeptide.

The MS/MS spectrum is acquired for the precursor ion with m/z 942. The product ion m/z 893, a predominant neutral loss of 98 Da (owing to H_3PO_4 loss), presents in the MS/MS spectrum.

Phosphoproteomics research is generating a wealth of novel information. Studies provide important information such as: a list of known phosphoproteins in a particular biological system; novel phosphorylation sites in known phosphoproteins; phosphorylated proteins which have not previously been reported to be phosphorylated; phosphorylation of a novel protein. Therefore, major efforts have been directed towards integration of this information, and towards an effective dissemination to the scientific community.

An important compilation of information on protein phosphorylation (and on other PTMs) is contained in the annotations of the Swiss-Prot protein sequence database. A Swiss-Prot annotation page for a particular protein entry will include information on the location of a phosphorylation site as well as relevant literature references. In addition to Swiss-Prot annotations, new resources related to phosphorylation and other PTMs have been developed. Table 1-2 lists some of the Internet-based resources for phosphoproteomics research.

Several knowledgebases dedicated to protein phosphorylation have been created. One of the most comprehensive knowledgebases is PhosphoSite. PhosphoSite (www.phosphosite.org) is a systems biology resource focused on in vivo protein phosphorylation sites in human, mouse, and other mammalian proteomes. It includes a wealth of information such as the phosphorylated residue, orthologous sites, domains and motifs, additional functionalities etc. Thus, PhosphoSite provides an accurate, comprehensive source of information about mammalian protein phosphorylation sites.

To further the insight derived form large-scale phosphoproteomics studies, bioinformatics tools for additional phosphorylation-related examination have been developed. For example, phosphopeptide sequences identified from phosphoproteomic screens can be analyzed with the Scansite tool to predict protein kinases and/or phosphorylation-dependent binding motifs. Scansite (http://scansite.mit.edu) searches for motifs within proteins that are likely to be phosphorylated by specific protein kinases or bind to domains (Obenauer et al., 2003).

1.6 Summary and Research Aims

Rapid development of proteomic technologies for studying prostate cancer shows a great promise for gaining new scientific knowledge that will contribute to the ultimate goal of finding more effective cancer diagnostic methods and therapies. In-gel and gel-free-based methodologies have already been applied in prostate cancer studies of cultured cells and tissue specimens. In the last few years proteomic studies have generated new information of potential diagnostic, prognostic, and therapeutic significance.

Diverse proteomics technologies have adapted for phosphoproteomics. Mass spectrometry-based phosphoproteomic platforms play a major role in current phosphoproteomics research, and advancements in the various components that comprise these platforms have been made, including optimized procedures for sample preparation,

Table 1-2 A list of major websites for phosphoproteomics.

Name	Comments	URL
Phosphorylation-site database		
Swiss-Prot	Protein annotation including phosphorylation sites and other post translational modification	http://expasy.org
PhosphoSite	Search known phosphorylation sites in human, mouse or rat	http://www.phosphosite.org
Phospho.ELM	Search phosphorylation sites in proteins	http://phospho.elm.eu.org
Phosphorylation-site prediction		
Scansite	Search for potential kinase motifs	http://scansite.mit.edu
Prosite	Database of protein domains, families and functional sites	http://expasy.org/prosite
Ascore	Phosphorylation site localization based on the presence and intensity of site-determining ions in MS/MS spectra.	http://ascore.med.harvard.edu

specific and sensitive methods for phosphospecific enrichment, mass spectrometers with lower detection limits and improved mass accuracy, alternative gas-phase dissociation strategies, expanded protein knowledgebases and other bioinformatics resources. These technological advances make it feasible to perform large-scale phosphoproteomic examinations of prostate cancer.

It is an accepted fact that no single bioanalytical platform can be universally applied to proteomics or phosphoproteomics. Due to diverse nature of biological samples, different research objectives, different resources available to investigators, various bioanalytical platforms are being utilized for phosphoproteomics (Neverova and Van Eyk, 2005). Each bioanalytical platform has its unique strengths (and also limitations). Improvements of existing platforms and development of new platforms is a critical aspect of the field of proteomics, since a continued expansion of analytical capabilities will bring more power to penetrate deeper into a proteome or phosphoproteome, to more accurately capture its dynamics, and to integrate information into a systems-level understanding.

In our research group, the long-term focus is on proteomics of human cells, tissues, and biological fluids. Our team has contributed to the efforts directed towards analytical method development. We introduced a new platform that combines IEF and tandem mass spectrometry, and adapted this platform to phosphoproteomics (Beranova-Giorgianni et al., 2006; Giorgianni et al., 2004; Zhao et al., 2005).

Over the past years, our group has pursued research on the prostate cancer proteome and phosphoproteome, focusing on cultured prostate cancer cell lines and on

human tumor specimens. There were two broad objectives that I set out to achieve in my doctoral research: (1) to build on the successful foundation from previous research in our laboratory to obtain an expanded atlas of the human prostate cancer phosphoproteome; and (2) to complete a first phase of a new collaborative research program aimed at differential profiling of prostate cancer tissue for mechanistic studies of molecular effects of novel anticancer therapies.

The specific aims of my research were:

Specific aim 1 (Chapter 2) was to adapt our newly developed analytical method - termed in-gel IEF LC-MS/MS - to mapping of prostate cancer phosphoproteome to characterize on a global scale the phosphoproteome in the LNCaP human prostate cancer cell line.

Specific aim 2 (Chapter 3) was to apply a gel-free analytical platform to mapping the phosphoprotein signatures in human prostate cancer tissues for biomarkers discovery.

Specific aim 3 (Chapter 4) was to develop a 2-DE based platform combined with phospho-specific staining to characterize the phosphoproteome in the LNCaP prostate cancer cells.

Specific aim 4 (Chapter 5) was to identify proteins that are differentially expressed in control and bicalutamide/embelin treated mouse prostate tumor specimens, which will aid in the revealing of molecular mechanism of bicalutamide/embelin combination therapy.

CHAPTER 2. CHARACTERIZATION OF THE PHOSPHOPROTEOME IN LNCAP PROSTATE CANCER CELLS BY IN-GEL ISOELECTRIC FOCUSING AND TANDEM MASS SPECTROMETRY

2.1 Introduction

Prostate cancer is a leading type of cancer in men, and it is the second leading cause of cancer death (Jemal et al., 2008). Despite recent declines in the mortality from prostate cancer, prostate cancer remains a serious public health issue. Therefore, a large number of research efforts aims to increase our understanding of the mechanisms underlying the formation and progression of prostate cancer, in order to improve current diagnostic methods and to discover new drug targets. Analysis of the molecular machinery in prostate cancer cells by proteomics approaches is an integral part of these efforts.

Phosphoproteomics has recently emerged as an approach that focuses on examination of protein phosphorylation on a global-scale. Many fundamental cellular processes are controlled by reversible protein phosphorylation; it is estimated that in mammalian cells, 30% of proteins are phosphorylated at any given time (Cohen, 2000). Disruptions of phosphorylation-mediated cell signaling are associated with various diseases, including cancer (Benzeno et al., 2006; Iakoucheva et al., 2004; Lim, 2005; Stephens et al., 2005). Therefore, large-scale examination of the prostate cancer phosphoproteome will bring unique mechanistic insight about perturbations of protein networks relevant to cancer. Several recent reviews summarized numerous phosphoproteomic methodologies that have been developed. These methodologies used various combinations of separation strategies, in conjunction with mass spectrometry (Collins et al., 2007; Gafken and Lampe, 2006; Hoffert and Knepper, 2008).

In our research group, the long-term focus is on proteomics of prostate cancer. We have initiated a phosphoproteomic study that aims to map the phosphoproteome in the LNCaP cell line, including an exact description of the sites of phosphorylation. Towards the aim, we have recently applied a simple gel-free analytical methodology to obtain a first panel of the LNCaP phosphoproteins, 137 phosphorylation sites in 81 phosphoproteins (Giorgianni et al., 2007). That pilot study underscored the need to enhance the coverage of the LNCaP phosphoproteome through modifications of our analytical strategy.

The aim of this study was to adapt a newly developed analytical methodology, termed in-gel IEF LC-MS/MS (Giorgianni et al., 2003; Zhao et al., 2005), to phosphoproteomics study for prostate cancer, to characterize on a global scale the phosphoproteome in LNCaP human prostate cancer cell line. An outline of the in-gel IEF LC-MS/MS strategy is shown in Figure 2-1.

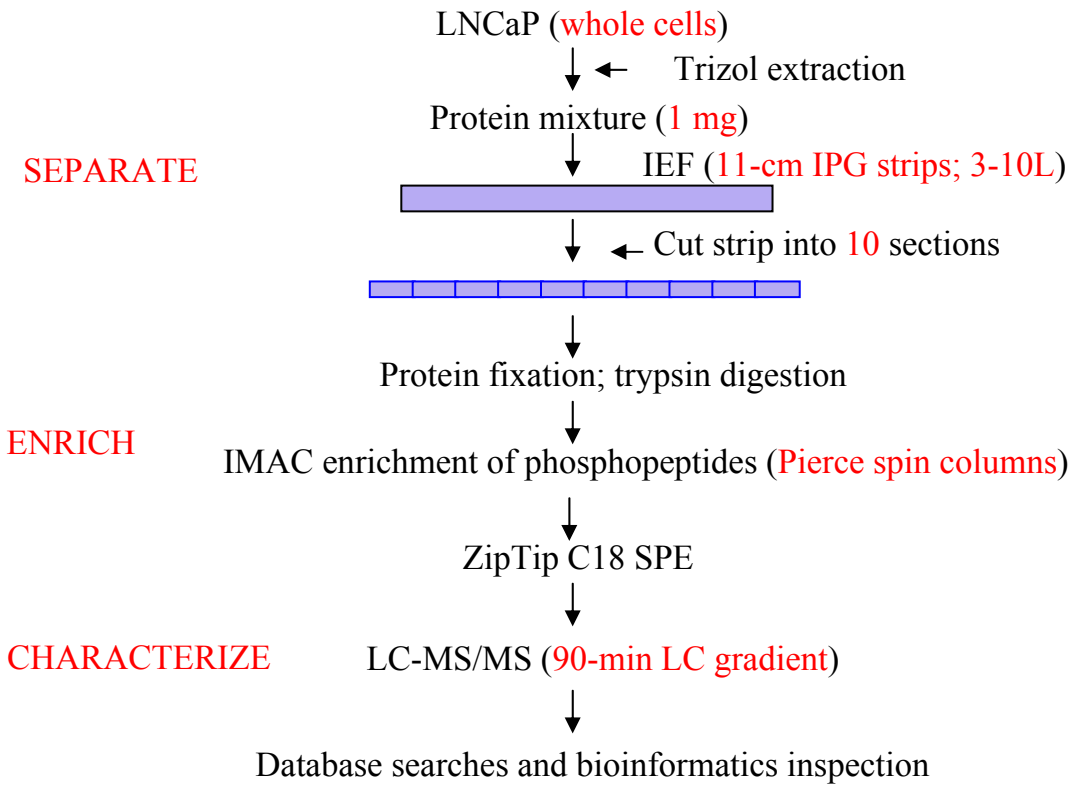

Figure 2-1 Outline of the in-gel IEF LC-MS/MS strategy.

The LNCaP proteins were extracted with Trizol reagent, and separated by IEF in IPG strips. After sectioning of the strips, the proteins in each gel section were fixed, and digested with trypsin. The digests were subjected to IMAC to isolate phosphorylated peptides. The samples were desalted and concentrated by SPE, and analyzed with LC-MS/MS. The LC-MS/MS datasets were used to identify the phosphorylated peptides and proteins via searches of a protein sequence database.

2.2 Materials and Methods

2.2.1 Protein Extraction from LNCaP Cells

The LNCaP human prostate cancer cells (American Type Culture Collection, Manassas, VA) were cultured under conditions described previously (Giorgianni et al., 2007). Briefly, the LNCaP cells were cultured in RPMI-1640 with 2 mM L-glutamine (American Type Culture Collection, Manassas, VA) supplemented with 10% fetal bovine serum (Hyclone, Logan, UT) in a 37 °C, 5% CO2 incubator. The cells were collected while in log-phase growth (approximately 85% confluency). The media were aspirated from the plates; 0.25% trypsin-0.53 mM EDTA (American Type Culture Collection) was added. After a few minutes, complete media were added to the plates to stop the trypsinization, and cells were resuspended and transferred to a conical tube for centrifugation. Cells were pelleted at 150×g for 4 min, and resuspended in PBS. The cells were processed for protein extraction in two tubes, each containing 5×10^6 cells. The cells in each tube were resuspended in 1.0 mL of Trizol reagent (Invitrogen, Carlsbad, CA) containing 5 µL of a phosphatase inhibitor cocktail (Sigma, St. Louis, MO), and the cells were lysed by repetitive pipetting. A total of 1 mg of protein was extracted using Trizol reagent following a procedure provided by the manufacturer.

Briefly, cells were resuspended in 1.0 mL of Trizol reagent containing 5 µL of a phosphatase inhibitor cocktail, and the samples were pipetted until full disruption of the cells was achieved. The samples were incubated for 5 minutes at room temperature to permit the complete dissociation of nucleoprotein complexes. Chloroform was added at a proportion of 0.2 mL per 1 mL of Trizol reagent. The mixtures were vigorously mixed by hand for 15 seconds. The mixtures were incubated at room temperature for 3 minutes. Centrifugation was performed at 12,000 x g for 15 minutes at 4 °C. Following centrifugation, the mixture separated into a lower red phenol-chloroform phase, an interphase and a colorless upper aqueous phase. The organic phase was retained after carefully removing the aqueous phase (containing RNA). Absolute ethanol was added at a proportion of 0.3 mL per 1 mL of Trizol reagent used for the initial homogenization. Samples were mixed by inversion, and were incubated at room temperature for 3 minutes followed by sedimentation of DNA by centrifugation at 2,000 x g for 5 minutes at 4 °C. The protein-containing phenol-ethanol supernatant was retained. Isopropyl alcohol was added to the supernatant at a proportion of 1.5 mL per 1 mL of Trizol reagent used for the initial homogenization. The mixture was stored at room temperature for 10 minutes followed by protein sedimentation by centrifugation at 12,000 x g for 10 minutes at 4 °C. Supernatant was removed and protein pellets were washed twice with 0.3 M guanidinium hydrochloride in 95% ethanol, followed by a single wash with ethanol. The proteins were dried in vacuum centrifuge for 5 minutes.

2.2.2 In-gel IEF

The proteins were solubilized in 600 µL of a rehydration buffer containing urea (7 M), thiourea (2 M), CHAPS (2%, w/v), IPG buffer pH 3-10 (2%, w/v), DTT (0.3%, w/v), and a trace of Bromophenol Blue dye. The mixture was kept at room temperature for 1 h; during that time, the mixture was sonicated for 20 s three times. The mixture was divided into three aliquots and centrifuged for 5 min at 12,000×g. The aliquots of the sample solution were loaded onto three IPG strips (pH 3-10, 11cm; GE Healthcare). The strips were allowed to rehydrate overnight in a reswelling tray. The IEF was carried out in a Multiphor II unit (GE Healthcare, Piscataway, NJ) according to manufacturer's instructions. In brief, the Multitemp water circulator was set to 20 °C, and apparatus was leveled, and all cables were connected. The DryStrip tray and the Immobiline strip aligner were placed according to the instructions. The grooves were lined up with the pattern on the cooling plate. The rehydrated IPG strip was taken out of the reswelling tray, and was rinsed slightly with water to remove any residual oil. The strip was placed into a groove in the strip aligner with the gel side up, and anode towards the rear. Two moistened electrode strips were placed on top of the aligned strip, one across the cathode and one across the anode edges. The strip made at least partial contact with the gel surface. Oil was used to completely cover the IPG strip. Focusing was performed at 20 ºC under the following conditions: 100 V (gradient over 1 min); 100 V (fixed for 120 min); 500 V (gradient over 1 min); 3500 V (gradient over 90 min); 3500 V (fixed for 6 h). After IEF, the IPG strips were stored at -80 ºC until further analysis.

2.2.3 In-gel Digestion

After IEF, the IPG strips were rinsed with water, and cut into 10 sections of identical size (1.10 cm× 0.36 cm). The gel sections were peeled off from the plastic backing with a clean scalpel. The same gel sections from the three strips were combined. Proteins in the IPG strip sections were fixed in 20% trichloroacetic acid (TCA) for 30min (Zhao et al., 2005). All gel pieces were washed with water and incubated in 200 µL of 200 mM ammonium bicarbonate for 10 min, followed by dehydration with 200 µL of acetonitrile (ACN). The gel pieces were dried in a vacuum centrifuge. The gel pieces were rehydrated with 100 µL of ammonium bicarbonate (50 mM) containing sequencing-grade trypsin (Promega, Madison, WI) at a concentration of 40 ng/µL. The samples were incubated overnight at 37 ºC.

2.2.4 Enrichment of Phosphopeptides with IMAC

The digests from each gel section were dried in a vacuum centrifuge, and re-dissolved in 50 µL of 10% acetic acid. The phosphopeptides were isolated with an IMAC Gallium (III) spin-column (Phosphopeptide Isolation Kit; Pierce, Rockford, IL). The sample solution was bound to the column by incubation at room temperature for 1 h. The column was washed with the following solutions: two portions of 40 µL of 0.1% AcOH, two portions of 40 µL of 0.1% AcOH/10% ACN, and two portions of 40 µL of

water. The phosphopeptides were eluted from the IMAC column with two aliquots of 30µL of 200 mM sodium phosphate (pH 8.4), followed by a single elution with 30 µL of 100 mM sodium phosphate/ 50% ACN. The eluates were combined and dried under vacuum. Prior to LC-MS/MS analyses, the IMAC-enriched phosphopeptides were reconstituted with 15 µL of 0.1% trifloroacetic acid (TFA) and desalted with ZipTipC18 (Millipore, Billerica, MA), using the procedure provided by the manufacturer. In brief, the ZipTipC18 column was conditioned with 10 µL ACN / 0.1% TFA (3 times), 50% ACN / 0.1% TFA (3 times) and water / 0.1% TFA (3 times). The peptide mixture was aspirated 10 times in order for the peptides to bind to the cartridge. The cartridge was washed 3 times with 10 µL 0.1% TFA / water. The phosphopeptides were eluted from the ZipTipC18 column with 3 µL of 50% ACN/0.1% TFA, and diluted with 3 µL of 0.1% AcOH.

2.2.5 LC-MS/MS Analysis

LC-MS/MS experiments were performed on an LTQ linear ion trap mass spectrometer (Thermo Electron, San Jose, CA) coupled to a nanoflow LC system (Dionex, Sunnyvale, CA). Each IMAC-enriched digest obtained from specific IPG gel section was analyzed in triplicate. The peptide mixtures were manually injected onto a PicoTip fused-silica micro-capillary column/spray needle (15 cm length, 75 µm ID; New Objective, MA) packed in-house with C18 stationary phase (Michrom Bioresources, Auburn, CA). The peptides were separated using a 90 min-gradient from 0% to 90% mobile phase B. The composition of mobile phase B was 90% MeOH/10 %water/0.05% FA; the composition of mobile phase A was 2% MeOH/98% water/0.05% FA. The LTQ mass spectrometer was operated in positive ion mode and data-dependent acquisition was performed. One data-dependent acquisition cycle encompassed a full-range MS scan followed by 7 MS/MS scans on the most abundant ions from the MS scan.

2.2.6 Database Searches

The datasets obtained in the LC-MS/MS analyses of the enriched digests from each gel section were used for database searches with the TurboSEQUEST search engine (Thermo Electron) that is part of Bioworks version 3.2. Using the target-decoy database searching strategy (Ballif et al., 2008; Elias and Gygi, 2007), the data were searched against a composite database containing human protein sequences and their reversed complements. The searches were performed with the following parameters: full-trypsin specificity, dynamic modification of oxidized Met (+15.9949), and dynamic modifications of phosphorylated Ser, Thr, and Tyr (+79.9663). The search results were filtered using the cutoffs of $\Delta Cn = 0.14$, and XCorr of 3.0, 4.0 for doubly and triply charged precursor ions, respectively; this filtering procedure produced a phosphopeptide set with an estimated false-positive rate of 0.8% (Elias and Gygi, 2007). All entries within this set were manually validated. In addition, lower-scoring phosphopeptides were subjected to manual validation, and those peptides that fulfilled the validation criteria were included in the final phosphopeptide panel. The manual validation involved

inspection of the corresponding MS/MS data. The criteria used for manual validation included: the presence of a diagnostic product ion corresponding to neutral loss of phosphoric acid (DeGnore and Qin, 1998); and high-quality spectrum in terms of signal-to-noise ratio for the sequence-determining product ions. Furthermore, assignments of exact sites of phosphorylation were validated manually through inspection of the corresponding product ions.

2.3 Results and Discussion

2.3.1 In-gel IEF LC-MS/MS Approach

The analytical methodology, outlined in Figure 2-1, encompassed seven steps: (1) Trizol-based extraction of proteins from the LNCaP cells; (2) separation of the protein mixture by isoelectric focusing in immobilized pH gradient (IPG) strips; (3) sectioning of the IPG strips; (4) protein fixation followed by digestion of the proteins in each gel section; (5) enrichment of phosphopeptides in the digests by IMAC; (6) analysis of the enriched digests by LC-MS/MS; and (7) identification of the phosphopeptides/proteins through database searches, and assignment of the sites of phosphorylation in these proteins. A representative example of an MS/MS spectrum from the LC-MS/MS datasets is shown in Figure 2-2.

The objective of the study presented here was to obtain an expanded panel of the LNCaP phosphoproteome through application of an improved analytical strategy. In-gel IEF LC-MS/MS, which included separation of the prostate proteins by IEF, was used to provide an additional dimension of separation of the complex mixture. Fractionation of the original protein mixture simplified the samples to be subsequently analyzed by LC-MS/MS. The concomitant decrease in throughput (multiple fractions had to be analyzed) was offset by the increase in the amount of information that was gained in the overall output of the analysis.

In combination with IEF separation, phosphopeptide enrichment and a more sensitive mass spectrometer (LTQ vs LCQ Deca XP plus), this bioanalytical strategy yielded a significantly larger phosphoprotein panel, compared to our pilot study of the LNCaP phosphoproteome (Giorgianni et al., 2007). As shown in Table 2-1, a total of 625 phosphorylation sites were identified in 558 phosphopeptides. Together, these phosphopeptides mapped to 296 different proteins. This panel of the LNCaP phosphoproteins was 3.6-fold larger than the panel obtained in our previous work, which attested to the power of the chosen analytical methodology. A full list of the phosphopeptides and phosphoproteins characterized in this study is provided in Table A-1. Phosphorylation sites were assigned based on manual inspection of product ion series in the MS/MS spectrum. The full information for each phosphorylation site assignment is provided in Table A-2.

One of tasks we faced in the analysis of tandem mass spectra was to validate

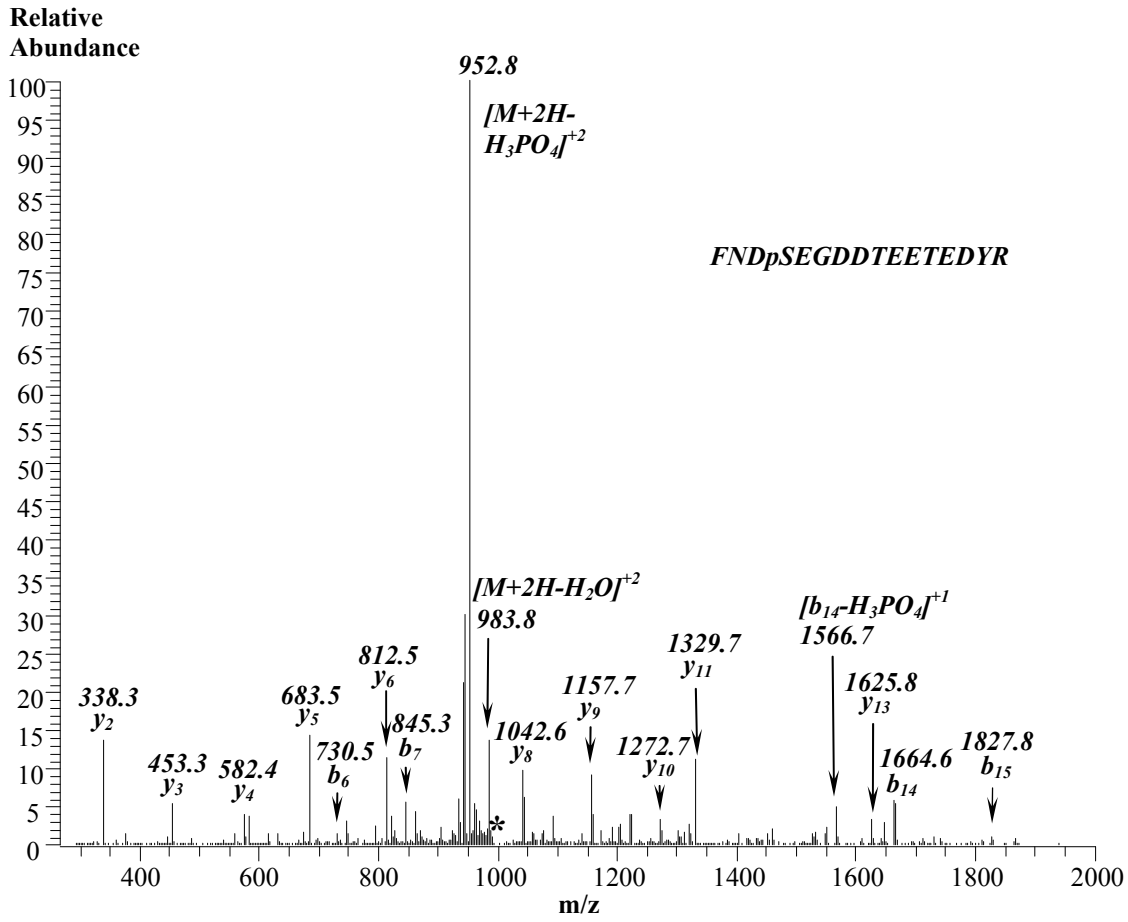

Figure 2-2 A representative MS/MS spectrum obtained in the LC-MS/MS analysis of IMAC-enriched digest from gel section 4.

The spectrum contains a phosphate-diagnostic product ion at m/z 952, and series of other product ions that determine the sequence of the peptide. Based on these data, the phosphopeptide FNDpSEGDDTEETEDYR (m/z of the $[M+2H]^{2+}$ molecular ion is 1001.4, marked as * into the spectrum) was identified that belongs to Bcl-2-Associated Transcription Factor 1.

Table 2-1 Summary of the LNCaP phosphoproteome characterization results: in-gel IEF LC-MS/MS vs. gel-free methodology.

Method	Number of phosphosites	Number of phosphopeptides	Number of phosphoproteins
Gel-free platform	137	115	81
In-gel IEF LC-MS/MS	625	558	296

peptide-spectrum matched identification. Tandem mass based peptide identifications are dependent on the quality of the match between the observed and predicted sequence spectra. However, in practice matches between observed and expected spectra are not perfect. Therefore, manual inspection of MS/MS spectra of the individual search results is very critical after database search. For the large phosphorylation data set generated by in-gel IEF LC-MS/MS study, we performed a composite target-decoy search strategy (Ballif et al., 2008; Elias and Gygi, 2007), the data were searched against a composite database containing human protein sequences and their reversed complements. The target-decoy strategy helped to estimate how many false positive were associated with the entire data set. We determined the cutoff value for the filters required to achieve a < 1% false-positive rate. Moreover, we performed manual validation of all hits and included the lower-scoring validated hits in our final panel. Combination the target-decoy strategy and the manual validation strategy allowed us to balance the need to minimize false positive with the need to also reduce false negatives.

2.3.2 Characteristics of Identified Phosphoproteins/phosphopeptides

Distribution of the identified phosphoprotein/phosphopeptides across the IPG strip is shown in Figure 2-3. As expected, the largest numbers of phosphoproteins were found in gel sections 4 and 5, corresponding to pH range 5.1 to 6.5. In addition, a number of acidic or basic phosphoproteins were found at the extreme positions in the pH 3-10 IPG strip. For example, a high-pI protein, Cysteine and Glycine-Rich Protein 1 (theoretical pI is 8.90) was identified in gel section 9. These results showed that phosphoproteins with a wide range of physicochemical characteristics were probed by our methodology. It should be noted that the experimental pI information on the intact protein was preserved, unlike in the gel-free approach or other methods that focus on analyses at the peptide level. As shown in Figure 2-4, the majority of the identified phosphopeptides were singly phosphorylated; doubly phosphorylated peptides accounted for 20-30 % of all phosphopeptides, and fewer than 10% were triply phosphorylated.

The phosphoproteins characterized in the study were evaluated based on their subcellular locations and function, as presented below. The full information for each phosphoprotein is available in Table A-3.

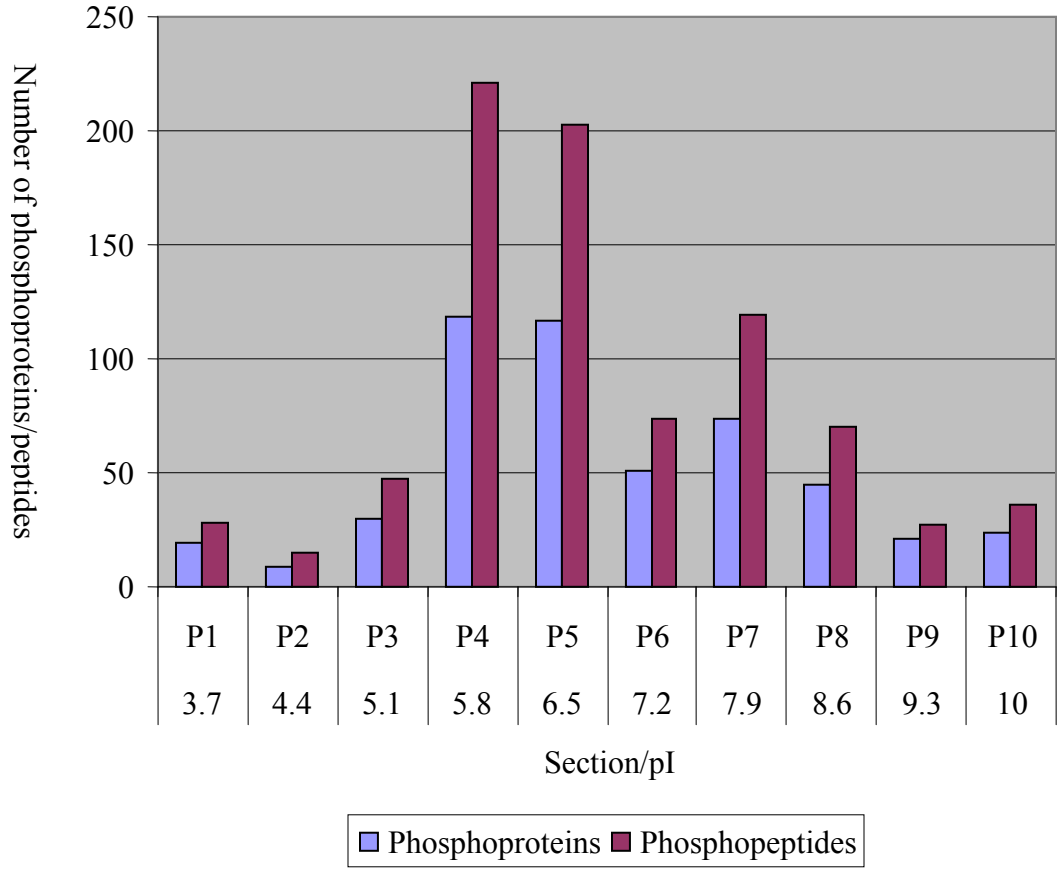

Figure 2-3 Distribution of phosphoproteins/phosphopeptides in the IPG strip sections.

An 11-cm IPG strip (pH range 3-10L) was used and divided into 10 sections of equal size. The labels on the x axis showed the IPG strip section numbers and corresponding pI values.

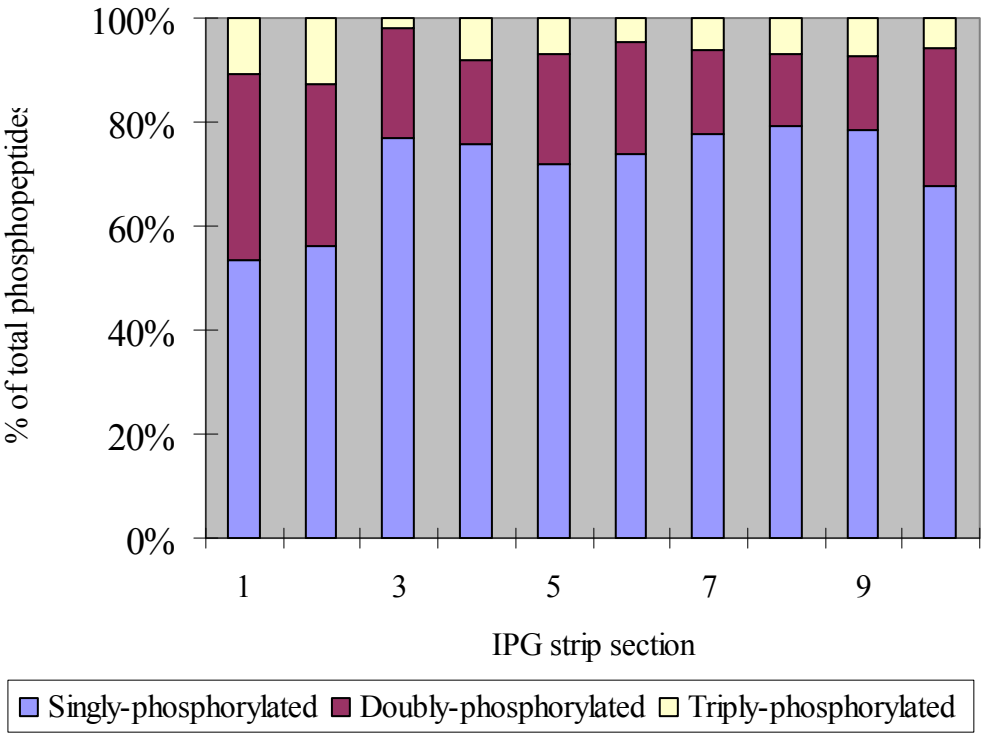

Figure 2-4 Distribution of singly, doubly, and triply phosphorylated peptides.

2.3.3 Classifications of Identified Phosphoproteins

The characterized phosphoproteins belong to various subcellular locations. The subcellular locations of the identified phosphoproteins were assigned based on Swiss-Prot annotations: among the 296 phosphoproteins, 205 proteins were annotated and 91 proteins could not be classified. As depicted in Figure 2-5, proteins from various subcellular compartments were sampled: nucleus, cytoplasm, multiple (that is, proteins that can be found in more than one subcellular location), membrane and mitochondria. It should be noted that the largest group sampled in the study were nuclear proteins and proteins that belong to a cytoplasm/nucleus subgroup within the "multiple" category.

The phosphoproteins characterized in the study are functionally diverse. We grouped the identified phosphoproteins into several categories based on their biological function as annotated in the Swiss-Prot database. The distribution of the phosphoproteins among the various functional categories is shown in Figure 2-6. The largest group was represented by proteins playing a role in transcription, including transcription factors and RNA-processing proteins. Other two large groups were represented by proteins involved in translation and signal transduction.

2.3.4 Selected Examples of Identified Phosphoproteins

Selected examples of identified phosphoproteins that are of particular interest in the normal and disease prostate physiology included kinases, steroid-receptor interacting proteins, and other proteins relevant to cancer.

The LNCaP phosphoprotein panel included a number of kinases, for example RAC-alpha Serine/threonine-Protein Kinase, Mitogen-Activated Protein Kinase 2, Serine/threonine-Protein Kinase TAO2, Serine/threonine-protein Kinase D1, and Protein Kinase C. Some of these kinases were known to play a role in prostate cancer. For example, RAC-Alpha Serine/Threonine-Protein Kinase (Protein Kinase B) is part of a central signaling pathway in prostate cancer (Lee et al., 2008); phosphorylation of the site that was found in this study (S473) regulates the activity of this kinase, and phosphorylation at S473 correlates with clinical outcome in prostate cancer (Kreisberg et al., 2004).

A number of other cancer-relevant proteins were identified. RNA-Binding Protein 5 is a tumor suppressor protein that promotes apoptosis and cell cycle arrest. Bcl-2-Associated Transcription Factor 1 is a transcriptional repressor that promotes apoptosis. Transforming Acidic Coiled-Coil-Containing Protein 2 is a candidate breast tumor suppressor and biomarker for tumor progression. It may protect nonmalignant cells from tumorigenic conversion by promoting proper cellular organization and tissue morphogenesis (Chen et al., 2000). Programmed Cell Death Protein 4 (Pdcd4) is a novel tumor suppressor. The Pdcd4 gene was first identified as a differentially expressed mRNA when cells were treated with apoptosis inducers. Pdcd4 might suppress tumor progression by regulating the expression of the kinase MAP4K1 (Yang et al., 2006).

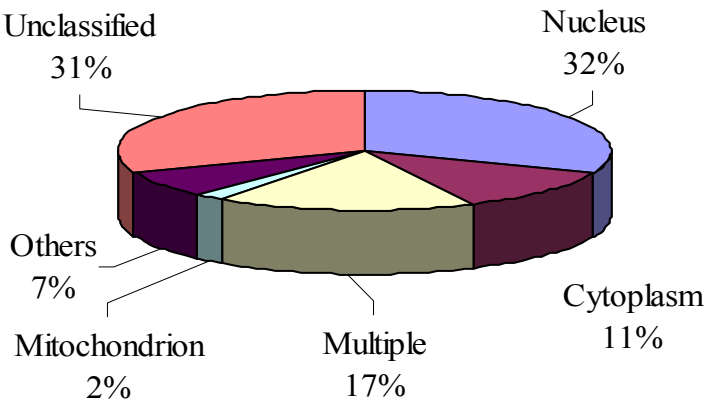

Figure 2-5 Summary of the sub-cellular locations of the LNCaP phosphoproteins characterized by in-gel IEF LC-MS/MS.

Note: The information was compiled from Swiss-Prot annotations.

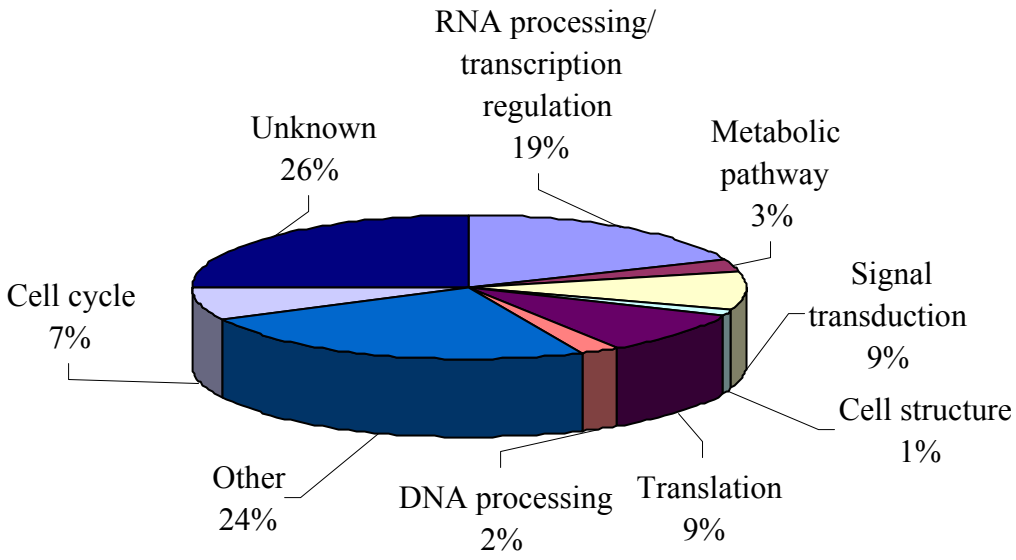

Figure 2-6 Classification of the characterized LNCaP phosphoproteins based on their involvement in cellular processes.

Note: This information was gathered based on Swiss-Prot annotations.

Several members of the androgen receptor (AR) response pathway were characterized. Several phosphorylated sites in protein from the heat-shock protein (HSP) family were found, such as HSP86, HSPB1 and HSP84. HSPs are bound by the ligand-free AR which is sequestered in the cytoplasm. HSPs function as chaperones to stabilize the AR during folding, protecting it from degradation. When dihydrotestosterone (DHT) binds to the AR, inducing a conformation change, which allows dissociation of HSPs, AR then forms a homo-dimer and is phosphorylated at several sites (Edwards and Bartlett, 2005; Lee and Chang, 2003).

Phosphorylation sites were identified for mitogen-activated protein kinase (MAPK) Ser164, Ser331 and protein kinase C (PKC) Ser354. These kinases help AR sensitize low circulating level of DHT to induce phosphorylation at specific sites of AR and then translocate AR to the nucleus (Rochette-Egly, 2003). PKC is a phospholipid-dependent cytoplasmic, serine/threonine kinase, which may be activated by TGF-β or intercellular activators such as calcium and diacylglycerol (Lahn et al., 2004). There are PKC phosphorylation consensus sites on the AR at Ser81 and Ser650. This indicates that activating PKC signaling can affect AR phosphorylation.

We also identified proteins involved in Ras signaling: Ras GTPase-activating protein-binding protein 1 (G3BP-1), Ras GTPase-activating protein-binding protein 2 (G3BP-2), and Rab-GTPase. Ras subfamily proteins control signal transduction between the membrane and the nucleus, and activation of Ras-mediated signaling has been implicated in the progression of prostate cancer to androgen independence (Gioeli, 2005).

2.4 Conclusions

With in-gel IEF based analytical platform, we have characterized over 600 different phosphorylation sites in 296 phosphoproteins in the LNCaP prostate cancer cell line. This panel of the LNCaP phosphoproteins was 3-fold larger than the panel obtained in our previous work, and was the largest phosphoproteins panel in prostate cancer to date. The phosphoproteins identified in this study belonged to various locations within the cell and were involved in various processes including cell differentiation, transcription regulation, and intercellular signal transduction. The expanded phosphoproteome map obtained in this study was of a satisfactory size to serve as a foundation for future quantitative studies of the effects of pharmaceuticals on the LNCaP prostate cancer cells.

CHAPTER 3. INVESTIGATION OF PHOSPHOPROTEIN SIGNATURES IN ARCHIVED HUMAN PROSTATE CANCER TISSUES VIA PROTEOMIC ANALYSIS

3.1 Introduction

Early stage detection and diagnosis of cancers decrease the mortality rate of these diseases. The prostate specific antigen (PSA) screen is a commonly used, serum based, biomarker test for the early detection of prostate cancer. It is well known that the PSA screen suffers for low specificity and poor sensitivity (Lin et al., 2007). Therefore, the discovery of new biomarkers of prostate cancer, featuring high specificity and sensitivity, would dramatically improve the survival rate of prostate cancer patients.

Because of its importance, the human prostate tissue has been a prime target of proteomics research efforts. To date, several studies have applied the proteomics approach to study the protein expression patterns in prostate cancer (Sardana et al., 2008b; Semmes et al., 2006; Solassol et al., 2005) as compared to healthy prostate tissues. Most of these studies had a common goal: the discovery of novel biomarkers, and all studies used mass spectrometry (MS) based platforms for their discovery efforts. As a result of these efforts, a large number of molecular markers have been identified; to date none of them has reached clinical use (Sardana et al., 2008a). It is thought that patterns revealed in a panel of proteins (known as a "protein signature") associated with a form of cancer might have better diagnostic and predictive capabilities than the current "one biomarker" approach.

An alternative approach to protein expression analysis for the discovery of disease biomarkers is the comprehensive characterization of protein phosphorylation. Protein phosphorylation is the most widespread signaling mechanism in eukaryotic cells, and it is involved in all fundamental cellular processes. Reversible phosphorylation forms the basis of cell signaling networks and phosphorylation-based signaling networks are key to the cell ability to quickly respond to external and internal environmental changes. The elucidation of the phosphoprotein networks in prostate cancer would therefore deepen our understanding of the mechanisms involved in its formation and progression, and it would improve the accuracy of early detection and it would speed up the discovery rate of targeted and more effective drugs.

We have already applied the gel-free platform to study phosphoproteins in LNCaP cells to obtain the first phosphoprotein networks in a prostate cancer cell line (Giorgianni et al., 2007). Since tissues based proteomic analyses are considered to be potentially more useful for relating protein status directly to diseases, the aim of this study was to apply the gel-free analytical platform to identify phosphoproteins on a global scale in archived prostate cancer tissues for biomarker discovery. An outline of the gel-free approach is shown in Figure 3-1.

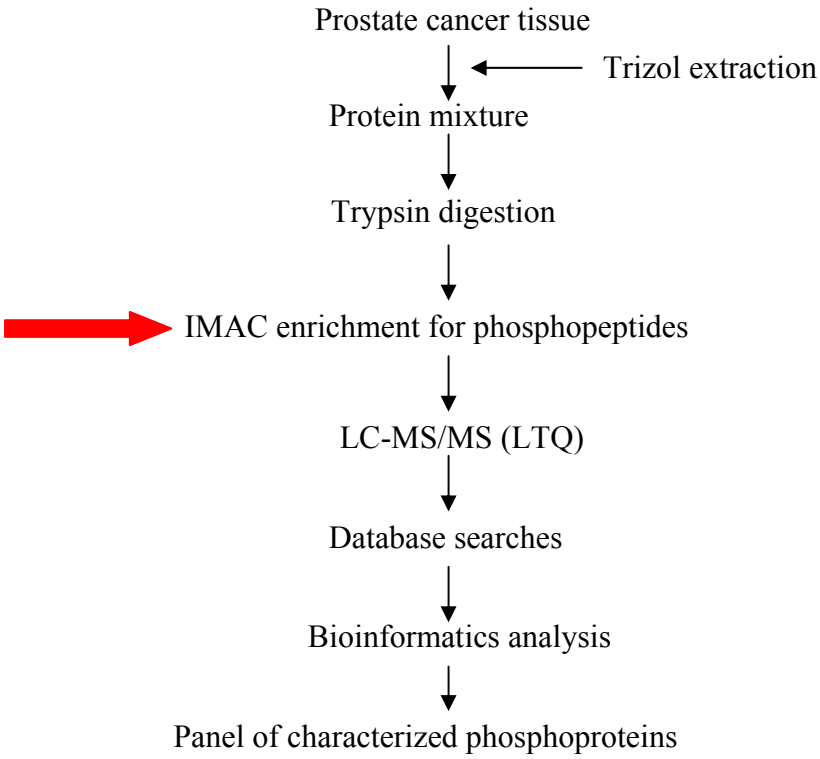

Figure 3-1 Outline of the gel-free analytical methodology.

Proteins from prostate cancer tissues were extracted with Trizol reagent, and then in-solution digested with trypsin. The digests were subjected to IMAC to isolate phosphorylated peptides. Enriched peptides were analyzed with LC-MS/MS. The MS/MS datasets were used to identify the phosphorylated peptides and proteins via searches of a protein sequence database. Bioinformatics analyses were performed for the panel of characterized phosphoproteins.

3.2 Materials and Methods

3.2.1 Characteristics of Clinical Samples

A total of 5 bulk prostate cancer specimens (99-010, 99-029, 98-065, 99-045, 99-067) have been used in the study. The specimens were obtained from the University of Tennessee Department of Urology Specimen and Tissue Bank. The research project was approved by the UTHSC IRB. The specimens were procured during radical prostatectomy, and were stored in liquid nitrogen until transfer from the Bank; afterwards, they were stored at -80 °C until processing. All specimens have been evaluated by a pathologist to confirm the presence of cancer, and to determine the Gleason score. The characteristics of specimens are summarized in Table 3-1.

3.2.2 Protein Extraction

Each prostate tumor tissue specimen (50-200 mg wet weight) was quickly minced with a scalpel and the pieces were suspended in 1.0 mL of Trizol reagent (Invitrogen, Carlsbad, CA) containing 5 µL of phosphatase inhibitor cocktail (Sigma, St. Louis, MO). The samples were homogenized until full disruption of the tissue was achieved. The protein, free of nucleic acids, was extracted from each lysate using Trizol reagent according the manufacturer's instruction (details described in Chapter 2). Protein pellets were washed three times with 0.3 M Guanidinium hydrochloride in 95% ethanol, followed by a single wash with ethanol. Proteins were dried under vacuum for 30 min, and were resuspended in 50 mM ammonium bicarbonate. The protein concentration of the extracts was determined by Bradford assay (GE Healthcare, Piscataway, NJ).

3.2.3 In-solution Digestion of Proteins

The extracted proteins (approximately 1 mg) were re-suspended in 50 mM ammonium bicarbonate buffer (pH 8) through vigorous vortexing. To produce a homogeneous protein suspension, the samples were sonicated three times for 20 s each time, with 30 s intervals between the sonication. Sequencing-grade trypsin (Promega,

Table 3-1 Characteristics of prostate cancer specimens used in the study.

Specimen code	Donor age	Donor race	Diagnosis (total Gleason score)
99-010	50	African American	Cancer (5)
99-029	59	African American	Cancer (7)
98-065	62	African American	Cancer (6)
99-045	66	Caucasian	Cancer (6)
99-067	67	Caucasian	Cancer (6)

Madison, WI, USA) was added to the protein mixture at an enzyme-to-protein ratio of 1:60 (w/w). The digestion proceeded overnight at 37 °C with gentle agitation. After 16 hours of digestion, undigested protein was visible in some of the samples. Therefore, additional trypsin was added to achieve complete digestion.

3.2.4 Enrichment of Phosphopeptides with IMAC

The tryptic digests were dried in a vacuum centrifuge, and re-dissolved in 50 µL of 90% water/10% AcOH. The resulting solution was applied to an IMAC spin-column (Phosphopeptide Isolation Kit; Pierce, Rockford, IL), and the phosphopeptides were bound by incubation at room temperature for 1 h. The column was washed with the following solutions: 40 µL of 0.1% AcOH (2 washes), 40 µL of 0.1% AcOH/10% ACN (2 washes), and 40 µL of water (2 washes). The phosphopeptides were eluted from the IMAC column with three 30 µL-aliquots of 200 mM sodium phosphate (pH 8.4), followed by a single elution with 30 µL of 100 mM sodium phosphate/50% ACN. The eluates were combined and dried under vacuum. Prior to LC-MS/MS analysis, the IMAC-enriched phosphopeptides were reconstituted with 15 µL of water/2.5% FA and desalted with ZipTipC18 (Millipore, Billerica, MA), using the procedure provided by the manufacturer. The phosphopeptides retained on the ZipTipC18 column were eluted with 3 µL of 50% ACN/0.1% FA and diluted with 6 µL of 0.5% FA, then analyzed by LC-MS/MS.

3.2.5 LC-MS/MS

LC-MS/MS experiments were performed on a LTQ linear ion trap mass spectrometer (Thermo Electron, San Jose, CA) coupled to a nanoflow HPLC system (Dionex, Sunnyvale, CA). Each sample was analyzed in triplicate. Peptide mixtures were loaded onto a fused-silica micro-capillary column/spray needle (Picofrit^{TM} , 15 cm length, 75 µm ID; New Objective, MA) packed in-house with C18 stationary phase (Michrom Bioresources, Inc., Auburn, CA). The peptides were separated using a 90-min linear gradient from 0% to 90% mobile phase B. Mobile phase B was 10% water/90% MeOH/0.05% FA; mobile phase A was 98% water/2% MeOH/0.05% FA. The LTQ mass spectrometer was operated in positive ion mode and data-dependent acquisition was performed. In brief, a scan cycle was initiated with a full MS, which was followed by MS/MS scans on the 7 most abundant precursor ions.

3.2.6 Database Searches

The MS/MS data were used to search the Swiss-Prot database (subset of human proteins) with the TurboSEQUEST search engine that was part of Bioworks version 3.2 software suite (Thermo Electron). Searches were performed with the following parameters: full-trypsin specificity, static modifications of oxidized Met (+15.9949), and dynamic modifications of phosphorylated Ser, Thr, and Tyr (+79.9663). All peptide

matches were filtered to include peptides retrieved with XCorr values ≥ 3.00, 2.00, and 3.50 for singly, doubly and triply charged ions, respectively. The MS/MS spectra of all phosphopeptide candidates that had passed this initial filtering were manually validated through inspection of the MS/MS spectra. This manual validation assessed the following: (1) whether a neutral-loss signal corresponding to $[M+2H-98]^{2+}$ for doubly charged ions or $[M+3H-98]^{3+}$ for triply charged ions was present in the spectrum; and (2) whether a good portion of the peptide sequence was covered by the b- and/or y product-ion series. The exact phosphorylation site assignment was validated by inspecting the b- and/or y-product ions that flanked the phosphorylation site assigned by software.

3.2.7 Additional Bioinformatics Analysis

Annotations of the Swiss-Prot database, and the PhosphoSite knowledgebase (www.phosphosite.org) were used to assess whether a particular site has been identified previously in prostate cancer tissue or in other biological systems. Gene Ontology (bioinfor.vanderbilt.edu/webgestalt) was used to classify identified proteins according to molecular function. The bioinformatics tool Scansite (scansite.mit.edu) was used to obtain information about potential kinase and/or phosphorylation-dependent binding motifs.

3.3 Results

In this study, a gel-free bioanalytical strategy was used to map the phosphoproteins in archived primary human prostate cancer tissue. One milligram of protein extracted from the tissue specimen was digested in-solution with trypsin. Generally, Trizol-extracted protein mixtures are denatured with 8 M urea and then diluted to 1-2 M urea prior to trypsin digestion. This strategy is used to digest highly complex protein mixtures, particularly when sample availability is a major concern. However, the urea present in the resulting digest complicates subsequent analysis. A clean, more efficient method for in-solution digestion of protein mixture has been recently reported (Kim et al., 2006), and this method was used in the study reported here. In this method, the extracted proteins were suspended in ammonium bicarbonate and digested with trypsin. The resulting tryptic peptides were dried in a speed vacuum concentrator to remove solvent and volatile buffers. This digestion method eliminated the need for removal of salts, urea or detergents prior to the IMAC step, and thus minimized sample loss.

A group of five archived human prostate tissue specimens was analyzed to obtain initial data on the prostate cancer tissue phosphoproteome. Peptide digests from each specimen were subjected to IMAC to enrich for phosphopeptides, and the enriched digests were analyzed by LC-MS/MS with an LTQ linear ion trap instrument. The phosphopeptides present in each digest were identified through searches of the Swiss-Prot protein sequence database. The identifications were based on MS/MS data that provide information on the peptide sequence and on location of the phosphorylation site(s) in the

peptide. The database search results were filtered to exclude low-scoring hits, and the phosphopeptides that passed the filters were validated through manual inspection of the corresponding MS/MS data. One of the features that provided supporting evidence for a phosphopeptide was the presence of a phosphate-diagnostic product ion in the MS/MS spectrum. An example of an MS/MS spectrum that illustrated this well-known phenomenon is shown in Figure 3-2. This spectrum displayed a prominent product ion at m/z 812.7, which corresponded to the loss of the elements of phosphoric acid from the doubly-charged precursor ion.

From each specimen, a number of phosphopeptides were detected; these phosphopeptides mapped to different phosphoproteins. A summary of the results is shown in Table 3-2. These results demonstrated that direct phosphoproteomics of archived tumor specimens was feasible. The size of the phosphoprotein panels ranged from 19 to 34 phosphoproteins encompassing between 25-45 different phosphorylation sites (Table 3-2). The phosphopeptides and sites found for each phosphoprotein are shown in Table 3-3. Additional details on the phosphopeptide/protein identification are provided in Table A-4. Based on an in silico analyses using the Scansite tool, some of the phosphorylation sites were part of known sequence motifs involved in kinase and/or phosphorylation-dependent binding interaction. Information on sites involved in such motifs is provided in Table A-5.

The phosphopeptide signatures varied from specimen to specimen. The overall distribution of the identified phosphopeptides is shown in Figure 3-3. Fifty-three percent of phosphopeptides were uniquely found in each specimen; 17% were common to all the specimens; 13% found in 4 out of 5 specimens and 17% in 2 or 3 out of 5 specimens. The results highlighted the heterogeneity of tissue samples and the need to investigate a larger specimen group. Nevertheless, a number of phosphoproteins were consistenly present in multiple specimens. Among the identified phosphoproteins, nine phosphoproteins were found in most of the specimens. These phosphoproteins included Caldesmone, Desmin, Heat Shock protein beta-6 (HSPB6), Heat Shock protein beta-1 (HSPB1), Synaptopodin-2, Filamin-C, DnaJ homolog subfamily C member 5, Tensin-1, and Glyceraldehyde-3-phosphate dehydrogenase. Eleven phosphoproteins were found in two or three out of five specimens, such as Myosin-11(MYH11), Septin-2, Desmocollin-1 precursor, Cysteine and glycine-rich protein 1, Transgelin, and Vimentin (Table 3-3).

The characterized phosphoproteins were grouped into functional categories based on GO annotation of the level 2 (Figure 3-4). The characterized phosphoproteins were involved in various cellular functions, such as binding, catalytic activity, enzyme regulator, signal transduction, cell structure, and transcription regulation.

3.4 Discussion

Advances in mass spectrometry-based technologies make it feasible to characterize phosphoproteins in complex mixtures, in a high-throughput, large-scale fashion. These technologies have been applied to investigations of cell cultures, tissues

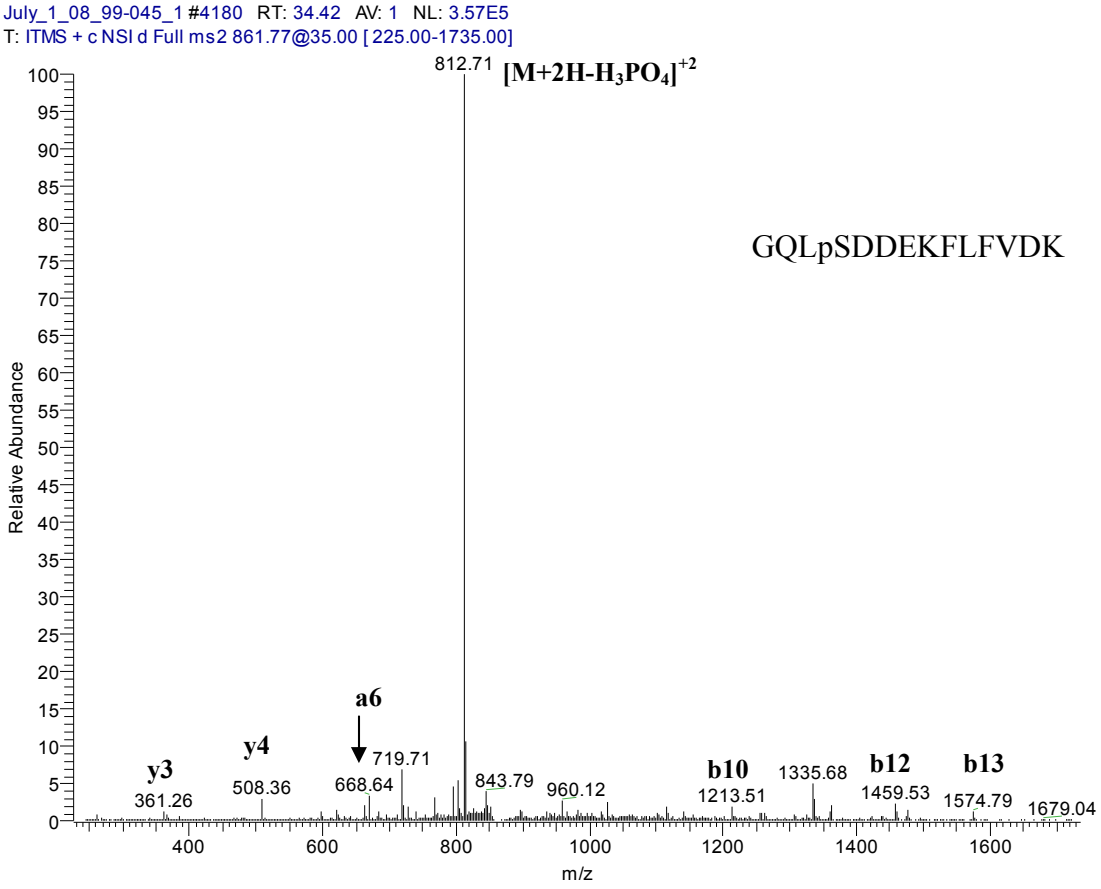

Figure 3-2 An example of MS/MS spectrum of GQLpSDDEKFLFVDK**.**

The spectrum contains a phosphate diagnostic product ion at m/z 812, and series of other product ions that determine the sequence of the peptide. Based on these data, the phosphopeptide with the sequence GQLpSDDEKFLFVDK (m/z of the $[M+2H]^{2+}$ molecular ion is 861.4) was retrieved. The sequence mapped to protein Myosin-11 and included a phosphorylated serine at position 8.

Table 3-2 Summary of results for the analyses of the phosphoproteome in human prostate cancer tissue.

Specimen	Number of phosphorylation sites	Number of phosphopeptides	Number of phosphoproteins
99-010	27	24	24
99-029	27	24	19
98-065	25	26	21
99-045	45	40	34
99-067	31	34	25

Table 3-3 Phosphoproteins characterized in the prostate cancer specimens.

Accession number	Protein	Peptide	Site
	Phosphoproteins found in all 5 specimens		
Q05682	Caldesmon	RGS*IGENQVEVMVEEK	S202
		RGS*IGENQVEVM#VEEK	S202
P17661	Desmin	TFGGAPGFPLGSPLSS*PVFPR	S32
		TFGGAPGFPLGS*PLSSPVFPR	S28
		TFGGAPGFPLGS*PLSS*PVFPR	S32
P04792	Heat-shock protein beta-1	QLS*SGVSEIR	S82
		GPS*WDPFR	S15
		GPS*WDPFRDWYPHSR	S15
Q9UMS6	Synaptopodin-2	AQS*PTPSLPASWK	S902
		AQS*PTPS*LPASWK	S906
		TAKPFPGSVNQPATPFS*PTR	S604
		PFPGSVNQPATPFS*PTR	S604
		GVSS*PIAGPAQPPPWPQPAPWSQPAFYDSSER	S638
		SKS*PDPDPNLSHDR	S226
	Phosphoproteins found in 4 out of 5 specimens		
O14558	Heat-shock protein beta-6 (Heat-shock 20 kDa-like protein)	RAS*APLPGLSAPGR	S16
Q14315	Filamin-C	LGS*FGSITR	S2233
Q9H3Z4	DnaJ homolog subfamily C member 5	S*LSTSGESLYHVLGLDK	S8
		SLSTS*GESLYHVLGLDK	S12
Q9HBL0	Tensin-1	RMS*VGDR	S1393
		WDS*YDNFSGHR	S338
		EAT*SDPSRTPEEEPLNLEGLVAHR	T854
		T*PTQPLLESGFR	T1105
		EATSDPSRT*PEEEPLNLEGLVAHR	T860
		SQS*FSEAEPQLPPAPVR	S621
P04406	Glyceraldehyde-3-phosphate dehydrogenase	VIHDNFGIVEGLMTTVHAITAT*QK	T182
	Phosphoproteins found in 3 out of 5 specimens		
P35749	Myosin-11	GQLS*DDEKFLFVDK	S8
		VIENADGS*EEETDTR	S1954
		RVIENADGS*EEETDTR	S1954

Table 3-3 (continued).

Accession number	Protein	Peptide	Site
	Phosphoproteins found in 2 out of 5 specimens		
Q15019	Septin-2	IYHLPDAES*DEDEDFKEQTR	S218
Q08554	Desmocollin-1 precursor	MKVQDQDLPNT*PHSK	T385
P21291	Cysteine and glycine-rich protein 1	GFGFGQGAGALVHS*E	S192
Q8N283	Ankyrin repeat domain-containing protein 35	QS*VGLLT*NELAM#EK	S672; T677
Q01995	Transgelin	HVIGLQMGS*NR	S181
P08670	Vimentin	ISLPLPNFS*SLNLR	S419
Q6P597	Kinesin light chain 3	APRTLSAST*QDLS*PH	T493; S497
O95425	Supervillin	S*LSDFTGPPQLQALK	S547
Q15746	Myosin light chain kinase	KSS*TGSPTSPLNAEK	S1773
Q63ZY3	Ankyrin repeat domain-containing protein 25	ALAMPGRPES*PPVFR	S375
		KIS*ITER	S406
	Phosphoproteins found in 1 out of 5 specimens		
Q92736	Ryanodine receptor 2	SSSENAKVTS*LDS*SSHR	S4546; S4549
P13796	Plastin-2	GS*VSDEEMMELR	S5
Q15283	Ras GTPase-activating protein 2	S*SFKETFMCEFFK	S559
P43353	Aldehyde dehydrogenase 3B1	FDY*IFFTGS*PR	Y183; S189
P24844	Myosin regulatory light chain 2	ATS*NVFAMFDQSQIQEFK	S20
P27816	Microtubule-associated protein 4	DMES*PTKLDVTLAK	S280
P17252	Protein kinase C alpha type	STLNPQWNES*FTFK	S226
Q8IYX7	Uncharacterized protein C9orf138	EY*QKGPIPMEGLTTSR	Y59
O75069	Transmembrane and coiled-coil domains protein 2	GAS*LHS*SSGGGSS*GSSSRRTK	S166; S169
P27216	Annexin A13	YQKS*LSDMVRSDTSGDFR	S294
Q6PCE3	Phosphoglucomutase-2-like 1	AVAGVMITAS*HNR	S175
P01854	Ig epsilon chain C region	VAHTPS*STDWVDNK	S92

Table 3-3 (continued).

Accession number	Protein	Peptide	Site
Q8TCU4	Alstrom syndrome protein 1	SPLQEAES*KVSMALEETLR	S2367
P80421	Ig heavy chain V-I region DOT	DRLVMSSDTSANTVS*MQLR	S79
Q8TAP8	Putative uncharacterized protein C7orf47	S*SLALGLELR	S108
P36871	Phosphoglucomutase-1	AIGGIILTAS*HNPGGPNGDFGIK	S117
P60174	Triosephosphate isomerase	KQS*LGELIGTLNAAK	S21
Q9NZN4	EH domain-containing protein 2	GPDEAMEDGEEGS*DDEAEWVVTK	S438
P22059	Oxysterol-binding protein 1	GDMS*DEDDENEFFDAPEIITMPENL GHK	S351
Q32MZ4	Leucine-rich repeat flightless-interacting protein 1	RGS*GDTSISIDTEASIR	S120
Q9UBT6	DNA polymerase kappa	CDS*YKDDLLLR	S10
Q9Y385	Ubiquitin-conjugating enzyme E2 J1	RLS*TSPDVIQGHQPR	S266
Q86SQ6	Probable G-protein coupled receptor 123	QVT*KKAPLCLDTDQPPYPR	T833
Q9Y618	Nuclear receptor corepressor 2	REGTPPPPPPS*R	S1390
Q9H2J4	Phosducin-like protein 3	LS*ES*GAIMTDLEENPK	S199; S201
P09496	Clathrin light chain A	LQS*EPESIR	S105
O43237	Cytoplasmic dynein 1 light intermediate chain 2	SGQKT*VLSNVQEELDR	T463
P35558	Phosphoenolpyruvate carboxykinase	WM#S*EEDFEK	S118
P05386	60S acidic ribosomal protein P1	KEES*EES*DDDMGFGLFD	S101; S104
P13861	cAMP-dependent protein kinase type II-alpha regulatory subunit	GDS*ES*EEDEDLEVPVPSR	S77; S79
Q6P9B9	Integrator complex subunit 5	FQAPSPS*TLLR	S1012
Q14195	Dihydropyrimidinase-related protein 3	GSPT*RPNPPVR	T524
Q13618	Cullin-3	FLLES*FNNDRLFK	S359
P48681	Nestin	S*LGEQDQMTLRPPEK	S767
Q9NSE4	Isoleucyl-tRNA synthetase	GLVYRS*Y*KPVFWSPSSR	S239; Y240
O43432	Eukaryotic translation initiation factor 4 gamma 3	SS*ASSLNR	S1194
P27824	Calnexin precursor	AEEDEILNRS*PR	S583

Table 3-3 (continued).

Accession number	Protein	Peptide	Site
Q96KP6	TNFAIP3-interacting protein 3	CS*FSEDCLR	S175
P20711	Aromatic-L-amino-acid decarboxylase	GLQAY*IR	Y377
O76041	Nebulette	SMQHS*PNLR	S953
P08238	Heat shock protein HSP 90-beta (HSP 90)	IEDVGS*DEEDDSGKDKK	S254
O75385	Serine/threonine-protein kinase ULK1	KM#S*LGGGR	S495
Q9Y5C1	Angiopoietin-related protein 3 precursor	NMSLELNS*K	S122
Q6KC79	Nipped-B-like protein	QNEST*IVEPK	T667
P58107	Epiplakin	QPLQAT*FRGLRKQVS*AR	T1495, S1504
P02545	Lamin A/C	LRLS*PSPTSQR	S390
Q13242	Splicing factor, arginine/serine-rich 9	GS*PHYFSPFRPY	S211
Q13263	Transcription intermediary factor 1-beta	SRS*GEGEVSGLMR	S473
P07197	Neurofilament triplet M protein	GKSPVPKS*PVEEK	S645
P15924	Desmoplakin	GLPSPYNMSSAPGS*R	S2825
O00264	Membrane associated progesterone receptor component 1	LLKEGEEPTVYS*DEEEPKDESAR	S180

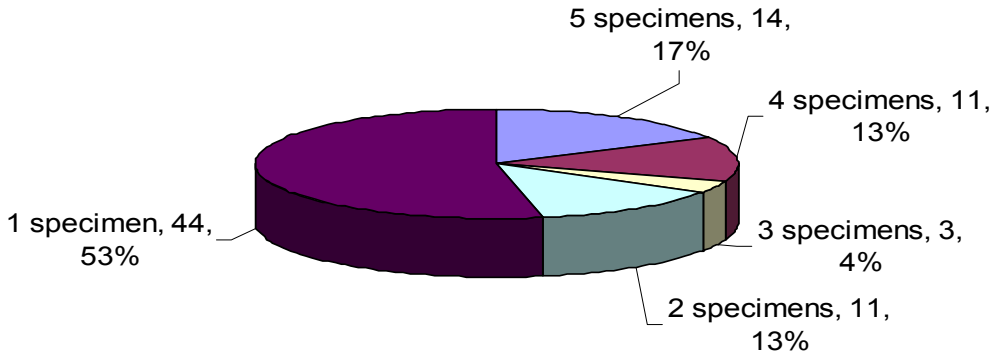

Figure 3-3 Distribution of identified phosphopeptides in five prostate tissues analyzed.

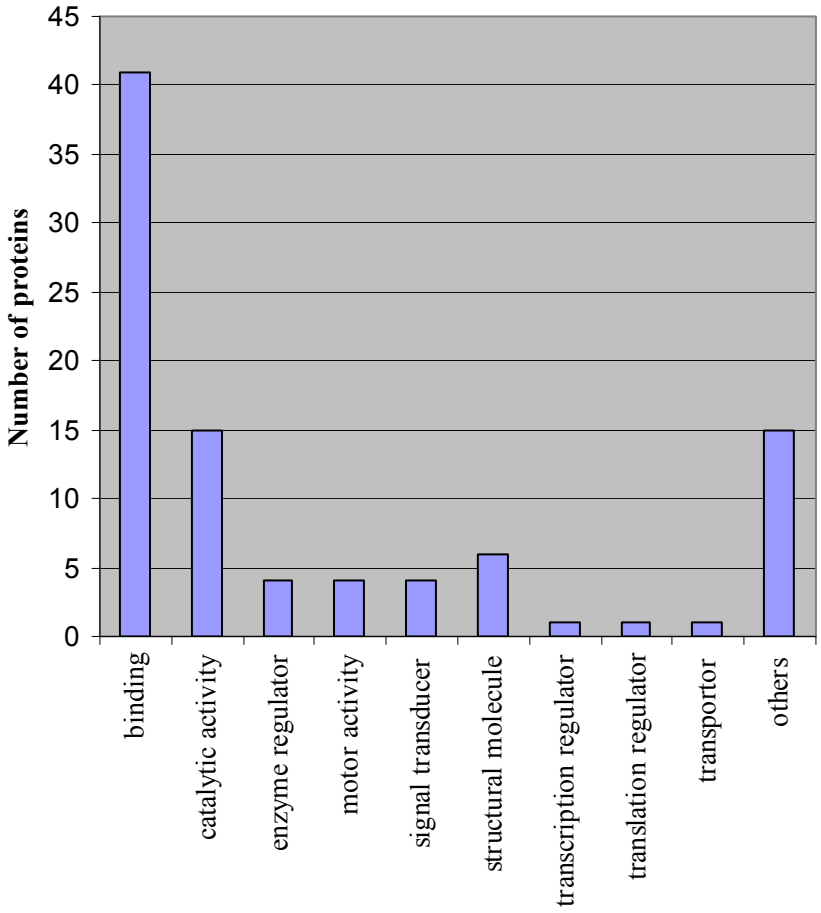

Figure 3-4 Classification of identified phosphoproteins by molecular function according to GO annotation at the level 2.

and biological fluids to discover cancer biomarkers (Lin et al., 2007; Sardana et al., 2008b; Semmes et al., 2006). Extensive efforts were involved in exploring theapplication of proteomic strategy to study biomarkers in prostate cancer cell lines or tissues, such as 2-DE, 2D-DIGE, multiple dimensional chromatography (Johansson et al., 2006; Lin et al., 2007; Rowland et al., 2007; Sardana et al., 2007; Ummanni et al., 2008; Whitaker et al., 2007). The cell lines PC-3, DU 145, and LNCaP are spontaneously established from human prostate cancer metastases and are frequently used in prostate cancer research. However, these cell lines only partly mimic the biology of prostate cancer. Recently, increased efforts have been directed towards tissue-based proteomic analysis because it can directly reflect the relationship of proteins to diseases. A gel-free bioanalytical methodology has been used in our group to map the phosphoproteome in the LNCaP human prostate cancer cell line (Giorgianni et al., 2007). Recently, we have produced an expanded LNCaP phosphoproteome panel through the application of in-gel IEF LC-MS/MS, which involves one-dimensional protein separation.

In this study, we employed a gel-free methodology to investigate phosphoprotein signatures in archived human prostate cancer tissues. Because of the limited size of a human tissue sample compared to that of cultured cells, it is critical to minimize the loss of sample during the various steps in the analytical workflow. In our previous study of cultured cells (LNCaP) phosphoproteome, we used guanidinium hydrochloride to aid protein solubilization prior to in-solution digestion. With this procedure, the peptide digest had to be subjected to solid phase extraction (SPE) cleanup with a C18 Sep-Pak cartridge before IMAC enrichment. For the present work on human prostate tissue, we sought to avoid this SPE step that may be associated with significant sample loss. Therefore, we adopted a modified protein digestion methodology to our study that was based on recently published report.

Genetic and environmental variability, together with sampling variations due to different cell types, results in the heterogeneity of human prostate cancer tissue specimens. A unique set of phosphoproteins was identified in each tissue specimen. Nevertheless, it was also demonstrated that a subset of the phosphoprotein panel was preserved across multiple specimens; 30% of the phosphopeptides were identified in ≥4 out of the 5 specimens analyzed.

The characterized phosphoproteins were functionally diverse. Based on published literature, a number of these phosphoproteins were relevant to prostate cancer mechanism. Some of the identified phosphoproteins have previously been reported to be differentially regulated in tumors, including prostate tumors. For example, HSPB1, MYH11, VIME, DESM, TAGL, HSP90A and SEPT2 have been reported as differentially expressed in prostate cancer (Lin et al., 2007; Rowland et al., 2007).

Among the groups of phosphoproteins identified, there were several chaperones, including HSPB1 (HSP27), HSPB6 and HS90B. HSP27, which has been reported up-regulated in prostate cancer (Rocchi et al., 2004), is involved in various cellular processes including apoptosis, cell growth and differentiation, actin reorganization and polypeptide renaturation. Cell proliferative activity in prostate cancer specimens was significantly

associated with HSP27 expression (Kurahashi et al., 2007). HSP 27 is involved in cooperative interaction with androgen receptor (AR), which enhances AR stability, shuttling, and transcriptional activity, thereby increasing prostate cancer cell survival. Androgen-bound AR induces rapid HSP27 phosphorylation on Ser (78) and Ser (82) residues. Phosphorylated HSP27 displaces HSP90 from a complex with AR to chaperone AR into the nucleus and interact with its response elements to enhance its genomic activity. Inhibition of HSP27 phosphorylation, or knockdown using the antisense drug, shifted the association of AR with HSP90 to MDM2, increased AR degradation, decreased AR transcriptional activity, and increased prostate cancer LNCaP cell apoptotic rates (Zoubeidi et al., 2007). Previous study showed increased HSP27 expression was linked with hormone resistance and a poor prostate cancer prognosis (Miyake et al., 2006). HSP27 expression was also highly up-regulated in prostate cancer cells after androgen withdrawal or chemotherapy, to become uniformly highly expressed in androgen-independent prostate cancer. Silencing of HSP27 in prostate cancer cells by siRNA increased apoptotic rates and caused inhibition of cell growth in LNCaP and PC-3 cells (Rocchi et al., 2006). These findings suggested the expression level of HSP27 in prostate cancer tissue could be used as a useful predictor of prostate cancer, and also illustrated the potential utility of HSP27 as future targeted therapy in enhancing the efficacy of chemotherapy in advanced prostate cancer.

Tensin was another important protein found in prostate tissues, which is one of components of phosphatase and tensin homologue deleted on chromosome 10 (PTEN). PTEN has been shown to be inactivated in a wide variety of cancers, and the role of this gene as a tumor suppressor has been well established. PTEN has been found to work as a predictor of prostate cancer in combination with other proteins. Differentiation related gene 1(Drg-1) gene, one of the potential targets of PTEN, has been shown to suppress tumor metastasis in animal models of prostate and colon cancer, and the expression of this gene was significantly reduced with advancement of prostate and breast cancers in clinical setting. PTEN controls Drg-1 by an Akt-dependent pathway, overexpression of PTEN significantly augments the endogenous expression of Drg-1 protein. Combination of the two markers, PTEN and Drg-1, emerged as a significantly better predictor of prostate and breast cancer patient survival than either marker alone (Bandyopadhyay et al., 2004). PTEN, in combination with pAkt, was a better predictor of the risk of biochemical recurrence compared with pAkt alone. Loss of PTEN expression, together with increased Akt phosphorylation and Gleason score, was of significant predictive value for determining, at the time of prostatectomy, the risk of biochemical recurrence (Bedolla et al., 2007). PTEN was found to strongly inhibit the growth of human prostate tumors, especially when combined with radiation therapy, and this effect was mediated by the induction of apoptosis and by the inhibition of angiogenesis and cellular proliferation (Anai et al., 2006). PTEN/phosphatidylinositol 3-kinase (PI3K)/AKT constitute an important pathway regulating the signaling of multiple biological processes such as apoptosis, metabolism, cell proliferation and cell growth. Tissue-specific deletions of PTEN usually provoke cancer. Moreover, an absence of PTEN cooperated with an absence of p53 to promote cancer (Blanco-Aparicio et al., 2007).

A number of filament proteins (desmin, vimentin and caldesmon) were identified

in our study. Intermediate filaments (IFs) are an important structural feature of eukaryotic cells. They, along with microtubules and actin microfilaments, make up the cytoskeleton. Based on current knowledge, a main function of IFs is to provide protection against various mechanical or other types of stresses. IFs are also involved in maintaining cell shape, and providing flexible scaffold, which undergoes disassembly and reorganization during certain cellular processes including cell division, migration and shape changes in response to their alterations in the microenvironment (Coulombe and Wong, 2004). IFs in smooth muscle are formed by polymerization of the proteins vimentin and desmin and constitute one of the major components of the cytoskeleton (Chang and Goldman, 2004).

Desmin is class-III intermediate filament found in muscle cells. Desmin is important in muscle cell architecture and structure since it connects many components of the cytoplasm. It has been shown that desmin phosphorylation occurred in cells/tissues in response to biological signal/treatment. It is possible that desmin phosphorylation may influence the temporal and spatial array of structural proteins or signal partners in smooth muscle (Tang, 2008).

Vimentin is also a member of class-III intermediate filament family of proteins. Vimentin has been found to be attached to the nucleus, endoplasmic reticulum, and mitochondria, either laterally or terminally. Therefore, vimentin played a significant role in supporting and anchoring the position of the organelles in the cytosol. Vimentin phosphorylation was also found to be associated with its disassembly and spatial reorganization in smooth muscle cells and tissues during agonist activation (Li et al., 2006). Vimentin has been shown to affect motility and invasiveness of prostate cancer cells. A low level of vimentin was expressed in the less invasive cell line, LNCaP, in contrast to the higher level in more aggressive cell lines, DU-145 and PC3 (Mitchell et al., 2000). Downregulation of vimentin expression in PC-3 cells led to a significant decrease in tumor cells motility and invasive activity (Wei et al., 2008; Zhao et al., 2008).

Caldesmon (CaD), a component of microfilaments in all cells and thin filaments in smooth muscle cells, is known to bind to actin, tropomyosin, calmodulin, and myosin and to inhibit actin-activated ATP hydrolysis by smooth muscle myosin. Thus, it is believed to regulate smooth muscle contraction, cell motility and the cytoskeletal structure. CaD has been found to bind to vimentin and desmin proteins. Assembly of vimentin and desmin into IF was also affected by CaD silencing, although their expression was not significantly altered when CaD was silenced. It indicated that CaD was necessary for the maintenance of actin microfilaments and IF in the cytoskeletal structure. Thus, the alternation of CaD expression might affect the cytoskeletal structure in smooth muscle, as in smooth muscle de-differentiation and in certain pathological conditions (Deng et al., 2007).

3.5 Conclusions

In this study, a gel-free approach was applied to characterize phosphoproteins of archived primary human prostate cancer tissue for biomarker discovery. The panels

obtained for human prostate cancer tissue contained 15-24 phosphoproteins. Some of the characterized phosphoproteins were present in all specimens; in addition, each specimen also produced a unique set of phosphoproteins. The findings provided a direct glimpse into the phosphoprotein machinery operating within the human prostate cancer tissue and demonstrated that phosphoproteins can be characterized directly from archived tissue specimens.

CHAPTER 4. IDENTIFICATION OF PHOSPHOPROTEINS IN THE LNCAP HUMAN PROSTATE CANCER CELL LINE BY A 2-DE AND PHOSPHO-SPECIFIC STAINING-BASED PROTEOMICS PLATFORM

4.1 Introduction

Two-dimensional polyacrylamide gel electrophoresis (2-DE) is one of the most commonly used protein separation techniques (Gorg et al., 2000). It can separate thousands of proteins in a specific cell, tissue or biological fluid. It has high resolution and high reproducibility. 2-DE coupled with mass spectrometry (MS) and database searches is a widely used platform in proteomics studies (Gorg et al., 2004). 2-DE combined with MS is able to get a rapid overview of proteomic alterations in different biological systems or physiological states. Combination with multiplexed protein staining makes it possible to investigate various post-translationally modified proteins by 2-DE (Wu et al., 2005).

Pro-Q^{TM} Diamond is a fluorescent stain specific for detection of phosphoproteins (Schulenberg et al., 2004; Steinberg et al., 2003). Pro-Q^{TM} Diamond can be used to detect phosphorylated serine, tyrosine, or threonine residues. It has been reported that Pro-Q^{TM} Diamond, combined with SDS-PAGE or 2-DE, was applied to efficiently detect phosphoproteins and to quantitatively measure phosphoprotein expression in various biological systems, such as spleen leukocytes (Wu et al., 2005), eye lenses (Schaefer et al., 2006), dentate gyrus (Chardonnet et al., 2008), heart muscle (Jacques et al., 2008), skeletal muscle (Gannon et al., 2008) et al.

The sub-aims of our study were: (1) to develop a platform for the identification of LNCaP phosphoproteins. This sub-aim included incorporation of multiplexed staining, and evaluation of selected technical aspects. (2) to apply the platform to identify selected phosphoproteins from the LNCaP phosphoproteome. In this study, we applied 2-DE as separation technique, Pro-Q^{TM} Diamond as detection method, LC-MS/MS and database searches as protein identification tools to investigate the phosphoproteins in the LNCaP prostate cancer cell line. An outline of the 2-DE with phsopho-specific staining strategy is shown in Figure 4-1.This approach did not require the pre-selection of protein candidates for analysis, rapidly generated a snapshot of the phosphoproteome in the LNCaP cells, and it was particularly useful for an initial screening of the phosphoproteome to evaluate the phosphoproteome coverage for further study of the expression of phosphoproteins in various physiological states.

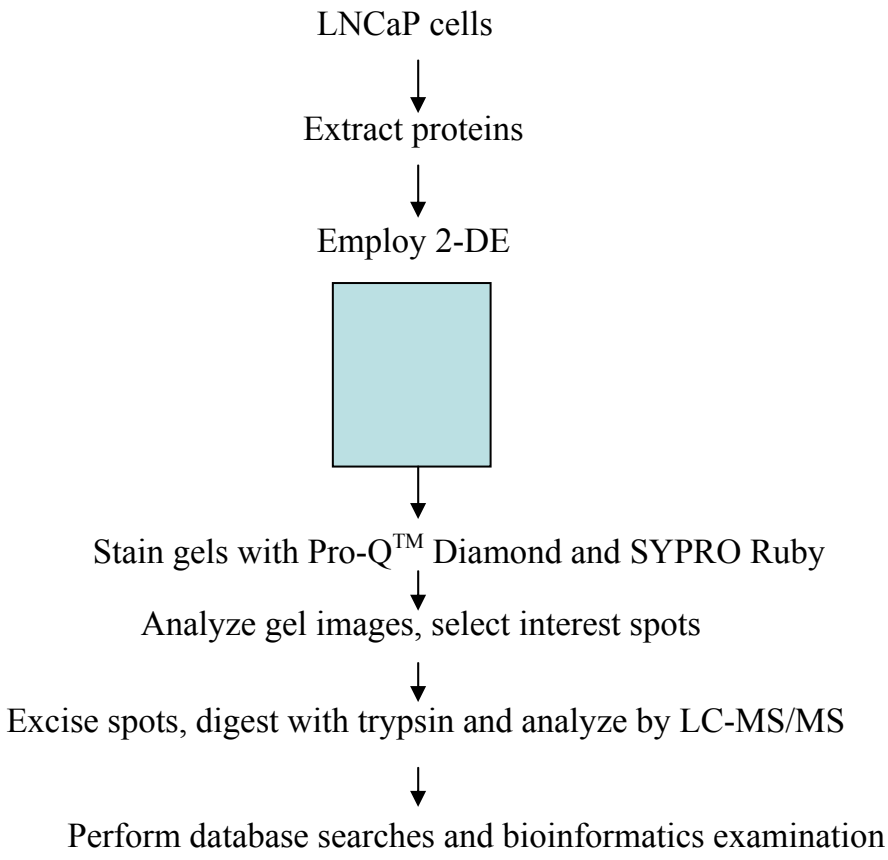

Figure 4-1 Schematic of 2-DE and phospho-specific staining based proteomics platform.

The LNCaP proteins were extracted with Trizol reagent. Proteins were separated with 2-DE. Gels were sequentially stained with Pro-Q™ Diamond and SYPRO Ruby staining. Gel images were computer-assisted analyzed. The spots of interest were excised and digested with trypsin. The digests were analyzed with LC-MS/MS. Proteins were identified through database searches and bioinformatics examination of the identified proteins was performed.

4.2 Materials and Methods

4.2.1 Protein Extraction from LNCaP Cells

A cell pellet containing 5×10^6 LNCaP cells was resuspended in 1.0 mL of Trizol reagent (Invitrogen, Carlsbad, CA) with 5 µL of phosphatase inhibitor cocktail (Sigma, St. Louis, MO). The cells were lysed thoroughly by repetitive pipetting. Approximately 1.0 mg of protein, free of nucleic acids, was extracted from this cell lysate using Trizol reagent according to the manufacturer's instructions (details described in Chapter 2). Protein pellets were washed twice with 0.3 M Guanidinium hydrochloride in 95% ethanol, followed by a single wash with ethanol. The protein pellet was dried with a vacuum centrifuge for 30 minutes, and was stored at -80 °C for further analysis.

4.2.2 Sample Preparation

4.2.2.1 Standard Rehydration Buffer

For 2-DE separations, the protein pellet was dissolved with a rehydration buffer that contained urea (7 M), thiourea (2 M), CHAPS detergent (2% w/v), IPG buffer 3-10 (2% v/v), DTT (0.3%, w/v) and a trace amount of Bromophenol Blue dye. The protein concentration of the extracts was determined by Bradford assay (GE Healthcare, Piscataway, NJ). The final protein concentration in the rehydration buffer was 0.61 µg/µL. The mixture was vortexed for 1 hour at room temperature. Following solubilization, the sample was centrifuged for 30 minutes at 21,000 x g. Protein sample (215 µg in 350 µL of rehydration buffer) was loaded onto a pre-cast immobilized pH gradient (IPG) strip (pH 3-10NL, 18 cm; GE Healthcare, Piscataway, NJ), and the strip was allowed to rehydrate overnight in a re-swelling tray or a strip holder.

4.2.2.2 Destreak Rehydration Buffer

For 2-DE separations, the protein pellet was dissolved with a DeStreak rehydration solution(Olsson et al., 2002) (GE Healthcare, Piscataway, NJ) with IPG buffer 3-10 (2% v/v), DTT (20 mM) and a trace amount of Bromophenol Blue dye. Protein concentration was determined by 2-D Quant Kit (GE Healthcare, Piscataway, NJ). The resulting solution (200 µg of proteins in 350 µL of the rehydration buffer) was vortexed for 1 hour at room temperature, followed by the centrifugation for 30 minutes at 21,000 x g. The supernatant was loaded onto a pre-cast IPG strip (pH 3-10NL, 18 cm), and the strip was allowed to rehydrate overnight in a re-swelling tray.

4.2.3 First Dimension: Isoelectric Focusing

4.2.3.1 IEF with Multiphor Unit

Isoelectric focusing was performed with a Multiphor II apparatus (GE Healthcare, Piscataway, NJ) according to manufacturer's instructions (details described in Chapter 2). The isoelectric focusing was performed under the following voltage program: 100 V (gradient over 1 minute); 100 V (fixed for 2 hours); 500 V (gradient over 1 minute); 3500 V (gradient over 90 minutes); 3500 V (fixed for 8 hours). After the focusing, the strip was wrapped loosely in plastic wrap and was stored at -80 °C until the next step.

4.2.3.2 IEF with IPGphor Unit

Isoelectric focusing was performed with the IPGphor apparatus (GE Healthcare, Piscataway, NJ) according to manufacturer's instructions. Briefly, the strip holder was chosen, and 350 μL of rehydration solution was applied into the holder. IPG strip was positioned in the holder with the gel side down and without bubbles, making sure that the IPG strip was in contact with the strip holder electrodes at each end. Cover fluid was applied to IPG strip and the cover was placed on the holder. The strip holder was positioned on the IPGphor platform with the two external electrodes of the instrument making contact with the electrodes of the strip holder. The isoelectric focusing was performed under the following voltage program: 30 V (fixed for 16 hours); 200 V (fixed for 1 hour); 500 V (fixed for 1 hour); 1000 V (fixed for 1 hour); 8000 V (gradient over 30 minutes); 8000 V (fixed for 4 hours). After the focusing, the strip was wrapped loosely in plastic wrap and was stored at -80 °C until the next step.

4.2.4 Second Dimension: SDS-PAGE

4.2.4.1 Gel Casting

To prepare eight of 12%, 20 × 20 cm SDS-PAGE gels, gel plates and plastic pads were assembled sequentially into the casting chamber placed on a flat surface. The casting chamber was clamped and the plates were leveled on the bottom. The casting chamber was put on the stand. All reagents were combined, including 120 mL of 40% acrylamide/bis, 100 mL of 1.5 M Tris-HCl (pH 8.8) and 180 mL distilled water and degassed for 15 minutes. When ready to pour the gel, the reagents of 2 mL of 10% ammonium persulfate and 100 μL TEMED were quickly added and gently mixed. The gel solution was transferred between the glass plates in the casting chamber to about 3/4 inch below the short plate. A small layer of butanol was added on the top of the gel prior to polymerization to straighten the level of the gel and remove unwanted air bubbles that may be present. Once the gel polymerized, the butanol was removed by rinsing the top layer of the gel with distilled water prior to the use.

4.2.4.2 SDS-PAGE with Dodeca Cell Unit

SDS-PAGE was performed with a ProteanPlus Dodeca Cell apparatus (Bio-Rad, Hercules, CA). The IPG strip was incubated for 15 minutes in an equilibration buffer (50 mM Tris/HCl pH 8.8, 6 M urea, 30% glycerol, 2% SDS) with 2.0% DTT and then in equilibration buffer with 2.5% iodoacetamide and a trace amount of bromophenol blue dye for an additional 15 minutes. The strip and a sample application piece with the Marker 12 MW maker (Invitrogen, Carisbad, CA) were put on the top of the self-cast 12%, 20 x 20 cm SDS-PAGE gel and were sealed with 1% agarose in gel running buffer, which contained 25 mM Tris (pH 8.3), 192 mM glycine and 0.1% SDS. The SDS-PAGE separation was performed with according to the manufacturer's instructions. Briefly, the temperature setting for the electrophoresis was 15 °C, the voltage applied was 200 V constant and the electrophoresis time was **ca.** 8 hours. The SDS-PAGE separation was completed when the Bromophenol Blue dye front migrated to the bottom of the gel.

4.2.5 Gel Staining

4.2.5.1 Pro-Q™ Diamond Staining

A series of stains was applied to each 2-DE gel, which was compatible with subsequent mass spectrometric analysis. Briefly, 2-DE gel was fixed in 200 mL of fixation solution (50% MeOH /10% AcOH /40% water) for 30 minutes or overnight. The gel was washed three times with distilled water with gentle agitation for 15 minutes each. The gel was incubated in dark with 170~190 mL of Pro-Q™ Diamond phosphoprotein gel stain (Molecular Probes, Eugene, OR) with gentle agitation for 2.5 hours. The gel was incubated with 190 mL of Pro-Q™ Diamond phosphoprotein gel destaining solution (Molecular Probes, Eugene, OR) for 2 hours with gentle agitation, followed by two washes with distilled water for 5 minutes each.

4.2.5.2 SYPRO Ruby Staining

After detection of phosphoproteins, the gel was stained in SYPRO Ruby protein stain (Molecular Probes, Eugene, OR). 2-DE gel was rinsed twice with distilled water for 15 minutes each, followed by incubation in 170 mL of SYPRO Ruby staining solution for 3 hours to overnight in the dark with gentle agitation. After incubation of the staining, the gel was incubated in 200 mL of 10% of MeOH /7% of AcOH /83% water for 30 minutes. The gel was rinsed twice with distilled water for 5 minutes each.

4.2.6 Gel Imaging

The images were acquired with an FX Fluorescence Laser Scanner (Bio-Rad, Hercules, CA). For Pro-Q™ Diamond stain, the laser was used with 532 nm excitation and 555 nm band pass emission; for SYPRO Ruby stain, proteins were detected using the laser scanner with the excitation 488 nm and 555 nm band pass emission. The images

were displayed with Adobe Photoshop 5.0 LE software, and saved as .TIFF files for future analysis. The Pro-Q^{TM} Diamond and SYPRO Ruby images were analyzed using the software PDQuest 7.1.0 (Bio-Rad, Hercules, CA).

4.2.7 Spot Excision

Spots in 2-DE gels were excised with cut-to-size 1 mL pipette tips, and the gel pieces were put into 1.5 mL siliconized Eppendorf microcentrifuge tubes.

4.2.8 In-gel Tryptic Digestion

The gel pieces were incubated in 50 mM ammonium bicarbonate for 10 minutes. After the incubation, the buffer was removed and the gel pieces were washed three times with 50% ACN/50% 50 mM ammonium bicarbonate for 10 minutes each. Gel pieces were dried under vacuum for 30 minutes. The dried gel pieces were rehydrated in a trypsin solution that contained 16.7 ng/µL trypsin (Promega, Madison, WI) in 50 mM ammonium bicarbonate (pH 8). The digestion solution was incubated at 37 °C overnight.

4.2.9 Peptide Processing

The tryptic digest was centrifuged at 1,000 x g for 1 minute, and the supernatant was transferred to a new 0.6 mL siliconized microcentrifuge tube. The gel piece was extracted with 60% ACN/0.01% TFA three times for 15 minutes each with gentle agitation or sonication. All supernatants were combined and dried with a vacuum centrifuge. Prior to LC-MS/MS analysis, the digest was reconstituted with 15 µL of 2.5% FA/97.5% water and desalted with ZipTipC18 column (Millipore, Billerica, MA, USA), using the procedure provided by the manufacturer (details described in Chapter 2). The peptides retained on the ZipTipC18 column were eluted with 1.5 µL of 50% ACN/0.1% FA and diluted with 2.5 µL of 0.5% FA.

4.2.10 LC-MS/MS Analysis

LC-MS/MS experiments were performed on a LTQ linear ion trap mass spectrometer (Thermo Electron, San Jose, CA). Peptide mixtures were loaded onto a fused-silica microcapillary column (15 cm length, 75 µm ID; New Objective, MA) packed in-house with C18 resin (Michrom Bioresources, Inc., Auburn, CA) and were separated using a 30-minute linear gradient from 0% to 90% solvent B (0.05% FA/90% MeOH/10% water). Solvent A was 0.05% FA/ 2% MeOH/98% water. The LTQ mass spectrometer was operated in positive ion mode and data-dependent acquisition was performed. In brief, a scan cycle was initiated with a full MS scan of wide mass range (m/z 400-2000), which was followed by MS/MS scans on the 7 most abundant precursor ions with dynamic exclusion of previously selected ions.

4.2.11 Database Searches

The MS/MS data were used to search the Swiss-Prot database (subset of human proteins) with the TurboSEQUEST search engine that is part of Bioworks version 3.2 (Thermo Electron, San Jose, CA). Searches were performed with the following parameters: full-trypsin specificity, dynamic modifications of phosphorylated Ser, Thr, and Tyr; dynamic modifications of oxidized methionine, and static modifications of cysteine by carbamidomethylation. All peptide matches were filtered by XCorr larger than 3.00, 2.50, and 3.50 used for singly, doubly and triply charged ions, respectively; peptide probability less than 1.0E-3; different peptides; and only top matches were considered. The peptides retrieved by the searches were validated by manual inspection of the MS/MS data. Criteria used for manual validation included: a high-quality spectrum with product ions clearly above the baseline noise; and sequential members of the b- and/or y-series present in the mass spectra.

4.2.12 Inspection of Protein Information

The experimental pI was estimated according to the pH gradient chart provided by the manufacturer (GE Healthcare, Piscataway, NJ) based on the relative migration of each protein spot.

A series of protein markers with known molecular weights were used to determine the experimental molecular weight of unknown proteins by comparing the migration distance relative to the markers. The relative migration (Rm) value of protein spots was determined by dividing the total distance they migrated by the distance migrated by the bromphenol blue dye. A straight reference line was plotted, using the Rm of each MW marker spot and the logarithm of that molecular weight. The relative molecular weight of each protein spot was calculated from that equation.

The theoretical pI and MW were computed with Swiss-Prot Compute pI/MW tool for each UniProt Knowledgebase entry. The status of protein phosphorylation was inspected in the Swiss-Prot annotations and the PhosphoSite knowledgebase. Information of protein function and subcellualr location was collected from Gene Ontology (http://bioinfo.vanderbilt.edu/webgestalt/) and Swiss-Prot annotation.

4.3 Results

4.3.1 Application of Different Rehydration Buffers: Standard vs. Destreak

In order to address the issue of streaking in the basic region of the pH gradient (pH 7-9), we employed the Destreak Rehydration solution in the sample preparation for the first dimension. Destreak Rehydration solution has been reported to transform the

protein thiol groups into a stable disulfides and hence to protect the disulfide groups from unspecific oxidation (Olsson et al., 2002).

We performed side-by-side separations of LNCaP proteins that were solubilized with standard rehydration buffer or with Destreak Rehydration solution. Comparison of 2-DE gel images of samples using standard rehydration buffer (Figure 4-2a) or Destreak rehydration solution (Figure 4-2b) showed that the protein spot pattern of Destreak-solubilized sample has somewhat improved compared to the patterns obtained using standard rehydration buffer; however, the streaking was not totally eliminated. Therefore, we opted to use IPG strips with pH range of 4-7 for subsequent experiments.

4.3.2 IPGphor vs. Multiphor

As the first dimension of 2-DE, the quality of IEF is critical for the overall success of 2-DE separation. Different configurations of IPG-based IEF equipment are commercially available. The IPGphor and Multiphor II are two widely used systems for IEF.

In the method development phase of our study, we assessed the 2-DE spot patterns of LNCaP proteins produced by the IPGphor and by the Multiphor units. The same amount of protein was loaded onto two 18-cm IPG strips (pH 4-7), and the strips were focused in Multiphor II and IPGphor, respectively.

Comparison of the 2-DE gel images from the Multiphor II (Figure 4-3a) and the IPGphor (Figure 4-3b) indicated both IEF systems separated proteins with a satisfactory resolution. Multiphor yielded a better separation of proteins in the basic region of the gel.

4.3.3 Detection of Proteins by Sequential Staining

In the study, 2-DE gels were first stained with the Pro-Q^{TM} Diamond stain; the gels were imaged to capture the phosphoprotein patterns. Subsequently, the gels were stained with SYPRO Ruby total protein stain, and images were obtained to detect the total protein pattern. It has been reported that Pro-Q^{TM} Diamond stain did not interfere with the SYPRO Ruby stain, even though there is some overlap in the wavelengths of fluorescence (Wu et al., 2005). The images obtained with Pro-Q^{TM} Diamond and with SYPRO Ruby stain are shown in Figure 4-4a and 4-4b, respectively.

Several spots seen with Pro-Q^{TM} Diamond stain were not present in the SYPRO Ruby-stained gel. Furthermore, intensities of some spots on Pro-Q^{TM} Diamond and SYPRO Ruby stain images are different.

(a)

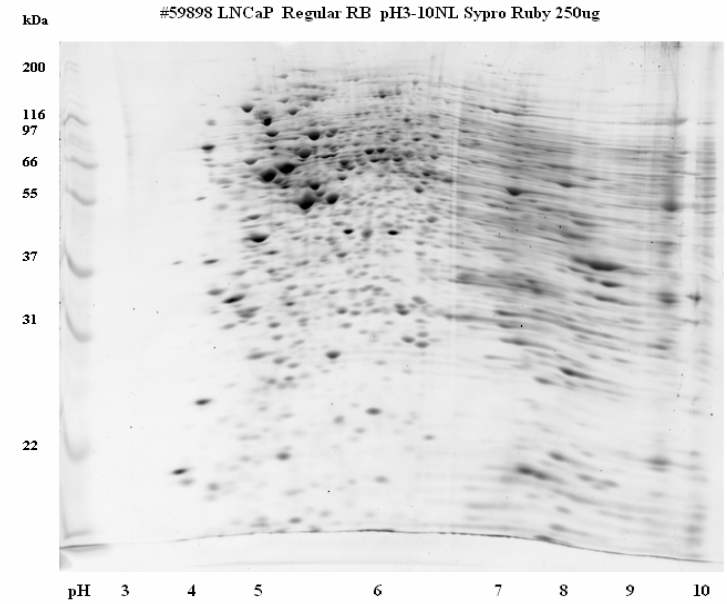

(b)

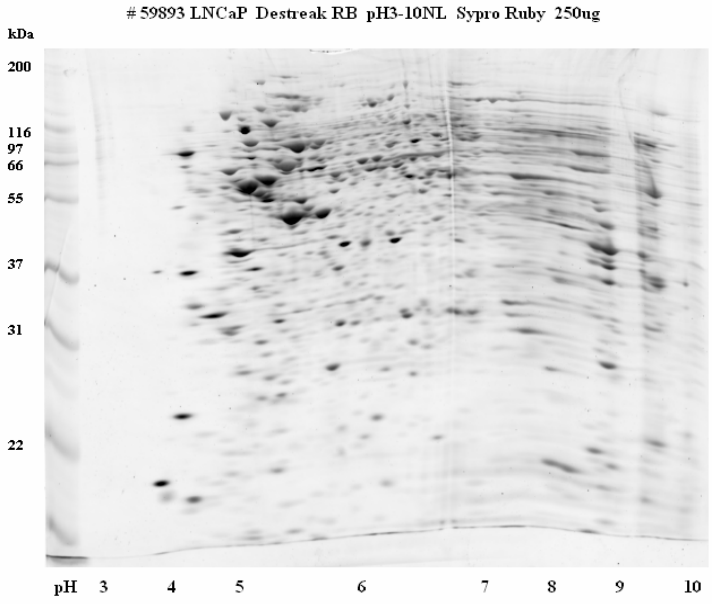

Figure 4-2 2-DE gels of LNCaP proteins with pH 3-10NL using different rehydration buffers (a) Standard rehydration buffer (b) Destreak rehydration solution.

(a)

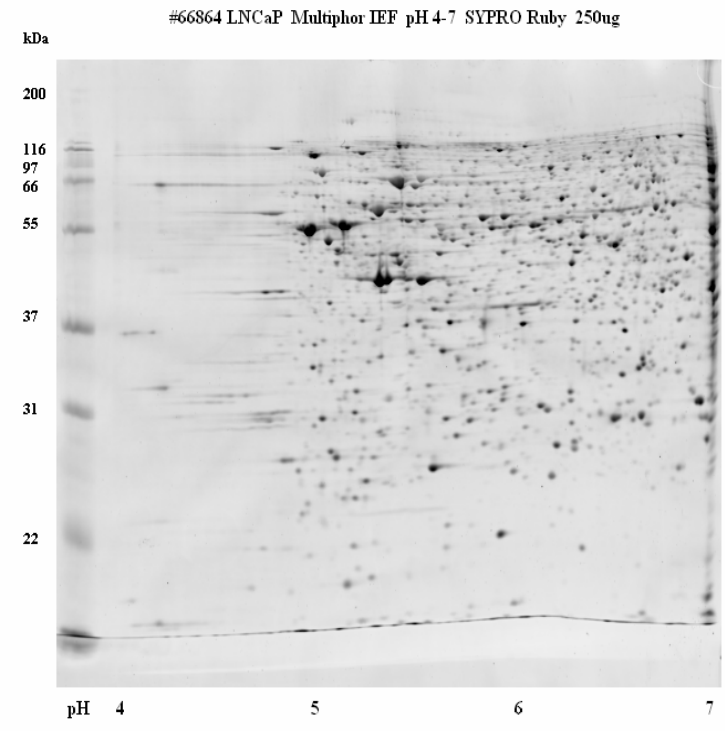

(b)

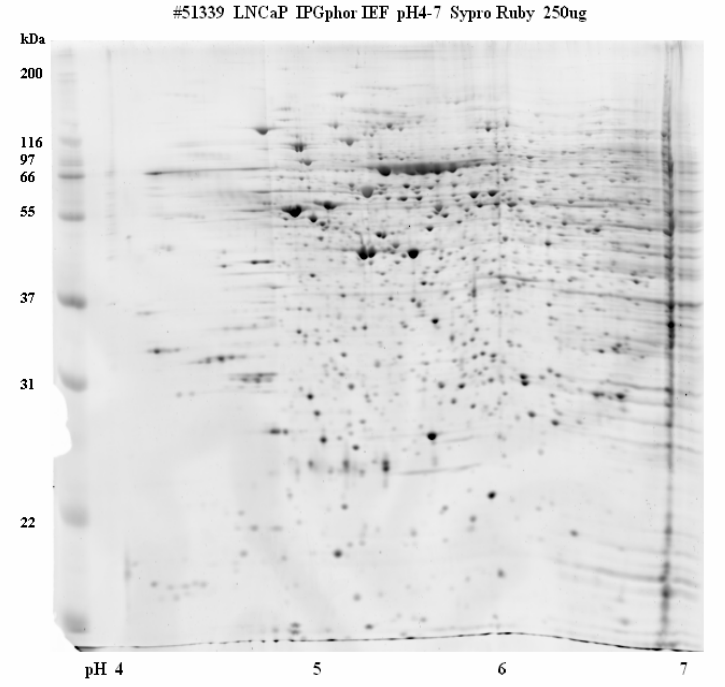

Figure 4-3 2-DE gels of LNCaP using different IEF units (a) Multiphor II (b) IPGphor.

(a)

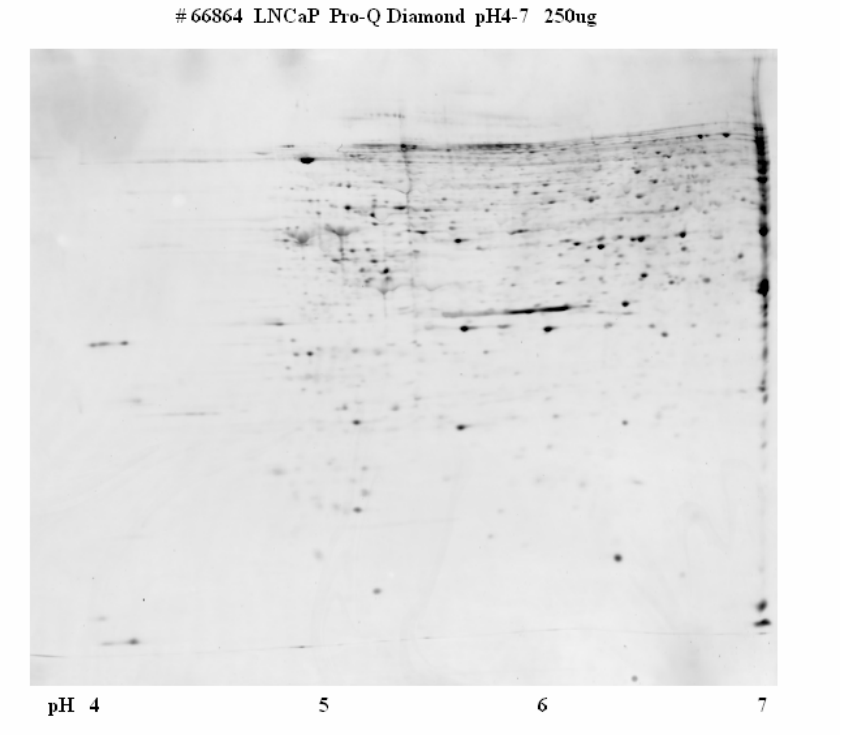

(b)

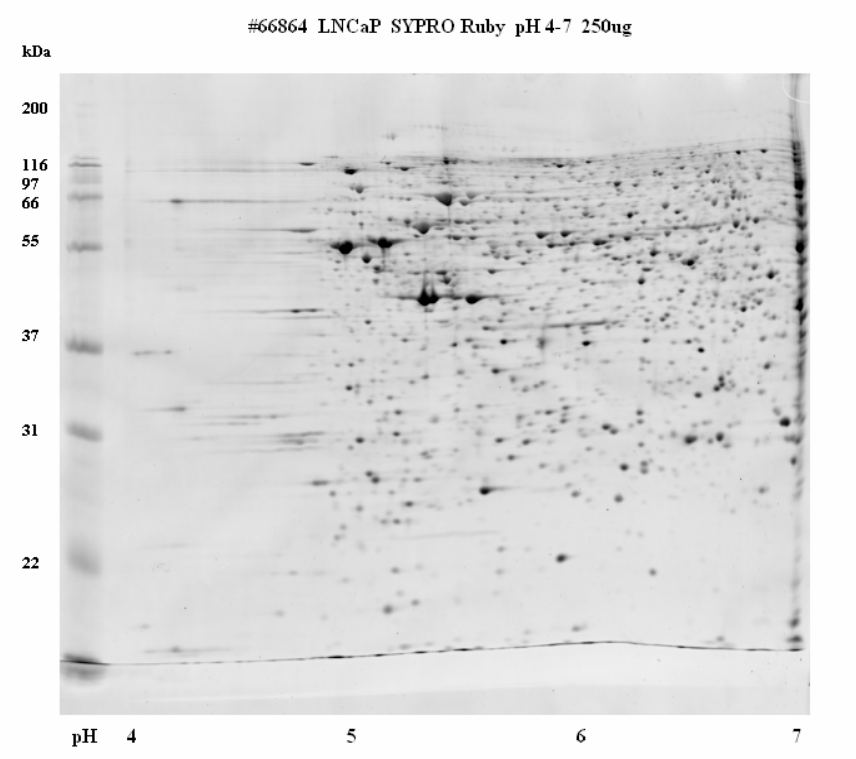

Figure 4-4 2-DE gels of LNCaP proteins detected with multiplexed staining (a) Pro-Q™ Diamond Phosphoprotein staining (b) SYPRO Ruby staining.

4.3.4 Protein Identification

We identified a set of proteins that were detected as intense spots in the Pro-Q™ Diamond-stained gels. For the identification, we selected 16 spots from the gel with pH range of 4-7. These spots are labeled in Figure 4-5. In addition, we selected 14 spots from another Pro-Q™ Diamond stained gel that included pH range 3-10 (Figure 4-6). As discussed above, the spot quality in the pH 3-10 gel was not sufficient for 2-DE-based analysis; however, we used this wide range pH gradient in our in-gel IEF LC-MS/MS phosphoproteomics platform (see Chapter 2). Therefore, we opted to identify proteins from the pH 3-10 gel to allow direct comparison of the data.

For identification, the spots were excised and subjected to in-gel tryptic digestion. The extracted peptides were analyzed by LC-MS/MS and the LC-MS/MS data were used for database searches to identify the proteins. Overall, proteins were identified from all thirty protein spots. The identification was based on the presence of $\geq$2 peptides. Since the spots were taken from a single gel (no pooling), the 100% success rate attested to the sensitivity of the LC-MS/MS system and to the overall power of our protein identification procedure. Protein identification results for the 14 spots from 2-DE gel with pH 3-10 are shown in Table 4-1; results for the16 spots from 2-DE gel with pH 4-7 are shown in Table 4-2. It should be noted that some of the proteins were identified in multiple spots; furthermore, some of the spots contained more than one protein. Both scenarios are frequently encountered in these types of analyses. For example, if several forms of the same protein are present in the mixture, each form will give rise to a different spot. Conversely, different proteins with very similar pI and MW values may co-migrate in 2-DE.

4.3.5. Additional Examination of the Phosphoprotein Panel

Inspection of the Swiss-Prot annotations and survey of the PhosphoSite knowledgebase revealed that most of the proteins identified in our study are known to be phosphorylated. This indicated a high specificity of the Pro-Q™ Diamond stain.

Gene Ontology and Swiss-Prot annotations were inspected to gather information on subcellular location and on protein function. This information is included in Tables 4-1 and 4-2.

We compared the phosphoprotein panel obtained in this study to the panel that was produced with in-gel IEF LC-MS/MS (Chapter 2). Out of the 30 proteins, 3 proteins (Lupus la protein, Stress-induced-phosphoprotein1 and Nucleophosmin) were also found with in-gel IEF LC-MS/MS. These results showed that the two platforms provided complementary data on the LNCaP phosphoproteome.

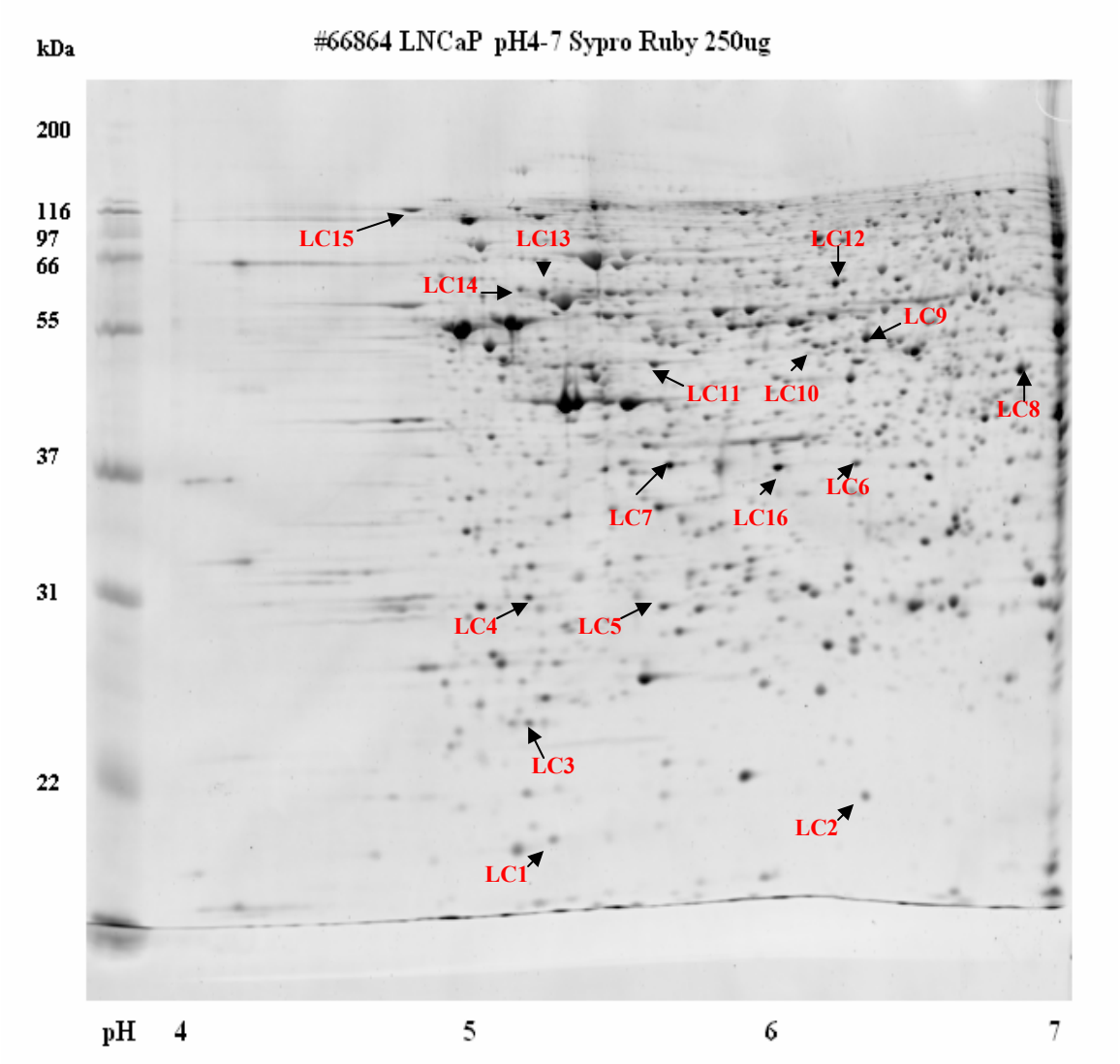

Figure 4-5 16 protein spots selected from 2-DE gel with pH 4-7.

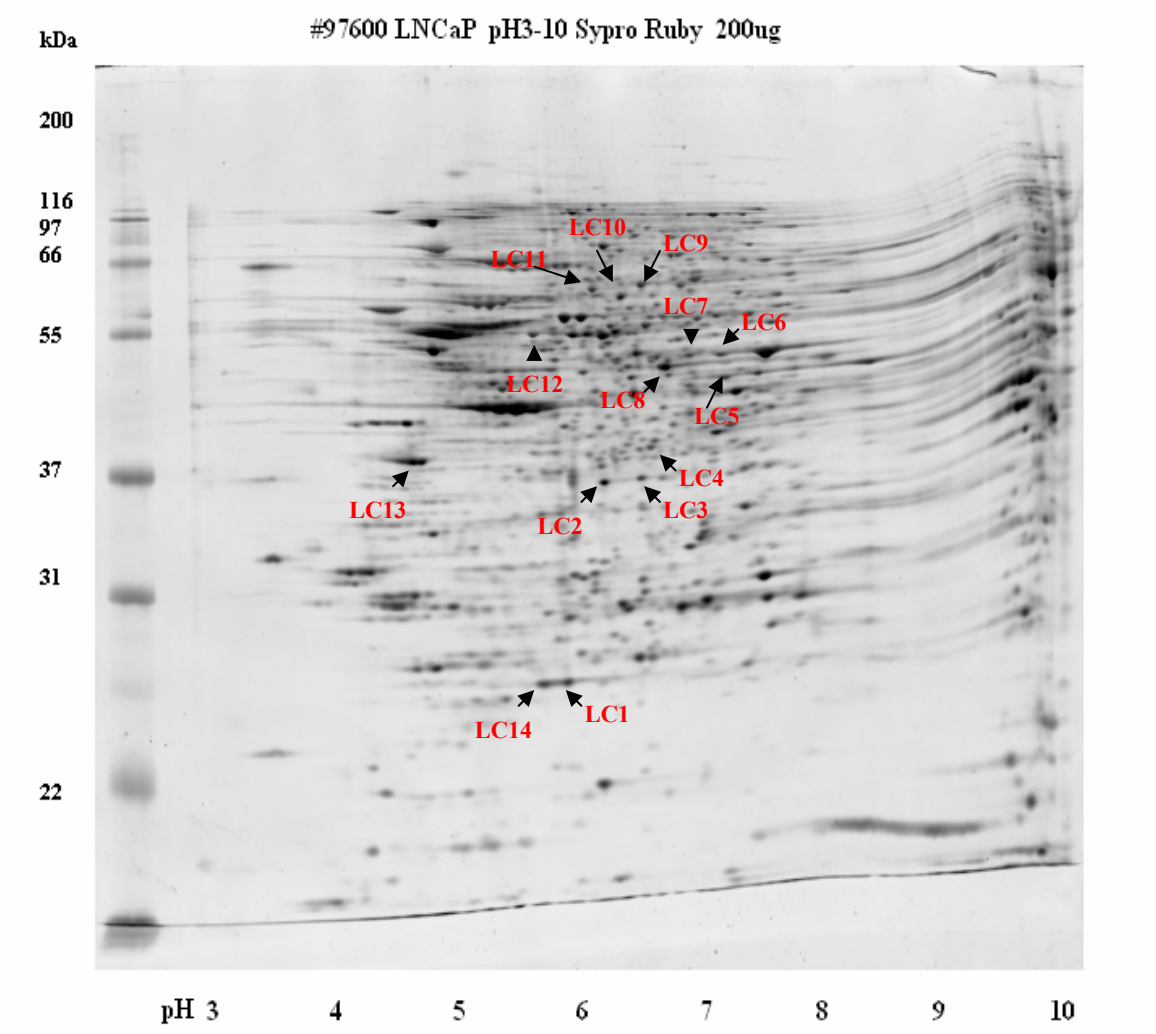

Figure 4-6 14 protein spots selected from 2-DE gel with pH 3-10.

Table 4-1 Protein identification results for Pro-Q™ Diamond-stained spots from pH 3-10 gel.

Spot	Swiss-Prot accession number	Protein name	MW Exp(Theo）	pI Exp(Theo)	Function [a]	Location [a]	Phosphorylated [b]
1	P32119 PRDX2_HUMAN	Peroxiredoxin-2	25.8 (21.9)	5.8 (5.66)	response to oxidative stress | regulation of apoptosis | anti-apoptosis	cytoplasm	Yes
	Q06830 PRDX1_HUMAN	Peroxiredoxin-1	25.8 (22.1)	5.8 (8.27)	cell proliferation | skeletal development	cytoplasm; melanosome	Yes
2	P04083 ANXA1_HUMAN	Annexin A1	42.9 (38.7)	6.3 (6.57)	cell surface receptor linked signal transduction | inflammatory response | keratinocyte differentiation | lipid metabolism | peptide cross-linking | anti-apoptosis | cell motility	nucleus; cytoplasm	Yes
3	P05388 RLA0_HUMAN	60S acidic ribosomal protein P0	42.9(34.3)	6.5 (5.72)	translational elongation | protein biosynthesis | ribosome biogenesis and assembly	cytosolic large ribosomal subunit	Yes
	P07195 LDHB_HUMAN	L-lactate dehydrogenase B chain	42.9 (36.6)	6.5 (5.71)	tricarboxylic acid cycle intermediate metabolism | anaerobic glycolysis	cytoplasm	Yes
4	P37837 TALDO_HUMAN	Transaldolase	46.2 (37.5)	6.6 (6.36)	metabolism | pentose-phosphate shunt | carbohydrate metabolism	cytoplasm	Yes
5	P49411 EFTU_HUMAN	Elongation factor Tu, mitochondrial precursor	55.5 (49.5)	7.2 (7.26)	translational elongation | protein biosynthesis	mitochondrion	Yes

Table 4-1 (continued).

Spot	Swiss-Prot accession number	Protein name	MW Exp(Theo）	pI Exp(Theo)	Function [a]	Location [a]	Phosphorylated [b]
6	P06733 ENOA_HUMAN	Alpha-enolase	58.6 (47.2)	7.2 (7.01)	glycolysis | growth control | hypoxia tolerance | allergic response | transcriptional repressor	cytoplasm; cell membrane nucleus	Yes
	P05455 LA_HUMAN	Lupus La protein	58.6 (46.8)	7.2 (6.68)	transcription from RNA polymerase III promoter | tRNA modification | RNA processing | RNA export from nucleus | histone mRNA metabolism	nucleus	Yes
7	P06733 ENOA_HUMAN	Alpha-enolase	58.6 (47.2)	6.9 (7.01)	glycolysis | growth control | hypoxia tolerance | allergic response | transcriptional repressor	cytoplasm; cell membrane nucleus	Yes
	P05455 LA_HUMAN	Lupus La protein	58.6 (46.8)	6.9 (6.68)	transcription from RNA polymerase III promoter | tRNA modification | RNA processing | RNA export from nucleus | histone mRNA metabolism	nucleus	Yes
8	P26641 EF1G_HUMAN	Elongation factor 1-gamma	57.6 (50.1)	6.6 (6.25)	translational elongation | protein biosynthesis	cytosol	Yes
9	P31948 STIP1_HUMAN	Stress-induced-phosphoprotein 1	70.5 (62.6)	6.5 (6.40)	response to stress	cytoplasm; nucleus	Yes

Table 4-1 (continued).

Spot	Swiss-Prot accession number	Protein name	MW Exp(Theo）	pI Exp(Theo)	Function [a]	Location [a]	Phosphorylated [b]
10	P40227 TCPZ_HUMAN	T-complex protein 1 subunit zeta	67.9 (58.0)	6.3 (6.24)	nucleotide binding | ATP binding | unfolded protein binding |	cytoplasm	Yes
11	P49368 TCPG_HUMAN	T-complex protein 1 subunit gamma	69.2 (60.5)	6.1 (6.10)	nucleotide binding | ATP binding | unfolded protein binding |	cytoplasm	Yes
12	P14923 PLAK_HUMAN	Junction plakoglobin	61.9 (81.6)	5.6 (5.95)	structural molecule activity | cytoskeletal protein binding |	cell junction; cytoplasm; membrane	Yes
	P49368 TCPG_HUMAN	T-complex protein 1 subunit gamma	61.9 (60.5)	5.6 (6.10)	nucleotide binding | ATP binding | unfolded protein binding |	cytoplasm	Yes
13	P06748 NPM_HUMAN	Nucleophosmin	45.3 (32.6)	4.6 (4.64)	Nucleotide binding | the assembly and/or transport of ribosome	nucleus	Yes
14	P32119 PRDX2_HUMAN	Peroxiredoxin-2	25.8 (21.9)	5.7 (5.66)	response to oxidative stress | regulation of apoptosis | anti-apoptosis	cytoplasm	Yes

a. Protein function and sucellular location were obtained based on Gene Ontology and Swiss-Prot annotation.
b. Status of protein phosphorylation was inspected in Swiss-Prot and PhosphoSite.

Table 4-2 Protein identification results for Pro-Q™ Diamond-stained spots from pH 4-7 gel.

Spot	Swiss-Prot accession number	Protein name	MW Exp(Theo)	pI Exp(Theo)	Function [a]	Location [a]	Phosphorylated [b]
1	P53999 TCP4_HUMAN	Activated RNA polymerase II transcriptional coactivator p15	16.7 (14.4)	5.3 (9.6)	single-stranded DNA binding | transcription coactivator activity | DNA binding	nucleus	Yes
2	P23528 COF1_HUMAN	Cofilin-1	18.8 (18.5)	6.5 (8.22)	actin binding | protein binding	nucleus	Yes
3	Q9Y5S9 RBM8A_HUMAN	RNA-binding protein 8A	22.3 (19.9)	5.0 (5.5)	mRNA binding | protein binding | nucleotide binding	cytoplasm; nucleus	Yes
	Q13185 CBX3_HUMAN	Chromobox protein homolog 3	22.3 (20.8)	5.0 (5.23)		nucleus	Yes
4	O43399 TPD54_HUMAN	Tumor protein D54	31.3 (22.2)	5.1 (5.26)	protein binding	unclassified	Yes
	P25788 PSA3_HUMAN	Proteasome subunit alpha type 3	31.3 (28.4)	5.1 (5.19)	threonine endopeptidase activity | protein binding	cytoplasm; nucleus	Yes
5	P04792 HSPB1_HUMAN	Heat-shock protein beta-1	30.4 (22.8)	5.6 (5.98)	protein binding	cytoplasm; nucleus	Yes
	O75489 NDUS3_HUMAN	NADH dehydrogenase [ubiquinone] iron-sulfur protein 3	30.4 (30.2)	5.6 (6.98)	NADH dehydrogenase activity | NADH dehydrogenase (ubiquinone) activity	mitochondrion	Yes

Table 4-2 (continued).

Spot	Swiss-Prot accession number	Protein name	MW Exp(Theo)	pI Exp(Theo)	Function [a]	Location [a]	Phosphorylated [b]
	Q9BTE7 DCNL5_HUMAN	DCN1-like protein 5	30.4 (27.5)	5.6 (5.44)		unclassified	No
6	O00487 PSDE_HUMAN	26S proteasome non-ATPase regulatory subunit 14	43.9 (34.6)	6.2 (6.06)	ubiquitin-dependent protein catabolism	unclassified	Yes
	Q14847 LASP1_HUMAN	LIM and SH3 domain protein 1	43.9 (29.7)	6.2 (6.61)	ion transporter activity | metal ion binding | actin binding | SH3/SH2 adaptor activity | zinc ion binding	cytoplasm	Yes
7	P05388 RLA0_HUMAN	60S acidic ribosomal protein P0	43.9 (34.3)	5.5 (5.72)	structural constituent of ribosome | RNA binding | protein binding	unclassified	Yes
	P06748 NPM_HUMAN	Nucleophosmin	43.9 (32.6)	5.5 (5.0)	Nucleotide binding | the assembly and/or transport of ribosome	nucleus	Yes
8	O75874 IDHC_HUMAN	Isocitrate dehydrogenase [NADP]	56.1 (46.7)	6.9 (6.53)	oxidoreductase activity | isocitrate dehydrogenase (NADP+) activity | oxidoreductase activity, acting on NADH or NADPH, NAD or NADP as acceptor |	cytoplasm	Yes
9	P50395 GDIB_HUMAN	Rab GDP dissociation inhibitor beta	60.5 (50.7)	6.3 (6.11)	Rab GDP-dissociation inhibitor activity | GTPase activator activity	cytoplasm; membrane	Yes
	P31150 GDIA_HUMAN	Rab GDP dissociation inhibitor alpha	60.5 (50.6)	6.3 (5.0)	Rab GDP-dissociation inhibitor activity | GTPase activator activity	cytoplasm	Yes

Table 4-2 (continued).

Spot	Swiss-Prot accession number	Protein name	MW Exp(Theo)	pI Exp(Theo)	Function [a]	Location [a]	Phosphorylated [b]
10	Q99816 TS101_HUMAN	Tumor susceptibility gene 101 protein	59.4 (43.9)	6.1 (6.06)	protein binding | transcription corepressor activity | DNA binding | ubiquitin-protein ligase activity	cytoplasm; membrane	Yes
	O75439 MPPB_HUMAN	Mitochondrial-processing peptidase subunit beta	59.4 (54.4)	6.1 (6.38)	mitochondrial processing peptidase activity | metal ion binding | zinc ion binding	mitochondrion	No
	Q9UQ80 PA2G4_HUMAN	Proliferation-associated protein 2G4	59.4 (43.8)	6.1 (6.13)	methionyl aminopeptidase activity | protein binding | transcription factor activity | hydrolase activity | RNA binding | cobalt ion binding	cytoplasm; nucleus	Yes
11	P31930 UQCR1_HUMAN	Ubiquinol-cytochrome-c reductase complex core protein 1	56.7 (52.6)	5.5 (5.94)	oxidoreductase activity | ubiquinol-cytochrome-c reductase activity	mitochondrion	Yes
	P02647 APOA1_HUMAN	Apolipoprotein A-I precursor	56.7 (30.8)	5.5 (5.56)	lipid binding | high-density lipoprotein binding | protein binding | lipid transporter activity	secreted	No
12	Q16222 UAP1_HUMAN	UDP-N-acetylhexosamine pyrophosphorylase	70.4 (58.8)	6.1 (5.92)	UDP-N-acetylglucosamine diphosphorylase activity | nucleotidyltransferase activity	cytoplasm	No

Table 4-2 (continued).

Spot	Swiss-Prot accession number	Protein name	MW Exp(Theo)	pI Exp(Theo)	Function [a]	Location [a]	Phosphorylated [b]
13	P10809 CH60_HUMAN	60 kDa heat shock protein, mitochondrial precursor	67.8 (61.1)	5.1 (5.7)	protein binding | nucleotide binding | chaperone binding | unfolded protein binding | ATP binding	mitochondrion	Yes
14	P61978 HNRPK_HUNMAN	Heterogeneous nuclear ribonucleoprotein K	69.1 (51.0)	5.0 (5.39)	nucleic acid binding | RNA binding | DNA binding | protein binding	cytoplasm/ nucleus	Yes
15	P45974 UBP5_HUMAN	Ubiquitin carboxyl-terminal hydrolase 5	75.9 (95.8)	4.9 (4.91)	protein binding | zinc ion binding | metal ion binding | cysteine-type endopeptidase activity | ubiquitin-specific protease 5 activity	unclassified	Yes
	P08238 HS90B_HUMAN	Heat shock protein HSP 90-beta	75.9 (83.3)	4.9 (4.97)	nitric-oxide synthase regulator activity | nucleotide binding | TPR domain binding	cytoplasm/ melanosome	Yes
	P07900 HS90A_HUMAN	Heat shock protein HSP 90-alpha	75.9 (84.7)	4.9 (4.94)	nitric-oxide synthase regulator activity | nucleotide binding | protein homodimerization activity | unfolded protein binding | molecular function unknown | ATP binding	cytoplasm/ melanosome	Yes
16	P05388 RLA0_HUMAN	60S acidic ribosomal protein P0	43.9 (34.3)	6.1 (5.72)	structural constituent of ribosome | RNA binding | protein binding	unclassified	Yes

a. Protein function and sucellular location were obtained based on Gene Ontology and Swiss-Prot annotation.
b. Status of protein phosphorylation was inspected in Swiss-Prot and PhosphoSite.

4.4 Discussion

Proteomic technologies enable the study of proteins and their interactions in a systematic manner. Because of the critical role that phosphorylation plays in biological systems, intensive efforts have been centered on the development of improved phosphoproteomic strategies, and many analytical options are available. Before large-scale application of a chosen bioanalytical platform to a new biological system, in a new setting, it is necessary to tailor the chosen strategy to the particular task, and to evaluate its performance. In this study, we applied 2-DE with multiplexed Pro-Q^{TM} Diamond phsopho-specific stain and SYPRO Ruby stain, followed by protein identification of selected spots using LC-MS/MS, to obtain an overview of phosphoproteins in the LNCaP human prostate cancer cell line.

We found that streaks were present in the pH range of 7-9 in our 2-DE gels. It is common that horizontal streaking is present at the basic pH range of 7-9 in a 2-DE gel. The primary reason of streaking is due to the depletion of the reducing agent at the basic end during IEF (Gorg et al., 2000; Olsson et al., 2002). Reducing agent, dithiothreitol (DTT), is a weak acid and therefore charged at a basic pH, which results in the migration of DTT towards the anode during IEF. The depletion of DTT at the cathode leads to oxidation of protein thiol groups and re-formation of inter- and intra- molecular disulfide bridges.

Destreak rehydration solution has been reported to transform the protein thiol groups into a stable disulfide and to protect the disulfide groups from unspecific oxidation (Olsson et al., 2002). We partially reduced streaks and improved the spot patterns on 2-DE gels with pH range of 3-10 by using the Destreak Rehydration solution. However, the major improvement expected was not reached. Another option to address this issue would be to perform two separations with two different strips: pH 4-7 and pH 6-9 (Hoving et al., 2002; Pennington et al., 2004). However, this would mean additional sample and time requirements, plus modification of the experimental procedure. Therefore, we decided to use IPG strips with pH range of 4-7 for subsequent experiments; with this option we can achieve an increased resolution in the pH region where most proteins appear.

Sample application plays an important role in the IPG-based isoelectric focusing. Previous studies showed the best protein recoveries are obtained for all protein loads when samples are applied to IPG strips during rehydration using a single device for both rehydration and IEF. In contrast, the recoveries are poorest when rehydration and IEF are performed in separate devices, and increasing protein loads using separate devices extensively increases sample losses (Zuo and Speicher, 2000).

Compared to Multiphor II that employs separate rehydration and IEF chambers, the IPGphor is an integrated equipment that consists of a high voltage power supply and a solid state cooling system. IPG strips are rehydrated and focused in the same strip holder by automatically programming the initial rehydration step, thus avoiding transfer of the IPG strip from the re-swelling tray to an IEF tray and eliminating further handling of the

strip. In addition, the advantage of the strip holder over the reswelling tray is that proteins that do not enter the IPG gel during rehydration can enter the gel during the focusing step. Zuo and Speicher reported that the application of low voltage during rehydration did not appear to significantly improve overall protein recovery, but it was beneficial for entry of specific proteins (Zuo and Speicher, 2000). In our study, both IEF systems demonstrated a satisfactory protein separation; either one can be applied in further study.

Both Pro-Q^{TM} Diamond stain and SYPRO Ruby stain are fluorescent stains and have similar sensitivity. They can be used subsequently to detect phosphoproteins and total proteins in a single gel. SYPRO Ruby stain has a low background, high resolution and dynamic range, and is easy to manipulate (Lopez et al., 2000). However, Pro-Q^{TM} Diamond staining is affected by the expertise that an investigator has with the technique. The stain and destain time points will affect background and resolution. We found that some of the spots that were present on both images sometimes differed in intensity; and there were a few spots only present on Pro-Q^{TM} Diamond image but not on SYPRO Ruby. This may be due to the specific proteins that are particularly sensitive to one staining but not to the other (Wu et al., 2005). This sequential staining of proteins in a single gel provided parallel determination of protein expression and preliminary characterization of post-translational modifications of proteins in individual spots on 2-DE gels.

In our determination of the protein identities, we considered the possibility of phosphorylation in our database searches; however, no phosphopeptides were retrieved for the identified proteins. This result was expected. In order to maximize the chance of direct detection of the phosphorylated peptide, an IMAC enrichment step must be included at the peptide level (analogously to the method in Chapter 2). This strategy is possible, and has been used to characterize exact phosphorylation sites, e.g. in the human growth hormone (Zhan et al., 2005). However, the strategy requires a much higher protein amount. In our 2-DE survey of LNCaP phosphoproteins, we chose to focus on maximizing the success rate of determination of protein identity, and we used information from published literature to provide supporting evidence for the phosphorylation status of the identified proteins. To gather this information, we used two bioinformatics resources. First, we inspected the Swiss-Prot annotations for each protein. These annotations summarize information on each Swiss-Prot database entry, including post-translational modifications. Second, we used the PhosphoSite knowledgebase to retrieve information on protein phosphorylation. This strategy takes advantage of the publicly available information sources. Instead of using PubMed, we performed our inspection in Swiss-Prot and PhosphoSite annotation because both of them are populated with information derived from published literatures and as complete and up-to-date as possible.

Another characteristic that we addressed for our phosphoprotein panel concerned relevance of the identified proteins to prostate cancer. Because our study was intended as a prelude to future differential expression studies in the context of prostate cancer, it is important to evaluate whether the phosphoproteins that we probed with the chosen bioanalytical strategy bear potential relevance to cancer. We evaluated this aspect by reviewing published literature. A number of identified proteins have been previously

reported to be differentially expressed in prostate cancer cell line, such as Peroxiredoxin-2, Annexin A1, Transaldolase, Nucleophosmin et al. The findings indicated that 2-DE strategy is feasible to study the phosphoprotein differential expression in LNCaP. A number of cancer relevant phosphoproteins identified in the present study was shown in Table 4-3 based on their functions.

Peroxiredoxins (PRDXs) are antioxidant enzymes expressed by most free-living organisms, often in multiple isoforms. Shen et al. demonstrated that prostate cancer cells were more sensitive to hydrogen peroxide or an organic hydroperoxide when PRDX1, 2, or 3 was partially suppressed (Shen and Nathan, 2002). Park et al. reported that PRDX1 acted as a key mediator in stimulating the activation of androgen receptor (AR). The high level of PRDX1 was expressed in the aggressive LN3, C4-2, and C4-2B prostate cancer cell lines derived from LNCaP, which displayed PRDX1 is able to sensitize a ligand-stimulated AR and serve as a new target in the management of prostate cancer (Park et al., 2007). PRDX2 have been reported to significantly up-regulate in highly metastatic prostate cancer cell line 1E8-H cells (Wu et al., 2007). Nevertheless, PRDX 2 and PRDX1 have been found lacking significant change in prostate needle biopsy speciments (Lin et al., 2007).

Annexin I (ANX I) is a promising prostate cancer biomarker identified by 2-DE and mass spectrometry. Studies have confirmed that ANX I was underexpressed in a majority of early stage prostate cancers (Kang et al., 2002; Ornstein and Tyson, 2006). ANX I expression were also decreased in androgen stimulated prostate cancer, androgen-independent prostate cancer and metastatic prostate cancer cell line (Smitherman et al., 2004; Wu et al., 2007). Although reduced expression levels of ANX I protein is a common finding in all stages of prostate cancer, a causative relationship between ANX I dysregulation and prostate cancer development has not yet been established. ANX I may have tumor suppressor functions in prostate cancer. Hsiang et al. reported that ANX I displayed its pro-apoptotic effect through involving in the activation of p38 and JNK, which appeared to shift the balance of signal transduction away from proliferation and toward apoptosis (Hsiang et al., 2006).

The nuclear protein B23, nucleophosmin (NPM), is an RNA-associated nucleolus phosphoprotein reported to be more abundant in malignant and growing cells than in

Table 4-3 Example of cancer relevant phosphorproteins identified in LNCaP.

Functional categories	Protein name
Apoptosis modulated protein	Peroxiredoxin-2, Annexin A1
Molecular chaperones	T-complex protein 1 subunit zeta, T-complex protein 1 subunit gamma, Nucleophosmin
Multifunctional enzyme	Alpha-enolase
Carbohydrate metabolism enzyme	Transaldolase
Stress response protein	Stress-induced-phosphoprotein 1, Peroxiredoxin-2

normal nondividing cells (Subong et al., 1999). Leotoing et al. reported the potential of NPM as a tumor marker for human prostate cancer. They found that NPM was overexpressed in prostate cancer compared to normal adjacent tissues, and could modulate AR functions by promoting assembly of AR-containing regulatory complexes. Thus, the high levels of NPM might alter AR functions in prostate cancer (Leotoing et al., 2008).

Two T-complex protein 1 (TCP) isoforms, T-complex protein 1 subunit zeta and T-complex protein 1 subunit gamma, were identified in the study. TCP's function is the binding of nucleotide, ATP and/or unfolded protein (Li et al., 1994). It involves the process of protein folding. Up-regulated TCP was found in highly metastatic prostate cancer cell line 1E8-H (Wu et al., 2007) and the cell line M12 (Liu et al., 2003). The high levels of TCP may reflect the alter AR functions in prostate cancer.

Enolase (ENOA or ENO1) is a multifunctional protein. Besides its role in basic metabolism, Enolase serves as a surface receptor for the binding of plasminogen (Andronicos et al., 1997; Lopez-Alemany et al., 2003). ENO1 has been implicated in numerous diseases, including cancers (Kanemoto et al., 2006; Katayama et al., 2006). Plow et al. have found that ENO1 involved tumor cell invasion and metastasis via initiating the activity of plasminogen activity on the cell surface (Plow et al., 1995). ENO1 has been reported highly expressed in tumor cells (Altenberg et al., 2006; Altenberg and Greulich, 2004). Pancholi demonstrated that the increased expression of ENO1 both at DNA level and at the protein level directly correlated the progression of tumors (Pancholi, 2001).

Transaldolase plays an important role in central metabolism. It is involved in oxidative stress and apoptosis, in multiple sclerosis, and in cancer (Samland and Sprenger, 2009). Transaldolase deficiency has been found to associate with liver cirrhosis in a new inborn (Verhoeven et al., 2001). Recently, Basta et al. demonstrated that genetic polymorphisms in Transaldolase were associated with squamous cell carcinoma of the head and neck (Basta et al., 2008).

4.5 Conclusions

In this study, we demonstrated the feasibility of using 2-DE with phsopho-specific staining and tandem mass spectrometry to investigate the phosphoproteins in the LNCaP human prostate cancer cell line. This methodology complements the other platforms that we used for prostate cancer phosphoproteomics research; it will be of particular value for future comparative studies of phosphoproteins in various physiological states. The phosphoproteins probed with the chosen analytical platform are known to be relevant to prostate cancer.

CHAPTER 5. PROTEOMIC ANALYSIS OF PROTEIN ALTERATIONS IN MOUSE PROSTATE CANCER TISSUE INDUCED BY BICALUTAMIDE/EMBELIN COMBINATION TREATMENT

5.1 Introduction

Prostate cancer is a major health problem in Western countries. It is the most common cancer and the third leading cause of male cancer death (Jemal et al., 2006). During the initial stage of prostate cancer, the tumor is dependent on androgen for growth (Isaacs, 1994; Miller et al., 2003). For those without metastatic disease, androgen withdrawal/androgen ablation is the most effective therapy. Early treatment with the non-steroidal antiandrogen bicalutamide significantly improves survival in patients with localized disease (Blackledge, 1996). However, the therapeutic success is temporary. Prolonged treatment results in the mutation of androgen receptor, which converts bicalutamide from an antagonist into an agonist, leading to drug resistance. Hence, in the majority of cases, the disease reappears within a few years as an androgen-independent form. There are no effective treatments for androgen-independent prostate cancer. Recently, clinical trials showed that docetaxel, in combination with estramustine could improve the survival of patients with metastatic, androgen-independent prostate cancer, as compared with mitoxantrone and prednisone (Petrylak et al., 2004). The combination of an androgen receptor antagonist (bicalutamide) and XIAP inhibitor (embelin) has been reported to cause regression of prostate tumors (Danquah et al., 2009). That result indicates that a treatment strategy with novel drug combination, delivered in a more effective way, is a promising way to treat androgen-independent prostate cancer.

X-Linked inhibitor of apoptosis protein (XIAP) is a promising molecular target for the design of new anticancer drugs aiming at promoting apoptosis in cancer cells. Embelin is a novel cell-permeable inhibitor of XIAP, which binds to the XIAP BIR3 domain to which Smac and caspase-9 bind. Embelin selectively inhibits cell growth, induces apoptosis, and activates caspase-9 in prostate cancer cells (Chen et al., 2006; Nikolovska-Coleska et al., 2004).

Bicalutamide is a non-steroidal antiandrogen with affinity for androgen receptor. The low solubility/dissolution rate of bicalutamide is still a key factor limiting its oral bioavailability (Le et al., 2009). The use of amphiphilic copolymer micelles as effective carriers for tumor-drug delivery has drawn more attention in the last few years (Blanco et al., 2007; Ishihara et al., 2008; Lee et al., 2006; Yang et al., 2008; Yasugi et al., 1999). The amphiphilic copolymer can form a micelle structure with a hydrophobic inner core and a hydrophilic outer shell in aqueous environments. The core-shell structure makes it easy to incorporate hydrophobic drugs and results in an increased drug concentration in body fluids.

Proteomics is a powerful approach which enables to survey a large number of proteins simultaneously. It has been extensively applied to examine protein expression in various types of human cancers and in the context of resistance to several drugs

(Cicchillitti et al., 2009; Di Michele et al., 2009; Ou et al., 2008; Rondepierre et al., 2009). Thus, proteomics offers excellent possibilities for determining proteins involved in the complex pharmacological effects of anticancer agents, and to provide an insight into the molecular mechanism of anticancer agents in prostate cancer.

The aim of this study was to identify proteins that are differentially expressed in control and bicalutamide/embelin treated mouse prostate tumor specimens. This study will aid in the revealing of molecular mechanism of bicalutamide/embelin combination therapy. A comparative proteomic approach based on 2-DE coupled with mass spectrometry (LC-MS/MS) was applied to mouse prostate tumors with bicalutamide/embelin combination treatment. An outline of the 2-DE based strategy is shown in Figure 5-1.

5.2 Materials and Methods

5.2.1 In Vivo Studies

This was a collaboration study with the group of Dr. Ram I. Mahato from the Department of Pharmaceutical Sciences, UTHSC. Dr. Mahato's group performed the in vivo studies. Briefly, all animal experiments were performed in accordance with NIH animal use guidelines and protocol approved by the Animal Care and Use Committee at the University of Tennessee Health Science Center. Xenograft flank tumors were induced in 8-weeks-old male BALB/C nude mice purchased from The Jackson Laboratory (Bar Harbor, ME) by subcutaneous injection of three million LNCaP cells suspended in 1:1 media and matrigel. When tumors reached approximately 150mm^3, mice were randomized into three groups of five mice, minimizing weight and tumor size difference. Each group was treated with intratumoral injection of saline, sonicated bicalutamide suspension or bicalutamide entrapped in PEG-PLA micelles (20 mg/kg) three times a week. Mice were treated for three weeks. After three weeks, treatments with bicalutamide were terminated, and treatment with embelin was commenced and continued for two weeks. Mice were sacrificed after bicalutamide /embelin combination treatment. Tumors were surgically removed, frozen in liquid nitrogen and stored at -80 ºC.

5.2.2 Protein Preparation

Proteins were extracted from 200 mg of crushed tumor tissues by using 2 mL of Trizol reagent (Invitrogen, Carlsbad, CA) with 5 µL of protease inhibitor cocktail (Sigma, St. Louis, MO) according the manufacturer's instruction (details described in Chapter 2). For 2-DE separations, protein pellet was dissolved with a rehydration buffer that contained urea (7 M), thiourea (2 M), CHAPS detergent (2% w/v), IPG buffer 3-10 (2% v/v), DTT (0.3%, w/v) and a trace amount of Bromophenol Blue dye. The protein concentration of the extracts was determined by Bradford assay (GE Healthcare, Piscataway, NJ).

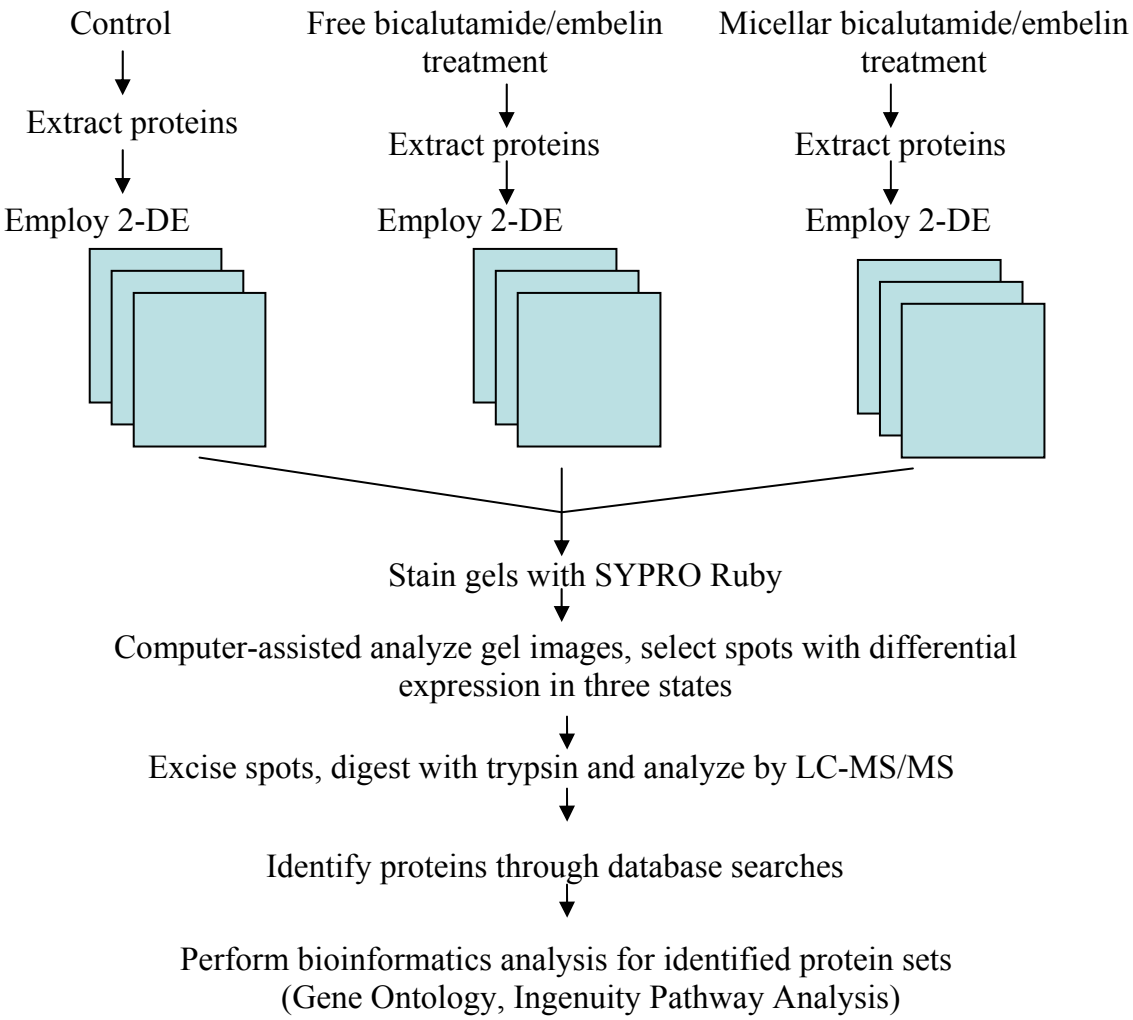

Figure 5-1 Outline of 2-DE based comparative proteomics platform.

Proteins were extracted from mouse prostate tumor tissues, and then separated by 2-DE. Protein spots on 2-DE gels were visualized by staining with SYPRO Ruby and gel images were analyzed with computer-assisted gel image analysis software. The spots found to be statistically significant ($p<0.05$) were excised, digested with trypsin, and analyzed by LC-MS/MS. Proteins were identified through database searches, and bioinformatics analyses were performed for final identified proteins.

5.2.3 2-DE

For the first dimension, protein samples (250 µg of protein in 350 µL of rehydration buffer) were loaded on pre-cast, 18-cm long immobilized pH gradient (IPG) stripes (pH 4-7) (GE Healthcare, Piscataway, NJ). Isoelectric focusing was performed with the IPGphor apparatus (GE Healthcare, Piscataway, NJ) according to manufacturer's instructions (details described in Chapter 4). The isoelectric focusing was performed under the following voltage program: 30 V (fixed for 16 hours); 200 V (fixed for 1 hour); 500 V (fixed for 1 hour); 1000 V (fixed for 1 hour); 8000 V (gradient over 30 minutes); 8000 V (fixed for 4 hours).

IPG strips were then incubated for 15 minutes in an equilibration buffer (50 mM Tris/HCl pH 8.8, 6 M urea, 30% glycerol, 2% SDS) with 2.0% DTT and then in equilibration buffer with 2.5% iodoacetamide for an additional 15 minutes. The second dimensional separations were carried out on 12% SDS- PAGE gels at 15 °C with 200 V constant voltage applied for about 8 hours in a Protean Plus Dodeca Cell (Bio-Rad, Hercules, CA), until the bromophenol blue dye front reached the end of the gels.

5.2.4 Gel Staining and Imaging

Gels were stained with SYPRO Ruby protein stain (Molecular Probes, Eugene, OR). The image was acquired on an FX Fluorescence Laser Scanner (Bio-Rad, Hercules, CA) with 488 nm laser excitation and 555 nm band pass emission filter for SYPRO Ruby stain. The images were displayed with Adobe Photoshop 5.0 LE software, and saved as .TIFF files for future analysis. The gel images were analyzed using two independent and commercially available image analysis software packages, PDQuest version 7.1.0 (Bio-Rad, Hercules, CA) and Progenesis SameSpots version 3.3 (Nonlinear USA Inc, Durham, NC).

Using PDQuest software package, gel images were performed with the "Automated spot detection and matching wizard" tool. After grouping the gels within a specified match set (control, free bicalutamide, or micelle bicalutamide) and spot detection, the software automatically generated a "match set master gel" image, which is a synthetic gel image made up of all the spots that were detected within the match set by PDQuest. Each spots was assigned a unique identified number across all the gels by the software to permit comparison between groups. The density of each spot was normalized to the total density in the gel image and was expressed in parts per million (PPM).

The same 2-DE gel images were also analyzed using Progenesis SameSpot software package. Briefly, gel images were grouped into three categories (control, free bicalutamide and micelle bicalutamide) for comparative analysis. A reference gel was selected from all gel set to serve as a universal index for spot numbering prior to matching analysis. Spot detection, filtering, and background subtraction were automatically performed by the software using its unique nonparametric algorithm and

applied to all the subgels in the particular group. Spots that did not match were manually warped and updated at the individual and reference gels.

Following confirmation of appropriate spot detection, matching and normalization, spot statistics were reviewed. ANOVA test was performed to quantify differential expression of spots among three groups. The spots found to be statistically significant ($p < 0.05$) were isolated for further investigation.

5.2.5 In-gel Tryptic Digestion

Spots of interest were excised from the gels. The gel pieces were extensively washed with 50 mM ammonium bicarbonate in 50% ACN for three times, and then dried under vacuum for 30 minutes. The dried gel pieces were rehydrated in a trypsin solution that contained 16.7 ng/μL of trypsin (Promega, Madison, WI) in 50 mM ammonium bicarbonate (pH 8). The digestion solution was incubated at 37 °C overnight. The resulting peptides were extracted with 0.01% TFA/ 60% ACN three times. All supernatants were combined and dried with a vacuum centrifuge. Prior to LC-MS/MS analysis, the digestions were reconstituted with 15 μL of 2.5% FA and desalted with ZipTipC18 (Millipore, Billerica, MA), using the procedure provided by the manufacturer (details described in Chapter 2). The peptides retained on the ZipTipC18 column were eluted with 1.5 μL of 50% ACN/0.1% FA and diluted with 2.5 μL of 0.5% FA.

5.2.6 LC-MS/MS Analysis

LC-MS/MS experiments were performed on a LTQ linear ion trap mass spectrometer (Thermo Electron, San Jose, CA). Peptide mixtures were loaded onto a fused-silica microcapillary column (15 cm length, 75 μm ID; New Objective, MA) packed in-house with C18 resin (Michrom Bioresources, Inc., Auburn, CA) and were separated using a 30-min gradient from 0% to 90% solvent B (0.05% FA/90% MeOH). Solvent A was 0.05% FA/ 2% MeOH. The LTQ mass spectrometer was operated in positive ion mode and data-dependent acquisition was performed. In brief, a scan cycle was initiated with a full scan of wide mass accuracy (m/z 400-2000) in the ion trap, which was followed by MS/MS scans in the linear ion trap on the 7 most abundant precursor ions with dynamic exclusion of previously selected ions.

5.2.7 Database Searches

The MS/MS data were used to search the Swiss-Prot database (subset of mouse proteins) with the TurboSEQUEST search engine (Thermo Electron) that is part of Bioworks version 3.2 (Thermo Electron, San Jose, CA). Searches were performed with the following parameters: full-trypsin specificity, dynamic modifications of oxidized methionine, and static modifications of cystein by carbamidomethylation. All peptide matches were filtered by XCorr larger than 3.00, 2.50, and 3.50 used for singly, doubly

and triply charged ions, respectively; peptide probability less than 1.0E-3; different peptides; and only the top matches were considered. The peptides retrieved by the searches were validated by manual inspection of the MS/MS data. Criteria used for manual validation included: the spectrum must be of good quality with fragment ion clearly above the baseline noise; sequential members of the b- or y-series were observable in the mass spectra.

5.2.8 Bioinformatics and Network Analysis

The proteins identified as being differentially expressed among treatment groups were compared to all annotated proteins using gene ontology (GO). This analysis was carried out using the Web-accessible program (http://bioinfo.vanderbilt.edu/webgestalt/). Proteins were classified with GO annotation at level 4 according to the molecular function that proteins normally carry out, the biological process that proteins are involved in, and the molecular component (subcellular location) of the proteins.

Identified proteins were also analyzed by Ingenuity Pathway Analysis (IPA; Ingenuity System, Mountain View, CA). IPA is a powerful curated database and analysis system for understanding how proteins work together to affect cellular changes. It builds hypothetical networks from identified proteins and other proteins, based on a regularly updated database which consists of millions of individual relationships between genes, proteins and other biological molecules, based on information compiled from published literature. It enables to pinpoint the biological mechanisms, pathways and functions most relevant to the experimental datasets or genes of interest. IPA generates a score for each possible network, which is calculated according to the fit of that network to the input proteins. The higher score indicates a lower possibility that the input proteins occur in a given network by random chance. Networks with scores of 10 or higher have a high confidence of not being generated by random chance alone.

5.3 Results

The aim of the study was to identify proteins whose differential expression relates to bicalutamide/embelin treatment in mouse prostate tumors and to reveal the molecular mechanism of prostate tumor regression induced by the combination of anticancer drugs.

We employed a 2-DE based approach coupled with mass spectrometry for protein identification. For gaining insight into the mechanisms of drug action, the ability to reproducibly measure the protein expression levels across the experiments is a key challenge. Hence, it is important to realize the contribution of technical variations in measuring quantitative differences. In the present study, technical variation was determined by employing three gels per sample.

Correlation analysis was used to determine the reproducibility of the spot volume within and between a set of gels (Zhan and Desiderio, 2003). The coefficient of

correlation of the normalized spot volum across three replicates per sample ranged from 0.89 to 0.98. The coefficient of variation (CV) is a quantitative index, describing the amount of the variation of volume among the matched-spots. The average CV was calculated from all spots matched on gels within an experiment set. The average CV for replicate 2-DE gels of all three sample types was 20.7±15.8%, which was comparable with the reported results 35.7±20.8% for Dodeca system by Zhan and Desiderio (Zhan and Desiderio, 2003). This result was also consistent with several other published reports on the degree of variation attributed to 2-DE in the hands of the users (Molloy et al., 2003; Saldanha et al., 2008).

In order to describe in the detail of the difference in the amount of variation of the normalized volume of the matched-spots, the proportion of the matched-spots among the different CV ranges of the normalized volume is described in Table 5-1. The majority of spots was matched within the low CV range (70% of matched spots with CV< 25 %, 90% of matched spots with CV< 50%). Small proportion of spots was matched in high CV range. The results was also similar to the previous reported results based on the Dodeca system of the study (77% of matched spots with CV< 50%) (Zhan and Desiderio, 2003). The degree of technical variation due to the 2-DE process established an important baseline for uncoupling biological variation from technical variation.

5.3.1 Profile of Mouse Prostate Tumor Specimens

To study the molecular mechanisms of bicalutamide/embelin combination therapy in prostate cancer, three groups of mouse prostate tumor specimens were used in this work. Prostate tumors from mice treated with saline were used as controls. The controls were compared to two combination treatments: free-bicalutamide/embelin and PEG-PLA bicalutamide micelles/embelin.

5.3.2 Proteomic Patterns of Bicalutamide/embelin Combination Treatment

2-DE was used to separate protein mixture and to locate differentially expressed proteins among control, free-bicalutamide/embelin and PEG-PLA bicalutamide micelles/embelin treated mouse prostate cancer tissues. Patterns from three different mouse specimens were analyzed and three replicate 2-DE gels per specimen were used. Figure 5-2 shows a representative 2-DE gel of proteins for mouse prostate tumor obtained by using an IPG 4-7 strips and a 12% SDS-PAGE gel. 2-DE patterns from the three treatment groups were obtained and analyzed with two different image analysis software packages (Bio-Rad PDQuest Version 7.1 software and Progenesis Samespots v3.3 software). Overall, more than 600 spots were resolved in the 2-DE gels and the protein expression profiles among the three groups were similar; a set of 33 protein spots exhibiting significantly differential expression by ANOVA test ($p < 0.05$) are located (Figure 5-2) and analyzed by nano-LC-MS/MS.

Table 5-1 Proportion of the matched spots among the different ranges of the CV of the normalized volume.

CV of normalized volume (%)	Control		Free bicalutamide		Micelle bicalutamide	
	Number of matched spots	Proportion (%)	Number of matched spots	Proportion (%)	Number of matched spots	Proportion (%)
<10	93	20.9	220	49.4	95	21.3
10-25	175	39.4	189	42.5	192	43.2
25-50	123	27.6	30	6.7	107	24.1
50-75	41	9.2	6	1.4	45	10.1
75-100	10	2.2	0	0	5	1.1
>100	3	0.7	0	0	1	0.2
Total	445	100	445	100	445	100

(a)

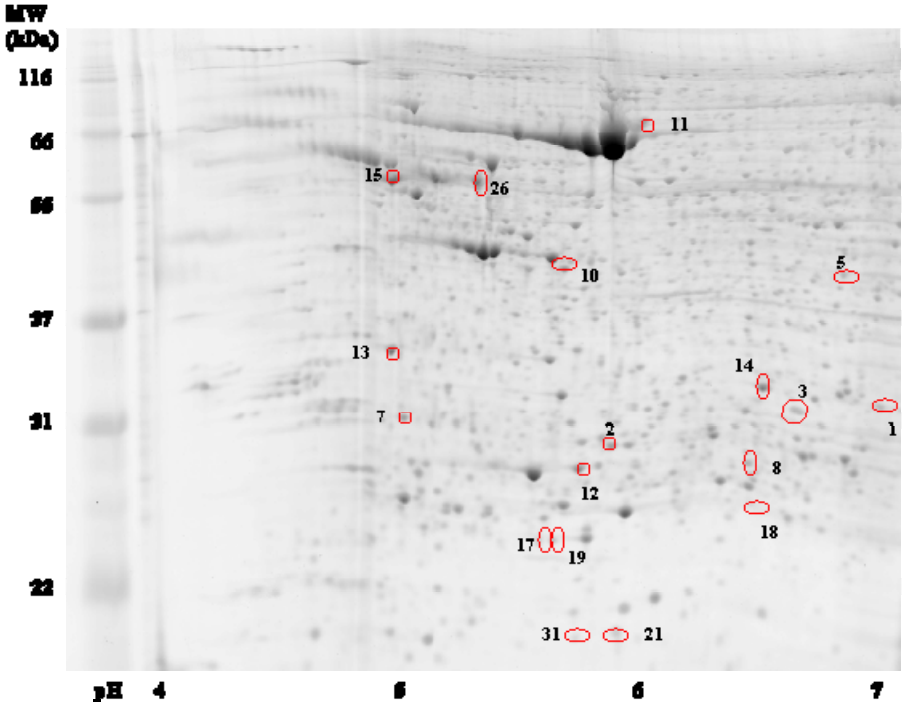

(b)

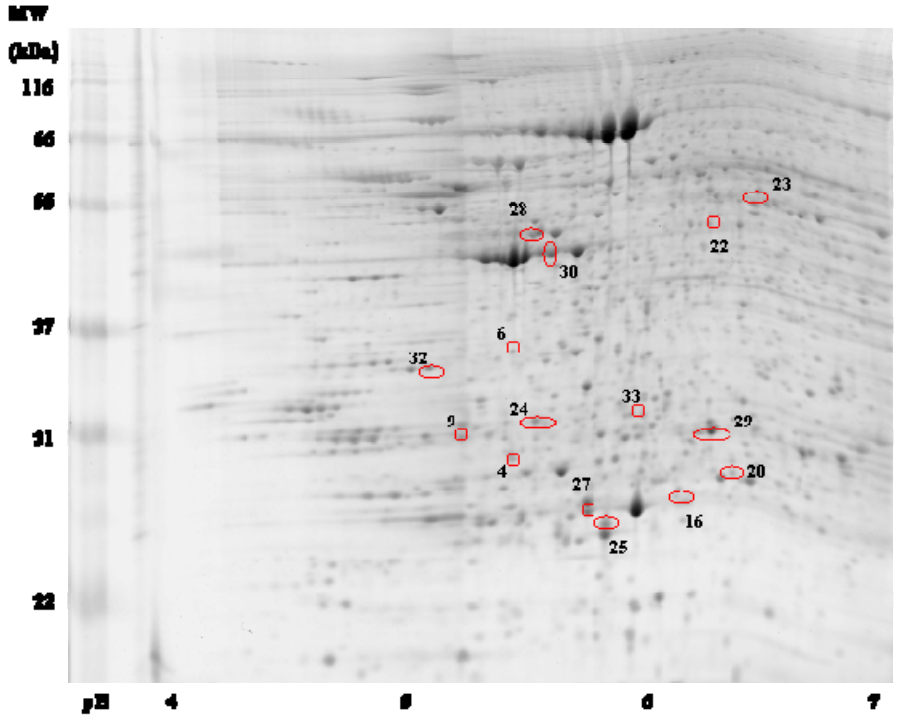

Figure 5-2 Representative 2-DE gels of mouse prostate cancer proteome (a) Control (b) Free bicalutamide/embelin treatment.

33 protein spots marked on the maps were differentially expressed ($p<0.05$) in the comparisons between control and treated samples; these proteins were identified by MS.

5.3.3 Identification of Candidate Protein Spots from 2-DE Gels

The selected protein spots from SYPRO Ruby stained gels were excised and subjected to in-gel tryptic digestion. The extracted peptides were analyzed by LC-MS/MS to generate sequence-diagnostic MS/MS data. Out of the 33 differentially expressed protein spots, 30 protein spots were successfully identified, corresponding to 38 different proteins (Table 5-2 and Table 5-3). Overall, 19 proteins were identified in protein spots which were significantly up-regulated in bicalutamide/embelin treated specimens compared with control tumor specimens, such as peroxiredoxin-1, Glutathione peroxidase 1, enolase, and peroxiredoxin-2. Moreover, 19 proteins were identified from down-regulated protein spots in bicalutamide/embelin treated specimens compared with control tumor specimens, including plasminogen, annexin 5 and pre-mRNA-splicing factor SPF27. The summary score, protein coverage, and change fold for spots are shown in Table 5-2 and Table 5-3. It should be noted that some of the proteins were identified in multiple spots; furthermore, some of the spots contained more than one protein.

5.3.4 Classification of Identified Proteins

To interpret the results systematically, identified proteins were classified with GO annotation of the level 4 according to molecular function that proteins normally carry out, biological process that proteins are involved in, and molecular component (subcellular location).

The majority of the identified proteins were associated with metabolic processes (cellular metabolism 51.5%, primary metabolism 51.5%, and macromolecular metabolism 33.3%). In addition to metabolic process, the biological processes which the differentially expressed proteins were involved in included localization (51.5%), transport (33.3%), response to stress (12.1%) and apoptosis (12.1%) (Figure 5-3). Based on GO annotations, identified proteins were involved in various molecular functions (Figure 5-4), such as binding (cation binding 21%, metal ion binding 24%, RNA binding 9%), oxidoreductase activity (9%), and peptidase activity (9%). The classification is redundant since a protein can be classified into more than one category.

To gain further insight in the differentially expressed protein results, separation was made into up-regulated and down-regulated identified proteins (Table 5-4). According to GO annotations, most identified proteins in both groups involved “binding” in molecular function. But proteins in the up-regulated group were associated with “oxidoreductase activity”, while very few proteins belonged to that category in the down-regulated group. In the category of biological process, both up- and down-regulated proteins were classified into “cellular physiological process” and “metabolism”.

Table 5-2 List of identified protein spots down-regulated by bicalutamide/embelin treatment.

Spot	Accession number	Protein name	Theor MW (kDa)/pI	Peptide number	Coverage (%)	Fold change (Progenesis)	P-value (Progenesis)	Fold change (PDQuest)	P-value (PDQuest)
1	P60909 RS3_MOUSE	40 S ribosomal protein S3	26.7/9.6	1	5.3	1.9	< 0.05	2	< 0.01
2	P01843 LAC1_MOUSE	Ig lambd-1 chain C region	11.6/5.8	3	46.7	1.6	< 0.05	3.2	< 0.01
3	P63159 HMGB1_MOUSE	High mobility group protein B1	24.9/5.6	4	19.1	2.6	< 0.01	Out of range	< 0.01
4	Q9D287 BCAS2_MOUSE	Pre-mRNA-splicing factor SPF27	26.1/5.4	2	11.1	1.3	> 0.05	1.2	< 0.01
5	Q61990 PCBP2_MOUSE	Poly(rC)-binding protein 2	38.2/6.3	9	33.1	1.4	> 0.05	1.4	< 0.01
	P61161 ARP2_MOUSE	Actin-related protein 2	44.8/6.2	6	19.8				
6	Q64674 SPEE_MOUSE	Spermidine synthase	33.9/5.3	5	29.1	1.6	< 0.05	1.1	< 0.01
7	Q99PT1 GDIR_MOUSE	Rho GDP-dissociation inhibitor 1	23.4/5.1	7	38.2	1.3	< 0.05	Out of range	< 0.01
8	P23506 PIMT_MOUSE	Protein-L-isoaspartate(D-aspartate) O-methyltransferase	24.6/7.1	5	26.4	1.8	< 0.05	2.6	< 0.01

Table 5-2 (continued).

Spot	Accession number	Protein name	Theor MW (kDa)/pI	Peptide number	Coverage (%)	Fold change (Progenesis)	P-value (Progenesis)	Fold change (PDQuest)	P-value (PDQuest)
9	Q99PT1 GDIR_MOUSE	Rho GDP-dissociation inhibitor 1	23.4/5.1	6	49.5	1.3	> 0.05	Out of range	< 0.01
	P34022 RANG_MOUSE	Ran-specific GTPase-activating protein	23.6/5.1	3	15.3				
10	Q8K0E8 FIBB_MOUSE	Fibrinogen beta chain precusor	54.8/6.6	15	33	2.5	< 0.01	Out of range	< 0.01
11	P20918 PLMN_MOUSE	Plasminogen precursor	90.8/6.2	18	31	2.3	< 0.05	5.6	< 0.01
	P07724 ALBU_MOUSE	Serum albumin precursor	68.7/5.7	23	49				
	Q91X72 HEMO_MOUSE	Hemopexin precursor	51.3/7.9	10	33.9				
12	Q00623 APOA1_MOUSE	Apolipoprotein A-I precursor	30.6/5.6	5	17.4	1.9	> 0.05	2.4	< 0.01
13	P48036 ANXA5_MOUSE	Annexin A5	35.8/4.8	7	22.3	1.7	< 0.01	Out of range	< 0.01
14	Q9R1P4 PSA1_MOUSE	Proteasome subunit alpha type-1	29.5/6.0	3	17.49	1.5	< 0.05	5.6	< 0.01
15	Q4R4X8 TBB4_MOUSE	Tubulin beta-4 chain	49.6/4.7	23	59.7	2.1	< 0.01	Out of range	< 0.01

Protein name, accession number and theoretical pI and MW are from Swiss-Prot database (release 20090311)
Out of range indicates spot was absent in replicate gels or was below the detection parameters set for the software package.

Table 5-3 List of identified protein spots up-regulated by bicalutamide/embelin treatment.

Spot	Accession number	Protein name	Theor MW/pI	Peptide number	Coverage (%)	Fold change (Progenesis)	P-value (Progenesis)	Fold change (PDQuest)	P-value (PDQuest)
16	P29391 FRIL1_MOUSE	Ferritin light chain1	20.8/5.6	6	47.0	1.3	> 0.05	Out of range	< 0.01
17	P09528 FRIH_MOUSE	Ferritin heavy chain	21.1/5.5	6	40.1	1.8	< 0.01	2.4	< 0.01
18	P35700 PRDX1_MOUSE	Peroxiredoxin-1	22.2/8.2	5	25.1	1.3	> 0.05	Out of range	< 0.01
19	P46638 RB11B_MOUSE	Ras-related protein Rab-11B	24.5/5.6	2	10.6	2.4	< 0.01	2.2	< 0.01
20	P11352 GPX1_MOUSE	Glutathione peroxidase 1	22.2/6.7	8	55.7	2	> 0.05	Out of range	< 0.01
	Q99LX0 PARK7_MOUSE	Protein DJ-1	20.0/6.3	1	7.90				
21	P29391 FRIL1_MOUSE	Ferritin light chain1	20.8/5.6	5	34.4	1.4	> 0.05	1.8	< 0.01
22	P50247 SAHH_MOUSE	Adenosylhomo-cysteinase	47.7/6.1	10	25.7	1.6	< 0.01	Out of range	< 0.01
23	Q9D8N0 EF1G_MOUSE	Elongation factor 1-gamma	50.1/6.3	10	30.4	1.9	< 0.05	Out of range	< 0.01
	P17182 ENOA_MOUSE	Alpha-enolase	47.1/6.3	3	8.80				
24	P01837 KAC_MOUSE	Ig kappa chain C region	11.8/5.2	2	26.4	ND	NA	Out of range	< 0.01
25	P09528 FRIH_MOUSE	Ferritin heavy chain	21.1/5.5	7	40.66	2.2	< 0.01	2.1	< 0.01

Table 5-3 (continued).

Spot	Accession number	Protein name	Theor MW/pI	Peptide number	Coverage (%)	Fold change (Progenesis)	P-value (Progenesis)	Fold change (PDQuest)	P-value (PDQuest)
26	P21614 VTDB_MOUSE	Vitamin D-binding protein precuosor	53.6/5.4	21	55.5	1.3	> 0.05	4.1	< 0.01
	Q9D554 SF3A3_MOUSE	Splicing factor 3A subunit 3	58.8/5.2	5	14.2				
27	P29391 FRIL1_MOUSE	Ferritin light chain 1	20.8/5.6	8	55.2	2.2	< 0.01	Out of range	< 0.01
	Q61171 PRDX2_MOUSE	Peroxiredoxin-2	21.8/5.2	1	5.50				
28	P60842 IF2A1_MOUSE	Eukaryotic initiation factor 4A-I	46.2/5.3	24	48.5	1.1	> 0.05	Out of range	< 0.01
	P10630 IF4A2_MOUSE	Eukaryotic initiation factor 4A-II	46.4/5.3	2	8.3				
	Q5RFJ1 ILF2_MOUSE	Interleukin enhancer-binding factor 2	43.1/5.2	5	21.0				
29	Q3U0B3 DHR11_MOUSE	Dehydrogenase/ reductase SDP family member 11 precursor	28.3/5.9	2	11.5	1.4	> 0.05	1.8	< 0.01
	Q9QUM9 PSA6_MOUSE	Proteasome subunit alpha type-6	27.4/6.3	5	22.8				
30	Q04447 KCRB_MOUSE	Creatine kinase B-type	42.7/5.4	11	35.7	1.7	> 0.05	2.6	< 0.01

Protein name, accession number and theoretical pI and MW are from Swiss-Prot database (release 20090311)
Out of range indicates spot was absent in replicate gels or was below the detection parameters set for the software package. ND means spots not been detected.

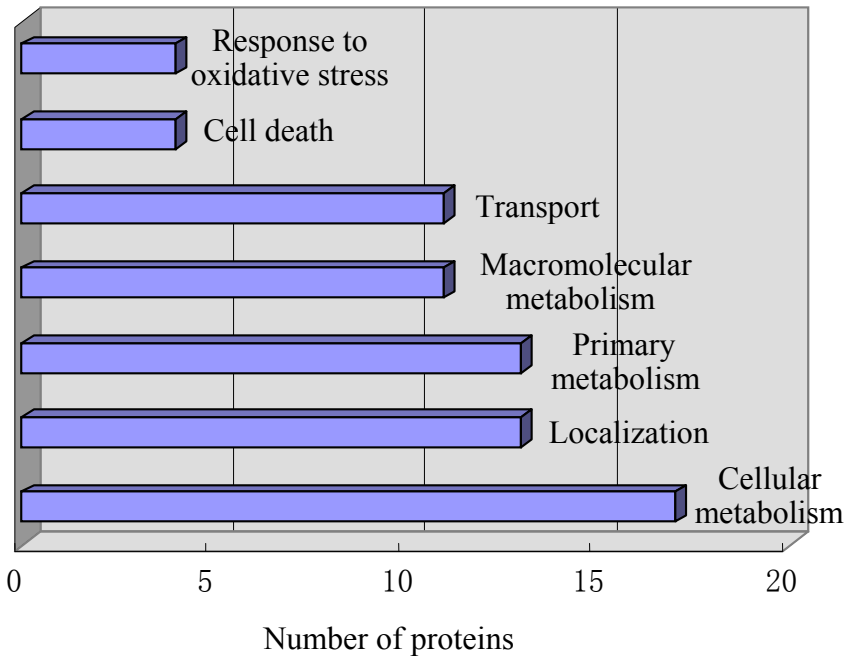

Figure 5-3 Classification of biological processes of identified proteins according to GO annotations.

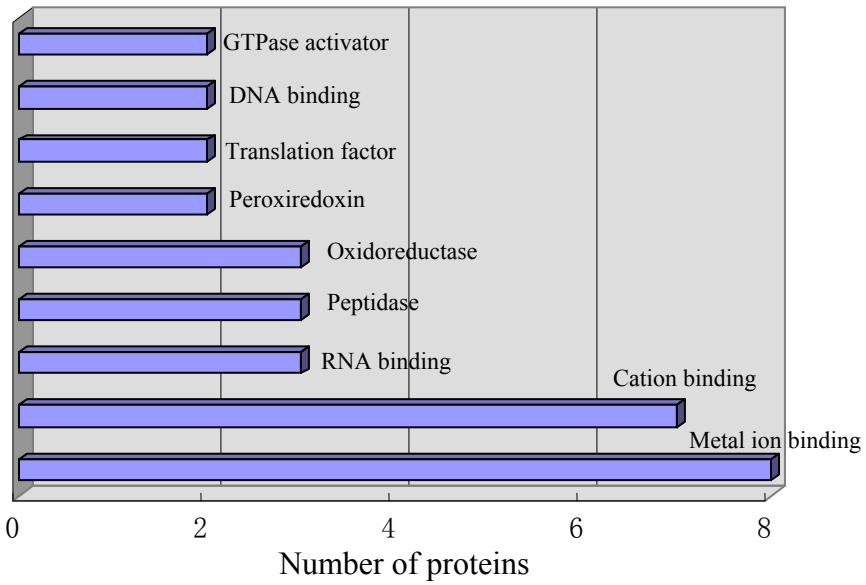

Figure 5-4 Classification of molecular functions of identified proteins according to GO annotations.

Table 5-4 Protein categories by Gene Ontology.

Molecular function	Ratio	Biological process	Ratio
Up-regulated proteins			
Protein binding	2/8	Cellular physiological process	14/24
Ion binding	3/8	Metabolism	10/18
Nucleic binding	3/6	Localization	6/13
Hydrolase activity	2/5	Response to stress	4/8
Oxidoreductase activity	5/5	death	2/4
Down-regulated proteins			
Protein binding	6/8	Cellular physiological process	10/24
Ion binding	5/8	Metabolism	8/18
Nucleic binding	3/6	Localization	7/13
Hydrolase activity	3/5	Response to stress	4/8
Oxidoreductase activity	0/5	death	2/4

5.3.5 Pathway Analysis of Proteins Modulated in Bicalutamide/embelin Treatment

To reveal the potential molecular mechanism of bicalutamide/embelin combination treatment in prostate cancer, pathway analysis was carried out on the dataset of identified proteins through the use of Ingenuity Pathway Analysis software. The most significant interaction networks associated with identified proteins were determined by using published interactions between genes, proteins and other biological molecules. Three high ranking networks were identified: (a) Small molecule biochemistry, tissue morphology; (b) RNA post-transcriptional modification, gene expression, RNA trafficking; (c) Behavior, cancer and carbohydrate metabolism (Table 5-5). Canonical pathways associated with altered proteins included acute phase response signaling, and metabolism. Figure 5-5 is the highest scored cluster of small molecule biochemistry. The score for the depicted network was 32, which indicated the possibility of matching the indicated proteins by a random chance was 10^{-32}.

5.4 Discussion

In the present work, a comparative proteomic study using 2-DE and mass spectrometry was performed and led to the identification of a set of differentially expressed proteins associated with bicalutamide/embelin treatment in mouse prostate tumors. This was the pilot study that examined the effects of bicalutamide/embelin combination treatment on prostate cancer. In this phase, we established a comparative proteomic methodology tailored to mouse tumor tissue, and obtained preliminary results on the effects of this new therapeutic strategy.

There are many proteomic technologies currently available, but 2-DE remains the most accessible platform to separate thousands of proteins simultaneously from multiple

Table 5-5 Representative networks associated with identified proteins by IPA software.

ID	Molecules in network	Score	Focus molecules	Top functions
1	**ALB, APOA1**, CDCP1, CLEC7A, **DHRS11, ENO1, FTH1, FTL,** FTMT, **GPX1, HMGB1 (includes EG:25459),** Ho, **HPX, IGKC**, IL1, IL1F5, IL1F6, IL1F8, IL1F9, KRT9, KRT16, LSP1, MIRN198 (includes EG:406975), NFkB (complex), **PCMT1,** PELI1, **PLG, PRDX1, PRDX2,** PRDX4, SETX, SRXN1, Tcf 1/3/4, TRPC4AP, UMOD	32	14	Small molecule biochemistry, tissue morphology, hair and skin development and function
2	**ACTR2, AHCY,** AHCYL2, **ANXA5, ARHGDIA,** CCDC44, CD44, CDC42, COMMD9, **EEF1G, EIF4A1, EIF4A2**, EPB41, ERLIN1, FAM62A, FTSJ1, **GC,** GOLIM4, HAL, HNF4A, MRP63, MRPL49, MRTO4, NUDT11, PABPC1, PAIP1, **PCBP2, PSMA1, PSMA6, RAB11B,** SCYL3, **SF3A3,** SLC2A4, TRAF6, TUT1	29	13	RNA post-transcriptional modification, gene expression, RNA trafficking
3	ALDH7A1, **BCAS2,** beta-estradiol, C1QTNF6, C21ORF126, **CKB,** DSCR3, ESR1, FAM105B, **FGB,** GHSR, GREB1, HCG 401283, HSF2BP, HSPA13, IL1B, KRT13, KRTAP10-6, **LOC389842,** LOC391282, LOC391322, MED7 (includes EG:66213), MMP2, NCRNA00162, ODF3B, **PARK7,** PNRC2 (includes EG:55629), PRDM2, SAPS2, SMS, **SRM,** UCRC, UMODL1, ZMAT5, ZNF398	11	6	Cellular growth and proliferation, cell-to-cell signaling and interaction, cancer

Genes in 2-DE analysis are shown with bold.

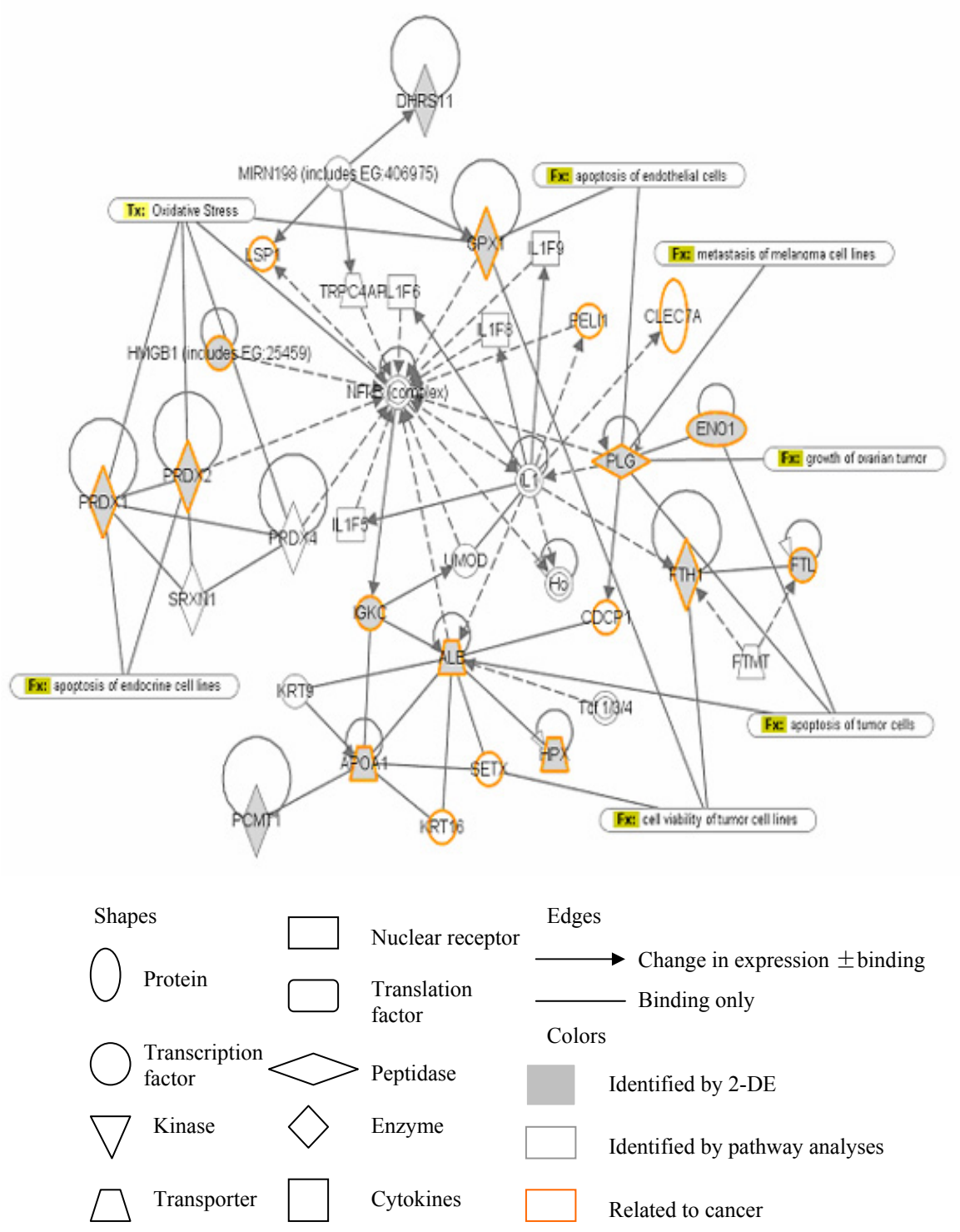

Figure 5-5 Network of small molecule biochemistry associated with modulated proteins identified in bicalutamide/embelin treatment in mouse prostate tumor tissue.

samples for subsequent protein identification and quantitative comparison (Li et al., 2009; Rondepierre et al., 2009; Tilton et al., 2007; Wu et al., 2007). To ensure high confidence in the identification of differentially expressed protein spots, two independent image analysis software packages, PDQUEST and Progenesis Samespots, were applied to analyze all 2-DE gel images in the study. In total, 33 spots were identified as having statistically significant differential expression, between both software packages. However, only 17 of these were identified using both programs, which is most likely due to the variations in algorithms between the software packages, such as background subtraction or noise correction (Saldanha et al., 2008). The scenarios have been reported by a number of previous publications about the use of independent image analysis packages for the analysis of a gel data set (Byrne et al., 2009; Rosengren et al., 2003; Saldanha et al., 2008).

Analysis of the gel images using PDQuest demanded extensive manual inspection of all gels and subsequent alignment of overlapping gel spots to the master gel image. Parameters were needed to be set up for the examination of the match for the individual gel images to the master gel. Whereas, the Progenesis analysis was entirely automated with minimal manual intervention. Although labor intensive, manual 2-DE image analysis allowed greater accuracy in definition of spot boundaries, especially for low abundance or poorly resolved spots (Saldanha et al., 2008). Apart from confident identification of differentially expressed spots, the application of two independent software programs could increase the coverage of candidate protein spots which might be missed because of different detection cutoff criteria used in the software packages.

In the present study, LC-MS/MS was used for protein spots identification. Protein identification was based on matching of peptide sequence data. Out of the 33 differentially expressed protein spots, 30 spots were identified with adequate coverage. Among the identified protein spots, we found some of the spots contained more than one protein with very similar pI and MW values. Furthermore, some of the proteins were identified in multiple spots, which may be due to post-translational modifications. Both scenarios are frequently encountered in these types of analyses. Multiple proteins in the same spot would require an independent confirmation through application of biochemical technologies (such as western blotting) to unambiguously pinpoint the exact differentially expressed protein.

Thirty eight differentially expressed proteins induced by bicalutamide/embellin treatment were identified by using 2-DE followed with MS. Both GO analysis and IPA indicated that metabolism and stress response were the two major biological processes associated with differentially expressed proteins in bicalutamide/embellin treatment. Small molecular biochemistry was the pathway in which most of identified proteins were involved. Some of the identified proteins have previously been reported to be modulated in bicalutamide-treated prostate cancer cell lines, supporting the findings of our study (Rowland et al., 2007).

The largest group of identified proteins belonged to the functional class of metabolism. The identified proteins and enzymes, such as Apolipoprotein A-I precursor,

Vitamin D-binding protein precursor, Dehydrogenase/reductase SDP family member 11, Proteasome subunit alpha type-6 and Proteasome subunit alpha type-1, were involved in different metabolic pathways. Enolase is a glycolytic enzyme expressed on the surface of eukaryotic cells and also serves as a surface receptor for the binding of plasminogen. Alpha enolase (ENO1) has been implicated in numerous diseases including cancers (Kanemoto et al., 2006; Katayama et al., 2006) and was highly expressed in tumor cells (Altenberg et al., 2006; Altenberg and Greulich, 2004). The role of ENO1 in tumor cell invasion and metastasis may be explained by initiating the activity of plasminogen activity on the cell surface, which implicates various physiological and pathological events such as wound healing, tissue modeling, embryogenesis and the cell spreading (Plow et al., 1995). Up-regulation of alpha-enolase may contribute to an increased metabolic capacity, but not to increased plasminogen activation in our study.

Apart from metabolism, another major group of proteins modulated by the combination treatment were proteins involved in stress response. Proteins in this group are mainly associated with oxidative stress. All proteins identified in this group were up-regulated in treated tissue, including peroxiredoxin 1 (PRDX1), peroxiredoxin 2 (PRDX2), glutathione peroxidase 1 (GPX1), protein DJ-1 (PARK7), and Dehydrogenase/reductase SDR family member 11 (DHR11).

Reactive oxygen species (ROS) are oxygen-containing free radicals, including superoxide radical ($O_2^{\cdot -}$), hydroxyl radical ($^{\cdot}OH$), hydrogen peroxide (H_2O_2) and reactive nitrogen species nitric oxide (NO) and peroxynitrite radical ($ONOO^{\cdot}$). These species can be generated either through endogenous sources (such as the mitochondrial respiratory chain, the cytochrome P450 metabolic pathway, the inflammatory response etc.), or from external sources (such as chlorinated compounds, metal ions and radiation) (Apel and Hirt, 2004). ROS, at normal physiological concentrations, play important roles in a variety of cellular processes (Muller et al., 2007; Stadtman, 1992).

Oxidative stress occurs through disturbance in the balance between ROS formation and the efficiency of antioxidant processes, which means the net amount of ROS exceeds the antioxidant capacity. Oxidative stress has been linked to a wide range of diseases including Parkinson's disease (Fang et al., 2007), Asthma (Larsen et al., 2006) and cancer (Visconti and Grieco, 2009). A high level of ROS in cancer cells may lead to a variety of biological responses, such as increased proliferation rate, induction of DNA mutations and genetic instability, and resistance to some drugs in anticancer therapy. To date, it is unclear if oxidative stress is the trigger of the disease, or if it is a consequence of the disease and causes the disease symptoms. Recently, Cohen et al.(Cohen et al., 2008) studied the dynamics and variability of the protein response of human cancer cells to a chemotherapy drug, camptothecin. All cells showed rapid translocation of proteins specific to the drug target, and slower nuclear localization changes including the oxidative stress response pathway. This indicated that the anticancer drug treatment led to the modulation of oxidative stress.

It has been reported that patients with prostate cancer or other pathological processes, such as chronic prostatitis or atrophic prostatitis, presented a decreased

antioxidant power and an increase of lipidic peroxidation (Lopez Laur et al., 2008). GPX is one of primary antioxidant enzymes; it reduces peroxides to their corresponding hydroxylated compounds using glutathione as a hydrogen donor. A recent study showed that the levels of antioxidant enzymes such Superoxide dismutase (SOD) and GPX in prostate cancer subjects were lower than in subjects with benign prostate hyperplasia and control subjects (Aydin et al., 2006). Overexpression of GPX3 in prostate cancer cell lines induced the suppression of colony formation and anchorage-independent growth of PC3, LNCaP, and Du145 cells (Yu et al., 2007b). Peroxiredoxins (PRDXs) are antioxidant enzymes expressed by most free-living organisms, often in multiple isoforms. Prostate cancer cells were shown to be more sensitive to hydrogen peroxide or an organic hydroperoxide when PRDX1, 2, or 3 was partially suppressed (Shen and Nathan, 2002). In the present study, overexpression of GPX, PRDX1 and PRDX2 indicated that administering bicalutamide/embelin perhaps shifts the redox balance within the tumor milieu, ultimately resulting in tumor suppression.

Protein DJ-1, also known as PARK7, is a multifunctional protein related to male fertility, identified as a hydroperoxide-responsive protein, and responsible for Parkinson's disease. Overexpression of DJ-1 has been associated with multiple cancers, including prostate cancer. It is known that DJ-1 is up-regulated by both androgen and antiandrogen treatment and that this increase is due to DJ-1 and androgen receptor protein stability (Pitkanen-Arsiola et al., 2006). It has also been shown that modulation of DJ-1 expression regulated AR transcriptional activity and may be involved in the development of androgen independence (Tillman et al., 2007). In our study, bicalutamide, as an antiandrogen in the combination treatment, resulted in overexpression of DJ-1 in mouse prostate tumors.

Another subgroup of differentially expressed proteins is comprised by proteins that are related to cancer cell metastasis. Annexin A5 is a calcium-dependent phospholipid binding protein, which is commonly used as a probe in Annexin A5 affinity assay to detect cell death. It was reported that down-regulated Annexin A5 reduced migration and invasion capacity of HaCaT cells which was even stronger in the oral carcinoma (Wehder et al., 2009). High mobility group protein B1 (HMGB1) is known to increase expression in carcinomas and exhibit association with proliferation and metastasis in many tumor types (Suzuki et al., 2009). Breast cancer amplified sequence 2 (BCAS2) was initially identified as a gene that was overexpressed and amplified in some breast cancer cell lines (Qi et al., 2005). In our study, expression levels of these proteins were down-regulated by bicalutamide/embelin combination treatment, indicating the decrease of cancer cell metastasis potential.

Several proteins involved in protein biosynthesis and modification were modulated by the combination treatment. Translation initiation factors (IF2A1, IF4A2) and elongation factor (EF1G) were up-regulated. Furthermore, 40S ribosomal protein (RS3), protein-L-isoaspartate(D-aspartate) O-methyltransferase (PIMT) and spermidine synthase (SPEE) were down-regulated.

In conclusion, bicalutamide/embelin treatment modulated molecular functions of

metabolism and biosynthesis, and in particular increased the expression levels of antioxidants to reduce oxidative stress.

5.5 Conclusions

The present study was the first comparative proteomics examination of the effects of bicalutamide/embelin combination treatment on prostate tumors. Protein alterations of mouse prostate tumors induced by bicalutamide/embelin treatment have been studied using 2-DE and mass spectrometry. This analytical strategy involved total protein separation with 2-DE and protein identification by using nanoLC-MS/MS. Differentially expressed proteins were further investigated by bioinformatics tools (GO and IPA) to reveal the associations with important biological functions and processes. The major functions were related to cancer, inflammatory disease, connective tissue disorders, and skeletal and muscular disorders. The molecular functions of differentially expressed protein were associated with metabolism and stress response.

CHAPTER 6. SUMMARY

Advances in technology and understanding of systems biology have provided tremendous strides towards improvement in modern human medicine. Recently, extensive efforts have been involved in the application of various proteomics technologies to the study of prostate cancer to obtain new mechanistic knowledge and to discover novel biomarkers. The desired outcomes of the efforts are markers that will aid in early detection and prognosis of prostate cancer, in monitoring of therapeutic response, and determining best course of therapy for cancer patients to improve clinical outcomes. Despite all these considerable efforts, it remains a challenge to perform a comprehensive proteome analysis.

In the current dissertation, I focused on the development and application of multiple mass spectrometry-based bioanalytical platforms for phosphoproteomic characterization in cell culture and clinical specimens of prostate cancer; and on application of optimized methods to analysis of differential protein expression to reveal molecular mechanism of drug action in mouse model of prostate cancer.

6.1 Discussion of Selected Analytical Aspects

In combination with IEF separation and phosphopeptide enrichment, in-gel IEF LC-MS/MS strategy yielded a significantly expanded phosphoprotein panel. This panel of the LNCaP phosphoproteins was 3.6-fold larger than the panel obtained in our previous work, which attests to the power of the chosen analytical methodology. The expanded phosphoproteome map obtained in this study will serve as a foundation for future quantitative studies of the effects of pharmaceuticals on the LNCaP prostate cancer cells; for this purpose, in-gel IEF LC-MS/MS will be combined with stable-isotope labeling such as stable isotope labeling with amino acids in cell culture (SILAC) (Mann, 2006). Furthermore, additional improvements of the in-gel IEF LC-MS/MS methodology will further enhance the coverage of the LNCaP phosphoproteome.

2-DE was one of the main separation methods applied in our studies. We applied 2-DE based platforms to investigation of phosphoproteins in the LNCaP prostate cancer cells, and to obtain protein profiling in mouse prostate tumor tissue treated by anticancer drugs. As an improvement, 2D-DIGE can be integrated into the platform for future continuation of this line of research. 2D-DIGE incorporates labeling of different protein populations with fluorescent molecules (CyDyes) prior to separation by 2-DE. Up to three different protein samples can be covalently labeled with fluorescent dyes and be separated by 2-DE in a single gel. The technique significantly reduces the inter-gel variability encountered with traditional 2-DE platforms (Alban et al., 2003; Minden et al., 2009).

Phosphorylation site assignment is one of challenges for site-specific identification in phosphoproteomics. In our mass spectrometry analyses, CID is the ion

activation/dissociation method for fragmentation of the peptide backbone and production of ions for sequence analysis and identification of phosphorylation sites. However, CID process often leads to elimination of the molecule of phosphoric acid from peptide ions containing phosphorylated serine and threonine residues; this predominant dissociation pathway results in lack of sequence information in MS/MS spectra. Assignment of phosphorylation sites, especially for peptides containing multiple phosphorylation sites, becomes a challenge. Recently, alternative dissociation methods, such as ETD(Chi et al., 2007; Molina et al., 2007), have been introduced as promising alternatives that provide more comprehensive backbone fragment ion series without loss of water, phosphate groups or phosphoric acid.

In our previous studies, protein function and subcellular location were manually classified based on Swiss-Prot annotations. In large-scale proteome studies, manual annotation strategy is subjective and also labor-intensive. Gene ontology (GO) is a collection of controlled vocabularies describing the biology of a gene product in any organism andit is commonly used to analyze results from high-throughput studies (Khatri and Draghici, 2005; Rhee et al., 2008). GO provides researchers with a broad overview of predominant activities of a specific group of proteins and assists in understanding of large-scale complex biological changes (Dimmer et al., 2008). GO analysis is broadly used in the proteomics community. To interpret our results systematically and to share our results with the research community, GO analysis was adopted in our studies to classify identified proteins according to molecular function, biological process, and molecular component (subcellular location).

Another bioinformatics resource newly applied in our research is the Ingenuity Pathway Analysis. IPA is a powerful curated database and analysis system, which can build hypothetical networks of physical and functional relationships between genes, proteins, and chemicals based on Ingenuity knowledge base. It can help to understand how proteins work together to effect cellular changes (Hoorn et al., 2005; Raponi et al., 2004). Ingenuity helped us to identify the biological mechanisms, pathways and functions most relevant to our experimental datasets of interest.

6.2 Summary

6.2.1 Characterization of the Phosphoproteome in Prostate Cancer

Our research aimed towards description of the phosphoproteome in prostate cancer focused on the LNCaP human prostate cancer cell line, and on human prostate cancer tissue.

For the LNCaP prostate cancer cell line, we applied a combination of analytical platforms: (1) a novel in-gel IEF LC-MS/MS analytical platform; (2) a 2-DE based platform combined with phospho-specific staining.

The in-gel IEF LC-MS/MS analytical methodology used in the study included separation of the LNCaP proteins by in-gel isoelectric focusing; digestion of the proteins with trypsin; enrichment of the digests for phosphopeptides with IMAC; analysis of the enriched digests by LC-MS/MS; and identification of the phosphorylated peptides/proteins through searches of the Swiss-Prot protein sequence database. With in-gel IEF based analytical platform, we have characterized over 600 different phosphorylation sites in 296 phosphoproteins in the LNCaP prostate cancer cell line. This panel of the LNCaP phosphoproteins was 3-fold larger than the panel obtained in our previous work (Giorgianni et al., 2007), and is the largest phosphoprotein panel in prostate cancer reported to date. The phosphoproteins identified in this study belonged to various locations within the cell and were involved in various processes including cell differentiation, transcription regulation, and intercellular signal transduction. The expanded phosphoproteome map obtained in this study was of a satisfactory size to serve as a foundation for future quantitative studies of the effects of pharmaceuticals on the LNCaP prostate cancer cells.

We also developed a 2-DE based platform, in combination with multiplexed staining and LC-MS/MS, for the identification of LNCaP phosphoproteins. In this study, we applied 2-DE as separation technique, Pro-Q^{TM} Diamond stain as phosphoprotein detection method, LC-MS/MS and database searches for protein identification to investigate the phosphoproteins in the LNCaP prostate cancer cell line. Proteins identified from spots of interest were shown to be highly relevant to prostate cancer. We demonstrated the feasibility of using 2-DE with phospho-specific stain and mass spectrometry to investigate the phosphoproteins in the LNCaP cell line. This methodology complements the in-gel IEF LC-MS/MS platform that we used for phosphoproteomics study; it will be of particular value for future comparative studies of phosphoproteins in various physiological states.

For prostate cancer tissue, a gel-free approach was applied to analyze five prostate cancer tissue specimens to obtain phosphoproteomic signatures of prostate cancer for biomarker discovery. Proteins were extracted with Trizol reagent, and then in-solution digested with trypsin. Phosphopeptides were enriched with IMAC, and the enriched digests were analzyed by LC-MS/MS with identification through searches of the Swiss-Prot protein sequence database. The panels obtained for prostate cancer tissue contain 15-24 phosphoproteins. Some of the characterized phosphoproteins were present in all five specimens; in addition, each specimen also produced a unique set of phosphoproteins. The findings provided a direct glimpse into the phosphoprotein machinery operating within the human prostate cancer tissue. This pilot study focused on a small set of specimens. The phosphoprotein panels that were obtained contained a number of proteins that were unique to a particular specimen. Analyses of a larger group of specimens will provide further knowledge on the phosphoprotein signatures to build the foundation for differential phosphoprotein profiling of cancer vs. control tissue for biomarker discovery.

6.2.2 Comparative Proteomics Study of Drug Effects in Prostate Cancer

We carried out the first comparative proteomics study of the effects of bicalutamide/embelin combination treatment on prostate tumors by characterizing the alterations in protein expression that were induced upon treatment of mice bearing prostate tumors with anticancer combination therapy.

A comparative proteomic strategy based on 2-DE coupled with LC-MS/MS was applied to analysis of mouse prostate tumor tissue. Proteins from the mouse prostate tumors were extracted with Trizol, and the protein mixtures were separated by 2-DE. Differences in the protein profiles for the different treatment groups were evaluated by computer-assisted analysis of SYPRO Ruby stained 2-DE gels. LC-MS/MS and database searches were used to identify differentially expressed proteins. Pathway analysis was carried out on the dataset of identified proteins with the Ingenuity bioinformatics tool. Out of the 33 differentially expressed protein spots, 30 protein spots were identified and grouped into various functional classes. The major protein categories were metabolism (52%), stress response (12%), protein biosynthesis (13%) and apoptosis (11%), suggesting that alterations in these processes may be involved in the mechanism of drug action. Proteins associated with oxidative stress were up-regulated, which indicated that treatment with bicalutamide/embelin may affect the redox balance within the prostate tumor, and this effect may contribute to tumor suppression.

Future plans for continuation of this study include incorporation of DIGE into the analytical methodology, examination of a larger group so that biological variability can be taken into account, evaluation of the proteomes at different points during the treatment course, etc. Ultimately, this research will bring new insights into the molecular mechanism of anticancer combination therapy.

In conclusion, in the research presented in this dissertation, multiple MS-based bioanalytical platforms were applied successfully to study the phosphoproteome and proteome in prostate cancer. The disease-related proteomic information obtained in my research will contribute to our understanding of the pathogenesis, and it will bring improvements in the diagnosis and treatment of prostate cancer.

LIST OF REFERENCES

2008, Screening for prostate cancer: U.S. Preventive Services Task Force recommendation statement: Ann.Intern.Med., v. 149, p. 185-191.

Alban, A, S O David, L Bjorkesten, C Andersson, E Sloge, S Lewis, I Currie, 2003, A novel experimental design for comparative two-dimensional gel analysis: two-dimensional difference gel electrophoresis incorporating a pooled internal standard: Proteomics., v. 3, p. 36-44.

Albuquerque, C P, M B Smolka, S H Payne, V Bafna, J Eng, H Zhou, 2008, A multidimensional chromatography technology for in-depth phosphoproteome analysis: Mol.Cell Proteomics., v. 7, p. 1389-1396.

Altenberg, B, C Gemuend, K O Greulich, 2006, Ubiquitous cancer genes: multipurpose molecules for protein micro-arrays: Proteomics., v. 6, p. 67-71.

Altenberg, B, K O Greulich, 2004, Genes of glycolysis are ubiquitously overexpressed in 24 cancer classes: Genomics, v. 84, p. 1014-1020.

Anai, S, S Goodison, K Shiverick, K Iczkowski, M Tanaka, C J Rosser, 2006, Combination of PTEN gene therapy and radiation inhibits the growth of human prostate cancer xenografts: Hum.Gene Ther., v. 17, p. 975-984.

Anderson, N L, N G Anderson, 1998, Proteome and proteomics: new technologies, new concepts, and new words: Electrophoresis, v. 19, p. 1853-1861.

Andronicos, N M, M Ranson, J Bognacki, M S Baker, 1997, The human ENO1 gene product (recombinant human alpha-enolase) displays characteristics required for a plasminogen binding protein: Biochim.Biophys.Acta, v. 1337, p. 27-39.

Apel, K, H Hirt, 2004, Reactive oxygen species: metabolism, oxidative stress, and signal transduction: Annu.Rev.Plant Biol., v. 55, p. 373-399.

Ashman, K, V E Lopez, 2009, Phosphoproteomics and cancer research: Clin.Transl.Oncol., v. 11, p. 356-362.

Aydin, A, Z Arsova-Sarafinovska, A Sayal, A Eken, O Erdem, K Erten, Y Ozgok, A Dimovski, 2006, Oxidative stress and antioxidant status in non-metastatic prostate cancer and benign prostatic hyperplasia: Clin.Biochem., v. 39, p. 176-179.

Ballif, B A, G R Carey, S R Sunyaev, S P Gygi, 2008, Large-scale identification and evolution indexing of tyrosine phosphorylation sites from murine brain: J.Proteome.Res., v. 7, p. 311-318.

Bandyopadhyay, S, S K Pai, S Hirota, S Hosobe, T Tsukada, K Miura, Y Takano, K Saito, T Commes, D Piquemal, M Watabe, S Gross, Y Wang, J Huggenvik, K Watabe, 2004, PTEN up-regulates the tumor metastasis suppressor gene Drg-1 in prostate and breast cancer: Cancer Res., v. 64, p. 7655-7660.

Basta, P V, J T Bensen, C K Tse, C M Perou, P F Sullivan, A F Olshan, 2008, Genetic variation in Transaldolase 1 and risk of squamous cell carcinoma of the head and neck: Cancer Detect.Prev., v. 32, p. 200-208.

Bedolla, R, T J Prihoda, J I Kreisberg, S N Malik, N K Krishnegowda, D A Troyer, P M Ghosh, 2007, Determining risk of biochemical recurrence in prostate cancer by immunohistochemical detection of PTEN expression and Akt activation: Clin.Cancer Res., v. 13, p. 3860-3867.

Benzeno, S, F Lu, M Guo, O Barbash, F Zhang, J G Herman, P S Klein, A Rustgi, J A Diehl, 2006, Identification of mutations that disrupt phosphorylation-dependent nuclear export of cyclin D1: Oncogene, v. 25, p. 6291-6303.

Beranova-Giorgianni, S, Y Zhao, D M Desiderio, F Giorgianni, 2006, Phosphoproteomic analysis of the human pituitary: Pituitary., v. 9, p. 109-120.

Bindukumar, B, S Schwartz, R Aalinkeel, S Mahajan, A Lieberman, K Chadha, 2008, Proteomic profiling of the effect of prostate-specific antigen on prostate cancer cells: Prostate, v. 68, p. 1531-1545.

Bjellqvist, B, K Ek, P G Righetti, E Gianazza, A Gorg, R Westermeier, W Postel, 1982, Isoelectric focusing in immobilized pH gradients: principle, methodology and some applications: J.Biochem.Biophys.Methods, v. 6, p. 317-339.

Blackledge, G R, 1996, Clinical progress with a new antiandrogen, Casodex (bicalutamide): Eur.Urol., v. 29 Suppl 2, p. 96-104.

Blackstock, W P, M P Weir, 1999, Proteomics: quantitative and physical mapping of cellular proteins: Trends Biotechnol., v. 17, p. 121-127.

Blanco, E, E A Bey, Y Dong, B D Weinberg, D M Sutton, D A Boothman, J Gao, 2007, Beta-lapachone-containing PEG-PLA polymer micelles as novel nanotherapeutics against NQO1-overexpressing tumor cells: J.Control Release, v. 122, p. 365-374.

Blanco-Aparicio, C, O Renner, J F Leal, A Carnero, 2007, PTEN, more than the AKT pathway: Carcinogenesis, v. 28, p. 1379-1386.

Byrne, J C, M R Downes, N O'Donoghue, C O'Keane, A O'Neill, Y Fan, J M Fitzpatrick, M Dunn, R W Watson, 2009, 2D-DIGE as a strategy to identify serum markers for the progression of prostate cancer: J.Proteome.Res., v. 8, p. 942-957.

Carter, H B, J D Pearson, E J Metter, L J Brant, D W Chan, R Andres, J L Fozard, P C Walsh, 1992, Longitudinal evaluation of prostate-specific antigen levels in men with and without prostate disease: JAMA, v. 267, p. 2215-2220.

Catalona, W J, J P Richie, J B deKernion, F R Ahmann, T L Ratliff, B L Dalkin, L R Kavoussi, M T MacFarlane, P C Southwick, 1994, Comparison of prostate specific antigen concentration versus prostate specific antigen density in the early detection of prostate cancer: receiver operating characteristic curves: J.Urol., v. 152, p. 2031-2036.

Chang, L, R D Goldman, 2004, Intermediate filaments mediate cytoskeletal crosstalk: Nat.Rev.Mol.Cell Biol., v. 5, p. 601-613.

Chardonnet, S, P Le Marechal, H Cheval, J P Le Caer, P Decottignies, O Laprevote, S Laroche, S Davis, 2008, Large-scale study of phosphoproteins involved in long-term potentiation in the rat dentate gyrus in vivo: Eur.J.Neurosci., v. 27, p. 2985-2998.

Chen, H M, K L Schmeichel, I S Mian, S Lelievre, O W Petersen, M J Bissell, 2000, AZU-1: a candidate breast tumor suppressor and biomarker for tumor progression: Mol.Biol Cell, v. 11, p. 1357-1367.

Chen, J, Z Nikolovska-Coleska, G Wang, S Qiu, S Wang, 2006, Design, synthesis, and characterization of new embelin derivatives as potent inhibitors of X-linked inhibitor of apoptosis protein: Bioorg.Med.Chem.Lett., v. 16, p. 5805-5808.

Chen, Z, K Southwick, C D Thulin, 2004, Initial analysis of the phosphoproteome of Chinese hamster ovary cells using electrophoresis: J.Biomol.Tech., v. 15, p. 249-256.

Chi, A, C Huttenhower, L Y Geer, J J Coon, J E Syka, D L Bai, J Shabanowitz, D J Burke, O G Troyanskaya, D F Hunt, 2007, Analysis of phosphorylation sites on proteins from Saccharomyces cerevisiae by electron transfer dissociation (ETD) mass spectrometry: Proc.Natl.Acad.Sci.U.S.A, v. 104, p. 2193-2198.

Cicchillitti, L, M Di Michele, A Urbani, C Ferlini, M B Donati, G Scambia, D Rotilio, 2009, Comparative proteomic analysis of paclitaxel sensitive A2780 epithelial ovarian cancer and its resistant counterpart A2780TC1 by 2D-DIGE: the role of ERp57: J.Proteome.Res., v. 8, p. 1902-1912.

Cohen, A A, N Geva-Zatorsky, E Eden, M Frenkel-Morgenstern, I Issaeva, A Sigal, R Milo, C Cohen-Saidon, Y Liron, Z Kam, L Cohen, T Danon, N Perzov, U Alon, 2008, Dynamic proteomics of individual cancer cells in response to a drug: Science, v. 322, p. 1511-1516.

Cohen, P, 2000, The regulation of protein function by multisite phosphorylation--a 25 year update: Trends Biochem.Sci., v. 25, p. 596-601.

Collins, M O, L Yu, J S Choudhary, 2007, Analysis of protein phosphorylation on a proteome-scale: Proteomics., v. 7, p. 2751-2768.

Corthals, G L, V C Wasinger, D F Hochstrasser, J C Sanchez, 2000, The dynamic range of protein expression: a challenge for proteomic research: Electrophoresis, v. 21, p. 1104-1115.

Coulombe, P A, P Wong, 2004, Cytoplasmic intermediate filaments revealed as dynamic and multipurpose scaffolds: Nat.Cell Biol., v. 6, p. 699-706.

Csucs, G, J J Ramsden, 1998, Interaction of phospholipid vesicles with smooth metal-oxide surfaces: Biochim.Biophys.Acta, v. 1369, p. 61-70.

Czupalla, C, B Nurnberg, E Krause, 2003, Analysis of class I phosphoinositide 3-kinase autophosphorylation sites by mass spectrometry: Rapid Commun.Mass Spectrom., v. 17, p. 690-696.

Dall'Era, M A, A Oudes, D B Martin, A Y Liu, 2007, HSP27 and HSP70 interact with CD10 in C4-2 prostate cancer cells: Prostate, v. 67, p. 714-721.

Danquah, M, F Li, C B Duke, III, D D Miller, R I Mahato, 2009, Micellar delivery of bicalutamide and embelin for treating prostate cancer: Pharm.Res., v. 26, p. 2081-2092.

DeGnore, J P, J Qin, 1998, Fragmentation of phosphopeptides in an ion trap mass spectrometer: J.Am.Soc.Mass Spectrom., v. 9, p. 1175-1188.

Deng, M, S Mohanan, E Polyak, S Chacko, 2007, Caldesmon is necessary for maintaining the actin and intermediate filaments in cultured bladder smooth muscle cells: Cell Motil.Cytoskeleton, v. 64, p. 951-965.

Di Michele, M, C A Della, L Cicchillitti, P Del Boccio, A Urbani, C Ferlini, G Scambia, M B Donati, D Rotilio, 2009, A proteomic approach to paclitaxel chemoresistance in ovarian cancer cell lines: Biochim.Biophys.Acta, v. 1794, p. 225-236.

Dimmer, E C, R P Huntley, D G Barrell, D Binns, S Draghici, E B Camon, M Hubank, P J Talmud, R Apweiler, R C Lovering, 2008, The gene ontology - providing a functional role in proteomic studies: Proteomics., v. 8, p. 2-11.

Dubrovska, A, S Souchelnytskyi, 2005, Efficient enrichment of intact phosphorylated proteins by modified immobilized metal-affinity chromatography: Proteomics., v. 5, p. 4678-4683.

Dunn, M J, 1987, Two-dimensional gel electrophoresis of proteins: J.Chromatogr., v. 418, p. 145-185.

Edwards, J, J M Bartlett, 2005, The androgen receptor and signal-transduction pathways in hormone-refractory prostate cancer. Part 1: Modifications to the androgen receptor: BJU.Int., v. 95, p. 1320-1326.

Elias, J E, S P Gygi, 2007, Target-decoy search strategy for increased confidence in large-scale protein identifications by mass spectrometry: Nat.Methods, v. 4, p. 207-214.

Fang, J, E J Metter, P Landis, H B Carter, 2002, PSA velocity for assessing prostate cancer risk in men with PSA levels between 2.0 and 4.0 ng/ml: Urology, v. 59, p. 889-893.

Fang, J, T Nakamura, D H Cho, Z Gu, S A Lipton, 2007, S-nitrosylation of peroxiredoxin 2 promotes oxidative stress-induced neuronal cell death in Parkinson's disease: Proc.Natl.Acad.Sci.U.S.A, v. 104, p. 18742-18747.

Farwell, W R, J A Linder, A K Jha, 2007, Trends in prostate-specific antigen testing from 1995 through 2004: Arch.Intern.Med., v. 167, p. 2497-2502.

Feng, X, X Liu, Q Luo, B F Liu, 2008, Mass spectrometry in systems biology: an overview: Mass Spectrom.Rev., v. 27, p. 635-660.

Fenn, J B, M Mann, C K Meng, S F Wong, C M Whitehouse, 1989, Electrospray ionization for mass spectrometry of large biomolecules: Science, v. 246, p. 64-71.

Ficarro, S B, M L McCleland, P T Stukenberg, D J Burke, M M Ross, J Shabanowitz, D F Hunt, F M White, 2002, Phosphoproteome analysis by mass spectrometry and its application to Saccharomyces cerevisiae: Nat.Biotechnol., v. 20, p. 301-305.

Gafken, P R, P D Lampe, 2006, Methodologies for characterizing phosphoproteins by mass spectrometry: Cell Commun.Adhes., v. 13, p. 249-262.

Gannon, J, L Staunton, K O'Connell, P Doran, K Ohlendieck, 2008, Phosphoproteomic analysis of aged skeletal muscle: Int.J.Mol.Med., v. 22, p. 33-42.

Garbis, S D, S I Tyritzis, T Roumeliotis, P Zerefos, E G Giannopoulou, A Vlahou, S Kossida, J Diaz, S Vourekas, C Tamvakopoulos, K Pavlakis, D Sanoudou, C A Constantinides, 2008, Search for potential markers for prostate cancer diagnosis, prognosis and treatment in clinical tissue specimens using amine-specific isobaric tagging (iTRAQ) with two-dimensional liquid chromatography and tandem mass spectrometry: J.Proteome.Res., v. 7, p. 3146-3158.

Gianazza, E, P G Righetti, 2009, Immobilized pH gradients: Electrophoresis, v. 30 Suppl 1, p. S112-S121.

Gioeli, D, 2005, Signal transduction in prostate cancer progression: Clin.Sci.(Lond), v. 108, p. 293-308.

Gioeli, D, S B Ficarro, J J Kwiek, D Aaronson, M Hancock, A D Catling, F M White, R E Christian, R E Settlage, J Shabanowitz, D F Hunt, M J Weber, 2002, Androgen receptor phosphorylation. Regulation and identification of the phosphorylation sites: J.Biol.Chem., v. 277, p. 29304-29314.

Giorgianni, F, S Beranova-Giorgianni, D M Desiderio, 2004, Identification and characterization of phosphorylated proteins in the human pituitary: Proteomics., v. 4, p. 587-598.

Giorgianni, F, D M Desiderio, S Beranova-Giorgianni, 2003, Proteome analysis using isoelectric focusing in immobilized pH gradient gels followed by mass spectrometry: Electrophoresis, v. 24, p. 253-259.

Giorgianni, F, Y Zhao, D M Desiderio, S Beranova-Giorgianni, 2007, Toward a global characterization of the phosphoproteome in prostate cancer cells: identification of phosphoproteins in the LNCaP cell line: Electrophoresis, v. 28, p. 2027-2034.

Glen, A, C S Gan, F C Hamdy, C L Eaton, S S Cross, J W Catto, P C Wright, I Rehman, 2008, iTRAQ-facilitated proteomic analysis of human prostate cancer cells identifies proteins associated with progression: J.Proteome.Res., v. 7, p. 897-907.

Goodman, T, B Schulenberg, T H Steinberg, W F Patton, 2004, Detection of phosphoproteins on electroblot membranes using a small-molecule organic fluorophore: Electrophoresis, v. 25, p. 2533-2538.

Gorg, A, C Obermaier, G Boguth, A Harder, B Scheibe, R Wildgruber, W Weiss, 2000, The current state of two-dimensional electrophoresis with immobilized pH gradients: Electrophoresis, v. 21, p. 1037-1053.

Gorg, A, W Weiss, M J Dunn, 2004, Current two-dimensional electrophoresis technology for proteomics: Proteomics., v. 4, p. 3665-3685.

Hart, S R, M D Waterfield, A L Burlingame, R Cramer, 2002, Factors governing the solubilization of phosphopeptides retained on ferric NTA IMAC beads and their analysis by MALDI TOFMS: J.Am.Soc.Mass Spectrom., v. 13, p. 1042-1051.

Henzel, W J, T M Billeci, J T Stults, S C Wong, C Grimley, C Watanabe, 1993, Identifying proteins from two-dimensional gels by molecular mass searching of peptide fragments in protein sequence databases: Proc.Natl.Acad.Sci.U.S.A, v. 90, p. 5011-5015.

Hoffert, J D, M A Knepper, 2008, Taking aim at shotgun phosphoproteomics: Anal.Biochem., v. 375, p. 1-10.

Hoffmann, P, M A Olayioye, R L Moritz, G J Lindeman, J E Visvader, R J Simpson, B E Kemp, 2005, Breast cancer protein StarD10 identified by three-dimensional separation using free-flow electrophoresis, reversed-phase high-performance liquid chromatography, and sodium dodecyl sulfate-polyacrylamide gel electrophoresis: Electrophoresis, v. 26, p. 1029-1037.

Hoorn, E J, J D Hoffert, M A Knepper, 2005, Combined proteomics and pathways analysis of collecting duct reveals a protein regulatory network activated in vasopressin escape: J.Am.Soc.Nephrol., v. 16, p. 2852-2863.

Hopper, R K, S Carroll, A M Aponte, D T Johnson, S French, R F Shen, F A Witzmann, R A Harris, R S Balaban, 2006, Mitochondrial matrix phosphoproteome: effect of extra mitochondrial calcium: Biochemistry, v. 45, p. 2524-2536.

Hoving, S, B Gerrits, H Voshol, D Muller, R C Roberts, J van Oostrum, 2002, Preparative two-dimensional gel electrophoresis at alkaline pH using narrow range immobilized pH gradients: Proteomics., v. 2, p. 127-134.

Hsiang, C H, T Tunoda, Y E Whang, D R Tyson, D K Ornstein, 2006, The impact of altered annexin I protein levels on apoptosis and signal transduction pathways in prostate cancer cells: Prostate, v. 66, p. 1413-1424.

Iakoucheva, L M, P Radivojac, C J Brown, T R O'Connor, J G Sikes, Z Obradovic, A K Dunker, 2004, The importance of intrinsic disorder for protein phosphorylation: Nucleic Acids Res., v. 32, p. 1037-1049.

Ibel, K, R P May, K Kirschner, H Szadkowski, E Mascher, P Lundahl, 1990, Protein-decorated micelle structure of sodium-dodecyl-sulfate--protein complexes as determined by neutron scattering: Eur.J.Biochem., v. 190, p. 311-318.

Ide, H, D B Seligson, S Memarzadeh, L Xin, S Horvath, P Dubey, M B Flick, B M Kacinski, A Palotie, O N Witte, 2002, Expression of colony-stimulating factor 1 receptor during prostate development and prostate cancer progression: Proc.Natl.Acad.Sci.U.S.A, v. 99, p. 14404-14409.

Isaacs, J T, 1994, Role of androgens in prostatic cancer: Vitam.Horm., v. 49, p. 433-502.

Ishihara, T, M Goto, H Kanazawa, M Higaki, Y Mizushima, 2008, Efficient entrapment of poorly water-soluble pharmaceuticals in hybrid nanoparticles: J.Pharm.Sci., v. 98, p. 2357-2363.

Jacques, A M, O Copeland, A E Messer, C E Gallon, K King, W J McKenna, V T Tsang, S B Marston, 2008, Myosin binding protein C phosphorylation in normal, hypertrophic and failing human heart muscle: J.Mol.Cell Cardiol., v. 45, p. 209-216.

Jemal, A, R Siegel, E Ward, Y Hao, J Xu, T Murray, M J Thun, 2008, Cancer statistics, 2008: CA Cancer J.Clin., v. 58, p. 71-96.

Jemal, A, R Siegel, E Ward, T Murray, J Xu, C Smigal, M J Thun, 2006, Cancer statistics, 2006: CA Cancer J.Clin., v. 56, p. 106-130.

Johansson, B, M R Pourian, Y C Chuan, I Byman, A Bergh, S T Pang, G Norstedt, T Bergman, A Pousette, 2006, Proteomic comparison of prostate cancer cell lines LNCaP-FGC and LNCaP-r reveals heatshock protein 60 as a marker for prostate malignancy: Prostate, v. 66, p. 1235-1244.

Kalume, D E, H Molina, A Pandey, 2003, Tackling the phosphoproteome: tools and strategies: Curr.Opin.Chem.Biol., v. 7, p. 64-69.

Kanemoto, K, H Satoh, H Ishikawa, K Sekizawa, 2006, Neurone-specific enolase and liver metastasis in small cell lung cancer: Clin.Oncol.(R.Coll.Radiol.), v. 18, p. 505.

Kang, J S, B F Calvo, S J Maygarden, L S Caskey, J L Mohler, D K Ornstein, 2002, Dysregulation of annexin I protein expression in high-grade prostatic intraepithelial neoplasia and prostate cancer: Clin.Cancer Res., v. 8, p. 117-123.

Katayama, M, H Nakano, A Ishiuchi, W Wu, R Oshima, J Sakurai, H Nishikawa, S Yamaguchi, T Otsubo, 2006, Protein pattern difference in the colon cancer cell lines examined by two-dimensional differential in-gel electrophoresis and mass spectrometry: Surg.Today, v. 36, p. 1085-1093.

Kaufmann, H, J E Bailey, M Fussenegger, 2001, Use of antibodies for detection of phosphorylated proteins separated by two-dimensional gel electrophoresis: Proteomics., v. 1, p. 194-199.

Khatri, P, S Draghici, 2005, Ontological analysis of gene expression data: current tools, limitations, and open problems: Bioinformatics., v. 21, p. 3587-3595.

Kim, J E, S R Tannenbaum, F M White, 2005, Global phosphoproteome of HT-29 human colon adenocarcinoma cells: J.Proteome.Res., v. 4, p. 1339-1346.

Kim, S C, Y Chen, S Mirza, Y Xu, J Lee, P Liu, Y Zhao, 2006, A clean, more efficient method for in-solution digestion of protein mixtures without detergent or urea: J.Proteome.Res., v. 5, p. 3446-3452.

Kreisberg, J I, S N Malik, T J Prihoda, R G Bedolla, D A Troyer, S Kreisberg, P M Ghosh, 2004, Phosphorylation of Akt (Ser473) is an excellent predictor of poor clinical outcome in prostate cancer: Cancer Res., v. 64, p. 5232-5236.

Kurahashi, T, H Miyake, I Hara, M Fujisawa, 2007, Expression of major heat shock proteins in prostate cancer: correlation with clinicopathological outcomes in patients undergoing radical prostatectomy: J.Urol., v. 177, p. 757-761.

Kweon, H K, K Hakansson, 2006, Selective zirconium dioxide-based enrichment of phosphorylated peptides for mass spectrometric analysis: Anal.Chem., v. 78, p. 1743-1749.

Kweon, H K, K Hakansson, 2008, Metal oxide-based enrichment combined with gas-phase ion-electron reactions for improved mass spectrometric characterization of protein phosphorylation: J.Proteome.Res., v. 7, p. 749-755.

Lahn, M, K Sundell, M Gleave, F Ladan, C Su, S Li, D Ma, B M Paterson, T F Bumol, 2004, Protein kinase C-alpha in prostate cancer: BJU.Int., v. 93, p. 1076-1081.

Larsen, K, J Malmstrom, M Wildt, C Dahlqvist, L Hansson, G Marko-Varga, L Bjermer, A Scheja, G Westergren-Thorsson, 2006, Functional and phenotypical comparison of myofibroblasts derived from biopsies and bronchoalveolar lavage in mild asthma and scleroderma: Respir.Res., v. 7, p. 11.

Larsen, M R, T E Thingholm, O N Jensen, P Roepstorff, T J Jorgensen, 2005, Highly selective enrichment of phosphorylated peptides from peptide mixtures using titanium dioxide microcolumns: Mol.Cell Proteomics., v. 4, p. 873-886.

Le, Y, H Ji, J F Chen, Z Shen, J Yun, M Pu, 2009, Nanosized bicalutamide and its molecular structure in solvents: Int.J.Pharm., v. 370, p. 175-180.

Lee, H J, C Chang, 2003, Recent advances in androgen receptor action: Cell Mol.Life Sci., v. 60, p. 1613-1622.

Lee, J T, B D Lehmann, D M Terrian, W H Chappell, F Stivala, M Libra, A M Martelli, L S Steelman, J A McCubrey, 2008, Targeting prostate cancer based on signal transduction and cell cycle pathways: Cell Cycle, v. 7, p. 1745-1762.

Lee, W C, Y C Li, I M Chu, 2006, Amphiphilic poly(D,L-lactic acid)/poly(ethylene glycol)/poly(D,L-lactic acid) nanogels for controlled release of hydrophobic drugs: Macromol.Biosci., v. 6, p. 846-854.

Leitner, A, A Foettinger, W Lindner, 2007, Improving fragmentation of poorly fragmenting peptides and phosphopeptides during collision-induced dissociation by malondialdehyde modification of arginine residues: J.Mass Spectrom., v. 42, p. 950-959.

Leotoing, L, L Meunier, M Manin, C Mauduit, M Decaussin, G Verrijdt, F Claessens, M Benahmed, G Veyssiere, L Morel, C Beaudoin, 2008, Influence of nucleophosmin/B23 on DNA binding and transcriptional activity of the androgen receptor in prostate cancer cell: Oncogene, v. 27, p. 2858-2867.

Li, Q F, A M Spinelli, R Wang, Y Anfinogenova, H A Singer, D D Tang, 2006, Critical role of vimentin phosphorylation at Ser-56 by p21-activated kinase in vimentin cytoskeleton signaling: J.Biol.Chem., v. 281, p. 34716-34724.

Li, W H, X H Miao, Z T Qi, W Ni, S Y Zhu, F Fang, 2009, Proteomic analysis of differently expressed proteins in human hepatocellular carcinoma cell lines HepG2 with transfecting hepatitis B virus X gene: Chin Med.J.(Engl.), v. 122, p. 15-23.

Li, W Z, P Lin, J Frydman, T R Boal, T S Cardillo, L M Richard, D Toth, M A Lichtman, F U Hartl, F Sherman, 1994, Tcp20, a subunit of the eukaryotic TRiC chaperonin from humans and yeast: J.Biol.Chem., v. 269, p. 18616-18622.

Li, Y, X Xu, D Qi, C Deng, P Yang, X Zhang, 2008, Novel Fe3O4@TiO2 core-shell microspheres for selective enrichment of phosphopeptides in phosphoproteome analysis: J.Proteome.Res., v. 7, p. 2526-2538.

Lim, Y P, 2005, Mining the tumor phosphoproteome for cancer markers: Clin.Cancer Res., v. 11, p. 3163-3169.

Lim, Y P, C Y Wong, L L Ooi, B J Druker, R J Epstein, 2004, Selective tyrosine hyperphosphorylation of cytoskeletal and stress proteins in primary human breast cancers: implications for adjuvant use of kinase-inhibitory drugs: Clin.Cancer Res., v. 10, p. 3980-3987.

Lin, J F, J Xu, H Y Tian, X Gao, Q X Chen, Q Gu, G J Xu, J D Song, F K Zhao, 2007, Identification of candidate prostate cancer biomarkers in prostate needle biopsy specimens using proteomic analysis: Int.J.Cancer, v. 121, p. 2596-2605.

Lin, K, R Lipsitz, T Miller, S Janakiraman, 2008, Benefits and harms of prostate-specific antigen screening for prostate cancer: an evidence update for the U.S. Preventive Services Task Force: Ann.Intern.Med., v. 149, p. 192-199.

Liu, X, Y Wu, Z E Zehner, C Jackson-Cook, J L Ware, 2003, Proteomic analysis of the tumorigenic human prostate cell line M12 after microcell-mediated transfer of chromosome 19 demonstrates reduction of vimentin: Electrophoresis, v. 24, p. 3445-3453.

Liu, Z, S Bengtsson, M Krogh, M Marquez, S Nilsson, P James, A Aliaya, A R Holmberg, 2007, Somatostatin effects on the proteome of the LNCaP cell-line: Int.J.Oncol., v. 30, p. 1173-1179.

Lopez Laur, J D, M Abud, F C Lopez, J Silva, Y Cisella, E R Perez, A Ortiz, 2008, [Antioxidant power and cellular damage in prostate cancer]: Arch.Esp.Urol., v. 61, p. 563-569.

Lopez, M F, K Berggren, E Chernokalskaya, A Lazarev, M Robinson, W F Patton, 2000, A comparison of silver stain and SYPRO Ruby Protein Gel Stain with respect to protein detection in two-dimensional gels and identification by peptide mass profiling: Electrophoresis, v. 21, p. 3673-3683.

Lopez-Alemany, R, C Longstaff, S Hawley, M Mirshahi, P Fabregas, M Jardi, E Merton, L A Miles, J Felez, 2003, Inhibition of cell surface mediated plasminogen activation by a monoclonal antibody against alpha-Enolase: Am.J.Hematol., v. 72, p. 234-242.

Malik, G, E Rojahn, M D Ward, M B Gretzer, A W Partin, O J Semmes, R W Veltri, 2007, SELDI protein profiling of dunning R-3327 derived cell lines: identification of molecular markers of prostate cancer progression: Prostate, v. 67, p. 1565-1575.

Mann, M, 2006, Functional and quantitative proteomics using SILAC: Nat.Rev.Mol.Cell Biol., v. 7, p. 952-958.

Marcantonio, M, M Trost, M Courcelles, M Desjardins, P Thibault, 2008, Combined enzymatic and data mining approaches for comprehensive phosphoproteome analyses: application to cell signaling events of interferon-gamma-stimulated macrophages: Mol.Cell Proteomics., v. 7, p. 645-660.

Meany, D L, Z Zhang, L J Sokoll, H Zhang, D W Chan, 2009, Glycoproteomics for prostate cancer detection: changes in serum PSA glycosylation patterns: J.Proteome.Res., v. 8, p. 613-619.

Meng, S, D Tripathy, S Shete, R Ashfaq, B Haley, S Perkins, P Beitsch, A Khan, D Euhus, C Osborne, E Frenkel, S Hoover, M Leitch, E Clifford, E Vitetta, L Morrison, D Herlyn, L W Terstappen, T Fleming, T Fehm, T Tucker, N Lane, J Wang, J Uhr, 2004, HER-2 gene amplification can be acquired as breast cancer progresses: Proc.Natl.Acad.Sci.U.S.A, v. 101, p. 9393-9398.

Miller, D C, K S Hafez, A Stewart, J E Montie, J T Wei, 2003, Prostate carcinoma presentation, diagnosis, and staging: an update form the National Cancer Data Base: Cancer, v. 98, p. 1169-1178.

Minden, J S, S R Dowd, H E Meyer, K Stuhler, 2009, Difference gel electrophoresis: Electrophoresis, v. 30 Suppl 1, p. S156-S161.

Mitchell, S, P Abel, M Ware, G Stamp, E Lalani, 2000, Phenotypic and genotypic characterization of commonly used human prostatic cell lines: BJU.Int., v. 85, p. 932-944.

Miyake, H, M Muramaki, T Kurahashi, K Yamanaka, I Hara, M Fujisawa, 2006, Enhanced expression of heat shock protein 27 following neoadjuvant hormonal therapy is associated with poor clinical outcome in patients undergoing radical prostatectomy for prostate cancer: Anticancer Res., v. 26, p. 1583-1587.

Molina, H, D M Horn, N Tang, S Mathivanan, A Pandey, 2007, Global proteomic profiling of phosphopeptides using electron transfer dissociation tandem mass spectrometry: Proc.Natl.Acad.Sci.U.S.A, v. 104, p. 2199-2204.

Molloy, M P, E E Brzezinski, J Hang, M T McDowell, R A VanBogelen, 2003, Overcoming technical variation and biological variation in quantitative proteomics: Proteomics., v. 3, p. 1912-1919.

Moser, K, F M White, 2006, Phosphoproteomic analysis of rat liver by high capacity IMAC and LC-MS/MS: J.Proteome.Res., v. 5, p. 98-104.

Muller, F L, M S Lustgarten, Y Jang, A Richardson, H Van Remmen, 2007, Trends in oxidative aging theories: Free Radic.Biol.Med., v. 43, p. 477-503.

Ndassa, Y M, C Orsi, J A Marto, S Chen, M M Ross, 2006, Improved immobilized metal affinity chromatography for large-scale phosphoproteomics applications: J.Proteome.Res., v. 5, p. 2789-2799.

Neverova, I, J E Van Eyk, 2005, Role of chromatographic techniques in proteomic analysis: J.Chromatogr.B Analyt.Technol.Biomed.Life Sci., v. 815, p. 51-63.

Nikolovska-Coleska, Z, L Xu, Z Hu, Y Tomita, P Li, P P Roller, R Wang, X Fang, R Guo, M Zhang, M E Lippman, D Yang, S Wang, 2004, Discovery of embelin as a cell-permeable, small-molecular weight inhibitor of XIAP through structure-based computational screening of a traditional herbal medicine three-dimensional structure database: J.Med.Chem., v. 47, p. 2430-2440.

Obenauer, J C, L C Cantley, M B Yaffe, 2003, Scansite 2.0: Proteome-wide prediction of cell signaling interactions using short sequence motifs: Nucleic Acids Res., v. 31, p. 3635-3641.

Olsson, I, K Larsson, R Palmgren, B Bjellqvist, 2002, Organic disulfides as a means to generate streak-free two-dimensional maps with narrow range basic immobilized pH gradient strips as first dimension: Proteomics., v. 2, p. 1630-1632.

Ornstein, D K, D R Tyson, 2006, Proteomics for the identification of new prostate cancer biomarkers: Urol.Oncol., v. 24, p. 231-236.

Ou, K, K Yu, D Kesuma, M Hooi, N Huang, W Chen, S Y Lee, X P Goh, L K Tan, J Liu, S Y Soon, R S Bin Abdul, T C Putti, H Jikuya, T Ichikawa, O Nishimura, M Salto-Tellez, P Tan, 2008, Novel breast cancer biomarkers identified by integrative proteomic and gene expression mapping: J.Proteome.Res., v. 7, p. 1518-1528.

Pancholi, V, 2001, Multifunctional alpha-enolase: its role in diseases: Cell Mol.Life Sci., v. 58, p. 902-920.

Pang, B, H Zhang, J Wang, W Z Chen, S H Li, Q G Shi, R X Liang, B X Xie, R Q Wu, X L Qian, L Yu, Q M Li, C F Huang, J G Zhou, 2009, Ubiquitous mitochondrial creatine kinase is overexpressed in the conditioned medium and the extract of LNCaP lineaged androgen independent cell lines and facilitates prostate cancer progression: Prostate., v. 69, p. 1176-1187.

Parekh, D J, D P Ankerst, D Troyer, S Srivastava, I M Thompson, 2007, Biomarkers for prostate cancer detection: J.Urol., v. 178, p. 2252-2259.

Park, S Y, X Yu, C Ip, J L Mohler, P N Bogner, Y M Park, 2007, Peroxiredoxin 1 interacts with androgen receptor and enhances its transactivation: Cancer Res., v. 67, p. 9294-9303.

Patterson, S D, R Aebersold, 1995, Mass spectrometric approaches for the identification of gel-separated proteins: Electrophoresis, v. 16, p. 1791-1814.

Patton, W F, 1999, Proteome analysis. II. Protein subcellular redistribution: linking physiology to genomics via the proteome and separation technologies involved: J.Chromatogr.B Biomed.Sci.Appl., v. 722, p. 203-223.

Patton, W F, 2000, A thousand points of light: the application of fluorescence detection technologies to two-dimensional gel electrophoresis and proteomics: Electrophoresis, v. 21, p. 1123-1144.

Pennington, K, E McGregor, C L Beasley, I Everall, D Cotter, M J Dunn, 2004, Optimization of the first dimension for separation by two-dimensional gel electrophoresis of basic proteins from human brain tissue: Proteomics., v. 4, p. 27-30.

Petrylak, D P, C M Tangen, M H Hussain, P N Lara, Jr., J A Jones, M E Taplin, P A Burch, D Berry, C Moinpour, M Kohli, M C Benson, E J Small, D Raghavan, E D Crawford, 2004, Docetaxel and estramustine compared with mitoxantrone and prednisone for advanced refractory prostate cancer: N.Engl.J.Med., v. 351, p. 1513-1520.

Pinkse, M W, P M Uitto, M J Hilhorst, B Ooms, A J Heck, 2004, Selective isolation at the femtomole level of phosphopeptides from proteolytic digests using 2D-NanoLC-ESI-MS/MS and titanium oxide precolumns: Anal.Chem., v. 76, p. 3935-3943.

Pitkanen-Arsiola, T, J E Tillman, G Gu, J Yuan, R L Roberts, M Wantroba, G A Coetzee, M S Cookson, S Kasper, 2006, Androgen and anti-androgen treatment modulates androgen receptor activity and DJ-1 stability: Prostate, v. 66, p. 1177-1193.

Plow, E F, T Herren, A Redlitz, L A Miles, J L Hoover-Plow, 1995, The cell biology of the plasminogen system: FASEB J., v. 9, p. 939-945.

Posewitz, M C, P Tempst, 1999, Immobilized gallium(III) affinity chromatography of phosphopeptides: Anal.Chem., v. 71, p. 2883-2892.

Qi, C, Y T Zhu, J Chang, A V Yeldandi, M S Rao, Y J Zhu, 2005, Potentiation of estrogen receptor transcriptional activity by breast cancer amplified sequence 2: Biochem.Biophys.Res.Commun., v. 328, p. 393-398.

Rabilloud, T, 1996, Solubilization of proteins for electrophoretic analyses: Electrophoresis, v. 17, p. 813-829.

Rabilloud, T, 2009, Solubilization of proteins in 2DE: an outline: Methods Mol.Biol., v. 519, p. 19-30.

Rabilloud, T, C Adessi, A Giraudel, J Lunardi, 1997, Improvement of the solubilization of proteins in two-dimensional electrophoresis with immobilized pH gradients: Electrophoresis, v. 18, p. 307-316.

Rao, A R, H G Motiwala, O M Karim, 2008, The discovery of prostate-specific antigen: BJU.Int., v. 101, p. 5-10.

Raponi, M, R T Belly, J E Karp, J E Lancet, D Atkins, Y Wang, 2004, Microarray analysis reveals genetic pathways modulated by tipifarnib in acute myeloid leukemia: BMC.Cancer, v. 4, p. 56.

Rhee, S Y, V Wood, K Dolinski, S Draghici, 2008, Use and misuse of the gene ontology annotations: Nat.Rev.Genet., v. 9, p. 509-515.

Rocchi, P, P Jugpal, A So, S Sinneman, S Ettinger, L Fazli, C Nelson, M Gleave, 2006, Small interference RNA targeting heat-shock protein 27 inhibits the growth of prostatic cell lines and induces apoptosis via caspase-3 activation in vitro: BJU.Int., v. 98, p. 1082-1089.

Rocchi, P, A So, S Kojima, M Signaevsky, E Beraldi, L Fazli, A Hurtado-Coll, K Yamanaka, M Gleave, 2004, Heat shock protein 27 increases after androgen ablation and plays a cytoprotective role in hormone-refractory prostate cancer: Cancer Res., v. 64, p. 6595-6602.

Rochette-Egly, C, 2003, Nuclear receptors: integration of multiple signalling pathways through phosphorylation: Cell Signal., v. 15, p. 355-366.

Rondepierre, F, B Bouchon, J Papon, M Bonnet-Duquennoy, R Kintossou, N Moins, J Maublant, J C Madelmont, M D'Incan, F Degoul, 2009, Proteomic studies of B16 lines: involvement of annexin A1 in melanoma dissemination: Biochim.Biophys.Acta, v. 1794, p. 61-69.

Rosengren, A T, J M Salmi, T Aittokallio, J Westerholm, R Lahesmaa, T A Nyman, O S Nevalainen, 2003, Comparison of PDQuest and Progenesis software packages in the analysis of two-dimensional electrophoresis gels: Proteomics., v. 3, p. 1936-1946.

Ross, L E, R J Coates, N Breen, R J Uhler, A L Potosky, D Blackman, 2004, Prostate-specific antigen test use reported in the 2000 National Health Interview Survey: Prev.Med., v. 38, p. 732-744.

Rowland, J G, J L Robson, W J Simon, H Y Leung, A R Slabas, 2007, Evaluation of an in vitro model of androgen ablation and identification of the androgen responsive proteome in LNCaP cells: Proteomics., v. 7, p. 47-63.

Saldanha, R G, N Xu, M P Molloy, D A Veal, M S Baker, 2008, Differential proteome expression associated with urokinase plasminogen activator receptor (uPAR) suppression in malignant epithelial cancer: J.Proteome.Res., v. 7, p. 4792-4806.

Salomon, A R, S B Ficarro, L M Brill, A Brinker, Q T Phung, C Ericson, K Sauer, A Brock, D M Horn, P G Schultz, E C Peters, 2003, Profiling of tyrosine phosphorylation pathways in human cells using mass spectrometry: Proc.Natl.Acad.Sci.U.S.A, v. 100, p. 443-448.

Samland, A K, G A Sprenger, 2009, Transaldolase: from biochemistry to human disease: Int.J.Biochem.Cell Biol., v. 41, p. 1482-1494.

Sardana, G, B Dowell, E P Diamandis, 2008a, Emerging biomarkers for the diagnosis and prognosis of prostate cancer: Clin.Chem., v. 54, p. 1951-1960.

Sardana, G, K Jung, C Stephan, E P Diamandis, 2008b, Proteomic analysis of conditioned media from the PC3, LNCaP, and 22Rv1 prostate cancer cell lines: discovery and validation of candidate prostate cancer biomarkers: J.Proteome.Res., v. 7, p. 3329-3338.

Sardana, G, J Marshall, E P Diamandis, 2007, Discovery of candidate tumor markers for prostate cancer via proteomic analysis of cell culture-conditioned medium: Clin.Chem., v. 53, p. 429-437.

Schaefer, H, D C Chamrad, M Herrmann, J Stuwe, G Becker, J Klose, M Blueggel, H E Meyer, K Marcus, 2006, Study of posttranslational modifications in lenticular alphaA-Crystallin of mice using proteomic analysis techniques: Biochim.Biophys.Acta, v. 1764, p. 1948-1962.

Schulenberg, B, T N Goodman, R Aggeler, R A Capaldi, W F Patton, 2004, Characterization of dynamic and steady-state protein phosphorylation using a fluorescent phosphoprotein gel stain and mass spectrometry: Electrophoresis, v. 25, p. 2526-2532.

Schwartz, J C, M W Senko, J E Syka, 2002, A two-dimensional quadrupole ion trap mass spectrometer: J.Am.Soc.Mass Spectrom., v. 13, p. 659-669.

Semmes, O J, G Malik, M Ward, 2006, Application of mass spectrometry to the discovery of biomarkers for detection of prostate cancer: J.Cell Biochem., v. 98, p. 496-503.

Shen, C, C Nathan, 2002, Nonredundant antioxidant defense by multiple two-cysteine peroxiredoxins in human prostate cancer cells: Mol.Med., v. 8, p. 95-102.

Skvortsova, I, S Skvortsov, T Stasyk, U Raju, B A Popper, B Schiestl, E von Guggenberg, A Neher, G K Bonn, L A Huber, P Lukas, 2008, Intracellular signaling pathways regulating radioresistance of human prostate carcinoma cells: Proteomics., v. 8, p. 4521-4533.

Smith, R A, V Cokkinides, O W Brawley, 2009, Cancer screening in the United States, 2009: a review of current American Cancer Society guidelines and issues in cancer screening: CA Cancer J.Clin., v. 59, p. 27-41.

Smitherman, A B, J L Mohler, S J Maygarden, D K Ornstein, 2004, Expression of annexin I, II and VII proteins in androgen stimulated and recurrent prostate cancer: J.Urol., v. 171, p. 916-920.

Solassol, J, P Marin, E Demettre, P Rouanet, J Bockaert, T Maudelonde, A Mange, 2005, Proteomic detection of prostate-specific antigen using a serum fractionation procedure: potential implication for new low-abundance cancer biomarkers detection: Anal.Biochem., v. 338, p. 26-31.

Spahr, C S, S A Susin, E J Bures, J H Robinson, M T Davis, M D McGinley, G Kroemer, S D Patterson, 2000, Simplification of complex peptide mixtures for proteomic analysis: reversible biotinylation of cysteinyl peptides: Electrophoresis, v. 21, p. 1635-1650.

Stadtman, E R, 1992, Protein oxidation and aging: Science, v. 257, p. 1220-1224.

Stasyk, T, S Morandell, R Bakry, I Feuerstein, C W Huck, G Stecher, G K Bonn, L A Huber, 2005, Quantitative detection of phosphoproteins by combination of two-dimensional difference gel electrophoresis and phosphospecific fluorescent staining: Electrophoresis, v. 26, p. 2850-2854.

Steinberg, T H, B J Agnew, K R Gee, W Y Leung, T Goodman, B Schulenberg, J Hendrickson, J M Beechem, R P Haugland, W F Patton, 2003, Global quantitative phosphoprotein analysis using Multiplexed Proteomics technology: Proteomics., v. 3, p. 1128-1144.

Stephens, B J, H Han, V Gokhale, D D Von Hoff, 2005, PRL phosphatases as potential molecular targets in cancer: Mol.Cancer Ther., v. 4, p. 1653-1661.

Subong, E N, M J Shue, J I Epstein, J V Briggman, P K Chan, A W Partin, 1999, Monoclonal antibody to prostate cancer nuclear matrix protein (PRO:4-216) recognizes nucleophosmin/B23: Prostate, v. 39, p. 298-304.

Suzuki, S, K Takeshita, M Asamoto, S Takahashi, H Kandori, K Tsujimura, F Saito, K Masuko, T Shirai, 2009, High mobility group box associated with cell proliferation appears to play an important role in hepatocellular carcinogenesis in rats and humans: Toxicology, v. 255, p. 160-170.

Sweet, S M, A J Creese, H J Cooper, 2006, Strategy for the identification of sites of phosphorylation in proteins: neutral loss triggered electron capture dissociation: Anal.Chem., v. 78, p. 7563-7569.

Tang, D D, 2008, Intermediate filaments in smooth muscle: Am.J.Physiol Cell Physiol, v. 294, p. C869-C878.

Thingholm, T E, T J Jorgensen, O N Jensen, M R Larsen, 2006, Highly selective enrichment of phosphorylated peptides using titanium dioxide: Nat.Protoc., v. 1, p. 1929-1935.

Tholey, A, J Reed, W D Lehmann, 1999, Electrospray tandem mass spectrometric studies of phosphopeptides and phosphopeptide analogues: J.Mass Spectrom., v. 34, p. 117-123.

Thompson, I M, D K Pauler, P J Goodman, C M Tangen, M S Lucia, H L Parnes, L M Minasian, L G Ford, S M Lippman, E D Crawford, J J Crowley, C A Coltman, Jr., 2004, Prevalence of prostate cancer among men with a prostate-specific antigen level < or =4.0 ng per milliliter: N.Engl.J.Med., v. 350, p. 2239-2246.

Tillman, J E, J Yuan, G Gu, L Fazli, R Ghosh, A S Flynt, M Gleave, P S Rennie, S Kasper, 2007, DJ-1 binds androgen receptor directly and mediates its activity in hormonally treated prostate cancer cells: Cancer Res., v. 67, p. 4630-4637.

Tilton, R G, S J Haidacher, W S Lejeune, X Zhang, Y Zhao, A Kurosky, A R Brasier, L Denner, 2007, Diabetes-induced changes in the renal cortical proteome assessed with two-dimensional gel electrophoresis and mass spectrometry: Proteomics., v. 7, p. 1729-1742.

Topoglidis, E, T Lutz, R L Willis, C J Barnett, A E Cass, J R Durrant, 2000, Protein adsorption on nanoporous TiO2 films: a novel approach to studying photoinduced protein/electrode transfer reactions: Faraday Discuss., p. 35-46.

Tsai, C F, Y T Wang, Y R Chen, C Y Lai, P Y Lin, K T Pan, J Y Chen, K H Khoo, Y J Chen, 2008, Immobilized metal affinity chromatography revisited: pH/acid control toward high selectivity in phosphoproteomics: J.Proteome.Res., v. 7, p. 4058-4069.

Ummanni, R, H Junker, U Zimmermann, S Venz, S Teller, J Giebel, C Scharf, C Woenckhaus, F Dombrowski, R Walther, 2008, Prohibitin identified by proteomic analysis of prostate biopsies distinguishes hyperplasia and cancer: Cancer Lett., v. 266, p. 171-185.

Unlu, M, M E Morgan, J S Minden, 1997, Difference gel electrophoresis: a single gel method for detecting changes in protein extracts: Electrophoresis, v. 18, p. 2071-2077.

Verhoeven, N M, J H Huck, B Roos, E A Struys, G S Salomons, A C Douwes, M S van der Knaap, C Jakobs, 2001, Transaldolase deficiency: liver cirrhosis associated with a new inborn error in the pentose phosphate pathway: Am.J.Hum.Genet., v. 68, p. 1086-1092.

Visconti, R, D Grieco, 2009, New insights on oxidative stress in cancer: Curr.Opin.Drug Discov.Devel., v. 12, p. 240-245.

Washburn, M P, D Wolters, J R Yates, III, 2001, Large-scale analysis of the yeast proteome by multidimensional protein identification technology: Nat.Biotechnol., v. 19, p. 242-247.

Wehder, L, S Arndt, U Murzik, A K Bosserhoff, R Kob, F von Eggeling, C Melle, 2009, Annexin A5 is involved in migration and invasion of oral carcinoma: Cell Cycle, v. 8, p. 1552-1558.

Wei, J, G Xu, M Wu, Y Zhang, Q Li, P Liu, T Zhu, A Song, L Zhao, Z Han, G Chen, S Wang, L Meng, J Zhou, Y Lu, S Wang, D Ma, 2008, Overexpression of vimentin contributes to prostate cancer invasion and metastasis via src regulation: Anticancer Res., v. 28, p. 327-334.

Welch, H G, L M Schwartz, S Woloshin, 2005, Prostate-specific antigen levels in the United States: implications of various definitions for abnormal: J.Natl.Cancer Inst., v. 97, p. 1132-1137.

Whitaker, H C, D P Stanbury, C Brinham, J Girling, S Hanrahan, N Totty, D E Neal, 2007, Labeling and identification of LNCaP cell surface proteins: a pilot study: Prostate, v. 67, p. 943-954.

Wu, J, N J Lenchik, M J Pabst, S S Solomon, J Shull, I C Gerling, 2005, Functional characterization of two-dimensional gel-separated proteins using sequential staining: Electrophoresis, v. 26, p. 225-237.

Wu, M, X Bai, G Xu, J Wei, T Zhu, Y Zhang, Q Li, P Liu, A Song, L Zhao, C Gang, Z Han, S Wang, J Zhou, Y Lu, D Ma, 2007, Proteome analysis of human androgen-independent prostate cancer cell lines: variable metastatic potentials correlated with vimentin expression: Proteomics., v. 7, p. 1973-1983.

Yang, H S, C P Matthews, T Clair, Q Wang, A R Baker, C C Li, T H Tan, N H Colburn, 2006, Tumorigenesis suppressor Pdcd4 down-regulates mitogen-activated protein kinase kinase kinase kinase 1 expression to suppress colon carcinoma cell invasion: Mol.Cell Biol, v. 26, p. 1297-1306.

Yang, Z L, X R Li, K W Yang, Y Liu, 2008, Amphotericin B-loaded poly(ethylene glycol)-poly(lactide) micelles: preparation, freeze-drying, and in vitro release: J.Biomed.Mater.Res.A, v. 85, p. 539-546.

Yasugi, K, Y Nagasaki, M Kato, K Kataoka, 1999, Preparation and characterization of polymer micelles from poly(ethylene glycol)-poly(D,L-lactide) block copolymers as potential drug carrier: J.Control Release, v. 62, p. 89-100.

Yates, J R, III, 2000, Mass spectrometry. From genomics to proteomics: Trends Genet., v. 16, p. 5-8.

Yates, J R, III, J K Eng, A L McCormack, D Schieltz, 1995, Method to correlate tandem mass spectra of modified peptides to amino acid sequences in the protein database: Anal.Chem., v. 67, p. 1426-1436.

Yates, J R, C I Ruse, A Nakorchevsky, 2009, Proteomics by mass spectrometry: approaches, advances, and applications: Annu.Rev.Biomed.Eng, v. 11, p. 49-79.

Yu, L R, Z Zhu, K C Chan, H J Issaq, D S Dimitrov, T D Veenstra, 2007a, Improved titanium dioxide enrichment of phosphopeptides from HeLa cells and high confident phosphopeptide identification by cross-validation of MS/MS and MS/MS/MS spectra: J.Proteome.Res., v. 6, p. 4150-4162.

Yu, Y P, G Yu, G Tseng, K Cieply, J Nelson, M Defrances, R Zarnegar, G Michalopoulos, J H Luo, 2007b, Glutathione peroxidase 3, deleted or methylated in prostate cancer, suppresses prostate cancer growth and metastasis: Cancer Res., v. 67, p. 8043-8050.

Zahedi, R P, A J Begonja, S Gambaryan, A Sickmann, 2006, Phosphoproteomics of human platelets: A quest for novel activation pathways: Biochim.Biophys.Acta, v. 1764, p. 1963-1976.

Zhan, X, D M Desiderio, 2003, Differences in the spatial and quantitative reproducibility between two second-dimensional gel electrophoresis systems: Electrophoresis, v. 24, p. 1834-1846.

Zhan, X, F Giorgianni, D M Desiderio, 2005, Proteomics analysis of growth hormone isoforms in the human pituitary: Proteomics., v. 5, p. 1228-1241.

Zhao, Y, F Giorgianni, D M Desiderio, B Fang, S Beranova-Giorgianni, 2005, Toward a global analysis of the human pituitary proteome by multiple gel-based technology: Anal.Chem., v. 77, p. 5324-5331.

Zhao, Y, Q Yan, X Long, X Chen, Y Wang, 2008, Vimentin affects the mobility and invasiveness of prostate cancer cells: Cell Biochem.Funct., v. 26, p. 571-577.

Zoubeidi, A, A Zardan, E Beraldi, L Fazli, R Sowery, P Rennie, C Nelson, M Gleave, 2007, Cooperative interactions between androgen receptor (AR) and heat-shock protein 27 facilitate AR transcriptional activity: Cancer Res., v. 67, p. 10455-10465.

Zuo, X, D W Speicher, 2000, Quantitative evaluation of protein recoveries in two-dimensional electrophoresis with immobilized pH gradients: Electrophoresis, v. 21, p. 3035-3047.

APPENDIX

Table A-1 Full list of phosphopeptides and phosphoproteins characterized in LNCaP cells.

Accession number	Peptide	MH+	z	XC	Site # in Swiss/Phosphosite (06/17/08)	Present in Phosphosite (06/17/08)
P07900	HS90A_HUMAN Heat shock protein HSP 90-alpha (HSP 86)			20.21		
	K.ESEDKPEIEDVGS*DEEEEK.K	2272.88640	2	4.15	263 Swiss/ 263 phos	Yes
	K.ESEDKPEIEDVGS*DEEEEKK.D	2400.98137	3	3.93	see line 4	
	R.DKEVS*DDEAEEK.E	1473.56282	2	4.89	231 Swiss/ 231 phos	Yes
Q15019	SEPT2_HUMAN Septin-2 (Protein NEDD5)			10.27		
	K.IYHLPDAES*DEDEDFKEQTR.L	2517.04530	3	4.28	see line 10	
	R.YLHDES*GLNR.R	1283.54158	2	2.41	134 NEW	No
	K.IYHLPDAES*DEDEDFK.E	2002.79534	2	3.37	218 Swiss/ 218 phos	Yes
Q15185	TEBP_HUMAN Prostaglandin E synthase 3 (Cytosolic prostaglandin E2 synthase)			10.35		
	K.DWEDDS*DEDMSNFDR.F	1955.62729	2	5.85	113 Swiss/ 113 phos	Yes
	K.DWEDDS*DEDM#SNFDR.F	1971.62219	2	2.92	see line 12	
O60716	CTND1_HUMAN Catenin delta-1 (p120 catenin)			70.35		
	R.LRSY*EDMIGEEVPSDQYYWAPLAQHER.G	3362.48235	3	6.95	321 Swiss/ 321 phos	Yes
	R.HYEDGYPGGSDNYGS*LSR.V	2053.79232	2	4.83	230 Swiss/ 230 phos	Yes
	R.SQSSHSYDDST*LPLIDR.N	2000.85968	3	4.73	869 Swiss	No
	R.S*YEDMIGEEVPSDQYYWAPLAQHER.G	3093.29718	3	3.65	320 Swiss/ 320 phos	Yes
	R.VGGS*SVDLHR.F	1106.49898	2	3.19	268 Swiss/ 268 phos	Yes
	R.S*GDLGDMEPLK.G	1241.51192	2	3.14	920 NEW	No
	R.TLDRS*GDLGDMEPLK.G	1726.77171	2	2.77	920 NEW	No
	R.S*MGYDDLDYGMMSDYGTAR.R	2227.80177	2	5.45	288 Swiss/ 288 phos	Yes
	R.T*LDRSGDLGDMEPLK.G	1726.77171	2	2.65	916 Swiss/ 916 phos	Yes
	R.HYEDGYPGGS*DNY*GSLSRVT*RIEER.Y	3097.21249	3	3.04	228 Swiss/ 228 phos	Yes

Table A-1 (continued).

Accession number	Peptide	MH+	z	XC	Site # in Swiss/Phosphosite (06/17/08)	Present in Phosphosite (06/17/08)
	R.S*MGYDDLDYGMMSDYGTAR.R	2227.80177	2	3.41	see line 22	
	R.VGGS*SVDLHR.F	1106.49898	2	2.44	see line 19	
	K.WAHDKFS*GEEGEIEDDES*GTENR.E	2797.02977	3	6.50	939 Swiss/ 939 phos	Yes
	K.WAHDKFS*GEEGEIEDDESGTENR.E	2717.06347	3	5.99	928 Swiss/ 928 phos	Yes
	K.WAHDKFS*GEEGEIEDDESGT*ENREEK.D	3183.20992	3	3.70	941 Swiss/ 941 phos	Yes
	R.ERS*PALKS*PLQSVVVR.R	1925.96089	3	3.42	248 Swiss/248 phos & 253 Swiss/ 253 phos	Yes
	R.IDIS*PSTFR.K	1115.51324	2	3.28	682 Swiss/ 682 phos	Yes
	R.ASAVSELS*PR.E	1096.50340	2	3.01	243 Swiss/ 243 phos	Yes
	K.S*PPSTGSTYGSSQK.E	1463.60496	2	2.82	320 Swiss/ 320 phos	Yes
	R.DSS*HS*RERS*AEK.T	1628.55019	2	2.35	747 NEW & 749 NEW & 753 NEW	No
	R.RIDIS*PSTFR.K	1271.61435	2	2.15	see line 32	
	K.SPPSTGST*Y*GSS*QK.E	1623.53756	2	2.09	324 Swiss/ 324 phos & 325 NEW & 328 NEW	Yes & No & No
P08651	NFIC_HUMAN Nuclear factor 1 C-type (Nuclear factor 1/C)			20.25		
	R.NWTEDMEGGISS*PVK.K	1729.71386	2	4.96	323 Swiss/ 323 phos	Yes
	R.NWTEDMEGGISS*PVKK.T	1857.80883	2	4.41	see line 39	
Q13283	G3BP1_HUMAN Ras GTPase-activating protein-binding protein 1 (G3BP-1)			20.26		
	K.SSS*PAPADIAQTVQEDLR.T	1964.89606	2	4.55	232 Swiss/ 232 phos	Yes
	R.YQDEVFGGFVTEPQEES*EEEVEEPEER.Q	3296.33143	3	3.25	149 Swiss/ 149 phos	Yes
Q9Y608	LRRF2_HUMAN Leucine-rich repeat flightless-interacting protein 2			20.25		
	R.RGS*GDTSSLIDPDTSLSELR.D	2185.99723	2	4.94	328 Swiss/ 328 phos	Yes
	R.IS*S*ARSS*PGFTNDDTASIVSSDRASR.G	2924.18594	3	3.04	231 NEW & 232 NEW & 236 NEW	No
	R.PSSRNS*ASATT*PLSGNSS*R.R	2116.80966	2	2.34	312 NEW & 317 NEW & 324 NEW	Yes
Q5VTR2	BRE1A_HUMAN Ubiquitin-protein ligase BRE1A (BRE1-A)			20.18		
	K.ALVVPEPEPDSDS*NQER.K	1961.84878	2	3.70	138 Swiss/ 138 phos	Yes

Table A-1 (continued).

Accession number	Peptide	MH+	z	XC	Site # in Swiss/Phosphosite (06/17/08)	Present in Phosphosite (06/17/08)
	K.PDSEDLSSQSS*AS*KASQEDANEIK.S	2683.06549	3	3.42	548 NEW & 550 NEW	No
Q8N6T3	ARFG1_HUMAN ADP-ribosylation factor GTPase-activating protein 1			20.21		
	R.RSS*DSWEVWGSASTNR.N	1904.79226	2	3.98	see line 54	
	R.EFLESQEDY*DPCWS*LQEK.Y	2405.89201	2	2.15	93 New & 98 New	No
	R.SS*DSWEVWGSASTNR.N	1748.69115	2	4.03	361 Swiss/ New in phos	No
	K.ASELGHS*LNENVLKPAQEK.V	2144.03831	3	3.39	246 Swiss/ 246 phos	Yes
Q9Y6G9	DC1L1_HUMAN Cytoplasmic dynein 1 light intermediate chain 1			30.31		
	R.DFQEYVEPGEDFPAS*PQR.R	2190.90154	2	5.94	207 Swiss/ 207 phos	Yes
	K.KTGSPGGPGVSGGS*PAGGAGGGSS*GLPPSTKK.S	2811.27095	3	3.77	468 NEW & 478 NEW	No
	K.PVT*VS*PTTPTSPTEGEAS*	1997.74287	2	2.22	508 NEW & 510 Swiss/510 phos & 523 NEW	No & Yes & No
Q9Y2U5	M3K2_HUMAN Mitogen-activated protein kinase kinase kinase 2			40.21		
	R.DRSS*PPPGYIPDELHQVAR.N	2214.03389	3	4.27	164 Swiss/ 164 phos	Yes
	R.AQS*YPDNHQEFSDYDNPIFEK.F	2624.06129	3	3.87	239 NEW	No
	K.RLS*IIGPTSR.D	1179.62452	2	2.62	153 NEW	No
	R.GS*DIDNPT*LTVM#DISPPSR.S	2190.90250	2	2.38	331 Swiss/ 331 phos & 337 NEW	Yes & No
O00193	SMAP_HUMAN Small acidic protein			10.34		
	R.S*ASPDDDLGSSNWEAADLGNEER.K	2514.98925	2	6.76	15 Swiss/ 15 phos	Yes
O95218	ZRAB2_HUMAN Zinc finger Ran-binding domain-containing protein 2			20.20		
	R.ENVEYIEREES*DGEYDEFGR.K	2545.00383	3	3.45	see line 69	
	R.EES*DGEYDEFGR.K	1512.51621	2	3.21	120 Swiss/ 120 phos	Yes
	K.YNLDAS*EEEDSNK.K	1593.59519	2	5.17	188 Swiss/ 188 phos	Yes
	K.EVEDKES*EGEEEDEDEDLSK.Y	2419.90318	3	3.62	153 Swiss/ 153 phos	Yes
	R.S*SSRS*S*SPSSSRSR.S	1694.59312	2	2.06	213 NEW & 217 NEW & 218 NEW	No

Table A-1 (continued).

Accession number	Peptide	MH+	z	XC	Site # in Swiss/Phosphosite (06/17/08)	Present in Phosphosite (06/17/08)
Q8N5F7	NKAP_HUMAN NF-kappa-B-activating protein			10.23		
	R.IGELGAPEVWGLS*PK.N	1632.80327	2	4.59	149 Swiss/ 149 phos	Yes
	K.Y*S*EDS*DSDSDSETDSSDEDNK.R	2566.70622	3	3.41	209 NEW & 210 NEW & 213 NEW	No
Q9NSK0	KLC4_HUMAN Kinesin light chain 4 (KLC 4) (Kinesin-like protein 8)			10.25		
	R.AAS*LNYLNQPSAAPLQVSR.G	2080.02226	2	5.05	590 Swiss/ 590 phos	Yes
Q9H1E3	NUCKS_HUMAN Nuclear ubiquitous casein and cyclin-dependent kinases substrate			10.28		
	K.VVDYSQFQES*DDADEDYGR.D	2317.87684	2	5.65	19 Swiss/ 19 phos	Yes
Q92625	ANKS1_HUMAN Ankyrin repeat and SAM domain-containing protein 1A (Odin)			10.21		
	K.SPS*FASEWDEIEK.I	1604.65158	2	4.30	663 Swiss/ 662 phos	Yes (same AA, diff #)
O00192	ARVC_HUMAN Armadillo repeat protein deleted in velo-cardio-facial syndrome			20.28		
	R.S*LAADDEGGPELEPDYGTATR.R	2243.93396	2	5.66	267 Swiss/ 267 phos	Yes
	R.NFDT*LDLPK.R	1142.51290	2	2.61	642 Swiss/ 642 phos	Yes
O15027	K0310_HUMAN Uncharacterized protein KIAA0310			10.23		
	R.FTGS*FDDDPDPHRDPYGEEVDR.R	2646.04162	3	4.15	1149 Swiss/ New in phos	No
Q14247	SRC8_HUMAN Src substrate cortactin (Amplaxin) (Oncogene EMS1)			30.24		
	R.LPSS*PVYEDAASFK.A	1590.70870	2	4.83	418 Swiss/ 418 phos	Yes
	K.TQT*PPVS*PAPQPTEER.L	1894.79830	2	4.19	401 Swiss/ 401 phos & 405 Swiss/ 405 phos	Yes & Yes
	R.VDKSAVGFDY*QGKT*EK.H	1931.81871	2	2.19	178 NEW in Swiss/ 178 phos & 182 NEW	Yes & No
	K.GRY*GLFPANY*VELR.Q	1814.80260	3	3.27	538 NEW & 545 NEW	No
	K.LS*KHCS*QVDSVRGFGGK.F	1964.84488	2	2.12	109 NEW & 113 Swiss/ 113 phos	No & Yes
	R.LPSS*PVY*EDAASFK.A	1670.67500	2	2.47	418 Swiss/ 418 phos & 412 Swiss/ 412 phos	Yes & Yes
Q14498	RBM39_HUMAN RNA-binding protein 39 (RNA-binding motif protein 39)			20.26		
	K.DKS*PVREPIDNLTPEER.D	2074.98046	3	5.11	136 Swiss/ 136 phos	
	R.YRS*PYSGPK.F	1134.49792	2	2.90	97 Swiss/ 97 phos	

Table A-1 (continued).

Accession number	Peptide	MH+	z	XC	Site # in Swiss/Phosphosite (06/17/08)	Present in Phosphosite (06/17/08)
Q6ICG6	CV009_HUMAN Uncharacterized protein C22orf9			10.20		
	K.SHS*ANDSEEFFR.E	1505.56925	2	3.98	324 NEW	No
Q9NYF8	BCLF1_HUMAN Bcl-2-associated transcription factor 1 (Btf)			80.23		
	K.FNDS*EGDDTEETEDYR.Q	2001.68692	2	4.61	397 Swiss/ 397 phos	Yes
	R.AEGEWEDQEALDYFS*DKESGK.Q	2513.00277	3	4.42	385 Swiss/ 385 phos	Yes
	K.KAEGEPQEES*PLK.S	1521.68321	2	4.20	177 Swiss/ 177 phos	Yes
	K.DLFDYS*PPLHK.N	1411.62933	2	3.84	512 Swiss/ 512 phos	Yes
	K.LKDLFDYS*PPLHK.N	1652.80836	3	3.04	see line 103	
	R.IDIS*PSTLR.K	1081.52889	2	2.83	658 Swiss/ 658 phos	Yes
	R.YSPS*QNS*PIHHIPSR.R	1879.78874	2	2.81	287 Swiss/ 287 phos & 290 Swiss/ 290 phos	Yes & Yes
	R.AEGEWEDQEALDYFS*DK.E	2111.81172	2	2.64	385 Swiss/ 385 phos	Yes
	R.RIDIS*PSTLR.K	1237.63000	2	2.02	see line 105	
	R.SSSSS*AS*PSSPSS*REEK.E	1936.66093	2	2.10	755 NEW & 757 NEW & 763 NEW	No & No & No
	R.S*SSSRSSSPYSKSPVS*K.R	1917.79903	2	2.01	141 NEW & 156 NEW	No & No
	R.YSPS*QNS*PIHHIPSR.R	1879.78874	2	2.34	see line 106	
P42167	LAP2B_HUMAN Lamina-associated polypeptide 2, isoforms beta/gamma			20.23		
	K.GPPDFS*SDEEREPTPVLGSGAAAAGR.S	2650.17805	3	4.54	66 Swiss/ 66 phos	Yes
	R.SST*PLPTISSSAENTR.Q	1727.78472	2	2.99	160 Swiss/ 160 NEW in phos	No
	K.GPPDFSSDEEREPT*PVLGSGAAAAGR.S	2650.17805	3	4.12	174 Swiss/ 173 phos	Yes (same AA, diff #)
	R.EQGTES*RSST*PLPTISSSAENTR.Q	2595.09706	3	3.03	156 Swiss/ 155 phos & 160 Swiss/ 159 phos	Yes (same AA, diff #)
P54578	UBP14_HUMAN Ubiquitin carboxyl-terminal hydrolase 14			10.30		
	R.AS*GEMASAQYITAALR.D	1719.77713	2	5.99	143 Swiss/ 142 phos	Yes (same AA, diff #)
	R.AS*GEM#ASAQYITAALR.D	1735.77203	2	2.67	see line 118	
	K.S*S*KISRLPAYLTIQMVR.F	2123.04833	2	2.06	314 NEW & 315 NEW	No & No

Table A-1 (continued).

Accession number	Peptide	MH+	z	XC	Site # in Swiss/Phosphosite (06/17/08)	Present in Phosphosite (06/17/08)
Q8NDX5	PHC3_HUMAN Polyhomeotic-like protein 3 (hPH3) (Homolog of polyhomeotic 3)			10.33		
	R.MDRT*PPPPTLS*PAAITVGR.G	2136.99121	3	5.84	609 Swiss/ 609 phos & 616 Swiss/ 616 phos	Yes & Yes
Q8IYB3	SRRM1_HUMAN Serine/arginine repetitive matrix protein 1			50.35		
	K.KETES*EAEDNLDDLEK.H	1944.79574	2	6.65	874 Swiss/ 874 phos	Yes
	K.KPPAPPS*PVQSQS*PSTNWSPAVPVK.K	2743.28916	3	5.37	769 Swiss/ 769 phos & 775 Swiss/ 775 phos	Yes & Yes
	K.KPPAPPS*PVQSQS*PSTNWS*PAVPVK.K	2823.25546	3	4.63	see line 125 also 781 Swiss/ 781 phos	Yes
	K.EKT*PELPEPSVK.V	1433.69232	2	2.41	220 Swiss/ 220 phos	Yes
	K.SRVS*VS*PGR.T	1104.45980	2	2.06	429 Swiss/ 429 phos & 431 Swiss/ 431 phos	Yes & Yes
	R.RYS*PPIQR.R	1096.52989	2	2.20	597 Swiss/ 597 phos	Yes
	R.RLS*PSAS*PPR.R	1227.52822	2	2.09	389 Swiss/ 389 phos & 393 Swiss/ 393 phos	Yes & Yes
	R.HRPS*PPAT*PPPK.T	1441.63883	2	2.56	402 Swiss/ 402 phos & 406 Swiss/ 406 phos	Yes & Yes
P10644	KAP0_HUMAN cAMP-dependent protein kinase type I-alpha regulatory subunit			10.20		
	R.EDEIS*PPPPNPVVK.G	1597.75090	2	3.90	83 Swiss/ 83 phos	Yes
	R.TDSREDEIS*PPPPNPVVK.G	2056.95866	2	2.86	see line 133	
P06748	NPM_HUMAN Nucleophosmin (NPM) (Nucleolar phosphoprotein B23)			20.30		
	K.DELHIVEAEAMNYEGS*PIK.V	2224.98316	2	5.47	70 Swiss/ 70 phos	Yes
	K.DELHIVEAEAMNYEGS*PIKVTLATLK.M	2951.44714	3	3.33	see line 136	
P31943	HNRH1_HUMAN Heterogeneous nuclear ribonucleoprotein H (hnRNP H)			10.30		
	R.PSGEAFVELES*EDEVK.L	1844.78372	2	3.17	63 Swiss/ New in phos	No
P16949	STMN1_HUMAN Stathmin (Phosphoprotein p19) (pp19)			10.15		
	K.ESVPEFPLS*PPK.K	1406.66029	2	2.42	38 Swiss/ 37 in phos	Yes (same AA, diff #)
	R.ASGQAFELILS*PR.S	1468.71954	2	4.00	25 Swiss/ 24 in phos	Yes (same AA, diff #)
Q14694	UBP10_HUMAN Ubiquitin carboxyl-terminal hydrolase 10			10.27		
	K.NHSVNEEEQEEQGEGS*EDEWEQVGPR.N	3107.21338	3	5.31	576 Swiss/ 576 phos	Yes

Table A-1 (continued).

Accession number	Peptide	MH+	z	XC	Site # in Swiss/Phosphosite (06/17/08)	Present in Phosphosite (06/17/08)
Q9UK76	HN1_HUMAN Hematological and neurological expressed 1 protein			10.29		
	R.RNS*SEASSGDFLDLK.G	1705.74285	2	5.40	87 Swiss/ 87 phos	Yes
	R.NS*SEASSGDFLDLK.G	1549.64174	2	5.22	see line 146	
Q13263	TIF1B_HUMAN Transcription intermediary factor 1-beta (TIF1-beta)			20.24		
	R.STAPSAAASASASASAAASS*PAGGGAEALELLEHCGVCR.E	3408.51954	3	4.90	50 Swiss/ New in phos	No
	R.SRS*GEGEVSGLMR.K	1444.62499	2	2.88	473 Swiss/ 473 phos	Yes
	R.S*GEGEVSGLMR.K	1201.49185	2	4.01	see line 150	
Q53SF7	CBLL1_HUMAN Cordon-bleu protein-like 1			10.24		
	R.AGS*LQLSSMSAGNSSLR.R	1745.78876	2	4.78	382 NEW	No
	R.QS*SLTFQSSDPEQMR.Q	1820.75204	2	2.48	1146 Swiss/ New in phos	No
O75821	IF34_HUMAN Eukaryotic translation initiation factor 3 subunit 4 (eIF-3 delta)			10.19		
	K.GIPLATGDT*SPEPELLPGAPLPPPK.E	2544.29967	3	3.15	41 Swiss/ 41 phos	Yes
Q9UKL0	RCOR1_HUMAN REST corepressor 1 (Protein CoREST)			10.17		
	R.EREES*EDELEEANGNNPIDIEVDQNK.E	3095.29605	3	3.44	257 Swiss/ 257 phos	Yes
Q6PKG0	LARP1_HUMAN La-related protein 1			30.23		
	K.GLSAS*LPDLDSENWIEVK.K	2052.95251	2	4.67	548 Swiss/ 548 phos	Yes
	R.S*LPTTVPESPNY*R.N	1620.67058	2	2.21	766 Swiss/ 766 phos	Yes
	R.SLPTTVPES*PNYR.N	1540.70428	2	2.17	774 Swiss/ 774 phos	Yes
	K.ILIVTQT*PHYMR.R	1551.77528	2	3.86	649 Swiss/ 649 phos	Yes
	R.EHRPRTASISSS*PSEGTPT*VGSYGCTPQSLPK.F	3474.53959	3	3.77	851 Swiss/ 851 phos & 858 New in Swiss/ 858 phos	Yes & Yes
	K.QEVENFKKVNM#IS*R.E	1817.86152	2	2.70	716 NEW	No
O43741	AAKB2_HUMAN 5'-AMP-activated protein kinase subunit beta-2 (AMPK beta-2 chain)			10.18		
	R.DLSSS*PPGPYGQEMYAFR.S	2081.86740	2	3.58	184 New in Swiss/ 184 phos	Yes

Table A-1 (continued).

Accession number	Peptide	MH+	z	XC	Site # in Swiss/Phosphosite (06/17/08)	Present in Phosphosite (06/17/08)
Q9Y2V2	CHSP1_HUMAN Calcium-regulated heat stable protein 1			10.12		
	R.GNVVPS*PLPTR.R	1216.60853	2	2.47	41 Swiss/ 41 phos	Yes
P12694	ODBA_HUMAN 2-oxoisovalerate dehydrogenase subunit alpha, mitochondrial precursor			20.23		
	R.S*VDEVNYWDK.Q	1334.53001	2	4.36	347 Swiss/ 347 phos	Yes
	R.IGHHS*TSDDSSAYR.S	1612.63872	3	3.68	337 Swiss/ 337 phos	Yes
Q8NEY8	PPHLN_HUMAN Periphilin-1 (Gastric cancer antigen Ga50)			10.16		
	R.DNTFFRES*PVGR.K	1504.65800	2	3.12	133 Swiss/ 133 phos	Yes
Q96JM3	K1802_HUMAN Zinc finger protein KIAA1802			70.24		
	R.KPSPSES*PEPWKPFPAVS*PEPR.R	2606.17274	3	3.89	286 Swiss/ New in phos & 297 NEW	No & No
	R.KPSGS*PDLWK.L	1194.55544	2	3.88	445 Swiss/ New in phos	No
	R.KPS*PS*ESPEPWKPFPAVSPEPR.R	2606.17274	3	3.41	282 Swiss/ New in phos & 284 NEW	No & No
	K.TAPTLS*PEHWK.A	1346.61401	2	3.05	405 Swiss/ New in phos	No
	R.RPAPAVS*PGSWK.P	1332.64598	2	2.96	308 Swiss/ 308 phos	Yes
	R.GGS*PDLWK.S	939.39714	2	2.23	476 Swiss/ 476 phos	Yes
	R.KPGPPLS*PEIR.S	1270.65548	2	2.17	427 Swiss/ 427 phos	Yes
	R.KTS*PASLDFPESQK.S	1614.74106	2	4.31	459 Swiss/ New in phos	No
	R.KT*SPASLDFPES*QKS*SR.G	2104.83883	2	2.27	458 NEW & 468 NEW & 471 NEW	No & No & No
Q15459	SF3A1_HUMAN Splicing factor 3 subunit 1 (Spliceosome-associated protein 114)			10.25		
	K.FGESEEVEMEVES*DEEDDKQEK.A	2697.02806	3	3.62	329 Swiss/ 329 phos	Yes
Q9UL54	TAOK2_HUMAN Serine/threonine-protein kinase TAO2			20.19		
	K.MLLARHS*LDQDLLR.E	1760.88769	3	3.51	656 NEW	No
	R.HS*LDQDLLR.E	1176.54085	2	2.14	see line 188	

Table A-1 (continued).

Accession number	Peptide	MH+	z	XC	Site # in Swiss/Phosphosite (06/17/08)	Present in Phosphosite (06/17/08)
Q15139	KPCD1_HUMAN Serine/threonine-protein kinase D1 (nPKC-D1)			20.21		
	R.RLS*NVS*LTGVSTIR.T	1662.79752	2	4.19	205 Swiss/ 205 phos & 208 New in Swiss/ 208 phos	Yes & Yes
	R.RLS*NVSLTGVSTIR.T	1582.83122	2	3.50	see line 191	
	R.T*SS*AELST*SAPDEPLLQKSPSESFIGREK.R	3331.44188	3	3.04	217 NEW & 219 New in Swiss/ 219 phos & 224 NEW	No & Yes & No
Q9UEW8	STK39_HUMAN STE20/SPS1-related proline-alanine-rich protein kinase			20.27		
	K.TEDGDWEWS*DDEMDEK.S	2066.68447	2	4.93	387 New in Swiss/ 387 phos	Yes
	K.ADMWSFGITAIELATGAAPY*HKY*PPMK.V	3126.39053	3	3.26	275 NEW & 278 NEW	No & No
Q9H0B6	KLC2_HUMAN Kinesin light chain 2 (KLC 2)			30.21		
	R.RDS*APYGEYGGSWYK.A	1758.71591	2	4.27	428 NEW	No
	R.ASS*LNFLNK.S	1073.50267	2	3.81	528 Swiss/ 528 phos	Yes
	R.TLSSS*SMDLSR.R	1263.52863	2	3.67	610 New in Swiss/ 610 phos	Yes
Q32MZ4	LRRF1_HUMAN Leucine-rich repeat flightless-interacting protein 1			10.20		
	R.RGS*GDTSISIDTEASIR.E	1844.83855	2	3.99	120 New in Swiss/ 120 phos	Yes
Q15052	ARHG6_HUMAN Rho guanine nucleotide exchange factor 6			10.16		
	R.MS*GFIYQGK.I	1110.46893	2	2.94	488 Swiss/ 488 phos	Yes
P21127	CD2L1_HUMAN PITSLRE serine/threonine-protein kinase CDC2L1			10.13		
	K.AYT*PVVVTLWYR.A	1547.76576	2	2.68	595 Swiss/ 595 phos	Yes
P17812	PYRG1_HUMAN CTP synthase 1 (UTP--ammonia ligase 1)			20.29		
	R.SGSSS*PDSEITELK.F	1516.64141	2	4.44	575 Swiss/ 575 phos	Yes
	K.YIDSADLEPITS*QEEPVR.Y	2141.96381	2	2.29	347 NEW	No
P25490	TYY1_HUMAN Transcriptional repressor protein YY1 (Yin and yang 1) (YY-1)			20.22		
	K.DIDHETVVEEQIIGENS*PPDYSEYMTGK.K	3275.39735	3	4.41	247 Swiss/ 247 phos	Yes
	R.EEVVGGDDS*DGLR.A	1427.56858	2	2.26	118 Swiss/ 118 phos	Yes

Table A-1 (continued).

Accession number	Peptide	MH+	z	XC	Site # in Swiss/Phosphosite (06/17/08)	Present in Phosphosite (06/17/08)
Q16637	SMN_HUMAN Survival motor neuron protein (Component of gems 1) (Gemin-1)			10.23		
	R.GTGQS*DDSDIWDDTALIK.A	2016.84336	2	4.67	28 Swiss/ 28 phos	Yes
Q13177	PAK2_HUMAN Serine/threonine-protein kinase PAK 2 (p21-activated kinase 2)			10.19		
	K.YLS*FTPPEK.D	1161.52274	2	3.52	141 Swiss/ 141 phos	Yes
Q08945	SSRP1_HUMAN FACT complex subunit SSRP1			10.22		
	K.EGMNPSYDEYADS*DEDQHDAYLER.M	2929.07780	3	4.21	444 Swiss/ 444 phos	Yes
P35221	CTNA1_HUMAN Catenin alpha-1 (Cadherin-associated protein)			20.28		
	R.S*RTS*VQTEDDQLIAGQSAR.A	2221.94855	2	5.64	652 Swiss/ 652 phos & 655 Swiss/ 655 phos	Yes & Yes
	R.T*SVQTEDDQLIAGQSAR.A	1898.84911	2	2.85	654 Swiss/ 654 phos	Yes
Q13242	SFRS9_HUMAN Splicing factor, arginine/serine-rich 9			30.19		
	R.GSPHYFS*PFRPY	1534.65146	2	3.57	216 Swiss/ 216 phos	Yes
	R.GS*PHYFS*PFRPY	1614.61776	2	2.81	211 Swiss/ 211 phos & 216 Swiss/ 216 phos	Yes & Yes
	R.STS*YGYSR.S	1000.37714	2	2.13	189 Swiss/ 189 phos	Yes
	R.GRDS*PYQSR.G	1145.47350	2	2.73	204 Swiss/ 204 phos	Yes
O93594	AGM1_HUMAN Phosphoacetylglucosamine mutase (PAGM)			10.24		
	K.STIGVMVTAS*HNPEEDNGVK.L	2164.95801	2	4.61	64 Swiss/ New in phos	No
Q9Y6X9	MORC2_HUMAN MORC family CW-type zinc finger protein 2			10.26		
	R.SVAVS*DEEEVEEEAER.R	1886.75387	2	5.30	743 Swiss/ 743 phos	Yes
Q92934	BAD_HUMAN Bcl2 antagonist of cell death (BAD) (Bcl-2-binding component 6)			30.23		
	R.RMS*DEFVDSFK.K	1440.58648	2	4.58	118 Swiss/ 118 phos	Yes
	R.HSS*YPAGTEDDEGMGEEPSPFR.G	2474.94421	2	3.50	75 Swiss/ 75 phos	Yes
	R.S*APPNLWAAQR.Y	1290.59903	2	3.42	99 Swiss/ 99 phos	Yes

Table A-1 (continued).

Accession number	Peptide	MH+	z	XC	Site # in Swiss/Phosphosite (06/17/08)	Present in Phosphosite (06/17/08)
Q9C0C2	TB182_HUMAN 182 kDa tankyrase 1-binding protein			10.20		
	R.RFS*EGVLQSPSQDQEK.L	1914.85928	2	3.98	429 New in Swiss/ 429 phosq	Yes
	R.S*QEADVQDWEFR.K	1589.62676	2	3.95	836 Swiss/ 836 phos	Yes
	K.VST*LRES*SAMAS*PLPR.E	1941.79413	2	2.04	5 NEW & 9 NEW & 14 NEW	No & No & No
Q96B36	AKTS1_HUMAN Proline-rich AKT1 substrate 1 (40 kDa proline-rich AKT substrate)			10.22		
	R.AATAARPPAPPPAPQPPS*PTPS*PPRPTLAR.E	3124.54923	3	4.30	88 Swiss/ 88 phos & 92 Swiss/ 92 phos	Yes & Yes
	K.S*LPVSVPVWGFK.E	1395.70718	2	3.70	183 Swiss/ 183 phos	Yes
	R.LNT*SDFQK.L	1032.43974	2	2.56	246 Swiss/ 246 phos	Yes
	R.AAT*AARPPAPPPAPQPPS*PT*PSPPR.P	2666.19280	2	2.55	73 NEW & 88 Swiss/ 88 phos & 90 NEW	No & Yes & No
Q14671	PUM1_HUMAN Pumilio homolog 1 (Pumilio-1) (HsPUM)			10.20		
	R.RDS*LTGSSDLYK.R	1421.63079	2	4.05	709 New in Swiss/ 709 phos	Yes
	R.S*ASSASSLFSPSSTLFSS*SR.L	2152.88349	2	2.23	797 NEW	No
P08559	ODPA_HUMAN Pyruvate dehydrogenase E1 component alpha subunit			20.25		
	R.YHGHS*MSDPGVS*YR.T	1752.62365	2	4.94	293 Swiss/ 293 phos & 300 Swiss/ 300 phos	Yes & Yes
	R.YGMGTS*VER.A	1079.42271	2	3.43	232 Swiss/ 232 phos	Yes
	R.YHGHSMS*DPGVSYR.T	1672.65735	3	3.83	295 Swiss/ 295 phos	Yes
Q9UQ35	SRRM2_HUMAN Serine/arginine repetitive matrix protein 2			30.31		
	R.HGGS*PQPLATTPLSQEPVNPPSEAS*PTR.D	3012.34993	3	6.13	377 Swiss/ 377 phos & 398 Swiss/ 398 phos	Yes & Yes
	K.SST*PPGESYFGVSSLQLK.G	1963.90483	2	3.36	1043 Swiss/ 1043 phos	Yes
	R.S*RT*PLLPR.K	1099.50603	2	2.13	2032 Swiss/ 2032 phos & 2034 Swiss/ 2034 phos	Yes & Yes
	R.GPS*PEGSS*ST*ESSPEHPPK.S	2133.74499	2	2.18	1648 NEW & 1653 NEW & 1655 NEW	No & No & No
	R.AHRSTSADS*ASSS*DTS*R.S	1962.66266	2	2.07	268 NEW & 272 NEW & 275 NEW	No & No & No
	R.QS*PSRS*SSPQPK.V	1445.58210	2	2.01	908 Swiss/ 908 phos & 912 NEW	Yes & No

Table A-1 (continued).

Accession number	Peptide	MH+	z	XC	Site # in Swiss/Phosphosite (06/17/08)	Present in Phosphosite (06/17/08)
P98175	RBM10_HUMAN RNA-binding protein 10 (RNA-binding motif protein 10)			20.16		
	R.HRHS*PTGPPGFPR.D	1522.70629	3	3.06	189 NEW	No
	R.Y*GATDRSQDDGGENRS*R.D	2043.75527	2	2.07	16 NEW	No
Q9BW71	HIRP3_HUMAN HIRA-interacting protein 3			10.24		
	K.SLKES*EQES*EEEILAQK.K	2136.89847	2	4.73	223 Swiss/ 223 phos & 227 Swiss/ 227 phos	Yes
Q9BSJ8	FA62A_HUMAN Protein FAM62A (Membrane-bound C2 domain-containing protein)			10.12		
	R.KLDVSVKSNS*SFMS*R.E	1844.80128	2	2.43	1063 NEW & 1067 NEW	No & No
Q9UKS6	PACN3_HUMAN Protein kinase C and casein kinase substrate in neurons protein 3			10.23		
	R.DGTAPPPQSPGSPGTGQDEEWS*DEESPR.K	2990.19594	3	4.58	354 Swiss/ 354 phos	Yes
P24844	MLRN_HUMAN Myosin regulatory light chain 2, smooth muscle isoform			10.19		
	R.ATS*NVFAMFDQSQIQEFK.E	2170.95147	2	3.81	20 Swiss/ 20 phos	Yes
P04792	HSPB1_HUMAN Heat-shock protein beta-1 (HspB1) (Heat shock 27 kDa protein)			20.26		
	R.QLS*SGVSEIR.H	1155.54051	2	2.96	82 Swiss/ 82 phos	Yes
	R.GPS*WDPFR.D	1041.41894	2	2.81	15 Swiss/ 15 phos	Yes
P05455	LA_HUMAN Lupus La protein (Sjoegren syndrome type B antigen)			20.26		
	K.FAS*DDEHDEHDENGATGPVK.R	2249.86186	3	3.37	366 Swiss/ 366 phos	Yes
	R.SPS*KPLPEVTDEYK.N	1669.77203	2	3.12	94 NEW	No
O60841	IF2P_HUMAN Eukaryotic translation initiation factor 5B (eIF-5B)			10.20		
	K.NKPGPNIES*GNEDDDASFK.I	2113.87097	2	4.07	214 Swiss/ 214 phos	Yes
P51114	FXR1_HUMAN Fragile X mental retardation syndrome-related protein 1 (hFXR1p)			20.27		
	R.RGPNYTSGYGTNSELSNPS*ETESER.K	2812.16934	3	5.34	409 Swiss/ 409 phos	Yes
	R.RGPNYTSGYGTNSELS*NPS*ETESER.K	2892.13564	3	3.84	406 Swiss/ 406 phos & 409 Swiss/ 409 phos	Yes & Yes

Table A-1 (continued).

Accession number	Peptide	MH+	z	XC	Site # in Swiss/Phosphosite (06/17/08)	Present in Phosphosite (06/17/08)
P08238	HS90B_HUMAN Heat shock protein HSP 90-beta (HSP 84) (HSP 90)			30.23		
	K.IEDVGS*DEEDDSGKDK.K	1817.69602	2	4.59	255 Swiss/ 254 phos	Yes (same AA, diff #)
	K.IEDVGS*DEEDDSGK.D	1574.57412	2	3.78	see line 281	
	K.IEDVGS*DEEDDSGKDKK.K	1945.79099	3	3.00	see line 281	
	R.EKEIS*DDEAEEEK.G	1630.63672	2	4.07	226 Swiss/ 225 phos	Yes (same AA, diff #)
Q9UEE9	CFDP1_HUMAN Craniofacial development protein 1 (Bucentaur)			10.18		
	K.LDWES*FKEEEGIGEELAIHNR.G	2581.16061	3	3.66	250 New in Swiss/ 250 phos	Yes
Q9Y383	LC7L2_HUMAN Putative RNA-binding protein Luc7-like 2			10.18		
	R.AMLDQLMGTS*R.D	1302.55815	2	3.69	18 New in Swiss/ 18 phos	Yes
Q99613	IF38_HUMAN Eukaryotic translation initiation factor 3 subunit 8 (eIF3 p110)			10.13		
	K.QPLLLS*EDEEDTKR.V	1752.80512	2	2.05	39 Swiss 39 phos	Yes
O14974	MYPT1_HUMAN Protein phosphatase 1 regulatory subunit 12A			20.22		
	K.TGS*YGALAEITASK.E	1448.66684	2	4.43	445 Swiss/ 445 phos	Yes
	K.SPLIES*TANMDNNQSQKTFKNK.E	2575.18578	2	2.49	304 NEW	No
	R.RST*QGVTLTDLQEAEK.T	1855.87968	2	5.08	696 Swiss/ 696 phos	Yes
	R.KTGS*YGALAEITASK.E	1576.76180	2	4.22	see line 292	
Q9Y3S2	ZN330_HUMAN Zinc finger protein 330 (Nucleolar cysteine-rich protein)			10.20		
	R.KDS*DTESSDLFTNLNLGR.T	2091.92300	2	4.00	291 NEW	No
P61978	HNRPK_HUMAN Heterogeneous nuclear ribonucleoprotein K			20.27		
	R.GSY*GDLGGPIITTQVTIPK.D	1996.99907	2	4.79	380 New in Swiss/ 380 phos	Yes
	R.RDYDDMS*PR.R	1234.45580	2	2.26	284 Swiss/ 284 phos	Yes
	R.GSY*GDLGGPIITT*QVTIPK.D	2076.96537	2	3.32	see line 299	
	R.DYDDMS*PR.R	1078.35469	2	2.55	see line 300	

Table A-1 (continued).

Accession number	Peptide	MH+	z	XC	Site # in Swiss/Phosphosite (06/17/08)	Present in Phosphosite (06/17/08)
P51858	HDGF_HUMAN Hepatoma-derived growth factor (HDGF)			10.13		
	R.AGDLLEDS*PK.R	1124.48708	2	2.54	165 Swiss/ 165 phos	Yes
	R.RAGDLLEDS*PK.R	1280.58819	2	3.54	see line 304	
	R.AGDLLEDS*PKRPK.E	1505.73592	2	2.64	see line 304	
	K.GNAEGS*S*DEEGKLVIDEPAK.E	2204.89953	2	5.87	132 Swiss/ 132 phos & 133 Swiss/ 133 phos	Yes & Yes
	K.KGNAEGS*S*DEEGKLVIDEPAK.E	2332.99450	3	3.80	see line 307	
	K.GNAEGS*SDEEGKLVIDEPAK.E	2124.93323	2	4.76	132 Swiss/ 132 phos	Yes
P22059	OSBP1_HUMAN Oxysterol-binding protein 1			20.20		
	R.TGS*NISGASSDISLDEQYK.H	2051.88047	2	4.00	379 Swiss/ 379 phos	Yes
	K.GDMS*DEDDENEFFDAPEIITMPENLGHK.R	3275.30682	3	3.34	351 Swiss/ 351 phos	Yes
Q8NE71	ABCF1_HUMAN ATP-binding cassette sub-family F member 1			20.17		
	K.LSVPTS*DEEDEVPAPK.P	1792.78880	2	3.36	109 Swiss/ 109 phos	Yes
	K.LSVPTS*DEEDEVPAPKPR.G	2045.94268	2	3.26	see line 314	
P55795	HNRH2_HUMAN Heterogeneous nuclear ribonucleoprotein H' (hnRNP H') (FTP-3)			10.28		
	K.HTGPNS*PDTANDGFVR.L	1764.73369	2	4.12	104 Swiss/ 104 phos	Yes
Q9BYG3	MK67I_HUMAN MKI67 FHA domain-interacting nucleolar phosphoprotein			10.19		
	K.S*QVAELNDDDKDDEIVFK.Q	2159.93799	2	3.71	247 Swiss/ 247 phos	Yes
P02545	LMNA_HUMAN Lamin-A/C (70 kDa lamin) (Renal carcinoma antigen NY-REN-32)			30.20		
	R.NKS*NEDQSMGNWQIK.R	1858.77892	2	3.00	458 NEW	No
	R.LRLS*PSPTSQR.S	1321.66236	2	2.65	390 Swiss/ 390 phos	Yes
	R.KLEST*ES*RSSFSQHAR.T	2009.84771	2	2.05	424 Swiss/ 424 phos	Yes
	R.LRLS*PS*PTSQR.S	1401.62866	2	3.69	390 Swiss/ 390 phos & 392 Swiss/ 392 phos	Yes & Yes
	R.SVGGS*GGGSFGDNLVTR.S	1646.71697	2	2.11	632 Swiss/ 632 phos	Yes

Table A-1 (continued).

Accession number	Peptide	MH+	z	XC	Site # in Swiss/Phosphosite (06/17/08)	Present in Phosphosite (06/17/08)
P06493	CDC2_HUMAN Cell division control protein 2 homolog (p34 protein kinase)			10.16		
	R.VYT*HEVVTLWYR.S	1645.77739	2	3.27	161 Swiss/ 161 phos	Yes
P49585	PCY1A_HUMAN Choline-phosphate cytidylyltransferase A			10.23		
	R.MLQAIS*PK.Q	967.46820	2	2.61	315 Swiss/ 315 phos	Yes
	K.T*SPPCS*PANLSR.H	1389.52690	2	3.20	342 New in Swiss/ 324 phos & 347 Swiss/ 347 phos	Yes & Yes
Q16204	CCDC6_HUMAN Coiled-coil domain-containing protein 6 (H4 protein)			40.26		
	R.PIS*PGLSYASHTVGFTPPTSLTR.A	2466.20644	3	5.14	367 Swiss/ New in phos	No
	R.T*VSSPIPYTPSPSSSR.P	1742.79964	2	4.29	349 NEW	No
	R.PIS*PGLSYASHTVGFT*PPTSLTR.A	2546.17274	3	3.02	367 Swiss/ New in phos & 380 NEW	No & No
	R.QLSESES*SLEMDDER.Y	1834.70481	2	2.68	327 NEW	No
	K.LDQPVS*APPS*PR.D	1423.60178	2	3.09	240 Swiss/ 240 phos & 244 Swiss/ 244 phos	Yes & Yes
Q9NTJ3	SMC4_HUMAN Structural maintenance of chromosomes protein 4			10.16		
	R.T*ESPATAAETASEELDNR.S	1971.81787	2	3.25	39 NEW	No
	K.S*S*LAMNRS*R.G	1261.41964	2	2.25	588 NEW & 589 NEW & 595 NEW	No
Q8TAQ2	SMRC2_HUMAN SWI/SNF-related matrix-associated actin-dependent regulator of chromatin subfamily C member 2			10.15		
	R.KRS*PSPSPT*PEAK.K	1541.67600	2	2.81	302 Swiss/ 302 phos	Yes
	K.DMDEPS*PVPNVEEVTLPK.T	2075.92425	2	3.05	347 Swiss/ 347 phos	Yes
Q14676	MDC1_HUMAN Mediator of DNA damage checkpoint protein 1			10.14		
	R.LLLAEDS*EEEVDFLSER.R	2073.92636	2	2.88	168 Swiss/ 168 phos	Yes
Q8WUA2	PPIL4_HUMAN Peptidyl-prolyl cis-trans isomerase-like 4 (PPIase)			10.16		
	R.INHTVILDDPFDDPPDLLIPDRSPEPT*R.E	3277.57763	3	3.15	182 NEW	No
	R.INHTVILDDPFDDPPDLLIPDRS*PEPTR.E	3277.57763	3	5.89	178 Swiss/ 178 phos	Yes
P18887	XRCC1_HUMAN DNA-repair protein XRCC1			10.20		
	K.TKPTQAAGPSS*PQKPPT*PEETK.A	2437.10472	3	4.07	447 Swiss/ 447 phos & 453 Swiss/ 453 phos	Yes & Yes

Table A-1 (continued).

Accession number	Peptide		MH+	z	XC	Site # in Swiss/Phosphosite (06/17/08)	Present in Phosphosite (06/17/08)
P07814	SYEP_HUMAN Bifunctional aminoacyl-tRNA synthetase				10.14		
	6580	K.EYIPGQPPLSQSSDSS*PTR.N	2125.94374	2	2.87	886 Swiss/ 886 phos	Yes
	7439	R.AKIDM#SS*NNGCMRDPTLY*R.C	2347.92695	2	2.07	346 NEW	No
	9047	K.HPKNPEVGLKPVWY*S*PK.V	2136.00784	2	2.00	546 NEW & 547 NEW	No & No
P27824	CALX_HUMAN Calnexin precursor				10.10		
		K.AEEDEILNRS*PR.N	1508.67405	2	2.01	583 Swiss/ 583 phos	Yes
O75494	FUSIP_HUMAN FUS-interacting serine-arginine-rich protein 1				10.23		
		R.S*FDYNYR.R	1044.38222	2	3.10	133 Swiss/ 133 phos	Yes
		R.S*RS*FDYNYR.R	1367.48166	2	2.14	131 Swiss/ 131 phos & 133 Swiss/ 133 phos	Yes & Yes
Q15773	MLF2_HUMAN Myeloid leukemia factor 2				20.16		
		R.QHMS*RMLSGGFGY*SPFLSIT*DGNMPGTR.P	3284.31644	3	3.26	29 NEW & 37 NEW & 44 NEW	No & No & No
		R.LAIQGPEDS*PSR.Q	1349.60966	2	2.53	238 Swiss/ 238 phos	Yes
Q15366	PCBP2_HUMAN Poly(rC)-binding protein 2 (Alpha-CP2) (hnRNP-E2)				10.16		
		K.PSSS*PVIFAGGQDR.Y	1497.67332	2	3.22	189 Swiss/ 189 phos	Yes
P30622	CLIP1_HUMAN Restin (Cytoplasmic linker protein 170 alpha-2) (CLIP-170)				20.21		
		K.LT*NLQENLSEVSQVKETLEK.E	2382.17995	2	3.75	822 Swiss/ 822 phos	Yes
		K.TISSEKAS*S*TPSS*ETQEEFVDDFRVGER.V	3358.34362	3	3.20	43 NEW & 44 NEW & 48 NEW	No & No & No
		R.VM#ATTSASLKRSPSASSLSSMS*SVASS*VSSR.P	3222.44184	3	3.19	320 NEW & 325 NEW	No & No
		R.SPSASSLS*SMS*SVASSVSSRPSR.T	2401.01016	2	2.02	317 NEW & 320 NEW	No & No
		K.RS*PSASS*LSSM#SSVASSVSSR.P	2232.92027	2	2.01	310 NEW & 315 NEW	No & No
		K.EPSATPPIS*NLTKTAS*ESISNLSEAGS*IK.K	3169.39895	3	3.11	186 NEW & 193 NEW & 204 Swiss/ 204 phos	No & No & Yes
P11717	MPRI_HUMAN Cation-independent mannose-6-phosphate receptor precursor				30.17		
		K.LVSFHDDS*DEDLLHI	1834.78947	2	2.22	2484 Swiss/ 2484 phos	Yes

Table A-1 (continued).

Accession number	Peptide	MH+	z	XC	Site # in Swiss/Phosphosite (06/17/08)	Present in Phosphosite (06/17/08)
O00567	NOP56_HUMAN Nucleolar protein Nop56 (Nucleolar protein 5A)			10.15		
	K.EELMSS*DLEETAGSTSIPK.R	2103.90391	2	3.07	520 Swiss/ 520 phos	Yes
P52756	RBM5_HUMAN RNA-binding protein 5 (RNA-binding motif protein 5)			10.18		
	R.GLVAAYSGDS*DNEEELVER.L	2132.90193	2	3.53	624 Swiss/ 624 phos	Yes
Q8ND30	LIPB2_HUMAN Liprin-beta-2			10.16		
	R.T*QSGNFYTDTLGMAEFR.R	2017.83610	2	3.11	510 NEW	No
P40222	TXLNA_HUMAN Alpha-taxilin			10.13		
	R.RPEGPGAQAPSS*PR.V	1486.67980	2	2.58	515 Swiss/ 515 phos	Yes
Q8IWS0	PHF6_HUMAN PHD finger protein 6 (PHD-like zinc finger protein)			10.17		
	K.TAHNSEADLEESFNEHELEPSS*PK.S	2777.15737	3	3.42	155 Swiss/ 155 phos	Yes
Q13595	TRA2A_HUMAN Transformer-2 protein homolog (TRA-2 alpha)			30.15		
	R.PTHS*GGGGGGGGGGGGGGGRRR.D	1901.82228	3	3.05	215 NEW	No
	R.AHT*PTPGIYMGR.P	1380.61297	2	2.77	202 NEW	No
	R.RS*PS*PYYSR.Y	1272.48093	2	2.09	260 Swiss/ 260 phos & 262 Swiss/ 262 phos	Yes & Yes
	R.S*PS*PYYSR.Y	1116.37982	2	2.99	see line 386	
	R.RRDSY*YDR.G	1210.50005	2	2.27	237 NEW	No
	R.RRS*PSPYY*SR.Y	1428.58204	2	2.02	260 Swiss/ 260 phos & 265 New in Swiss/ 265 in phos	Yes & Yes
Q13489	BIRC3_HUMAN Baculoviral IAP repeat-containing protein 3			10.19		
	-.M#NIVENS*IFLS*NLMK.S	1928.82979	2	3.74	7 NEW & 11 NEW	No & No
P49736	MCM2_HUMAN DNA replication licensing factor MCM2			10.15		
	R.GLLYDS*DEEDEERPAR.K	1973.81239	2	2.73	139 Swiss/ 139 phos	Yes
	R.VM#LES*FIDTQK.F	1406.62726	2	2.69	801 NEW	No

Table A-1 (continued).

Accession number	Peptide	MH+	z	XC	Site # in Swiss/Phosphosite (06/17/08)	Present in Phosphosite (06/17/08)
Q12968	NFAC3_HUMAN Nuclear factor of activated T-cells, cytoplasmic 3 (NF-ATc3)			10.13		
	R.PS*S*DSGCSHDSVLS*GQR.S	1958.63875	2	2.66	730 NEW & 731 NEW & 742 NEW	No & No & No
Q9H410	CT172_HUMAN Uncharacterized protein C20orf172			10.20		
	K.SLHLS*PQEQSASYQDR.R	1925.83888	2	3.94	81 NEW	No
Q9ULU4	PKCB1_HUMAN Protein kinase C-binding protein 1 (Rack7)			10.15		
	R.RIS*LSDMPR.S	1154.53874	2	2.48	425 New in Swiss/ 425 phos	Yes
	K.S*DSSDSEYISDDEQK.S	1784.63817	2	2.95	595 NEW	No
P31321	KAP1_HUMAN cAMP-dependent protein kinase type I-beta regulatory subunit			10.14		
	-.M#ASPPACPS*EEDESLK.G	1786.69106	2	2.77	9 NEW	No
Q7L7X3	TAOK1_HUMAN Serine/threonine-protein kinase TAO1			10.14		
	R.AS*DPQSPPQVS*R.H	1428.55555	2	2.22	417 New in Swiss/ 417 phos	Yes
P51587	BRCA2_HUMAN Breast cancer type 2 susceptibility protein			10.15		
	K.VFADIQS*EEILQHNQNMSGLEKVS*K.I	3004.35223	3	3.01	1926 NEW	No
Q8TF66	LRC15_HUMAN Leucine-rich repeat-containing protein 15 precursor (hLib)			10.13		
	R.M#LANLQNIS*LQNNRLR.Q	1994.00007	2	2.64	371 NEW	No
Q5VT25	MRCKA_HUMAN Serine/threonine-protein kinase MRCK alpha			20.12		
	R.HSTAS*NSS*NLSSPPS*PASPR.K	2220.83587	2	2.16	1700 NEW & 1703 NEW & 1710 NEW	No & No & No
	R.TVFSGS*VSIPS*ITK.S	1582.71647	2	2.05	1611 NEW & 1616 NEW	No & No
Q9UMY1	NOL7_HUMAN Nucleolar protein 7 (Nucleolar protein of 27 kDa)			10.15		
	K.VQSVS*QNKSY*LAVRLK.D	1979.97146	2	2.94	167 NEW & 172 NEW	No & No
P28161	GSTM2_HUMAN Glutathione S-transferase Mu 2 (GSTM2-2) (GST class-mu 2)			10.16		
	K.S*S*RFLPRPVFTK.M	1594.75419	2	3.02	200 NEW & 201 NEW	No & No

Table A-1 (continued).

Accession number	Peptide	MH+	z	XC	Site # in Swiss/Phosphosite (06/17/08)	Present in Phosphosite (06/17/08)
Q9UKX3	MYH13_HUMAN Myosin-13 (Myosin heavy chain 13)			10.14		
	R.VEEKES*LISQLT*K.S	1663.75906	2	2.79	1300 NEW & 1306 NEW	No & No
P55199	ELL_HUMAN RNA polymerase II elongation factor ELL			10.14		
	R.KSGAS*AVSGGS*GVS*QR.P	1674.62844	2	2.82	194 NEW & 200 NEW & 203 NEW	No & No & No
Q9BXT6	M10L1_HUMAN Putative helicase Mov10l1			20.13		
	K.WEDDSRNHGSPS*DCGPR.V	1994.74466	2	2.63	113 NEW	No
	K.SSQALT*S*AKTTVVVTAQK.R	1979.94497	2	2.59	472 NEW & 473 NEW	No & No
Q14181	DPOA2_HUMAN DNA polymerase subunit alpha B			10.17		
	R.GGAGNIS*LKVLGCPEALTGSYKSMFQK.L	2836.37728	3	3.42	192 NEW	No
Q12824	SNF5_HUMAN SWI/SNF-related matrix-associated actin-dependent regulator of chromatin subfamily B member 1			10.14		
	R.YPS*LWRRLATVEER.K	1855.92143	2	2.26	49 NEW	No
Q8IWV8	UBR2_HUMAN E3 ubiquitin-protein ligase UBR2 (N-recognin-2)			20.16		
	K.M#RES*SPTSPVAET*EGTIMEESSRDK.D	2930.18316	3	3.28	1005 NEW & 1014 NEW	No & No
	K.MRESS*PT*SPVAETEGTIMEES*SRDK.D	2994.15456	3	3.01	1006 NEW & 1008 NEW & 1022 NEW	No & No & No
P49006	MRP_HUMAN MARCKS-related protein (MARCKS-like protein 1)			30.22		
	R.GDVTAEEAAGAS*PAK.A	1453.62061	2	4.03	22 Swiss/ 21 phos	Yes (same AA, diff #)
	K.LSGLS*FK.R	831.40117	2	2.35	104 Swiss/ 103 phos	Yes (same AA, diff #)
	K.LSGLS*FKR.N	987.50228	2	2.21	see line 433	
Q99733	NP1L4_HUMAN Nucleosome assembly protein 1-like 4			10.24		
	R.REFITGDVEPTDAESEWHS*ENEEEEK.L	3172.29024	3	3.40	125 Swiss/ 125 phos	Yes
Q13541	4EBP1_HUMAN Eukaryotic translation initiation factor 4E-binding protein 1			20.24		
	R.VVLGDGVQLPPGDYSTT*PGGTLFSTT*PGGTR.I	3207.46462	3	4.48	37 Swiss/ 36 phos & 46 Swiss/ 45 phos	Yes (same AA, diff #)
	R.RVVLGDGVQLPPGDYSTT*PGGTLFSTT*PGGTR.I	3363.56573	3	4.23	see line 438	

Table A-1 (continued).

Accession number	Peptide	MH+	z	XC	Site # in Swiss/Phosphosite (06/17/08)	Present in Phosphosite (06/17/08)
Q9H6Z4	RANB3_HUMAN Ran-binding protein 3 (RanBP3)			10.18		
	R.TSS*LTQFPPSQSEER.S	1773.76907	2	3.57	126 Swiss/ 126 phos	Yes
P42566	EP15_HUMAN Epidermal growth factor receptor substrate 15 (Protein Eps15)			10.17		
	R.S*SPELLPSGVTDENEVTTAVTEK.V	2483.14362	2	3.43	562 Swiss/ New in phos	No
P62258	1433E_HUMAN 14-3-3 protein epsilon (14-3-3E)			10.32		
	K.AAFDDAIAELDTLS*EESYK.D	2167.93184	2	3.58	210 Swiss/ New in phos	No
O46021	RL1D1_HUMAN Ribosomal L1 domain-containing protein 1			10.12		
	K.ATNES*EDEIPQLVPIGK.K	1919.89975	2	2.09	361 Swiss/ 361 phos	Yes
P29966	MARCS_HUMAN Myristoylated alanine-rich C-kinase substrate (MARCKS)			20.11		
	K.LSGFS*FK.K	865.38552	2	2.27	170 Swiss/ 170 phos	Yes
	K.LSGFS*FKK.N	993.48048	2	2.25	see line 449	
O95400	CD2B2_HUMAN CD2 antigen cytoplasmic tail-binding protein 2			10.19		
	K.HSLDS*DEEEDDDDGGSSK.Y	2016.68256	2	3.71	49 Swiss/ 49 phos	Yes
P05783	K1C18_HUMAN Keratin, type I cytoskeletal 18 (Cytokeratin-18)			50.33		
	R.PVSSAAS*VYAGAGGSGSR.I	1660.73262	2	6.03	34 Swiss/ 33 phos	Yes (Same AA, diff #)
	R.LLEDGEDFNLGDALDSSNS*MQTIQK.T	2820.22810	3	4.90	401 Swiss/ 400 phos	Yes (Same AA, diff #)
	R.STS*FRGGM#GSGGLATGIAGGLAGMGGIQNEK.E	2935.34374	3	3.62	53 Swiss/ 52 phos	Yes (Same AA, diff #)
	R.ST*FSTNYR.S	1055.41934	2	2.57	8 Swiss/ 7 phos	Yes (Same AA, diff #)
	R.S*LGSVQAPSYGAR.P	1372.62564	2	2.47	15 Swiss/ New in phos	No
Q96QR8	PURB_HUMAN Transcriptional activator protein Pur-beta			30.26		
	R.DSLGDFIEHYAQLGPSS*PEQLAAGAEEGGGPR.R	3335.48519	3	5.18	101 Swiss/ 101 phos	Yes
	R.RGGGS*GGGEES*EGEEVDED	2011.64371	2	2.62	298 Swiss/ 298 phos & 304 Swiss/ 304 phos	Yes & Yes
	R.RGGGSGGGEES*EGEEVDED	1931.67741	2	2.41	see line 461	

Table A-1 (continued).

Accession number	Peptide	MH+	z	XC	Site # in Swiss/Phosphosite (06/17/08)	Present in Phosphosite (06/17/08)
Q5BKZ1	ZN326_HUMAN Zinc finger protein 326			10.21		
	R.SMDSYLNQS*YGMDNHSGGGGGSR.F	2456.92310	3	4.21	56 NEW	No
P29692	EF1D_HUMAN Elongation factor 1-delta (EF-1-delta)			10.20		
	R.ATAPQTQHVS*PMR.Q	1503.67736	2	3.75	133 Swiss/ New in phos	No
Q9UGV2	NDRG3_HUMAN Protein NDRG3			10.25		
	R.THS*TSSSLGSGESPFSR.S	1803.75448	2	5.00	331 Swiss/ 331 phos	Yes
Q05519	SFR11_HUMAN Splicing factor arginine/serine-rich 11			20.21		
	K.LNHVAAGLVS*PSLK.S	1485.78248	2	4.28	207 Swiss/ 207 New in pho	No
	R.DYDEEEQGYDS*EKEK.K	1943.70659	2	3.00	434 Swiss/ 434 phso	Yes
P25788	PSA3_HUMAN Proteasome subunit alpha type 3 (Proteasome component C8)			10.28		
	K.ESLKEEDES*DDDNM	1735.58878	2	5.58	250 Swiss/ 249 phos	Yes (Same AA, diff #)
Q6UN15	FIP1_HUMAN Pre-mRNA 3'-end-processing factor FIP1 (FIP1-like 1)			10.20		
	R.DHS*PTPSVFNSDEER.Y	1796.71228	2	3.83	492 Swiss/ 492 pho	Yes
Q9NYB0	TE2IP_HUMAN Telomeric repeat-binding factor 2-interacting protein 1			10.21		
	K.YLLGDAPVS*PSSQK.L	1541.72469	2	4.30	203 Swiss/ 203 phos	Yes
P27816	MAP4_HUMAN Microtubule-associated protein 4 (MAP 4)			40.27		
	K.DMES*PTKLDVTLAK.D	1627.76484	2	4.73	280 Swiss/ 280 phos	Yes
	K.VGS*LDNVGHLPAGGAVK.T	1670.82613	2	3.62	1073 Swiss/ 1073 phos	Yes
	K.DMS*PLSETEMALGK.D	1588.66341	2	3.06	507 Swiss/ 507 phos	Yes
	K.T*STSKAKTQPTSLPK.Q	1654.84111	2	2.19	712 NEW	No
	K.VGS*TENIK.H	927.41827	2	2.02	941 NEW	No
P08729	K2C7_HUMAN Keratin, type II cytoskeletal 7 (Cytokeratin-7)			20.32		
	R.T*LNETELTELQS*QISDTSVVLSMDNSR.S	3170.38472	3	6.39	227 NEW & 238 NEW	No & No
	R.T*LNETELT*ELQSQISDTSVVLSM#DNSR.S	3186.37962	3	4.13	227 NEW & 234 NEW	No & No

Table A-1 (continued).

Accession number	Peptide	MH+	z	XC	Site # in Swiss/Phosphosite (06/17/08)	Present in Phosphosite (06/17/08)
Q9H307	PININ_HUMAN Pinin (140 kDa nuclear and cell adhesion-related phosphoprotein)			10.20		
	K.S*LSPGKENVSALDMEK.E	1784.81358	2	3.95	441 Swiss/ 440 phos	Yes (Same AA, diff #)
Q9BQE3	TBA6_HUMAN Tubulin alpha-6 chain (Alpha-tubulin 6)			10.31		
	K.TIGGGDDS*FNTFFSETGAGK.H	2087.85934	2	5.65	48 Swiss/ 48 phos	Yes
Q93009	UBP7_HUMAN Ubiquitin carboxyl-terminal hydrolase 7 (Ubiquitin thioesterase 7)			10.21		
	K.AGEQQLS*EPEDMEMEAGDTDDPPR.I	2727.04333	3	4.29	18 Swiss/ 18 phos	Yes
P52597	HNRPF_HUMAN Heterogeneous nuclear ribonucleoprotein F (hnRNP F)			10.32		
	K.ATENDIYNFFS*PLNPVR.V	2076.94262	2	3.97	310 Swiss/ New in pho	No
Q13185	CBX3_HUMAN Chromobox protein homolog 3			10.27		
	K.SLS*DSESDDSK.S	1249.44673	2	3.53	95 Swiss/ 95 phos	Yes
Q8TE77	SSH3_HUMAN Protein phosphatase Slingshot homolog 3 (SSH-3L) (hSSH-3L)			20.26		
	R.S*PPGSGASTPVGPWDQAVQR.R	2073.93893	2	4.31	4 NEW	No
	R.RQS*FAVLR.G	1056.53497	2	3.05	37 New in Swiss/ 37 phos	Yes
Q9NR30	DDX21_HUMAN Nucleolar RNA helicase 2 (Nucleolar RNA helicase II)			10.20		
	K.NEEPS*EEEIDAPKPK.K	1791.76840	2	4.09	121 Swiss/ 121 pho	Yes
O95359	TACC2_HUMAN Transforming acidic coiled-coil-containing protein 2			10.18		
	K.LDNTPAS*PPRS*PAEPNDIPIAK.G	2460.12070	3	3.68	2317 Swiss/ New in phos & 2321 NEW	No & No
Q86W92	LIPB1_HUMAN Liprin-beta-1			10.26		
	R.SQS*TTFNPDDMSEPEFK.R	2039.79396	2	5.12	601 Swiss/ New in phos	No

Table A-1 (continued).

Accession number	Peptide	MH+	z	XC	Site # in Swiss/Phosphosite (06/17/08)	Present in Phosphosite (06/17/08)
P23588	IF4B_HUMAN Eukaryotic translation initiation factor 4B (eIF-4B)			50.27		
	K.SPPY*TAFLGNLPYDVTEESIK.E	2421.12612	2	4.84	96 NEW	No
	R.RES*EKS*LENETLNK.E	1836.77757	2	3.92	442 NEW & 445 Swiss/ New in phos	No & No
	R.ARPATDS*FDDYPPR.R	1687.71116	2	3.20	207 NEW	No
	R.HPS*WRS*EETQER.E	1701.64174	2	2.11	406 Swiss/ 406 phos & 409 NEW	Yes & No
	K.PRST*PEEDDSS*AS*TSQSTR.A	2277.79446	2	2.07	341 NEW & 348 NEW & 350 NEW	No & No & No
	K.YAALS*VDGEDENEGEDYAE	2155.78630	2	4.50	597 Swiss/ New in phos	No
O15164	TIF1A_HUMAN Transcription intermediary factor 1-alpha (TIF1-alpha)			20.16		
	K.SEWLDPSQKS*PLHVGETR.K	2145.99644	3	3.26	811 Swiss/ New in phos	No
	R.SILTSLLLNSS*QSS*T*SEETVLR.S	2605.14458	2	2.00	768 Swiss/ 768 phos & 771 NEW & 772 NEW	Yes & No & No
P46821	MAP1B_HUMAN Microtubule-associated protein 1B (MAP 1B)			20.18		
	K.LGDVS*PTQIDVSQFGSFK.E	2004.93138	2	3.59	1501 Swiss/ 1501 phos	Yes
	K.TTSPPEVS*GYS*Y*EK.T	1784.61039	2	2.12	1970 NEW & 1973 NEW & 1974 Swiss/ 1974 phos	No & No & Yes
Q06265	EXOS9_HUMAN Exosome complex exonuclease RRP45 (Exosome component 9)			20.20		
	K.APIDTS*DVEEK.A	1283.54024	2	3.89	306 NEW	No
Q8WUZ0	BCL7C_HUMAN B-cell CLL/lymphoma 7 protein family member C			20.28		
	K.GTEPS*PGGTPQPSRPVS*PAGPPEGVPEEAQPPR.L	3419.53041	3	5.64	114 Swiss/ 114 phos & 126 Swiss/ 126 phos	Yes & Yes
	K.GTEPS*PGGT*PQPSRPVSPAGPPEGVPEEAQPPR.L	3419.53041	3	3.07	118 Swiss/ 118 phos	Yes
O43290	SNUT1_HUMAN U4/U6.U5 tri-snRNP-associated protein 1			10.26		
	R.RVS*EVEEEKEPVPQPLPSDDTR.V	2616.21885	3	5.18	448 Swiss/ 448 phos	Yes
	R.DLQGLT*VEHAIDSFREGETMILT*LKDK.G	3219.50438	3	3.16	258 NEW	No
	K.KMSSS*DT*PLGT*VALLQEK.Q	2144.89865	2	2.08	762 NEW & 764 NEW & 768 NEW	No & No & No
	K.KMS*S*S*DTPLGTVALLQEKQK.A	2401.05220	2	2.36	760 NEW & 761 NEW & 762 NEW	No & No & No
	K.M#SS*SDT*PLGTVALLQEK.Q	1952.83229	2	2.13	761 NEW & 764 NEW	No & No

Table A-1 (continued).

Accession number	Peptide	MH+	z	XC	Site # in Swiss/Phosphosite (06/17/08)	Present in Phosphosite (06/17/08)
P30291	WEE1_HUMAN Wee1-like protein kinase (Wee1A kinase) (WEE1hu)			20.15		
	K.S*PAAPY*FLGSSFS*PVRCGGPGDASPR.G	2820.12888	3	3.04	127 Swiss/ New in phos & 132 NEW & 139 Swiss/ 139 phos	No & No & Yes
	K.S*RYTTEFHELEKIGS*GEFGSVFK.C	2808.23171	3	3.03	293 NEW & 307 NEW	No & No
P16333	NCK1_HUMAN Cytoplasmic protein NCK1 (NCK adaptor protein 1)			10.17		
	K.RKPS*VPDSASPADDSFVDPGER.L	2409.07179	3	3.42	85 Swiss/ 85 phos	Yes
Q9UNE7	STUB1_HUMAN STIP1 homology and U box-containing protein 1			10.20		
	R.LGAGGGS*PEKS*PSAQELK.E	1872.81395	2	3.92	19 Swiss/ 19 phos & 23 Swiss/ 23 phos	Yes & Yes
Q9BTC0	DIDO1_HUMAN Death-inducer obliterator 1 (DIO-1)			10.18		
	R.RNS*VERPAEPVAGAATPSLVEQQK.M	2614.29844	3	3.66	1456 Swiss/ New in phos	No
Q96I25	SPF45_HUMAN Splicing factor 45 (45 kDa-splicing factor)			20.20		
	R.S*MGGAAIAPPTSLVEK.D	1608.77026	2	4.06	169 NEW	No
	R.SPT*GPSNSFLANMGGTVAHK.I	2052.92084	2	3.75	224 NEW	No
Q53EL6	PDCD4_HUMAN Programmed cell death protein 4 (Nuclear antigen H731-like)			30.20		
	R.KDS*VWGSGGGQQSVNHLVK.E	2062.97056	3	3.98	313 NEW	No
	R.SGLTVPTS*PK.G	1066.51799	2	2.62	94 Swiss/ 94 phos	Yes
	K.NSSRDS*GRGDS*VS*DSGSDALR.S	2364.84896	2	2.17	71 NEW & 76 Swiss/ New in phos	No & No
Q9H2U2	IPYR2_HUMAN Inorganic pyrophosphatase 2, mitochondrial precursor (PPase 2)			20.28		
	R.SLVESVSSS*PNKESNEEEQVWHFLGK	3026.37787	3	5.60	317 Swiss/ 317 phos	Yes
	K.FKPGYLEATLNWFRLY*K.V	2226.11471	3	3.71	241 New in Swiss/ 241 phos	Yes
Q8ND56	LS14A_HUMAN LSM14 protein homolog A (Protein SCD6 homolog)			20.17		
	K.S*PTMEQAVQTASAHLPAPAAVGR.R	2370.12714	3	3.50	192 Swiss/ 192 phos	Yes
	R.SS*PQLDPLR.K	1092.50849	2	2.38	183 Swiss/ 183 phos	Yes
Q13247	SFRS6_HUMAN Splicing factor, arginine/serine-rich 6			20.18		
	R.SNS*PLPVPPSK.A	1202.58165	2	3.19	303 Swiss/ 303 phos	Yes
	R.LIVENLSS*R.C	1110.55544	2	3.14	119 NEW	No

Table A-1 (continued).

Accession number	Peptide	MH+	z	XC	Site # in Swiss/Phosphosite (06/17/08)	Present in Phosphosite (06/17/08)
Q9H7L9	SDS3_HUMAN Sin3 histone deacetylase corepressor complex component SDS3			10.24		
	K.RPAS*PSS*PEHLPATPAESPAQR.F	2443.08023	3	4.74	234 Swiss/ 234 phos	Yes
Q9BXP5	ARS2_HUMAN Arsenite-resistance protein 2			20.17		
	R.TQLWASEPGT*PPLPTSLPSQNPILK.N	2752.39569	3	3.35	544 Swiss/ 544 phos	Yes
	R.HELS*PPQK.R	1015.46081	2	2.44	74 Swiss/ 74 phos	Yes
P68366	TBA1_HUMAN Tubulin alpha-1 chain (Alpha-tubulin 1)			10.16		
	R.EDM#AALEKDY*EEVGIDSYEDEDEGEE	3105.14492	3	3.15	432 NEW	No
Q96D71	REPS1_HUMAN RalBP1-associated Eps domain-containing protein 1			30.20		
	R.TSADAQEPASPVVSPQQS*PPTS*PHTWR.K	3018.30298	3	4.01	118 Swiss/ New in phos & 122 Swiss/ New in phos	No & No
	R.RQS*SSYDDPWK.I	1448.58417	2	3.75	220 Swiss/ New in phos	No
	R.HAAS*YS*SDSENQGSY*SGVIPPPPGRGQVKK.G	3340.40717	3	3.14	63 NEW & 65 NEW & 74 New in Swis/s 74 phos	No & No & Yes
O94888	UBXD7_HUMAN UBX domain-containing protein 7			10.17		
	R.SESLIDASEDS*QLEAAIR.A	2013.90121	2	3.34	288 Swiss/ 288 phos	Yes
	R.SES*LIDASEDSQLEAAIR.A	2013.90121	2	5.19	280 Swiss/ 280 phos	Yes
	R.DFQT*ET*IRQEQELR.N	1952.81502	2	2.66	116 NEW & 118 NEW	No & No
P67809	YBOX1_HUMAN Nuclease sensitive element-binding protein 1			20.24		
	R.NYQQNYQNS*ESGEKNEGSESAPEGQAQQR.R	3337.36251	3	4.15	165 Swiss/ 165 phos	Yes
	K.NEGSES*APEGQAQQR.R	1667.66567	2	2.98	176 Swiss/ 176 phso	Yes
Q9UN36	NDRG2_HUMAN Protein NDRG2 (Protein Syld709613)			10.24		
	R.SRT*AS*LTSAASVDGNR.S	1752.73129	2	4.75	330 Swiss/ 330 phos & 332 Swiss/ 332 phos	Yes & Yes
O00264	PGRC1_HUMAN Membrane-associated progesterone receptor component 1 (mPR)			10.17		
	K.EGEEPTVYS*DEEEPKDESAR.K	2375.93984	3	3.38	181 Swiss/ 180 phos	Yes (Same AA, diff #)

Table A-1 (continued).

Accession number	Peptide		MH+	z	XC	Site # in Swiss/Phosphosite (06/17/08)	Present in Phosphosite (06/17/08)
Q9UBC2	EP15R_HUMAN Epidermal growth factor receptor substrate 15-like 1				20.23		
	7476	K.FHDTS*SPLMVTPPSAEAHWAVR.V	2516.14279	3	4.60	107 NEW	No
	9686	K.DS*LRSTPS*HGSVSSLNSTGSLSPKHS*LK.Q	3106.36424	3	3.07	235 NEW & 241 Swiss/ 241 phos	No & Yes
O00499	BIN1_HUMAN Myc box-dependent-interacting protein 1 (Bridging integrator 1)				20.22		
		K.S*PSPPDGS*PAATPEIR.V	1738.70843	2	4.46	296 Swiss/ 296 phos & 303 Swiss/ 303 phos	Yes & Yes
		K.S*PSPPDGSPAATPEIR.V	1658.74213	2	3.86	see line 582	
Q9BQI5	SGIP1_HUMAN SH3-containing GRB2-like protein 3-interacting protein 1				10.12		
		K.WVHFSDTSPEHVTPELT*PR.E	2315.04921	2	2.12	328 NEW	No
O95460	MATN4_HUMAN Matrilin-4 precursor				10.16		
		R.VGVIQYS*SQVQSVFPLR.A	1987.00482	2	3.13	79 NEW	No
Q9ULM3	YETS2_HUMAN YEATS domain-containing protein 2				10.14		
		K.T*EES*S*ELGNYVIK.I	1708.61548	2	2.85	1131 NEW & 1134 NEW & 1135 NEW	No & No & No
Q9Y233	PDE10_HUMAN cAMP and cAMP-inhibited cGMP 3',5'-cyclic phosphodiesterase 10A				10.15		
		K.S*QHLTGLTDEKVK.A	1535.74648	2	2.90	8 NEW	No
Q15054	DPOD3_HUMAN DNA polymerase subunit delta 3 (DNA polymerase subunit delta p66)				20.14		
		K.TEPEPPSVKS*S*SGENK.R	1832.73504	2	2.76	374 NEW & 375 NEW & 376 NEW	No & No & No
		K.S*KLAVT*ASIHVY*SIQK.A	1984.89450	2	2.16	90 NEW & 95 NEW & 101 NEW	No & No & No
		R.VALS*DDETKETENMR.K	1817.76227	2	2.38	307 Swiss/ New in phos	No
Q9UNZ2	NSF1C_HUMAN NSFL1 cofactor p47 (p97 cofactor p47)				10.17		
		R.KKS*PNELVDDLFK.G	1612.79818	2	3.44	114 Swiss/ 114 phos	Yes
Q9Y6W5	WASF2_HUMAN Wiskott-Aldrich syndrome protein family member 2				10.23		
		K.RS*SVVSPSHPPPAPPLGSPPGPK.P	2325.17508	3	4.64	292 NEW	No
		R.S*S*VVS*PSHPPPAPPLGSPPGPK.P	2329.00657	3	3.68	292 NEW & 293 NEW & 296 NEW	No & No & No

Table A-1 (continued).

Accession number	Peptide	MH+	z	XC	Site # in Swiss/Phosphosite (06/17/08)	Present in Phosphosite (06/17/08)
Q9BQA1	MEP50_HUMAN Methylosome protein 50 (MEP50 protein) (WD repeat protein 77)			10.16		
	R.KET*PPPLVPPAAR.E	1452.76101	2	3.22	5 Swiss/ 5 phos	Yes
P49407	ARRB1_HUMAN Beta-arrestin-1 (Arrestin beta 1)			10.16		
	R.KDLFVANVQS*FPPAPEDK.K	2081.99432	2	3.22	86 NEW	No
Q9P2B4	CT2NL_HUMAN CTTNBP2 N-terminal-like protein			10.12		
	7470 K.EQKKLS*SQLEEER.S	1683.79489	2	2.45	165 NEW	No
Q5JTD0	TJAP1_HUMAN Tight junction-associated protein 1 (Tight junction protein 4)			10.16		
	R.KDS*LTQAQEQGNLLN	1738.80070	2	3.19	545 Swiss/ 545 phos	Yes
P24043	LAMA2_HUMAN Laminin subunit alpha-2 precursor (Laminin M chain)			10.16		
	R.NS*HIAIAFDDT*KVKNR.L	1988.89902	2	3.24	2772 NEW & 2781 NEW	No & No
Q6Y7W6	PERQ2_HUMAN PERQ amino acid-rich with GYF domain-containing protein 2			10.14		
	R.PGT*PSDHQSQEASQFER.K	1980.80831	2	2.51	382 Swiss/ New in phos	No
Q86WB0	NIPA_HUMAN Nuclear-interacting partner of ALK			20.16		
	K.QSSQPAETDS*MSLSEKS*RK.V	2255.92504	3	3.15	479 NEW & 486 NEW	No & No
	R.SMGTGDT*PGLEVPSS*PLR.K	1960.81224	2	2.26	387 NEW & 395 Swiss/ 395 phos	No & Yes
Q12955	ANK3_HUMAN Ankyrin-3 (ANK-3) (Ankyrin-G)			10.15		
	R.RQS*FASLALR.K	1228.61977	2	2.97	1459 Swiss/ 1459 phos	Yes
Q15642	CIP4_HUMAN Cdc42-interacting protein 4			10.15		
	R.APSDS*SLGTPSDGRPELR.G	1921.86510	2	3.04	298 New in Swiss/ 298 phos	Yes
O15173	PGRC2_HUMAN Membrane-associated progesterone receptor component 2			10.18		
	R.LLKPGEEPSEY*TDEEDTK.D	2159.92675	3	3.57	210 New in Swiss/ 210 phos	Yes
Q8N5S9	KKCC1_HUMAN Calcium/calmodulin-dependent protein kinase kinase 1			20.12		
	R.KLS*LQER.P	953.48154	2	2.35	74 Swiss/ 74 phos	Yes
	R.LIPS*WTT*VILVKS*MLRK.R	2225.09690	2	2.14	443 NEW & 446 NEW & 452 NEW	No & No & No

Table A-1 (continued).

Accession number	Peptide		MH+	z	XC	Site # in Swiss/Phosphosite (06/17/08)	Present in Phosphosite (06/17/08)
P30086	PEBP1_HUMAN Phosphatidylethanolamine-binding protein 1 (PEBP-1)				10.23		
		K.NRPTS*ISWDGLDSGK.L	1712.76392	2	4.63	52 Swiss/ New in phos	No
Q9UQB8	BAIP2_HUMAN Brain-specific angiogenesis inhibitor 1-associated protein 2				10.22		
		K.LSDSYSNT*LPVR.K	1431.65152	2	3.93	340 New in Swiss/ 340 phos	Yes
O15530	PDPK1_HUMAN 3-phosphoinositide-dependent protein kinase 1 (hPDK1)				10.31		
		R.ANS*FVGTAQYVSPELLTEK.S	2134.01036	2	6.10	241 Swiss/ 241 phos	Yes
Q9H788	SH24A_HUMAN SH2 domain-containing protein 4A (Protein SH(2)A)				10.21		
		R.TLS*SSAQEDIIR.W	1399.64644	2	4.13	315 Swiss/ 315 phos	Yes
P18615	NELFE_HUMAN Negative elongation factor E (NELF-E) (RD protein)				10.18		
		R.SIS*ADDDLQESSR.R	1502.60061	2	3.56	115 Swiss/ 115 phos	Yes
		K.QPMLDAAT*GKSVWGS*LAVQNS*PKGCHR.D	3078.31268	3	3.44	340 NEW & 347 NEW & 353 Swiss/ 353 phos	No & No & Yes
		R.S*LSEQPVMDTATATEQAK.Q	1986.87255	2	3.56	49 NEW	No
Q9H1B7	CN004_HUMAN Protein C14orf4				20.18		
	3477	R.KAS*PEPPDSAEGALK.L	1576.72541	2	3.57	547 Swiss/ 547 phos	Yes
	3488	R.RNS*SS*PVSPASVPGQR.R	1785.76801	2	3.32	657 Swiss/ 657 phos & 659 Swiss/ 659 phos	Yes & Yes
	8184	R.QSPNSSSAAAS*VAS*RR.G	1735.71597	2	2.23	224 NEW & 227 Swiss/ New in phos	No & No
Q12857	NFIA_HUMAN Nuclear factor 1 A-type (Nuclear factor 1/A)				20.24		
		R.S*PGSGSQSSGWHEVEPGMPSPTTLK.K	2620.13849	3	4.79	300 Swiss/ 300 phos	Yes
		R.RSLPSTS*ST*SSTKR.L	1654.71966	2	2.49	273 NEW & 275 NEW	No & No
Q5UE93	PI3R6_HUMAN Phosphoinositide 3-kinase regulatory subunit 6				10.16		
		R.PS*GDGEM#LPGVSRLHTAR.V	1975.90551	2	3.21	401 NEW	No

Table A-1 (continued).

Accession number	Peptide	MH+	z	XC	Site # in Swiss/Phosphosite (06/17/08)	Present in Phosphosite (06/17/08)
P21675	TAF1_HUMAN Transcription initiation factor TFIID subunit 1			30.15		
	R.M#LLAAGS*AASGNNHRDDDTASVTSLNS*SATGR.C	3323.39946	3	3.04	1138 NEW & 1158 NEW	No & No
	R.TDPMVTLSSILES*IINDM#R.D	2231.03347	2	2.21	1391 NEW	No
	R.VGT*TVHCDYLNR.P	1457.62426	2	2.17		
	R.VGTTVHCDY*LNRPHK.S	1819.83090	2	2.89	1366 NEW	No
Q8N1N0	CLC4F_HUMAN C-type lectin domain family 4 member F			10.13		
	K.SSFDNT*S*AEIQFLR.G	1774.70843	2	2.70	313 NEW & 314 NEW	No & No
Q04726	TLE3_HUMAN Transducin-like enhancer protein 3 (ESG3)			20.18		
	R.ESSANNSVS*PSESLR.A	1643.69082	2	3.65	203 Swiss/ 203 phos	Yes
	K.DLGHNDKS*STPGLKSNTPT*PR.N	2382.04860	2	2.32	310 NEW	No
	K.SDDLVVDVSNEDPAT*PRVSPAHS*PPENGLDK.A	3417.48827	3	3.78	259 Swiss/ 259 New in phos & 267 Swiss/ 267 phos	No & Yes
	R.VS*PAHS*PPENGLDK.A	1607.65018	2	2.57	263 Swiss/ 263 phos & 267 Swiss/ 267 phos	Yes & Yes
Q5VV41	ARHGG_HUMAN Rho guanine nucleotide exchange factor 16			10.17		
	R.HQS*FGAAVLSR.E	1252.58338	2	3.25	107 NEW	No
Q12906	ILF3_HUMAN Interleukin enhancer-binding factor 3			10.16		
	K.RPMEEDGEEKS*PSK.K	1698.70403	3	3.13	382 Swiss/ 382 phos	Yes
Q96IT1	ZN496_HUMAN Zinc finger protein 496			10.16		
	R.PPS*QLS*GDPVLQDAFLLQEENVR.D	2712.23171	2	2.93	185 Swiss/ New in phos & 188 NEW	No & No
Q9UN86	G3BP2_HUMAN Ras GTPase-activating protein-binding protein 2 (G3BP-2)			10.17		
	K.STT*PPPAEPVSLPQEPPK.A	1951.94122	2	3.33	227 Swiss/ 227 phos	Yes
P55317	HNF3A_HUMAN Hepatocyte nuclear factor 3-alpha (HNF-3A)			10.17		
	K.TGQLEGAPAPGPAAS*PQTLDHSGATATGGASELK.T	3225.50593	3	3.46	332 NEW	No
P35579	MYH9_HUMAN Myosin-9 (Myosin heavy chain 9)			10.17		
	K.KMEDS*VGCLET*AEEVK.R	1927.74653	2	3.31	1376 NEW & 1382 NEW	No & No

Table A-1 (continued).

Accession number	Peptide	MH+	z	XC	Site # in Swiss/Phosphosite (06/17/08)	Present in Phosphosite (06/17/08)
P08621	RU17_HUMAN U1 small nuclear ribonucleoprotein 70 kDa (U1 snRNP 70 kDa)			10.18		
	R.YDERPGPS*PLPHR.D	1600.72675	3	3.68	226 Swiss/ 226 phos	Yes
	R.GGGGGQDNGLEGLGNDS*R.D	1739.69803	2	3.35	410 Swiss/ 410 phos	Yes
Q13315	ATM_HUMAN Serine-protein kinase ATM (Ataxia telangiectasia mutated)			20.16		
	K.RSLES*VYS*LYPTLSR.L	1930.87107	2	3.21	2165 NEW & 2168 NEW	No & No
	K.M#LQPIT*R.L	954.44778	2	2.01	2031 NEW	No
Q9UKM9	RALY_HUMAN RNA-binding protein Raly			10.13		
	R.GRLS*PVPVPR.A	1157.61904	2	2.68	135 Swiss/ 135 phos	Yes
	R.AAS*AIYSGYIFDYDYYR.D	2117.88918	2	5.64	206 NEW	No
Q9BSG1	ZNF2_HUMAN Zinc finger protein 2 (Zinc finger 2.2) (Zinc finger protein 661)			10.15		
	K.VFSSKS*SVIQHQR.R	1582.77370	2	2.67	410 NEW	No
Q6ZMT1	STAC2_HUMAN SH3 and cysteine-rich domain-containing protein 2			10.19		
	R.SSFSS*T*SESPTRSLSER.D	2004.79468	2	3.71	224 NEW & 225 NEW	No & No
P85037	FOXK1_HUMAN Forkhead box protein K1 (Myocyte nuclear factor)			20.14		
	R.S*APAS*PTHPGLMSPR.S	1665.68552	2	2.77	416 Swiss/ 416 phos & 420 Swiss/ 420 phos	Yes & Yes
	R.EGS*PIPHDPEFGSK.L	1576.66790	2	2.13	445 Swiss/ 445 phos	
O15062	ZBTB5_HUMAN Zinc finger and BTB domain-containing protein 5			10.13		
	K.HYLTTRTLPMS*PPSER.V	1965.92519	2	2.59	127 NEW	No\
Q9H2M9	RBGPR_HUMAN Rab3 GTPase-activating protein non-catalytic subunit			10.16		
	K.QDFS*PEVLKLANEER.D	1854.86330	2	3.28	952 NEW	No
P22626	ROA2_HUMAN Heterogeneous nuclear ribonucleoproteins A2/B1 (hnRNP A2 / hnRNP B1)			30.33		
	R.GFGDGYNGYGGGPGGGNFGGS*PGYGGGR.G	2575.00584	3	6.53	259 Swiss/ 259 pho	Yes
	R.NMGGPYGGGNYGPGGSGGS*GGYGGR.S	2269.87165	2	6.11	see line 693	
	R.GGNFGFGDS*R.G	1093.40983	2	3.41	212 Swiss/ 212 phos	Yes
	R.NMGGPYGGGNYGPGGS*GGSGGYGGR.S	2269.87165	2	3.97	341 Swiss/ 341 phos	Yes

Table A-1 (continued).

Accession number	Peptide	MH+	z	XC	Site # in Swiss/Phosphosite (06/17/08)	Present in Phosphosite (06/17/08)
Q9UHD8	SEPT9_HUMAN Septin-9 (MLL septin-like fusion protein)			10.29		
	R.S*FEVEEVETPNSTPPR.R	1897.82150	2	5.71	30 Swiss/ 30 phos	Yes
	K.RS*FEVEEVETPNSTPPR.R	2053.92261	2	3.64	see line 698	
	R.S*FEVEEVET*PNSTPPR.R	1977.78780	2	2.43	38 NEW & 30 Swiss/ 30 phos	No & Yes
Q8TEA8	DTD1_HUMAN Probable D-tyrosyl-tRNA(Tyr) deacylase 1			30.18		
	R.S*ASSGAEGDVSSEREP	1644.63845	2	3.65	194 NEW	No
	K.EDRS*ASSGAEGDVS*S*EREP	2204.74170	2	2.43	194 NEW & 204 Swiss/ 204 phos & 205 Swiss/ 205 phos	No & Yes & Yes
	K.EDRSAS*SGAEGDVS*S*ER.E	1978.64634	2	2.37	196 Swiss/ 196 phos & see line 703 for 204 & 205	Yes & Yes & Yes
Q5JSZ5	K0515_HUMAN Uncharacterized protein KIAA0515			10.22		
	K.LKFS*DDEEEEEVVK.D	1775.76225	2	4.37	388 Swiss/ 388 phos	Yes
P25205	MCM3_HUMAN DNA replication licensing factor MCM3			10.18		
	K.DGDSYDPYDFS*DTEEEMPQVHTPK.T	2882.10223	3	3.58	711 Swiss/ 711 phos	Yes
O95248	MTMR5_HUMAN SET-binding factor 1 (Sbf1) (Myotubularin-related protein 5)			10.16		
	R.RTTVPSGPPMT*AILER.C	1805.89792	2	3.18	546 NEW	No
Q6P6C2	ALKB5_HUMAN Alkylated repair protein alkB homolog 5			10.14		
	R.RGS*FSSENYWR.K	1468.60049	2	2.75	361 Swiss/ 361 phos	Yes
	K.YQEDS*DPERSDYEEQQLQK.E	2466.99327	3	3.45	64 New in Swiss/ 64 phos	Yes
	R.GS*FSSENYWR.K	1312.49938	2	2.31	see line 712	
	R.LET*KS*LSSSVLPPSYASDRLSGNNR.D	2838.30700	3	3.15	294 NEW & 296 NEW	Yes & Yes
Q9NX63	CHCH3_HUMAN Coiled-coil-helix-coiled-coil-helix domain-containing protein 3			10.26		
	R.YS*GAYGASVSDEELK.R	1655.68361	2	5.21	50 Swiss/ 50 phos	Yes
P21796	VDAC1_HUMAN Voltage-dependent anion-selective channel protein 1 (VDAC-1)			10.20		
	K.LTFDSSFS*PNTGK.K	1480.63554	2	3.97	104 Swiss/ 103 pho	Yes (Same AA, diff #)
Q76KP1	B4GN4_HUMAN N-acetyl-beta-glucosaminyl-glycoprotein 4-beta-N-acetylgalactosam			10.14		
	R.TLGPAAPTVDS*NLS*SEAR.P	1945.83033	2	2.81	616 NEW & 619 NEW	No & No

Table A-1 (continued).

Accession number	Peptide	MH+	z	XC	Site # in Swiss/Phosphosite (06/17/08)	Present in Phosphosite (06/17/08)
Q13573	SNW1_HUMAN SNW domain-containing protein 1 (Nuclear protein SkiP)			10.20		
	R.GPPS*PPAPVMHS*PSR.K	1673.69061	2	3.62	224 Swiss/ 224 phos & 232 Swiss/ 232 phos	Yes & Yes
Q9NPH0	PPA6_HUMAN Lysophosphatidic acid phosphatase type 6 precursor			10.13		
	R.GRRQTAS*LQPGIS*EDLK.K	2015.93105	2	2.42	223 NEW & 229 NEW	No & No
Q6WKZ4	RFIP1_HUMAN Rab11 family-interacting protein 1 (Rab11-FIP1)			10.27		
	K.HLFSS*TENLAAGSWK.E	1727.77885	2	5.33	357 Swiss/ New in phos	No
P23193	TCEA1_HUMAN Transcription elongation factor A protein 1			10.27		
	K.EPAITSQNS*PEAR.E	1479.64750	2	2.81	100 Swiss/ 100 phos	Yes
	K.KKEPAITSQNS*PEAR.E	1735.83742	3	3.12	see line 729	
O75446	SAP30_HUMAN Histone deacetylase complex subunit SAP30			10.15		
	K.DTLTYFIY*SVKNDK.N	1786.82988	2	3.06	202 NEW	No
Q07666	SAM68_HUMAN KH domain-containing, RNA-binding, signal transduction-associated protein 1			10.16		
	R.SGS*MDPSGAHPSVR.Q	1464.59369	2	3.21	20 Swiss/ 20 phos	Yes
Q9UHR4	BI2L1_HUMAN Brain-specific angiogenesis inhibitor 1-associated protein 2-like protein 1			10.21		
	K.TPASTPVSGT*PQAS*PMIER.S	2086.89155	2	4.27	257 Swis/ 257 phos & 261 Swiss/ 261 phos	Yes & Yes
P09651	ROA1_HUMAN Heterogeneous nuclear ribonucleoprotein A1			10.32		
	K.S*ESPKEPEQLR.K	1379.62022	2	2.54	4 Swiss/ 4 phos	Yes
	R.SS*GPYGGGGQYFAK.P	1455.59401	2	2.23	338 Swiss/ 338 phos	Yes
Q9Y446	PKP3_HUMAN Plakophilin-3			10.21		
	R.LS*SGFDDIDLPSAVK.Y	1643.75638	2	4.14	313 Swiss/ New in phos	No
	R.ADYDTLS*LR.S	1133.48742	2	2.91	180 New in Swiss/ 180 phos	Yes
Q96T21	SEBP2_HUMAN SECIS-binding protein 2			10.15		
	K.S*ARGSHHLSIYAENSLK.S	1949.92288	2	2.43	174 NEW	No
P52948	NUP98_HUMAN Nuclear pore complex protein Nup98-Nup96 precursor			10.17		
	R.DSENLAS*PSEYPENGER.F	1973.77601	2	3.38	623 Swiss/ 623 phos	Yes

Table A-1 (continued).

Accession number	Peptide	MH+	z	XC	Site # in Swiss/Phosphosite (06/17/08)	Present in Phosphosite (06/17/08)
P35527	K1C9_HUMAN Keratin, type I cytoskeletal 9 (Cytokeratin-9)			20.18		
	R.GSRGGSGGSY*GGGGS*GGGYGGGSGS*R.G	2331.78121	2	3.63	497 NEW & 502 NEW & 512 NEW	No & No & No
	R.GSRGGSGGS*Y*GGGGSGGGYGGGS*GSR.G	2331.78121	2	2.82	496 NEW & 497 NEW & 510 NEW	No & No & No
P51991	ROA3_HUMAN Heterogeneous nuclear ribonucleoprotein A3 (hnRNP A3)			20.29		
	R.SSGS*PYGGGYGSGGGSGGYGSR.R	1990.75627	2	5.90	358 Swiss/ 358 phos	Yes
	R.SSGSPY*GGGYGS*GGGS*GGYGSR.R	2150.68887	2	2.04	360 Swiss/ 360 phos & 366 NEW & 370 Swiss/ 370 phos	Yes & No & Yes
	R.SS*GSPY*GGGYGSGGGS*GGYGSRRF	2453.85840	3	3.00	356 Swiss/ 356 phos & see line 758 for 360 and 370	Yes & Yes & Yes
Q6P5R6	RL22L_HUMAN Ribosomal protein L22-like 1			10.19		
	R.YFQISQDEDES*ESED	1900.66439	2	3.83	118 Swiss/ 118 phos	Yes
Q96T37	RBM15_HUMAN Putative RNA-binding protein 15 (RNA-binding motif protein 15)			20.21		
	R.SLS*PGGAALGYR.D	1228.57215	2	2.74	294 Swiss/ 294 phos	Yes
	K.NS*S*GGGESRSSSRGGGGES*R.S	2107.72263	2	2.34	134 NEW & 135 NEW & 151 NEW	No & No & No
	R.SRS*PLDKDTY*PPSASVVGASVGGHR.H	2700.21779	3	4.27	259 New in Swiss/ 259 phos & 266 NEW	Yes & No
Q9UQF2	JIP1_HUMAN C-jun-amino-terminal kinase-interacting protein 1			10.14		
	K.QFVEYT*CPTEDIYLE	1929.78636	2	2.89	702 NEW	No
O96013	PAK4_HUMAN Serine/threonine-protein kinase PAK 4 (p21-activated kinase 4)			10.14		
	R.PFNT*YPR.A	974.41313	2	2.17	207 Swiss/ New in phos	No
Q15233	NONO_HUMAN Non-POU domain-containing octamer-binding protein (NonO protein)			10.24		
	R.FGQAATMEGIGAIGGT*PPAFNR.A	2243.03145	3	3.66	450 Swiss/ 450 phos	Yes
Q96PK6	RBM14_HUMAN RNA-binding protein 14 (RNA-binding motif protein 14)			10.13		
	R.RLS*ESQLSFR.R	1302.62016	2	2.27	618 Swiss/ 618 phos	Yes
P21291	CSRP1_HUMAN Cysteine and glycine-rich protein 1 (Cysteine-rich protein 1)			10.16		
	K.GFGFGQGAGALVHS*E	1513.64710	2	2.84	192 Swiss/ 191 phos	Yes (Same AA, diff #)
Q9P2K5	MYEF2_HUMAN Myelin expression factor 2 (MyEF-2) (MST156)			10.18		
	K.AEVPGATGGDS*PHLQPAEPPGEPR.R	2446.10343	3	3.66	17 Swiss/ 17 phos	Yes

Table A-1 (continued).

Accession number	Peptide	MH+	z	XC	Site # in Swiss/Phosphosite (06/17/08)	Present in Phosphosite (06/17/08)
Q96J84	KIRR1_HUMAN Kin of IRRE-like protein 1 precursor			10.15		
	R.FSQEPADQT*VVAGQR.A	1712.76392	2	2.98	31 NEW	No
Q9UHL0	DDX25_HUMAN ATP-dependent RNA helicase DDX25 (DEAD box protein 25)			10.18		
	K.WLTVEMIQDGHQVS*LLS*GELTVEQR.A	3028.38862	3	3.50	366 NEW & 369 NEW	No & No
Q5T8P6	RBM26_HUMAN RNA-binding protein 26 (RNA-binding motif protein 26)			10.13		
	K.T*QMQKELLDT*ELDLYKK.M	2256.02698	2	2.67	808 NEW & 817 NEW	No & No
Q9Y3Q4	HCN4_HUMAN Potassium/sodium hyperpolarization-activated cyclic nucleotide-gated channel 4			10.12		
	R.RGTPPLT*PGR.L	1131.56700	2	2.47	1075 NEW	No
Q8TEW8	PAR3L_HUMAN Partitioning-defective 3 homolog B (PAR3-beta)			10.20		
	R.T*QEELVAMLRST*K.Q	1665.73180	2	4.02	445 NEW	No
O60825	F262_HUMAN 6-phosphofructo-2-kinase/fructose-2,6-biphosphatase 2			10.16		
	R.RNS*FTPLSSSNTIR.R	1659.78499	2	3.16	446 Swiss/ 446 phos	Yes
Q96JC9	EAF1_HUMAN ELL-associated factor 1			10.16		
	K.T*SPLKDNPS*PEPQLDDIKR.E	2310.04139	2	3.15	158 Swiss/ 158 phos & 165 Swiss/ 165 phos	Yes & Yes
O43583	DENR_HUMAN Density-regulated protein (DRP) (Protein DRP1)			20.30		
	K.LTVENS*PKQEAGISEGQGTAGEEEEK.K	2797.24110	3	5.95	73 Swiss/ 73 phos	Yes
Q9C0C2	TB182_HUMAN 182 kDa tankyrase 1-binding protein			40.21		
	R.SPS*QDFSFIEDTEILDSAMYR.S	2531.06835	2	4.20	1554 Swiss/ 1554 phos	Yes
O14745	NHERF_HUMAN Ezrin-radixin-moesin-binding phosphoprotein 50 (EBP50)			30.33		
	R.S*ASSDTSEELNSQDSPPK.Q	1958.78624	2	6.59	288 Swiss/ 287 phos	Yes (Same AA, diff #)
	R.SAS*SDTSEELNSQDSPPK.Q	1958.78624	2	6.11	290 Swiss/ 289 phos	Yes (Same AA, diff #)
	R.EALAEAALES*PRPALVR.S	1872.95787	2	2.72	280 Swiss/ 279 phos	Yes (Same AA, diff #)
P42858	HD_HUMAN Huntingtin (Huntington disease protein) (HD protein)			10.16		
	R.VNHCLTICENIVAQS*VR.N	1978.92381	2	3.27	116 NEW	No

Table A-1 (continued).

Accession number	Peptide	MH+	z	XC	Site # in Swiss/Phosphosite (06/17/08)	Present in Phosphosite (06/17/08)
Q9Y266	NUDC_HUMAN Nuclear migration protein nudC			20.23		
	K.NGSLDS*PGKQDTEEDEEEDEKDK.G	2674.05230	3	4.56	139 Swiss/ 139 phos	Yes
O00264	PGRC1_HUMAN Membrane-associated progesterone receptor component 1 (mPR)			40.17		
	K.EGEEPTVYS*DEEEPK.D	1817.70005	2	2.75	181 Swiss/ 180 phos	Yes (Same AA, diff #)
Q9BVG4	CX026_HUMAN UPF0368 protein Cxorf26			10.16		
	K.GADS*GEEKEEGINR.E	1570.63806	2	3.20	197 NEW	No
Q13286	CLN3_HUMAN Battenin (Protein CLN3) (Batten disease protein)			10.14		
	R.RFS*DS*EGEET*VPEPR.L	1974.69183	2	2.88	12 Swiss/ 12 phos & 14 Swiss/ 14 phos & 19 NEW	Yes & Yes & No
Q5JTV8	TOIP1_HUMAN Torsin-1A-interacting protein 1			30.23		
	R.LQQQHSEQPPLQPS*PVMTR.R	2281.07946	3	3.90	143 Swiss/ 143 New in phos	No
	K.VNFSEEGET*EEDDQDSSHSSVTTVK.A	2836.13161	3	3.60	220 Swiss/ 220 New in phos	No
Q13501	SQSTM_HUMAN Sequestosome-1			10.15		
	R.LTPVS*PESSSTEEK.S	1570.68836	2	2.56	272 Swiss/ 272 phos	Yes
P20700	LMNB1_HUMAN Lamin-B1			30.30		
	R.LKLS*PS*PSSR.V	1231.54828	2	3.11	391 Swiss/ 390 phos & 393 Swiss/ 392 phos	Yes (Same AA, diff #)
	R.LKLS*PSPSSR.V	1151.58198	2	2.63	see line 810	
Q8IXT5	RB12B_HUMAN RNA-binding protein 12B (RNA-binding motif protein 12B)			20.18		
	R.FPPEDFRHS*PEDFR.R	1855.77991	3	3.55	575 Swiss/ 575 phos	Yes
O14578	CTRO_HUMAN Citron Rho-interacting kinase (CRIK)			10.16		
	R.TPLSQVNKVWDQS*S*V	1847.79758	2	2.53	2025 NEW & 2026 NEW	No & No
Q8WWM7	ATX2L_HUMAN Ataxin-2-like protein (Ataxin-2 domain protein)			10.17		
	K.EVDGLLTSEPMGS*PVSSK.T	1912.86092	2	3.27	594 Swiss/ 594 phos	Yes
P62995	TRA2B_HUMAN Arginine/serine-rich-splicing factor 10 (Transformer-2-beta)			10.26		
	K.RPHT*PTPGIYMGR.P	1562.72973	3	3.52	201 Swiss/ 201 phos	Yes

Table A-1 (continued).

Accession number	Peptide	MH+	z	XC	Site # in Swiss/Phosphosite (06/17/08)	Present in Phosphosite (06/17/08)
Q14157	UBP2L_HUMAN Ubiquitin-associated protein 2-like (Protein NICE-4)			30.22		
	R.RYPSSISSS*PQK.D	1416.65185	2	2.58	609 Swiss/ 609 phos	Yes
	K.NPS*DSAVHSPFTK.R	1466.63112	2	2.57	410 NEW	No
P31749	AKT1_HUMAN RAC-alpha serine/threonine-protein kinase (RAC-PK-alpha)			20.18		
	R.RPHFPQFS*YSASGTA	1732.74788	2	2.83	473 Swiss/ 473 phos	Yes
O14646	CHD1_HUMAN Chromodomain-helicase-DNA-binding protein 1			20.17		
	K.S*DSSPLPSEKSDEDDDK.L	1930.74370	2	3.06	1353 Swiss/ 1353 phos	Yes
	K.SDS*SPLPSEKSDEDDDK.L	1930.74370	2	2.75	1355 Swiss/ 1355 phos	Yes
O00257	CBX4_HUMAN E3 SUMO-protein ligase CBX4 (Chromobox protein homolog 4)			20.16		
	R.EEEVSGVS*DPQPQDAGSR.K	1966.80255	2	3.20	334 NEW	No
O14874	BCKD_HUMAN [3-methyl-2-oxobutanoate dehydrogenase [lipoamide]] kinase			20.15		
	R.ARS*TSAT*DTHHVEMAR.E	1929.76736	2	3.10	31 Swiss/ 31 phos & 35 Swiss/ 35 phos	Yes & Yes
Q15056	IF4H_HUMAN Eukaryotic translation initiation factor 4H (eIF-4H)			10.26		
	R.AY*SS*FGGGR.G	1061.34886	2	2.54	12 Swiss/ 11 phos & 14 NEW	Yes (Same AA, diff #) & No
Q8NC51	PAIRB_HUMAN Plasminogen activator inhibitor 1 RNA-binding protein			10.25		
	K.SKS*EEAHAEDSVMDHHFR.K	2191.88624	3	3.62	330 Swiss/ 330 phos	Yes
Q9Y478	AAKB1_HUMAN 5'-AMP-activated protein kinase subunit beta-1			10.24		
	R.S*HNNFVAILDLPEGEHQYK.F	2291.04921	3	4.80	108 Swiss/ 107 phos	Yes (Same AA, diff #)
P43243	MATR3_HUMAN Matrin-3			10.23		
	R.RDS*FDDR.G	990.36763	2	2.57	188 Swiss/ 188 phos	Yes
P18669	PGAM1_HUMAN Phosphoglycerate mutase 1 (Phosphoglycerate mutase isozyme B)			10.21		
	R.HGES*AWNLENR.F	1392.56919	2	3.91	11 Swiss/ 13 phos	Yes (Same AA, diff #)
Q96AT1	K1143_HUMAN Uncharacterized protein KIAA1143			10.20		
	R.IQPQPPDEDGDHS*DKEDEQPQVVVLK.K	3022.36770	3	3.96	50 Swiss/ 50 phos	Yes

Table A-1 (continued).

Accession number	Peptide	MH+	z	XC	Site # in Swiss/Phosphosite (06/17/08)	Present in Phosphosite (06/17/08)
P47736	RGP2_HUMAN Rap1 GTPase-activating protein 1 (Rap1GAP)			10.18		
	R.RSS*AIGIENIQEVQEK.R	1880.91132	2	3.68	499 NEW	No
Q9BUZ4	TRAF4_HUMAN TNF receptor-associated factor 4			10.17		
	R.GS*LDESSLGFGYPK.F	1536.66175	2	3.48	426 NEW	No
Q96T58	MINT_HUMAN Msx2-interacting protein (SPEN homolog)			10.17		
	K.FGKVTSVQIHGTS*EER.Y	1854.87454	2	2.66	374 NEW	No
Q5HYJ3	FA76B_HUMAN Protein FAM76B			10.17		
	K.ISNLS*PEEEQGLWK.Q	1709.77818	2	2.64	193 Swiss/ 193 phos	Yes
Q13427	PPIG_HUMAN Peptidyl-prolyl cis-trans isomerase G			10.17		
	R.RS*ET*PPHWR.Q	1325.51872	2	2.81	356 Swiss/ 356 phos & 358 Swiss/ 358 phos	Yes & Yes
Q9UDY2	ZO2_HUMAN Tight junction protein ZO-2 (Zonula occludens 2 protein)			10.16		
	R.DNS*PPPAFKPEPPK.A	1600.74067	2	3.20	986 Swiss/ 986 phos	Yes
Q9HC52	CBX8_HUMAN Chromobox protein homolog 8 (Polycomb 3 homolog)			10.14		
	R.HGS*GPPSSGGGLYR.D	1408.60049	2	2.62	311 New in Swiss/ 311 phos	Yes

Table A-2 Phosphorylation sites assigned by product ions in MS/MS spectrum.

Accession number	Scan(s)	Peptide	Phosphorylation sites
P07900	HS90A_HUMAN Heat shock protein HSP 90-alpha (HSP 86)		
		K.ESEDKPEIEDVGS*DEEEEK.K	S263 confirmed by y6, y7 S252 not phosphorylated by b4, b5
		K.ESEDKPEIEDVGS*DEEEEKK.D	S263 confirmed by y7, y9 S252 not phosphorylated by b4, b6
		R.DKEVS*DDEAEEK.E	S231 confirmed by y7, y8
Q15019	SEPT2_HUMAN Septin-2 (Protein NEDD5)		
		K.IYHLPDAES*DEDEDFKEQTR.L	S218 confirmed by y11 and y12 Y211 not phosphorylated by b2, b3 T228 not phosphorylated by y2, y4
		R.YLHDES*GLNR.R	S134 confirmed by y3, y5 Y129 not phosphorylated by b2, b4
		K.IYHLPDAES*DEDEDFK.E	S218 confirmed by y6, y10
Q15185	TEBP_HUMAN Prostaglandin E synthase 3 (Cytosolic prostaglandin E2 synthase)		
		K.DWEDDS*DEDMSNFDR.F	S113 confirmed by y9, y10
		K.DWEDDS*DEDM#SNFDR.F	
O60716	CTND1_HUMAN Catenin delta-1 (p120 catenin)		
		R.LRSY*EDMIGEEVPSDQYYWAPLAQHER.G	S320 not confirmed Y321 not confirmed S331 not phosphorylated by y13, y14 Y334 not phosphorylated by y10, y11 Y335 not phosphorylated by y9, y10
		R.HYEDGYPGGSDNYGS*LSR.V	S230 confirmed by y3, y5 Y217 not phosphorylated by b2, b3 Y221 not phosphorylated by b5, b6 S225 not phosphorylated by y8, y9 Y228 not phosphorylated by b12, b13 S232 not phosphorylated by y3
		R.SQSSHSYDDST*LPLIDR.N	T869 confirmed by y6, y7
		R.S*YEDMIGEEVPSDQYYWAPLAQHER.G	S320 not confirmed
		R.VGGS*SVDLHR.F	S268 confirmed by y6, y7
		R.S*GDLGDMEPLK.G	S920 confirmed by b3 and b4
		R.TLDRS*GDLGDMEPLK.G	S920 confirmed by y10, y11
		R.S*MGYDDLDYGMMSDYGTAR.R	S288 confirmed by b3 S300 not phosphorylated by y7
		R.T*LDRSGDLGDMEPLK.G	T916 confirmed by b3
		R.HYEDGYPGGS*DNY*GSLSRVT*RIEER.Y	Y228 not confirmed
		R.S*MGYDDLDYGMMSDYGTAR.R	S288
		R.VGGS*SVDLHR.F	S268
Q9Y2W1	TR150_HUMAN Thyroid hormone receptor-associated protein 3		
		K.WAHDKFS*GEEGEIEDDES*GTENR.E	S928 confirmed by b6, b9 S939 confirmed by y5, y6
		K.WAHDKFS*GEEGEIEDDESGTENR.E	S928 confirmed by b6, b9 S939 not phosphorylated by y5, y6

Table A-2 (continued).

Accession number	Scan(s)	Peptide	Phosphorylation sites
		K.WAHDKFS*GEEGEIEDDESGT*ENREEK.D	S928 confirmed by b6, b9 S939 not phosphorylated by y8, y9 T941 confirmed by y5, y8
		R.ERS*PALKS*PLQSVVVR.R	S248 not confirmed S253 confirmed by y8, y9
		R.IDIS*PSTFR.K	S682 confirmed by y5, y6
		R.ASAVSELS*PR.E	S243 confirmed by y2, y3. S240 not phosphorylated by y5, y6 S237 not phosphorylated by y8, y9
		K.S*PPSTGSTYGSSQK.E	S32o confirmed by b3 S323 not phosphorylated by y10, y11 S326 not phosphorylated by y7, y8 S330 not phosphorylated by y3, y4
		R.DSS*HS*RERS*AEK.T	S747 confirmed by y9, y10. S749 not confirmed. S753 confirmed by y3, y4
		R.RIDIS*PSTFR.K	S682 confirmed by y5, y6
		K.SPPSTGST*Y*GSS*QK.E	T324 confirmed by b7, b8 Y325 confirmed by b8, b9 S328 not confirmed
P08651	NFIC_HUMAN Nuclear factor 1 C-type (Nuclear factor 1/C)		
		R.NWTEDMEGGISS*PVK.K	S323 confirmed by y3, y4 S322 not phosphorylated by y4, y5 T313 not phosphorylated by y12, y13
		R.NWTEDMEGGISS*PVKK.T	S323 confirmed by y4, y5 S322 not phosphorylated by y5, y6 T313 not phosphorylated by y13, y14
Q13283	G3BP1_HUMAN Ras GTPase-activating protein-binding protein 1 (G3BP-1)		
		K.SSS*PAPADIAQTVQEDLR.T	S232 confirmed by y15, y16 T241 not phosphorylated by y6, y7
		R.YQDEVFGGFVTEPQEES*EEEVEEPEER.Q	S149 confirmed by y7, y14
Q9Y608	LRRF2_HUMAN Leucine-rich repeat flightless-interacting protein 2		
		R.RGS*GDTSSLIDPDTSLSELR.D	S328 confirmed by y17, y18 T331 not phosphorylated by y14, y15
		R.IS*S*ARSS*PGFTNDDTASIVSSDRASR.G	S231 & S232 & S236 not confirmed
		R.PSSRNS*ASATT*PLSGNSS*R.R	S312 & T317 & S324 not confirmed
Q5VTR2	BRE1A_HUMAN Ubiquitin-protein ligase BRE1A (BRE1-A)		
		K.ALVVPEPEPDSDS*NQER.K	S138 confirmed by y4, y5 S136 not phosphorylated by y5, y7
		K.PDSEDLSSQSS*AS*KASQEDANEIK.S	S548 confirmed by b10,b11 S550 confirmed by y11, y12
Q8N6T3	ARFG1_HUMAN ADP-ribosylation factor GTPase-activating protein 1		
		R.RSS*DSWEVWGSASTNR.N	S361 confirmed by y13, y14

Table A-2 (continued).

Accession number	Scan(s)	Peptide	Phosphorylation sites
		R.EFLESQEDY*DPCWS*LQEK.Y	Y93 not confirmed S98 confirmed by b13, b14
		R.SS*DSWEVWGSASTNR.N	S361
		K.ASELGHS*LNENVLKPAQEK.V	S246 not confirmed
Q9Y6G9	DC1L1_HUMAN Cytoplasmic dynein 1 light intermediate chain 1		
		R.DFQEYVEPGEDFPAS*PQR.R	S207 confirmed by y3, y5
		K.KTGSPGGPGVSGGS*PAGGAGGGSS*GLPPSTKK.S	S468 confirmed by b11, b15
		K.PVT*VS*PTTPTSPTEGEAS*	T508 confirmed by b3 S510 confirmed by y13, y14
Q9Y2U5	M3K2_HUMAN Mitogen-activated protein kinase kinase kinase 2		
		R.DRSS*PPPGYIPDELHQVAR.N	S164 confirmed by b3, b4
		R.AQS*YPDNHQEFSDYDNPIFEK.F	S239 confirmed by b3, b4
		K.RLS*IIGPTSR.D	S153 confirmed by y7, y8
		R.GS*DIDNPT*LTVM#DISPPSR.S	S331 confirmed by b3 T337 not confirmed
O00193	SMAP_HUMAN Small acidic protein		
		R.S*ASPDDDLGSSNWEAADLGNEER.K	S15 not confirmed
O95218	ZRAB2_HUMAN Zinc finger Ran-binding domain-containing protein 2		
		R.ENVEYIEREES*DGEYDEFGR.K	S120
		R.EES*DGEYDEFGR.K	S120 confirmed by y9, y10
		K.YNLDAS*EEEDSNK.K	S188 confirmed by y7, y8
		K.EVEDKES*EGEEEDEDEDLSK.Y	S153 confirmed by b7
		R.S*SSRS*S*SPSSSRSR.S	S213 & S217 & S218 not confirmed
Q8N5F7	NKAP_HUMAN NF-kappa-B-activating protein		
		R.IGELGAPEVWGLS*PK.N	S149 confirmed by b12, b13
		K.Y*S*EDS*DSDSDSETDSSDEDNK.R	Y209 &S 210 & S213 not confirmed
Q9NSK0	KLC4_HUMAN Kinesin light chain 4		
		R.AAS*LNYLNQPSAAPLQVSR.G	S590 confirmed by b3 Y593 not phosphorylated by y12, y14
Q9H1E3	NUCKS_HUMAN Nuclear ubiquitous casein and cyclin-dependent kinases substrate		
		K.VVDYSQFQES*DDADEDYGR.D	S19 confirmed by y8, y10
Q92625	ANKS1_HUMAN Ankyrin repeat and SAM domain-containing protein 1A (Odin)		
		K.SPS*FASEWDEIEK.I	S663 confirmed by y10, y11
O00192	ARVC_HUMAN Armadillo repeat protein deleted in velo-cardio-facial syndrome		
		R.S*LAADDEGGPELEPDYGTATR.R	S267 confirmed by b3

Table A-2 (continued).

Accession number	Scan(s)	Peptide	Phosphorylation sites
		R.NFDT*LDLPK.R	T642 confirmed by y5, y6
O15027	K0310_HUMAN Uncharacterized protein KIAA0310		
		R.FTGS*FDDDPDPHRDPYGEEVDR.R	S1149 confirmed by b2, b5 Y1161 not phosphorylated by y4, y7
Q14247	SRC8_HUMAN Src substrate cortactin		
		R.LPSS*PVYEDAASFK.A	S418 confirmed by y10, y11
		K.TQT*PPVS*PAPQPTEER.L	T401 confirmed by y13, y14 S405 confirmed by y9, y10
		R.VDKSAVGFDY*QGKT*EK.H	Y178 confirmed by b6, b10 T182 confirmed by b13, b14
		K.GRY*GLFPANY*VELR.Q	Y538 confirmed by b3 Y545 confirmed by y2, y5
		K.LS*KHCS*QVDSVRGFGGK.F	S109 confirmed by b3 S113 confirmed by y11, y13
		R.LPSS*PVY*EDAASFK.A	S418 confirmed by y10, y11 Y421 not confirmed
Q14498	RBM39_HUMAN RNA-binding protein 39		
		K.DKS*PVREPIDNLTPEER.D	S136 confirmed by b3 T146 not phosphorylated by y4, y5
		R.YRS*PYSGPK.F	S97 confirmed by y6, y7
Q6ICG6	CV009_HUMAN Uncharacterized protein C22orf9		
		K.SHS*ANDSEEFFR.E	S324 confirmed by y9, y10
Q9NYF8	BCLF1_HUMAN Bcl-2-associated transcription factor 1		
		K.FNDS*EGDDTEETEDYR.Q	S397 confirmed by y11, y13
		R.AEGEWEDQEALDYFS*DKESGK.Q	S385 not confirmed
		K.KAEGEPQEES*PLK.S	S177 confirmed by b9, b10
		K.DLFDYS*PPLHK.N	S512 confirmed by y5, y6
		K.LKDLFDYS*PPLHK.N	
		R.IDIS*PSTLR.K	S658 confirmed by y5, y6
		R.YSPS*QNS*PIHHIPSR.R	S287 not confirmed S 290 confirmed by y8, y9
		R.AEGEWEDQEALDYFS*DK.E	S385 confirmed by b14, b15
		R.RIDIS*PSTLR.K	S658
		R.SSSSS*AS*PSSPSS*REEK.E	S755 confirmed by b4, b5 S757 confirmed by b6, b7 S763 not confirmed
		R.S*SSSRSSSPYSKSPVS*K.R	S141 not confirmed S156 confirmed by y3
		R.YSPS*QNS*PIHHIPSR.R	
P42167	LAP2B_HUMAN Lamina-associated polypeptide 2, isoforms beta/gamma		
		K.GPPDFS*SDEEREPTPVLGSGAAAAGR.S	S66 not confirmed
		R.SST*PLPTISSSAENTR.Q	T160 confirmed by y13, y14
		K.GPPDFSSDEEREPT*PVLGSGAAAAGR.S	T174 confirmed by b12, b14
		R.EQGTES*RSST*PLPTISSSAENTR.Q	S156 not confirmed T160 confirmed by y13, y14

Table A-2 (continued).

Accession number	Scan(s)	Peptide	Phosphorylation sites
P54578	UBP14_HUMAN Ubiquitin carboxyl-terminal hydrolase 14		
		R.AS*GEMASAQYITAALR.D	S143 confirmed by b5, b6
		R.AS*GEM#ASAQYITAALR.D	see line 118
		K.S*S*KISRLPAYLTIQMVR.F	S314 & S315 not confirmed
Q8NDX5	PHC3_HUMAN Polyhomeotic-like protein 3		
		R.MDRT*PPPPTLS*PAAITVGR.G	T609 confirmed by b4, b5 S616 confirmed by y8, y9
Q8IYB3	SRRM1_HUMAN Serine/arginine repetitive matrix protein 1		
		K.KETES*EAEDNLDDLEK.H	S874 confirmed by y11, y12
		K.KPPAPPS*PVQSQS*PSTNWSPAVPVK.K	S769 confirmed by b5, b7 S775 confirmed by y12, y13
		K.KPPAPPS*PVQSQS*PSTNWS*PAVPVK.K	S 781 confirmed by y6, y7
		K.EKT*PELPEPSVK.V	T220 confirmed by y9, y10
		K.SRVS*VS*PGR.T	S429 confirmed by y5, y6 S431 confirmed by y3, y4
		R.RYS*PPIQR.R	S597 confirmed y5, y6
		R.RLS*PSAS*PPR.R	S389 confirmed by b2, b3 S393 confirmed by b6, b7
		R.HRPS*PPAT*PPPK.T	S402 confirmed by b5 T406 confirmed by y5
P10644	KAP0_HUMAN cAMP-dependent protein kinase type I-alpha regulatory subunit		
		R.EDEIS*PPPPNPVVK.G	S83 confirmed by y9, y10
		R.TDSREDEIS*PPPPNPVVK.G	
P06748	NPM_HUMAN Nucleophosmin		
		K.DELHIVEAEAMNYEGS*PIK.V	S70 confirmed by y3, y4
		K.DELHIVEAEAMNYEGS*PIKVTLATLK.M	
P31943	HNRH1_HUMAN Heterogeneous nuclear ribonucleoprotein H		
		R.PSGEAFVELES*EDEVK.L	S63 confirmed by y5, y6
P16949	STMN1_HUMAN Stathmin		
		K.ESVPEFPLS*PPK.K	S38 confirmed by y3, y4 S31 not phosphorylated by b2, b3
		R.ASGQAFELILS*PR.S	S25 confirmed by y3, y4
Q14694	UBP10_HUMAN Ubiquitin carboxyl-terminal hydrolase 10		
		K.NHSVNEEEQEEQGEGS*EDEWEQVGPR.N	S576 confirmed by y8, y11
Q9UK76	HN1_HUMAN Hematological and neurological expressed 1 protein		
		R.RNS*SEASSGDFLDLK.G	S87 confirmed by y12, y13 S88 not phosphorylated by y11, y12 S91 not phosphorylated by y8, y9
		R.NS*SEASSGDFLDLK.G	

Table A-2 (continued).

Accession number	Scan(s)	Peptide	Phosphorylation sites
Q13263	TIF1B_HUMAN Transcription intermediary factor 1-beta		
		R.STAPSAAASASASAAASS*PAGGGAEALELLEHCGVCR.E	S50 confirmed by b17, b18
		R.SRS*GEGEVSGLMR.K	S473 confirmed by b2, b3
		R.S*GEGEVSGLMR.K	
Q53SF7	CBLL1_HUMAN Cordon-bleu protein-like 1		
		R.AGS*LQLSSMSAGNSSLR.R	S382 confirmed by y14, y15
		R.QS*SLTFQSSDPEQMR.Q	S1146 confirmed by y14
O75821	IF34_HUMAN Eukaryotic translation initiation factor 3 subunit 4 (eIF-3 delta)		
		K.GIPLATGDT*SPEPELLPGAPLPPPK.E	T41 not confirmed
Q9UKL0	RCOR1_HUMAN REST corepressor 1		
		R.EREES*EDELEEANGNNPIDIEVDQNK.E	S257 confirmed by b4, b6
Q6PKG0	LARP1_HUMAN La-related protein 1		
		K.GLSAS*LPDLDSENWIEVK.K	S548 confirmed by y13, y14
		R.S*LPTTVPESPNY*R.N	S766 confirmed by b2 Y777 confirmed by b11,b12
		R.SLPTTVPES*PNYR.N	S774 confirmed by y4, y6
		K.ILIVTQT*PHYMR.R	T649 not confirmed
		R.EHRPRTASISSS*PSEGTPT*VGSYGCTPQSLPK.F	S851 not confirmed S858 not confirmed
		K.QEVENFKKVNM#IS*R.E	S716 not confirmed
O43741	AAKB2_HUMAN 5'-AMP-activated protein kinase subunit beta-2		
		R.DLSSS*PPGPYGQEMYAFR.S	S184 confirmed by y13, y14
Q9Y2V2	CHSP1_HUMAN Calcium-regulated heat stable protein 1		
		R.GNVVPS*PLPTR.R	S41 confirmed by y5, y6
P12694	ODBA_HUMAN 2-oxoisovalerate dehydrogenase subunit alpha, mitochondrial precursor		
		R.S*VDEVNYWDK.Q	S347 confirmed by b2, b3
		R.IGHHS*TSDDSSAYR.S	S337 not confirmed
Q8NEY8	PPHLN_HUMAN Periphilin-1		
		R.DNTFFRES*PVGR.K	S133 confirmed by y4, y5
Q96JM3	K1802_HUMAN Zinc finger protein KIAA1802		
		R.KPSPSES*PEPWKPFPAVS*PEPR.R	S286 confirmed by b6, b9 S 297 confirmed by y4, y7
		R.KPSGS*PDLWK.L	S445 confirmed by y5, y7
		R.KPS*PS*ESPEPWKPFPAVSPEPR.R	S282 not confirmed S284 not confirmed
		K.TAPTLS*PEHWK.A	S405 confirmed by y5, y6
		R.RPAPAVS*PGSWK.P	S308 confirmed by y5, y6
		R.GGS*PDLWK.S	S476 confirmed by y5, y6
		R.KPGPPLS*PEIR.S	S427 confirmed by y4, y5

Table A-2 (continued).

Accession number	Scan(s)	Peptide	Phosphorylation sites
		R.KTS*PASLDFPESQK.S	S459 not confirmed
		R.KT*SPASLDFPES*QKS*SR.G	S458 & S468 & S471 not confirmed
Q15459	SF3A1_HUMAN Splicing factor 3 subunit 1		
		K.FGESEEVEMEVES*DEEDDKQEK.A	S329 confirmed by y9, y10
Q9UL54	TAOK2_HUMAN Serine/threonine-protein kinase TAO2		
		K.MLLARHS*LDQDLLR.E	S656 confirmed by y7, y9
		R.HS*LDQDLLR.E	S656 confirmed by b5, b6
Q15139	KPCD1_HUMAN Serine/threonine-protein kinase D1		
		R.RLS*NVS*LTGVSTIR.T	S205 confirmed by y11. y12 S208 confirmed by y7, y9
		R.RLS*NVSLTGVSTIR.T	S205 confirmed by y11, y12
		R.T*SS*AELST*SAPDEPLLQKSPSESFIGREK.R	T217 & S219 & T224 not confirmed
Q9UEW8	STK39_HUMAN STE20/SPS1-related proline-alanine-rich protein kinase		
		K.TEDGDWEWS*DDEMDEK.S	S387 confirmed by y6, y9
		K.ADMWSFGITAIELATGAAPY*HKY*PPMK.V	Y275 & Y278 not confirmed
Q9H0B6	KLC2_HUMAN Kinesin light chain 2 (KLC 2)		
		R.RDS*APYGEYGSWYK.A	S428 confirmed by y11, y12
		R.ASS*LNFLNK.S	S528 confirmed by y6, y7
		R.TLSSS*SMDLSR.R	S610 confirmed by y6, y7
Q32MZ4	LRRF1_HUMAN Leucine-rich repeat flightless-interacting protein 1		
		R.RGS*GDTSISIDTEASIR.E	S120 confirmed by y14, y15
Q15052	ARHG6_HUMAN Rho guanine nucleotide exchange factor 6		
		R.MS*GFIYQGK.I	S488 confirmed by y7, y8,
P21127	CD2L1_HUMAN PITSLRE serine/threonine-protein kinase CDC2L1		
		K.AYT*PVVVTLWYR.A	T595 confirmed by y9, y10
P17812	PYRG1_HUMAN CTP synthase 1		
		R.SGSSS*PDSEITELK.F	S575 confirmed by y9, y10
		K.YIDSADLEPITS*QEEPVR.Y	S347 confirmed by y5, y7
P25490	TYY1_HUMAN Transcriptional repressor protein YY1		
		K.DIDHETVVEEQIIGENS*PPDYSEYMTGK.K	S247 confirmed by y11, y12
		R.EEVVGGDDS*DGLR.A	S118 confirmed by y4, y7
Q16637	SMN_HUMAN Survival motor neuron protein		

Table A-2 (continued).

Accession number	Scan(s)	Peptide	Phosphorylation sites
		R.GTGQS*DDSDIWDDTALIK.A	S28 confirmed by y13, y14
Q13177	PAK2_HUMAN Serine/threonine-protein kinase PAK 2		
		K.YLS*FTPPEK.D	S141 confirmed by y5, y7
Q08945	SSRP1_HUMAN FACT complex subunit SSRP1		
		K.EGMNPSYDEYADS*DEDQHDAYLER.M	S444 confirmed by b12, b14
P35221	CTNA1_HUMAN Catenin alpha-1		
		R.S*RTS*VQTEDDQLIAGQSAR.A	S652 no confirmed S 655 confirmed by y14, y16
		R.T*SVQTEDDQLIAGQSAR.A	T654 no confirmed
Q13242	SFRS9_HUMAN Splicing factor, arginine/serine-rich 9		
		R.GSPHYFS*PFRPY	S216 confirmed by y5, y6
		R.GS*PHYFS*PFRPY	S211 confirmed by b2 S216 confirmed by y5, y6
		R.STS*YGYSR.S	S189 confirmed by y5, y6
		R.GRDS*PYQSR.G	S204 not confirmed
O93594	AGM1_HUMAN Phosphoacetylglucosamine mutase (PAGM)		
		K.STIGVMVTAS*HNPEEDNGVK.L	S64 confirmed by y10, y12
Q9Y6X9	MORC2_HUMAN MORC family CW-type zinc finger protein 2		
		R.SVAVS*DEEEVEEEAER.R	S743 confirmed by y9, y12
Q92934	BAD_HUMAN Bcl2 antagonist of cell death		
		R.RMS*DEFVDSFK.K	S118 confirmed by b2, b4
		R.HSS*YPAGTEDDEGMGEEPSPFR.G	S75 no confirmed
		R.S*APPNLWAAQR.Y	S99 confirmed by b2, b7
Q9C0C2	TB182_HUMAN 182 kDa tankyrase 1-binding protein		
		R.RFS*EGVLQSPSQDQEK.L	S429 confirmed by b2, b4 S435 not phosphorylated by y7, y8 S437 not phosphorylated by y4, y7
		R.S*QEADVQDWEFR.K	S836 not confirmed
		K.VST*LRES*SAMAS*PLPR.E	T5 & S 9 & S14 not confirmed
Q96B36	AKTS1_HUMAN Proline-rich AKT1 substrate		
		R.AATAARPPAPPPAPQPPS*PTPS*PPRPTLAR.E	S88 confirmed by y12, y13 S92 confirmed by y8, y9
		K.S*LPVSVPVWGFK.E	S183 not confirmed
		R.LNT*SDFQK.L	T246 not confirmed
		R.AAT*AARPPAPPPAPQPPS*PT*PSPPR.P	T73 & S88 &T 90 not confirmed
Q14671	PUM1_HUMAN Pumilio homolog 1 (Pumilio-1)		
		R.RDS*LTGSSDLYK.R	S709 confirmed by y9, y10
		R.S*ASSASSLFSPSSTLFSS*SR.L	S797 not confirmed

Table A-2 (continued).

Accession number	Scan(s)	Peptide	Phosphorylation sites
P08559	ODPA_HUMAN Pyruvate dehydrogenase E1 component alpha subunit		
		R.YHGHS*MSDPGVS*YR.T	S293 confirmed by y9, y10 S300 confirmed by b11,b12
		R.YGMGTS*VER.A	S232 confirmed by y3, y4
		R.YHGHSMS*DPGVSYR.T	S295 not confirmed
Q9UQ35	SRRM2_HUMAN Serine/arginine repetitive matrix protein 2		
		R.HGGS*PQPLATTPLSQEPVNPPSEA S*PTR.D	S377 no confirmed S398 confirmed by y3, y4
		K.SST*PPGESYFGVSSLQLK.G	T1043 no confirmed
		R.S*RT*PLLPR.K	S2032 no confirmed T2034 confirmed by y5, y6
		R.GPS*PEGSS*ST*ESSPEHPPK.S	S1648 confirmed by b4 S1653 & T1655 not confirmed
		R.AHRSTSADS*ASSS*DTS*R.S	S268 &S 272 &T275 not confirmed
		R.QS*PSRS*SSPQPK.V	S908 & S912 not confirmed
P98175	RBM10_HUMAN RNA-binding protein 10		
		R.HRHS*PTGPPGFPR.D	S189 confirmed by b2, b4
		R.Y*GATDRSQDDGGENRS*R.D	Y16 confirmed by b3
Q9BW71	HIRP3_HUMAN HIRA-interacting protein 3		
		K.SLKES*EQES*EEEILAQK.K	S223 confirmed by y12, y14 S227 confirmed by b8, b9
Q9BSJ8	FA62A_HUMAN Protein FAM62A		
		R.KLDVSVKSNS*SFMS*R.E	S1063 no confirmed S1067 confirmed by y2, y4
Q9UKS6	PACN3_HUMAN Protein kinase C and casein kinase substrate in neurons protein 3		
		R.DGTAPPPQSPGSPGTGQDEEWS*D EESPR.K	S354 confirmed by y6, y7
P24844	MLRN_HUMAN Myosin regulatory light chain 2, smooth muscle isoform		
		R.ATS*NVFAMFDQSQIQEFK.E	S20 no confirmed
P04792	HSPB1_HUMAN Heat-shock protein beta-1 (HspB1) (Heat shock 27 kDa protein)		
		R.QLS*SGVSEIR.H	S82 confirmed by y7, y8 S83 not phosphorylated by y6, y7
		R.GPS*WDPFR.D	S15 confirmed by b2, b3
P05455	LA_HUMAN Lupus La protein (Sjoegren syndrome type B antigen)		
		K.FAS*DDEHDEHDENGATGPVK.R	S366 confirmed by b2, b3
		R.SPS*KPLPEVTDEYK.N	S94 confirmed by y11, y13
O60841	IF2P_HUMAN Eukaryotic translation initiation factor 5B		
		K.NKPGPNIES*GNEDDDASFK.I	S214 confirmed by y10, y11

Table A-2 (continued).

Accession number	Scan(s)	Peptide	Phosphorylation sites
P51114	FXR1_HUMAN Fragile X mental retardation syndrome-related protein 1 (hFXR1p)		
		R.RGPNYTSGYGTNSELSNPS*ETESER.K	S409 confirmed by y5, y7
		R.RGPNYTSGYGTNSELS*NPS*ETESER.K	S406 confirmed by y9, y10
P08238	HS90B_HUMAN Heat shock protein HSP 90-beta (HSP 84) (HSP 90)		
		K.IEDVGS*DEEDDSGKDK.K	S255 confirmed by b4, b6 S261 not phosphorylated by b11, b12
		K.IEDVGS*DEEDDSGK.D	S255 confirmed by y7, y10
		K.IEDVGS*DEEDDSGKDKK.K	
		R.EKEIS*DDEAEEEK.G	S226 confirmed by y8, y9
Q9UEE9	CFDP1_HUMAN Craniofacial development protein 1		
		K.LDWES*FKEEEGIGEELAIHNR.G	S250 confirmed by b4, b9
Q9Y383	LC7L2_HUMAN Putative RNA-binding protein Luc7-like 2		
		R.AMLDQLMGTS*R.D	S18 confirmed by y2, y3 T17 not phosphorylated by y3, y4
Q99613	IF38_HUMAN Eukaryotic translation initiation factor 3 subunit 8 (eIF3 p110)		
		K.QPLLLS*EDEEDTKR.V	S39 confirmed by y8, y9
O14974	MYPT1_HUMAN Protein phosphatase 1 regulatory subunit 12A		
		K.TGS*YGALAEITASK.E	S445 confirmed by y11,y12
		K.SPLIES*TANMDNNQSQKTFKNK.E	S304 confirmed by b5, b6
		R.RST*QGVTLTDLQEAEK.T	T696 not confirmed
		R.KTGS*YGALAEITASK.E	S445
Q9Y3S2	ZN330_HUMAN Zinc finger protein 330		
		R.KDS*DTESSDLFTNLNLGR.T	S291 confirmed by y15, y16
P61978	HNRPK_HUMAN Heterogeneous nuclear ribonucleoprotein K		
		R.GSY*GDLGGPIITTQVTIPK.D	Y380 confirmed by y14, y17
		R.RDYDDMS*PR.R	S284 confirmed by y2, y3
		R.GSY*GDLGGPIITT*QVTIPK.D	
		R.DYDDMS*PR.R	S284
P51858	HDGF_HUMAN Hepatoma-derived growth factor (HDGF)		
		R.AGDLLEDS*PK.R	S165 confirmed by y3, y4
		R.RAGDLLEDS*PK.R	
		R.AGDLLEDS*PKRPK.E	
		K.GNAEGS*S*DEEGKLVIDEPAK.E	S132 not confirmed S133 not confirmed
		K.KGNAEGS*S*DEEGKLVIDEPAK.E	
		K.GNAEGS*SDEEGKLVIDEPAK.E	S132 confirmed by b5, b6

Table A-2 (continued).

Accession number	Scan(s)	Peptide	Phosphorylation sites
P22059	OSBP1_HUMAN Oxysterol-binding protein 1		
		R.TGS*NISGASSDISLDEQYK.H	S379 confirmed by y16, y17
		K.GDMS*DEDDENEFFDAPEIITMPENLGHK.R	S351 not confirmed
Q8NE71	ABCF1_HUMAN ATP-binding cassette sub-family F member 1		
		K.LSVPTS*DEEDEVPAPK.P	S109 confirmed by y9, y11
		K.LSVPTS*DEEDEVPAPKPR.G	S109 confirmed by y12, y13
P55795	HNRH2_HUMAN Heterogeneous nuclear ribonucleoprotein H'		
		K.HTGPNS*PDTANDGFVR.L	S104 confirmed by y10, y11
Q9BYG3	MK67I_HUMAN MKI67 FHA domain-interacting nucleolar phosphoprotein		
		K.S*QVAELNDDDKDDEIVFK.Q	S247 confirmed by b3
P02545	LMNA_HUMAN Lamin-A/C (70 kDa lamin)		
		R.NKS*NEDQSMGNWQIK.R	S458 confirmed by b4
		R.LRLS*PSPTSQR.S	S390 confirmed by y7, y8
		R.KLEST*ES*RSSFSQHAR.T	T424 confirmed by y11, y12 S426 no confirmed
		R.LRLS*PS*PTSQR.S	S390 confirmed by y7, y8 S392 confirmed by y5, y6
		R.SVGGS*GGGSFGDNLVTR.S	S632 not confirmed
P06493	CDC2_HUMAN Cell division control protein 2 homolog (p34 protein kinase)		
		R.VYT*HEVVTLWYR.S	T161 confirmed by y9, y10
P49585	PCY1A_HUMAN Choline-phosphate cytidylyltransferase A		
		R.MLQAIS*PK.Q	S315 confirmed by b5,b6
		K.T*SPPCS*PANLSR.H	T342 not confirmed S347 confirmed by y6, y7
Q16204	CCDC6_HUMAN Coiled-coil domain-containing protein 6 (H4 protein)		
		R.PIS*PGLSYASHTVGFTPPTSLTR.A	S367 confirmed by b3
		R.T*VSSPIPYTPSPSSSR.P	T349 no confirmed
		R.PIS*PGLSYASHTVGFT*PPTSLTR.A	S367 confirmed by b3 T380 not confirmed
		R.QLSESES*SLEMDDER.Y	S327 no confirmed
		K.LDQPVS*APPS*PR.D	S240 confirmed by b5, b7 S244 confirmed by y2, y3
Q9NTJ3	SMC4_HUMAN Structural maintenance of chromosomes protein 4		
		R.T*ESPATAAETASEELDNR.S	T39 no confirmed
		K.S*S*LAMNRS*R.G	S588 & S589 not confirmed S595 confirmed by y3

Table A-2 (continued).

Accession number	Scan(s)	Peptide	Phosphorylation sites
Q8TAQ2	SMRC2_HUMAN SWI/SNF-related matrix-associated actin-dependent regulator of chromatin subfamily C member 2		
		R.KRS*PSPSPT*PEAK.K	S302 confirmed by b2, b3 T308 confirmed by y4, y6
		K.DMDEPS*PVPNVEEVTLPK.T	S347 confirmed by y12, y14
Q14676	MDC1_HUMAN Mediator of DNA damage checkpoint protein 1		
		R.LLLAEDS*EEEVDFLSER.R	S168 confirmed by y9, y11
Q8WUA2	PPIL4_HUMAN Peptidyl-prolyl cis-trans isomerase-like 4 (PPIase)		
		R.INHTVILDDPFDDPPDLLIPDRSPEPT*R.E	T182 not confirmed
		R.INHTVILDDPFDDPPDLLIPDRS*PEPTR.E	S178 confirmed by y5, y7
P18887	XRCC1_HUMAN DNA-repair protein XRCC1		
		K.TKPTQAAGPSS*PQKPPT*PEETK.A	S447 no confirmed T453 confirmed by y5, y7
P07814	SYEP_HUMAN Bifunctional aminoacyl-tRNA synthetase		
		K.EYIPGQPPLSQSSDSS*PTR.N	S886 confirmed by y3, y4
		R.AKIDM#SS*NNGCMRDPTLY*R.C	S346 not confirmed
		K.HPKNPEVGLKPVWY*S*PK.V	Y546 & S547 not confirmed
P27824	CALX_HUMAN Calnexin precursor		
		K.AEEDEILNRS*PR.N	S583 confirmed by b9, b10
O75494	FUSIP_HUMAN FUS-interacting serine-arginine-rich protein 1		
		R.S*FDYNYR.R	S133 confirmed by b2
		R.S*RS*FDYNYR.R	S131 confirmed by b2 S133 confirmed by b2, b4
Q15773	MLF2_HUMAN Myeloid leukemia factor 2		
		R.QHMS*RMLSGGFGY*SPFLSIT*DGNMPGTR.P	S29 & Y37 & T44 not confirmed
		R.LAIQGPEDS*PSR.Q	S238 confirmed by y3, y4
Q15366	PCBP2_HUMAN Poly(rC)-binding protein 2 (Alpha-CP2)		
		K.PSSS*PVIFAGGQDR.Y	S189 confirmed by b3, b4
P30622	CLIP1_HUMAN Restin		
		K.LT*NLQENLSEVSQVKETLEK.E	T822 confirmed by b4
		K.TISSEKAS*S*TPSS*ETQEEFVDDFRVGER.V	S43 & S44 & S48 not confirmed
		R.VM#ATTSASLKRSPSASSLSSMS*SVASS*VSSR.P	S320 & S325 not confirmed
		R.SPSASSLS*SMS*SVASSVSSRPSR.T	S317 confirmed by y15, y16 S320 not confirmed
		K.RS*PSASS*LSSM#SSVASSVSSR.P	S310 confirmed by b2 S315 not confirmed
		K.EPSATPPIS*NLTKTAS*ESISNLSEAGS*IK.K	S186 & S193 not confirmed S204 confirmed by y3, y4

Table A-2 (continued).

Accession number	Scan(s)	Peptide	Phosphorylation sites
P11717	MPRI_HUMAN Cation-independent mannose-6-phosphate receptor precursor		
		K.LVSFHDDS*DEDLLHI	S2484 confirmed by y6, y8
O00567	NOP56_HUMAN Nucleolar protein Nop56		
		K.EELMSS*DLEETAGSTSIPK.R	S520 confirmed by y13, y14
P52756	RBM5_HUMAN RNA-binding protein 5		
		R.GLVAAYSGDS*DNEEELVER.L	S624 confirmed by y9, y12
Q8ND30	LIPB2_HUMAN Liprin-beta-2		
		R.T*QSGNFYTDTLGMAEFR.R	T510 not confirmed
P40222	TXLNA_HUMAN Alpha-taxilin		
		R.RPEGPGAQAPSS*PR.V	S515 confirmed by y2, y3
Q8IWS0	PHF6_HUMAN PHD finger protein 6 (PHD-like zinc finger protein)		
		K.TAHNSEADLEESFNEHELEPSS*PK.S	S155 confirmed by y3
Q13595	TRA2A_HUMAN Transformer-2 protein homolog (TRA-2 alpha)		
		R.PTHS*GGGGGGGGGGGGGGGRRR.D	S215 not confirmed
		R.AHT*PTPGIYMGR.P	T202 confirmed by y9, y10
		R.RS*PS*PYYSR.Y	S260 confirmed by b2 S262 confirmed by b3, b4
		R.S*PS*PYYSR.Y	
		R.RRDSY*YDR.G	Y237 not confirmed
		R.RRS*PSPYY*SR.Y	S260 confirmed by b2, b3 Y265 confirmed by y2, y3
Q13489	BIRC3_HUMAN Baculoviral IAP repeat-containing protein 3		
		-.M#NIVENS*IFLS*NLMK.S	S7 confirmed by y7, y10 S11 confirmed by y4, y7
P49736	MCM2_HUMAN DNA replication licensing factor MCM2		
		R.GLLYDS*DEEDEERPAR.K	S139 confirmed by y9, y11
		R.VM#LES*FIDTQK.F	S801 confirmed by b3, b5
Q12968	NFAC3_HUMAN Nuclear factor of activated T-cells, cytoplasmic 3 (NF-ATc3)		
		R.PS*S*DSGCSHDSVLS*GQR.S	S730 not confirmed S731 not confirmed S742 confirmed by y3, y5
Q9H410	CT172_HUMAN Uncharacterized protein C20orf172		
		K.SLHLS*PQEQSASYQDR.R	S81 confirmed by y11, y12
Q9ULU4	PKCB1_HUMAN Protein kinase C-binding protein 1		
		R.RIS*LSDMPR.S	S425 confirmed by y6, y8 S427 not phosphorylated by y3, y5
		K.S*DSSDSEYISDDEQK.S	S595 not confirmed

Table A-2 (continued).

Accession number	Scan(s)	Peptide	Phosphorylation sites
P31321	KAP1_HUMAN cAMP-dependent protein kinase type I-beta regulatory subunit		
		-.M#ASPPACPS*EEDESLK.G	S9 confirmed by b8, b11
Q7L7X3	TAOK1_HUMAN Serine/threonine-protein kinase TAO1		
		R.AS*DPQSPPQVS*R.H	S417 confirmed by b3 S426 confirmed by b9, b11
P51587	BRCA2_HUMAN Breast cancer type 2 susceptibility protein		
		K.VFADIQS*EEILQHNQNMSGLEKVS*K.I	S1926 not confirmed
Q8TF66	LRC15_HUMAN Leucine-rich repeat-containing protein 15 precursor (hLib)		
		R.M#LANLQNIS*LQNNRLR.Q	S371 confirmed by y6, y9
Q5VT25	MRCKA_HUMAN Serine/threonine-protein kinase MRCK alpha		
		R.HSTAS*NSS*NLSSPPS*PASPR.K	S1700 & S1703 & S1710 not confirmed
		R.TVFSGS*VSIPS*ITK.S	1611 NEW & 1616 NEW
Q9UMY1	NOL7_HUMAN Nucleolar protein 7		
		K.VQSVS*QNKSY*LAVRLK.D	S167 confirmed by y11, y12 Y172 confirmed by y4, y7
P28161	GSTM2_HUMAN Glutathione S-transferase Mu 2 (GSTM2-2)		
		K.S*S*RFLPRPVFTK.M	S200 & S201 not confirmed
Q9UKX3	MYH13_HUMAN Myosin-13 (Myosin heavy chain 13)		
		R.VEEKES*LISQLT*K.S	S1300 confirmed by b4, b6 T1306 confirmed by b11, b12
P55199	ELL_HUMAN RNA polymerase II elongation factor ELL		
		R.KSGAS*AVSGGS*GVS*QR.P	S194 not confirmed S200 confirmed by b10, b12 S203 confirmed by y2, y3
Q9BXT6	M10L1_HUMAN Putative helicase Mov10l1		
		K.WEDDSRNHGSPS*DCGPR.V	S113 confirmed by b11, b12
		K.SSQALT*S*AKTTVVVTAQK.R	T472 & S473 not confirmed
Q14181	DPOA2_HUMAN DNA polymerase subunit alpha B		
		R.GGAGNIS*LKVLGCPEALTGSYKSMFQK.L	S192 confirmed by b5, b7
Q12824	SNF5_HUMAN SWI/SNF-related matrix-associated actin-dependent regulator of chromatin subfamily B member 1		
		R.YPS*LWRRLATVEER.K	S49 confirmed by b2,b6
Q8IWV8	UBR2_HUMAN E3 ubiquitin-protein ligase UBR2		
		K.M#RES*SPTSPVAET*EGTIMEESSRDK.D	S1005 not confirmed T1014 confirmed by y12, y13

Table A-2 (continued).

Accession number	Scan(s)	Peptide	Phosphorylation sites
		K.MRESS*PT*SPVAETEGTIMEES*SRDK.D	S1006 confirmed by b4, b5 T1008 confirmed by b6, b7 S1022 confirmed by y4, y5
P49006	MRP_HUMAN MARCKS-related protein		
		R.GDVTAEEAAGAS*PAK.A	S22 confirmed by y3, y4
		K.LSGLS*FK.R	S104 confirmed by y2, y3
		K.LSGLS*FKR.N	S104 confirmed by y3, y4
Q99733	NP1L4_HUMAN Nucleosome assembly protein 1-like 4		
		R.REFITGDVEPTDAESEWHS*ENEEEEK.L	S125 confirmed by y7, y9
Q13541	4EBP1_HUMAN Eukaryotic translation initiation factor 4E-binding protein 1		
		R.VVLGDGVQLPPGDYSTT*PGGTLFSTT*PGGTR.I	T37 confirmed by b16, b17 T46 confirmed by y5, y6
		R.RVVLGDGVQLPPGDYSTT*PGGTLFSTT*PGGTR.I	T37 confirmed by b17, b18 T46 confirmed by y5, y6
Q9H6Z4	RANB3_HUMAN Ran-binding protein 3 (RanBP3)		
		R.TSS*LTQFPPSQSEER.S	S126 confirmed by y12, y13
P42566	EP15_HUMAN Epidermal growth factor receptor substrate 15 (Protein Eps15)		
		R.S*SPELLPSGVTDENEVTTAVTEK.V	S562 not confirmed
P62258	1433E_HUMAN 14-3-3 protein epsilon (14-3-3E)		
		K.AAFDDAIAELDTLS*EESYK.D	S210 confirmed by y5, y6
O46021	RL1D1_HUMAN Ribosomal L1 domain-containing protein 1		
		K.ATNES*EDEIPQLVPIGK.K	S361 confirmed by b4, b6
P29966	MARCS_HUMAN Myristoylated alanine-rich C-kinase substrate (MARCKS)		
		K.LSGFS*FK.K	S170 confirmed by y2, y3
		K.LSGFS*FKK.N	
O95400	CD2B2_HUMAN CD2 antigen cytoplasmic tail-binding protein 2		
		K.HSLDS*DEEEDDDDGGSSK.Y	S49 confirmed by y13, y15
P05783	K1C18_HUMAN Keratin, type I cytoskeletal 18		
		R.PVSSAAS*VYAGAGGSGSR.I	S34 confirmed by y11, y12
		R.LLEDGEDFNLGDALDSSNS*MQTIQK.T	S401 confirmed by y6, y7
		R.STS*FRGGM#GSGGLATGIAGGLAGMGGIQNEK.E	S53 not confirmed
		R.ST*FSTNYR.S	T8 not confirmed
		R.S*LGSVQAPSYGAR.P	S15 confirmed by b2
Q96QR8	PURB_HUMAN Transcriptional activator protein Pur-beta		
		R.DSLGDFIEHYAQLGPSS*PEQLAAGAEEGGGPR.R	S101 confirmed by y15, y16
		R.RGGGS*GGGEES*EGEEVDED	S298 confirmed by b4, b8 S304 confirmed by b10, b11

Table A-2 (continued).

Accession number	Scan(s)	Peptide	Phosphorylation sites
		R.RGGGSGGGEES*EGEEVDED	S304 confirmed by b10, b12
Q5BKZ1	ZN326_HUMAN Zinc finger protein 326		
		R.SMDSYLNQS*YGMDNHSGGGGG SR.F	S56 not confirmed
P29692	EF1D_HUMAN Elongation factor 1-delta (EF-1-delta)		
		R.ATAPQTQHVS*PMR.Q	S133 confirmed by b9, b10
Q9UGV2	NDRG3_HUMAN Protein NDRG3		
		R.THS*TSSSLGSGESPFSR.S	S331 confirmed by y14, y15
Q05519	SFR11_HUMAN Splicing factor arginine/serine-rich 11		
		K.LNHVAAGLVS*PSLK.S	S207 confirmed by y4, y5
		R.DYDEEEQGYDS*EKEK.K	S434 confirmed by y4, y5
P25788	PSA3_HUMAN Proteasome subunit alpha type 3		
		K.ESLKEEDES*DDDNM	S250 confirmed by y5, y6
Q6UN15	FIP1_HUMAN Pre-mRNA 3'-end-processing factor FIP1		
		R.DHS*PTPSVFNSDEER.Y	S492 confirmed by b2, b3
Q9NYB0	TE2IP_HUMAN Telomeric repeat-binding factor 2-interacting protein 1		
		K.YLLGDAPVS*PSSQK.L	S203 confirmed by y5, y6
P27816	MAP4_HUMAN Microtubule-associated protein 4 (MAP 4)		
		K.DMES*PTKLDVTLAK.D	S280 confirmed by b2, b4
		K.VGS*LDNVGHLPAGGAVK.T	S1073 not confirmed
		K.DMS*PLSETEMALGK.D	S507 confirmed by b2, b3
		K.T*STSKAKTQPTSLPK.Q	T712 not confirmed
		K.VGS*TENIK.H	S941 not confirmed
P08729	K2C7_HUMAN Keratin, type II cytoskeletal 7 (Cytokeratin-7)		
		R.T*LNETELTELQS*QISDTSVVLSM DNSR.S	T227 not confirmed S238 confirmed by y15, y17
		R.T*LNETELT*ELQSQISDTSVVLSM #DNSR.S	T227 not confirmed T234 confirmed by b7, b11
Q9H307	PININ_HUMAN Pinin (140 kDa nuclear and cell adhesion-related phosphoprotein)		
		K.S*LSPGKENVSALDMEK.E	S441 confirmed by b2
Q9BQE3	TBA6_HUMAN Tubulin alpha-6 chain (Alpha-tubulin 6)		
		K.TIGGGDDS*FNTFFSETGAGK.H	S48 confirmed by y12, y13
Q93009	UBP7_HUMAN Ubiquitin carboxyl-terminal hydrolase 7		
		K.AGEQQLS*EPEDMEMEAGDTDDP PR.I	S18 confirmed by b6, b8
P52597	HNRPF_HUMAN Heterogeneous nuclear ribonucleoprotein F (hnRNP F)		
		K.ATENDIYNFFS*PLNPVR.V	S310 confirmed by y6, y7

Table A-2 (continued).

Accession number	Scan(s)	Peptide	Phosphorylation sites
Q13185	CBX3_HUMAN Chromobox protein homolog 3		
		K.SLS*DSESDDSK.S	S95 confirmed by y8, y9
Q8TE77	SSH3_HUMAN Protein phosphatase Slingshot homolog 3 (SSH-3L) (hSSH-3L)		
		R.S*PPGSGASTPVGPWDQAVQR.R	S4 not confirmed
		R.RQS*FAVLR.G	S37 confirmed by b2, b5
Q9NR30	DDX21_HUMAN Nucleolar RNA helicase 2		
		K.NEEPS*EEEIDAPKPK.K	S121 confirmed by b4, b6
O95359	TACC2_HUMAN Transforming acidic coiled-coil-containing protein 2		
		K.LDNTPAS*PPRS*PAEPNDIPIAK.G	S2317 not confirmed S2321 confirmed by y11, y12
Q86W92	LIPB1_HUMAN Liprin-beta-1		
		R.SQS*TTFNPDDMSEPEFK.R	S601 confirmed by y14, y15
P23588	IF4B_HUMAN Eukaryotic translation initiation factor 4B		
		K.SPPY*TAFLGNLPYDVTEESIK.E	Y96 not confirmed
		R.RES*EKS*LENETLNK.E	S442 confirmed by b2, b4 S445 confirmed by y8, y9
		R.ARPATDS*FDDYPPR.R	S207 confirmed by y7, y8
		R.HPS*WRS*EETQER.E	S406 confirmed by y9, y10 S409 confirmed by b5, b7
		K.PRST*PEEDDSS*AS*TSQSTR.A	T341 confirmed by b3, b5 S348 & S350 not confirmed
		K.YAALS*VDGEDENEGEDYAE	S597 confirmed by y14, y15
O15164	TIF1A_HUMAN Transcription intermediary factor 1-alpha		
		K.SEWLDPSQKS*PLHVGETR.K	S811 confirmed by b9, b10
		R.SILTSLLLNSS*QSS*T*SEETVLR.S	S768 confirmed by y11, y12 S771 & T772 not confirmed
P46821	MAP1B_HUMAN Microtubule-associated protein 1B (MAP 1B)		
		K.LGDVS*PTQIDVSQFGSFK.E	S1501 confirmed by y13, y14
		K.TTSPPEVS*GYS*Y*EK.T	S1970 & S1973 & Y1974 not confirmed
Q06265	EXOS9_HUMAN Exosome complex exonuclease RRP45 (Exosome component 9)		
		K.APIDTS*DVEEK.A	S306 confirmed by y4, y6
Q8WUZ0	BCL7C_HUMAN B-cell CLL/lymphoma 7 protein family member C		
		K.GTEPS*PGGTPQPSRPVS*PAGPPEGVPEEAQPPR.L	S114 not confirmed S126 confirmed by b16, b19
		K.GTEPS*PGGT*PQPSRPVSPAGPPEGVPEEAQPPR.L	T118 not confirmed

Table A-2 (continued).

Accession number	Scan(s)	Peptide	Phosphorylation sites
O43290	SNUT1_HUMAN U4/U6.U5 tri-snRNP-associated protein 1		
		R.RVS*EVEEEKEPVPQPLPSDDTR.V	S448 confirmed by b2, b4
		R.DLQGLT*VEHAIDSFREGETMILT*LKDK.G	T258 not confirmed
		K.KMSSS*DT*PLGT*VALLQEK.Q	S762 & T764 & T768 not confirmed
		K.KMS*S*S*DTPLGTVALLQEKQK.A	S760 & S761 & S762 not confirmed
		K.M#SS*SDT*PLGTVALLQEK.Q	S761&T764 not confirmed
P30291	WEE1_HUMAN Wee1-like protein kinase (Wee1A kinase)		
		K.S*PAAPY*FLGSSFS*PVRCGGPGDASPR.G	S127 & Y132 not confirmed S139 confirmed by y13, y14
		K.S*RYTTEFHELEKIGS*GEFGSVFK.C	S293 not confirmed S307 confirmed by y5, y9
P16333	NCK1_HUMAN Cytoplasmic protein NCK1		
		K.RKPS*VPDSASPADDSFVDPGER.L	S85 confirmed by b3, b4
Q9UNE7	STUB1_HUMAN STIP1 homology and U box-containing protein 1		
		R.LGAGGGS*PEKS*PSAQELK.E	S19 confirmed by b5, b7 S23 confirmed by y7, y9
Q9BTC0	DIDO1_HUMAN Death-inducer obliterator 1 (DIO-1)		
		R.RNS*VERPAEPVAGAATPSLVEQQK.M	S1456 confirmed by b2, b5
Q96I25	SPF45_HUMAN Splicing factor 45		
		R.S*MGGAAIAPPTSLVEK.D	S169 confirmed by b2
		R.SPT*GPSNSFLANMGGTVAHK.I	T224 not confirmed
Q53EL6	PDCD4_HUMAN Programmed cell death protein 4 (Nuclear antigen H731-like)		
		R.KDS*VWGSGGGQQSVNHLVK.E	S313 confirmed by b2,b3
		R.SGLTVPTS*PK.G	S94 confirmed by y2, y3
		K.NSSRDS*GRGDS*VS*DSGSDALR.S	S71 & S76 not confirmed
Q9H2U2	IPYR2_HUMAN Inorganic pyrophosphatase 2, mitochondrial precursor		
		R.SLVESVSSS*PNKESNEEEQVWHFLGK	S317 not confirmed
		K.FKPGYLEATLNWFRLY*K.V	Y241 not confirmed
Q8ND56	LS14A_HUMAN LSM14 protein homolog A		
		K.S*PTMEQAVQTASAHLPAPAAVGR.R	S192 confirmed by b2
		R.SS*PQLDPLR.K	S183 not confirmed
Q13247	SFRS6_HUMAN Splicing factor, arginine/serine-rich 6		
		R.SNS*PLPVPPSK.A	S303 confirmed by b2, b3
		R.LIVENLSS*R.C	S119 confirmed by y1, y2 S118 not phosphorylated by y2, y3

Table A-2 (continued).

Accession number	Scan(s)	Peptide	Phosphorylation sites
Q9H7L9	SDS3_HUMAN Sin3 histone deacetylase corepressor complex component SDS3		
		K.RPAS*PSS*PEHLPATPAESPAQR.F	S234 & S237 not confirmed
Q9BXP5	ARS2_HUMAN Arsenite-resistance protein 2		
		R.TQLWASEPGT*PPLPTSLPSQNPILK.N	T544 confirmed by b9, b10
		R.HELS*PPQK.R	S74 confirmed by y4, y5
P68366	TBA1_HUMAN Tubulin alpha-1 chain		
		R.EDM#AALEKDY*EEVGIDSYEDEDEGEE	Y432 confirmed by b9, b12
Q96D71	REPS1_HUMAN RalBP1-associated Eps domain-containing protein 1		
		R.TSADAQEPASPVVSPQQS*PPTS*PHTWR.K	S118 confirmed by y9, y10 S122 not confirmed
		R.RQS*SSYDDPWK.I	S220 confirmed by y8, y9
		R.HAAS*YS*SDSENQGSY*SGVIPPPPGRGQVKK.G	S63 & S65 & Y74 not confirmed
O94888	UBXD7_HUMAN UBX domain-containing protein 7		
		R.SESLIDASEDS*QLEAAIR.A	S288 confirmed by y5, y8
		R.SES*LIDASEDSQLEAAIR.A	S280 not confirmed
		R.DFQT*ET*IRQEQELR.N	T116 confirmed by b3, b4 T118 confirmed by y8, y10
P67809	YBOX1_HUMAN Nuclease sensitive element-binding protein 1		
		R.NYQQNYQNS*ESGEKNEGSESAPEGQAQQR.R	S165 not confirmed
		K.NEGSES*APEGQAQQR.R	S176 confirmed by y9, y10
Q9UN36	NDRG2_HUMAN Protein NDRG2 (Protein Syld709613)		
		R.SRT*AS*LTSAASVDGNR.S	T330 confirmed by y13, y14 S332 confirmed by y11, y12
O00264	PGRC1_HUMAN Membrane-associated progesterone receptor component 1 (mPR)		
		K.EGEEPTVYS*DEEEPKDESAR.K	S181 confirmed by y11, y12
Q9UBC2	EP15R_HUMAN Epidermal growth factor receptor substrate 15-like 1		
		K.FHDTS*SPLMVTPPSAEAHWAVR.V	S107 confirmed by b4, b5
		K.DS*LRSTPS*HGSVSSLNSTGSLSPKHS*LK.Q	S235 confirmed by b4 S241 confirmed by b7, b8
O00499	BIN1_HUMAN Myc box-dependent-interacting protein 1		
		K.S*PSPPDGS*PAATPEIR.V	S296 confirmed by b2 S303 confirmed by y8, y9
		K.S*PSPPDGSPAATPEIR.V	S296 confirmed by b2
Q9BQI5	SGIP1_HUMAN SH3-containing GRB2-like protein 3-interacting protein 1		
		K.WVHFSDTSPEHVTPELT*PR.E	T328 confirmed by y4

Table A-2 (continued).

Accession number	Scan(s)	Peptide	Phosphorylation sites
Q9ULM3	YETS2_HUMAN YEATS domain-containing protein 2		
		K.T*EES*S*ELGNYVIK.I	T1131 confirmed by b3 S1134 & S1135 not confirmed
Q9Y233	PDE10_HUMAN cAMP and cAMP-inhibited cGMP 3',5'-cyclic phosphodiesterase 10A		
		K.S*QHLTGLTDEKVK.A	S8 confirmed by b3
Q15054	DPOD3_HUMAN DNA polymerase subunit delta 3 (DNA polymerase subunit delta p66)		
		K.TEPEPPSVKS*S*SGENK.R	S374 & S375 not confirmed
		K.S*KLAVT*ASIHVY*SIQK.A	S90 confirmed by b3 T95 confirmed by b3, b6 Y101 not confirmed
		R.VALS*DDETKETENMR.K	S307 confirmed by b3, b5
Q9UNZ2	NSF1C_HUMAN NSFL1 cofactor p47 (p97 cofactor p47)		
		R.KKS*PNELVDDLFK.G	S114 confirmed by y10, y11
Q9Y6W5	WASF2_HUMAN Wiskott-Aldrich syndrome protein family member 2		
		K.RS*SVVSPSHPPPAPPLGSPPGPK.P	S292 not confirmed
		R.S*S*VVS*PSHPPPAPPLGSPPGPK.P	S292 & S293 & S296 not confirmed
Q9BQA1	MEP50_HUMAN Methylosome protein 50 (MEP50 protein) (WD repeat protein 77)		
		R.KET*PPPLVPPAAR.E	T5 confirmed by y10, y11
P49407	ARRB1_HUMAN Beta-arrestin-1 (Arrestin beta 1)		
		R.KDLFVANVQS*FPPAPEDK.K	S86 confirmed by y8, y10
Q9P2B4	CT2NL_HUMAN CTTNBP2 N-terminal-like protein 7470		
		K.EQKKLS*SQLEEER.S	S165 confirmed by b4, b6
Q5JTD0	TJAP1_HUMAN Tight junction-associated protein 1 (Tight junction protein 4)		
		R.KDS*LTQAQEQGNLLN	S545 confirmed by b3
P24043	LAMA2_HUMAN Laminin subunit alpha-2 precursor (Laminin M chain)		
		R.NS*HIAIAFDDT*KVKNR.L	S2772 confirmed by b4 T2781 confirmed by y5, y6
Q6Y7W6	PERQ2_HUMAN PERQ amino acid-rich with GYF domain-containing protein 2		
		R.PGT*PSDHQSQEASQFER.K	T382 confirmed by b3
Q86WB0	NIPA_HUMAN Nuclear-interacting partner of ALK		
		K.QSSQPAETDS*MSLSEKS*RK.V	S479 & S486 not confirmed
		R.SMGTGDT*PGLEVPSS*PLR.K	T387 & S395 not confirmed

Table A-2 (continued).

Accession number	Scan(s)	Peptide	Phosphorylation sites
Q12955	ANK3_HUMAN Ankyrin-3 (ANK-3) (Ankyrin-G)		
		R.RQS*FASLALR.K	S1459 confirmed by y7, y8
Q15642	CIP4_HUMAN Cdc42-interacting protein 4		
		R.APSDS*SLGTPSDGRPELR.G	S298 not confirmed
O15173	PGRC2_HUMAN Membrane-associated progesterone receptor component 2		
		R.LLKPGEEPSEY*TDEEDTK.D	Y210 not confirmed
Q8N5S9	KKCC1_HUMAN Calcium/calmodulin-dependent protein kinase kinase 1		
		R.KLS*LQER.P	S74 confirmed by y4, y5
		R.LIPS*WTT*VILVKS*MLRK.R	S443 not confirmed T446 confirmed by b6, b7 S452 confirmed by b10, b13
P30086	PEBP1_HUMAN Phosphatidylethanolamine-binding protein 1 (PEBP-1)		
		K.NRPTS*ISWDGLDSGK.L	S52 confirmed by y10, y11
Q9UQB8	BAIP2_HUMAN Brain-specific angiogenesis inhibitor 1-associated protein 2		
		K.LSDSYSNT*LPVR.K	T340 confirmed by y4, y6
O15530	PDPK1_HUMAN 3-phosphoinositide-dependent protein kinase 1 (hPDK1)		
		R.ANS*FVGTAQYVSPELLTEK.S	S241 confirmed by b4, b5
Q9H788	SH24A_HUMAN SH2 domain-containing protein 4A (Protein SH(2)A)		
		R.TLS*SSAQEDIIR.W	S315 confirmed by y9, y10
P18615	NELFE_HUMAN Negative elongation factor E (NELF-E) (RD protein)		
		R.SIS*ADDDLQESSR.R	S115 confirmed by y9, y11
		K.QPMLDAAT*GKSVWGS*LAVQNS*PKGCHR.D	T340 & S347 & S353 not confirmed
		R.S*LSEQPVMDTATATEQAK.Q	S49 not confirmed
Q9H1B7	CN004_HUMAN Protein C14orf4		
		R.KAS*PEPPDSAEGALK.L	S547 confirmed by b3
		R.RNS*SS*PVSPASVPGQR.R	S657 confirmed by b2, b3 S659 confirmed by y11, y12
		R.QSPNSSSAAAS*VAS*RR.G	S224 confirmed by y5, y7 S227 confirmed by b13, b15
Q12857	NFIA_HUMAN Nuclear factor 1 A-type (Nuclear factor 1/A)		
		R.S*PGSGSQSSGWHEVEPGMPSPTTLK.K	S300 confirmed by b3
		R.RSLPSTS*ST*SSTKR.L	S273 & T275 not confirmed
UE93	PI3R6_HUMAN Phosphoinositide 3-kinase regulatory subunit 6		
		R.PS*GDGEM#LPGVSRLHTAR.V	S401 confirmed by b3, y17

Table A-2 (continued).

Accession number	Scan(s)	Peptide	Phosphorylation sites
P21675	TAF1_HUMAN Transcription initiation factor TFIID subunit 1		
		R.M#LLAAGS*AASGNNHRDDDTASVTSLNS*SATGR.C	S1138 confirmed by b5, b9 S1158 not confirmed
		R.TDPMVTLSSILES*IINDM#R.D	S1391 confirmed by b12, b14
		R.VGT*TVHCDYLNR.P	T1360 not confirmed
		R.VGTTVHCDY*LNRPHK.S	Y1366 not confirmed
Q8N1N0	CLC4F_HUMAN C-type lectin domain family 4 member F		
		K.SSFDNT*S*AEIQFLR.G	T313 & S314 not confirmed
Q04726	TLE3_HUMAN Transducin-like enhancer protein 3 (ESG3)		
		R.ESSANNSVS*PSESLR.A	S203 confirmed by y6, y7
		K.DLGHNDKS*STPGLKSNTPT*PR.N	S310 confirmed by b7, b8
		K.SDDLVVDVSNEDPAT*PRVSPAHS*PPENGLDK.A	T259 confirmed by y15, y17 S267 not confirmed
		R.VS*PAHS*PPENGLDK.A	S263 not confirmed S267 not confirmed
Q5VV41	ARHGG_HUMAN Rho guanine nucleotide exchange factor 16		
		R.HQS*FGAAVLSR.E	S107 confirmed by y8, y9
Q12906	ILF3_HUMAN Interleukin enhancer-binding factor 3		
		K.RPMEEDGEEKS*PSK.K	S382 confirmed by y3, y5
Q96IT1	ZN496_HUMAN Zinc finger protein 496		
		R.PPS*QLS*GDPVLQDAFLLQEENVR.D	S185 confirmed by b4 S188 not confirmed
Q9UN86	G3BP2_HUMAN Ras GTPase-activating protein-binding protein 2 (G3BP-2)		
		K.STT*PPPAEPVSLPQEPPK.A	T227 not confirmed
P55317	HNF3A_HUMAN Hepatocyte nuclear factor 3-alpha		
		K.TGQLEGAPAPGPAAS*PQTLDHSGATATGGASELK.T	S332 confirmed by b10, b16
P35579	MYH9_HUMAN Myosin-9 (Myosin heavy chain 9)		
		K.KMEDS*VGCLET*AEEVK.R	S1376 confirmed by y11, y14 T1382 confirmed by b9, b12
P08621	RU17_HUMAN U1 small nuclear ribonucleoprotein 70 kDa (U1 snRNP 70 kDa)		
		R.YDERPGPS*PLPHR.D	S226 confirmed by y5, y7
		R.GGGGGQDNGLEGLGNDS*R.D	S410 confirmed by y2, y4
Q13315	ATM_HUMAN Serine-protein kinase ATM (Ataxia telangiectasia mutated)		
		K.RSLES*VYS*LYPTLSR.L	S2165 confirmed by b3, b5 S2168 confirmed by b7, b8
		K.M#LQPIT*R.L	T2031 confirmed by b5, b6

Table A-2 (continued).

Accession number	Scan(s)	Peptide	Phosphorylation sites
Q9UKM9	RALY_HUMAN RNA-binding protein Raly		
		R.GRLS*PVPVPR.A	S135 confirmed by y6, y7
		R.AAS*AIYSGYIFDYDYYR.D	S206 confirmed by b4
Q9BSG1	ZNF2_HUMAN Zinc finger protein 2 (Zinc finger 2.2) (Zinc finger protein 661)		
		K.VFSSKS*SVIQHQR.R	S410 not confirmed
Q6ZMT1	STAC2_HUMAN SH3 and cysteine-rich domain-containing protein 2		
		R.SSFSS*T*SESPTRSLSER.D	S224 & T225 not confirmed
P85037	FOXK1_HUMAN Forkhead box protein K1 (Myocyte nuclear factor)		
		R.S*APAS*PTHPGLMSPR.S	S416 confirmed by b4 S420 confirmed by y10, y11
		R.EGS*PIPHDPEFGSK.L	S445 confirmed by b3
O15062	ZBTB5_HUMAN Zinc finger and BTB domain-containing protein 5		
		K.HYLTTRTLPMS*PPSER.V	S127 confirmed by b9, b11
Q9H2M9	RBGPR_HUMAN Rab3 GTPase-activating protein non-catalytic subunit		
		K.QDFS*PEVLKLANEER.D	S952 confirmed by b3, b6
P22626	ROA2_HUMAN Heterogeneous nuclear ribonucleoproteins A2/B1		
		R.GFGDGYNGYGGGPGGGNFGGS*PGYGGGR.G	S259 confirmed by y7, y8
		R.NMGGPYGGGNYGPGGSGGS*GGYGGR.S	S259 confirmed by y6, y7
		R.GGNFGFGDS*R.G	S212 confirmed by b8, b9
		R.NMGGPYGGGNYGPGGS*GGSGGYGGR.S	S341 confirmed by y9, y10
Q9UHD8	SEPT9_HUMAN Septin-9 (MLL septin-like fusion protein)		
		R.S*FEVEEVETPNSTPPR.R	S30 confirmed by b3
		K.RS*FEVEEVETPNSTPPR.R	
		R.S*FEVEEVET*PNSTPPR.R	S38 confirmed by b6 T30 confirmed by y7, y8
Q8TEA8	DTD1_HUMAN Probable D-tyrosyl-tRNA(Tyr) deacylase 1		
		R.S*ASSGAEGDVSSEREP	S194 confirmed by b2
		K.EDRS*ASSGAEGDVS*S*EREP	S 194 confirmed by b3, b4 S204 & S205 not confirmed
		K.EDRSAS*SGAEGDVS*S*ER.E	S196 not confirmed S204 confirmed by b13, b14 S205 confirmed by b14, b16
Q5JSZ5	K0515_HUMAN Uncharacterized protein KIAA0515		
		K.LKFS*DDEEEEEVVK.D	S388 confirmed by y10, y11
O95460	MATN4_HUMAN Matrilin-4 precursor		
		R.VGVIQYS*SQVQSVFPLR.A	S79 not confirmed

Table A-2 (continued).

Accession number	Scan(s)	Peptide	Phosphorylation sites
P25205	MCM3_HUMAN DNA replication licensing factor MCM3		
		K.DGDSYDPYDFS*DTEEEMPQVHTPK.T	S711 confirmed by y13, y14
O95248	MTMR5_HUMAN SET-binding factor 1 (Sbf1) (Myotubularin-related protein 5)		
		R.RTTVPSGPPMT*AILER.C	T546 confirmed by y5, y6
Q6P6C2	ALKB5_HUMAN Alkylated repair protein alkB homolog 5		
		R.RGS*FSSENYWR.K	S361 confirmed by y8, y9
		K.YQEDS*DPERSDYEEQQLQK.E	S64 not confirmed
		R.GS*FSSENYWR.K	S361
		R.LET*KS*LSSSVLPPSYASDRLSGNNR.D	T294 & S296 not confirmed
Q9NX63	CHCH3_HUMAN Coiled-coil-helix-coiled-coil-helix domain-containing protein 3		
		R.YS*GAYGASVSDEELK.R	S50 confirmed by y14, b2
P21796	VDAC1_HUMAN Voltage-dependent anion-selective channel protein 1 (VDAC-1)		
		K.LTFDSSFS*PNTGK.K	S104 confirmed by y5, y6
Q76KP1	B4GN4_HUMAN N-acetyl-beta-glucosaminyl-glycoprotein 4-beta-N-acetylgalactosam		
		R.TLGPAAPTVDS*NLS*SEAR.P	S616 confirmed by b10, b12 S619 not confirmed
Q13573	SNW1_HUMAN SNW domain-containing protein 1 (Nuclear protein SkiP)		
		R.GPPS*PPAPVMHS*PSR.K	S224 confirmed by y11, y12 S232 confirmed by y3, y4
Q9NPH0	PPA6_HUMAN Lysophosphatidic acid phosphatase type 6 precursor		
		R.GRRQTAS*LQPGIS*EDLK.K	S223 confirmed by y10, y11 S229 confirmed by b12, b14
Q6WKZ4	RFIP1_HUMAN Rab11 family-interacting protein 1 (Rab11-FIP1)		
		K.HLFSS*TENLAAGSWK.E	S357 confirmed by y10, y11
P23193	TCEA1_HUMAN Transcription elongation factor A protein 1		
		K.EPAITSQNS*PEAR.E	S100 confirmed by y4, y5
		K.KKEPAITSQNS*PEAR.E	
O75446	SAP30_HUMAN Histone deacetylase complex subunit SAP30		
		K.DTLTYFIY*SVKNDK.N	Y202 confirmed by b7, b8
Q07666	SAM68_HUMAN KH domain-containing, RNA-binding, signal transduction-associated protein 1		
		R.SGS*MDPSGAHPSVR.Q	S20 not confirmed

Table A-2 (continued).

Accession number	Scan(s)	Peptide	Phosphorylation sites
Q9UHR4	BI2L1_HUMAN Brain-specific angiogenesis inhibitor 1-associated protein 2-like protein 1		
		K.TPASTPVSGT*PQAS*PMIER.S	T257 confirmed by y9, y11 S261 confirmed by y5, y6
P09651	ROA1_HUMAN Heterogeneous nuclear ribonucleoprotein A1		
		K.S*ESPKEPEQLR.K	S4 confirmed by b2
		R.SS*GPYGGGGQYFAK.P	S338 not confirmed
Q9Y446	PKP3_HUMAN Plakophilin-3		
		R.LS*SGFDDIDLPSAVK.Y	S313 confirmed by b2, y14
		R.ADYDTLS*LR.S	S180 confirmed by y2, y3
Q96T21	SEBP2_HUMAN SECIS-binding protein 2		
		K.S*ARGSHHLSIYAENSLK.S	S174 confirmed by b4
P52948	NUP98_HUMAN Nuclear pore complex protein Nup98-Nup96 precursor		
		R.DSENLAS*PSEYPENGER.F	S623 confirmed by y10, y11
P35527	K1C9_HUMAN Keratin, type I cytoskeletal 9 (Cytokeratin-9)		
		R.GSRGGSGGSY*GGGGS*GGGYGGGSGS*R.G	Y497 & S502 & S512 not confirmed
		R.GSRGGSGGS*Y*GGGGSGGGYGGGS*GSR.G	S496 & Y497 & S510 not confirmed
P51991	ROA3_HUMAN Heterogeneous nuclear ribonucleoprotein A3		
		R.SSGS*PYGGGYGSGGGSGGYGSR.R	S358 confirmed by y18, y20
		R.SSGSPY*GGGYGS*GGGS*GGYGSR.R	Y360 & S366 & S370 not confirmed
		R.SS*GSPY*GGGYGSGGGS*GGYGSRRF	S356 & Y360 not confirmed S370 confirmed by b13, b16
Q6P5R6	RL22L_HUMAN Ribosomal protein L22-like 1		
		R.YFQISQDEDES*ESED	S118 confirmed by b10, b12
Q96T37	RBM15_HUMAN Putative RNA-binding protein 15		
		R.SLS*PGGAALGYR.D	S294 confirmed by y9, y10
		K.NS*S*GGGESRSSSRGGGGES*R.S	S134 & S135 not confirmed S151 confirmed by b18, b19
		R.SRS*PLDKDTY*PPSASVVGASVGGHR.H	S259 & Y266 not confirmed
Q9UQF2	JIP1_HUMAN C-jun-amino-terminal kinase-interacting protein 1		
		K.QFVEYT*CPTEDIYLE	T702 confirmed by y9, y10
O96013	PAK4_HUMAN Serine/threonine-protein kinase PAK 4 (p21-activated kinase 4)		
		R.PFNT*YPR.A	T207 confirmed by y3, y5
Q15233	NONO_HUMAN Non-POU domain-containing octamer-binding protein		
		R.FGQAATMEGIGAIGGT*PPAFNR.A	T450 confirmed by y6, y8

Table A-2 (continued).

Accession number	Scan(s)	Peptide	Phosphorylation sites
Q96PK6	RBM14_HUMAN RNA-binding protein 14		
		R.RLS*ESQLSFR.R	S618 confirmed by y7, y8
P21291	CSRP1_HUMAN Cysteine and glycine-rich protein 1		
		K.GFGFGQGAGALVHS*E	S192 confirmed by y3
Q9P2K5	MYEF2_HUMAN Myelin expression factor 2 (MyEF-2) (MST156)		
		K.AEVPGATGGDS*PHLQPAEPPGEPR.R	S17 confirmed by y13, y14
Q96J84	KIRR1_HUMAN Kin of IRRE-like protein 1 precursor		
		R.FSQEPADQT*VVAGQR.A	T31 confirmed by b7, b11
Q9UHL0	DDX25_HUMAN ATP-dependent RNA helicase DDX25 (DEAD box protein 25)		
		K.WLTVEMIQDGHQVS*LLS*GELTVEQR.A	S366 & S369 not confirmed
Q5T8P6	RBM26_HUMAN RNA-binding protein 26		
		K.T*QMQKELLDT*ELDLYKK.M	T808 & T817 not confirmed
Q9Y3Q4	HCN4_HUMAN Potassium/sodium hyperpolarization-activated cyclic nucleotide-gated channel 4		
		R.RGTPPLT*PGR.L	T1075 confirmed by y2, y6
Q8TEW8	PAR3L_HUMAN Partitioning-defective 3 homolog B (PAR3-beta)		
		R.T*QEELVAMLRST*K.Q	T445 confirmed by b3 TT456 not confirmed
O60825	F262_HUMAN 6-phosphofructo-2-kinase/fructose-2,6-biphosphatase 2		
		R.RNS*FTPLSSSNTIR.R	S446 confirmed by b2, b3
Q96JC9	EAF1_HUMAN ELL-associated factor 1		
		K.T*SPLKDNPS*PEPQLDDIKR.E	T158 not confirmed S165 confirmed by y8, y11
O43583	DENR_HUMAN Density-regulated protein (DRP)		
		K.LTVENS*PKQEAGISEGQGTAGEEEEK.K	S73 confirmed by b5, b6
Q9C0C2	TB182_HUMAN 182 kDa tankyrase 1-binding protein		
		R.SPS*QDFSFIEDTEILDSAMYR.S	S1554 confirmed by b3
O14745	NHERF_HUMAN Ezrin-radixin-moesin-binding phosphoprotein 50 (EBP50)		
		R.S*ASSDTSEELNSQDSPPK.Q	S288 not confirmed
		R.SAS*SDTSEELNSQDSPPK.Q	S290 not confirmed
		R.EALAEAALES*PRPALVR.S	S280 confirmed by y7, y8

Table A-2 (continued).

Accession number	Scan(s)	Peptide	Phosphorylation sites
P42858	HD_HUMAN Huntingtin (Huntington disease protein) (HD protein)		
		R.VNHCLTICENIVAQS*VR.N	S116 confirmed by b13, b15
Q9Y266	NUDC_HUMAN Nuclear migration protein nudC		
		K.NGSLDS*PGKQDTEEDEEEDEKDK.G	S139 confirmed by b4, b9
O00264	PGRC1_HUMAN Membrane-associated progesterone receptor component 1 (mPR)		
		K.EGEEPTVYS*DEEEPK.D	S181 not confirmed
Q9BVG4	CX026_HUMAN UPF0368 protein Cxorf26		
		K.GADS*GEEKEEGINR.E	S197 confirmed by b3, b5
Q13286	CLN3_HUMAN Battenin (Protein CLN3)		
		R.RFS*DS*EGEET*VPEPR.L	S12 confirmed by y13 S14 confirmed by y10, y11 T19 confirmed by y5, y9
Q5JTV8	TOIP1_HUMAN Torsin-1A-interacting protein 1		
		R.LQQQHSEQPPLQPS*PVMTR.R	S143 not confirmed
		K.VNFSEEGET*EEDDQDSSHSSVTTVK.A	T220 confirmed by b7, b9
Q13501	SQSTM_HUMAN Sequestosome-1		
		R.LTPVS*PESSSTEEK.S	S272 confirmed by y9, y10
P20700	LMNB1_HUMAN Lamin-B1		
		R.LKLS*PS*PSSR.V	S391 confirmed by b3, b4 S393 confirmed by y4, y6
		R.LKLS*PSPSSR.V	S391 confirmed by y6, y7
Q8IXT5	RB12B_HUMAN RNA-binding protein 12B		
		R.FPPEDFRHS*PEDFR.R	S575 confirmed by y5, y6
O14578	CTRO_HUMAN Citron Rho-interacting kinase (CRIK)		
		R.TPLSQVNKVWDQS*S*V	S2025 not confirmed S2026 confirmed by y2
Q8WWM7	ATX2L_HUMAN Ataxin-2-like protein (Ataxin-2 domain protein)		
		K.EVDGLLTSEPMGS*PVSSK.T	S594 confirmed by y5, y7
P62995	TRA2B_HUMAN Arginine/serine-rich-splicing factor 10 (Transformer-2-beta)		
		K.RPHT*PTPGIYMGR.P	T201 confirmed by b2, b4
Q14157	UBP2L_HUMAN Ubiquitin-associated protein 2-like (Protein NICE-4)		
		R.RYPSSISSS*PQK.D	S609 confirmed by y3, y4
		K.NPS*DSAVHSPFTK.R	S410 confirmed by b3
P31749	AKT1_HUMAN RAC-alpha serine/threonine-protein kinase		
		R.RPHFPQFS*YSASGTA	S473 confirmed by b7, b8

Table A-2 (continued).

Accession number	Scan(s)	Peptide	Phosphorylation sites
O14646	CHD1_HUMAN Chromodomain-helicase-DNA-binding protein 1		
		K.S*DSSPLPSEKSDEDDDK.L	S1353 not confirmed
		K.SDS*PLPSEKSDEDDDK.L	S1355 confirmed by b3
O00257	CBX4_HUMAN E3 SUMO-protein ligase CBX4 (Chromobox protein homolog 4)		
		R.EEEVSGVS*DPQPQDAGSR.K	S334 not confirmed
O14874	BCKD_HUMAN [3-methyl-2-oxobutanoate dehydrogenase [lipoamide]] kinase		
		R.ARS*TSAT*DTHHVEMAR.E	S31 not confirmed T35 confirmed by y9, y10
Q15056	IF4H_HUMAN Eukaryotic translation initiation factor 4H (eIF-4H)		
		R.AY*SS*FGGGR.G	Y12 confirmed by b2 S14 not confirmed
Q8NC51	PAIRB_HUMAN Plasminogen activator inhibitor 1 RNA-binding protein		
		K.SKS*EEAHAEDSVMDHHFR.K	S330 confirmed by b2, b3
Q9Y478	AAKB1_HUMAN 5'-AMP-activated protein kinase subunit beta-1		
		R.S*HNNFVAILDLPEGEHQYK.F	S108 confirmed by b2
P43243	MATR3_HUMAN Matrin-3		
		R.RDS*FDDR.G	S188 confirmed by b2, b3
P18669	PGAM1_HUMAN Phosphoglycerate mutase 1		
		R.HGES*AWNLENR.F	S11 confirmed by y7, y8
Q96AT1	K1143_HUMAN Uncharacterized protein KIAA1143		
		R.IQPQPPDEDGDHS*DKEDEQPQVVVLK.K	S50 confirmed by y13, y14
P47736	RGP2_HUMAN Rap1 GTPase-activating protein 1 (Rap1GAP)		
		R.RSS*AIGIENIQEVQEK.R	S499 confirmed by y13, y14
Q9BUZ4	TRAF4_HUMAN TNF receptor-associated factor 4		
		R.GS*LDESSLGFGYPK.F	S426 confirmed by b2
Q96T58	MINT_HUMAN Msx2-interacting		
		K.FGKVTSVQIHGTS*EER.Y	S374 confirmed by b12, b13
Q5HYJ3	FA76B_HUMAN Protein FAM76B		
		K.ISNLS*PEEEQGLWK.Q	S193 confirmed by y9, y10
Q13427	PPIG_HUMAN Peptidyl-prolyl cis-trans isomerase G		
		R.RS*ET*PPHWR.Q	S356 confirmed by b2 T358 confirmed by y5, y6

Table A-2 (continued).

Accession number	Scan(s)	Peptide	Phosphorylation sites
Q9UDY2	ZO2_HUMAN Tight junction protein ZO-2 (Zonula occludens 2 protein)		
		R.DNS*PPPAFKPEPPK.A	S986 confirmed by b3, b4
Q9HC52	CBX8_HUMAN Chromobox protein homolog 8		
		R.HGS*GPPSSGGGLYR.D	S311 confirmed by b3, b5

Table A-3 Subcellular locations and functional categories of the characterized phosphoproteins.

Swissprot code	Protein name	Subcellular localization	Functional category
HS90A	HUMAN Heat shock protein HSP 90-alpha (HSP 86)	Cytoplasm	Molecular chaperone
SEPT2	HUMAN Septin-2 (Protein NEDD5)	unknown	Involved in cytokinesis
TEBP	HUMAN Prostaglandin E synthase 3 (Cytosolic prostaglandin E2 synthase)	Cytoplasm	RNA processing and Transcription regulation
CTND1	HUMAN Catenin delta-1 (p120 catenin)	Cytoplasm. Nucleus	Transcription regulation
TR150	HUMAN Thyroid hormone receptor-associated protein 3	Nucleus	RNA processing and Transcription regulation
NFIC	HUMAN Nuclear factor 1 C-type (Nuclear factor 1/C) (NF1-C)	Unknown	RNA processing and Transcription regulation
G3BP1	HUMAN Ras GTPase-activating protein-binding protein 1 (G3BP-1)	Cytoplasm. Cytoplasm; cytosol. Cell membrane. Nucleus.	DNA processing
LRRF2	HUMAN Leucine-rich repeat flightless-interacting protein 2	Unknown	Signal Transduction
BRE1A	HUMAN Ubiquitin-protein ligase BRE1A (BRE1-A) (hBRE1)	Nucleus	RNA processing and Transcription regulation
ARFG1	HUMAN ADP-ribosylation factor GTPase-activating protein 1	Cytoplasm	Unknown
DC1L1	HUMAN Cytoplasmic dynein 1 light intermediate chain 1	Unknown	May play a role in binding dynein to membranous organelles or chromosomes. May associate with the heavy chains in the dynein head where they might regulate enzyme activity

Table A-3 (continued).

Swissprot code	Protein name	Subcellular localization	Functional category
M3K2	HUMAN Mitogen-activated protein kinase kinase kinase 2	Cytoplasm	Signal transduction
SMAP	HUMAN Small acidic protein	Unknown	Unknown
ZRAB2	HUMAN Zinc finger Ran-binding domain-containing protein 2	Nucleus	Translation
NKAP	HUMAN NF-kappa-B-activating protein	Nucleus	Regulator of TNF and IL-1 induced NF-kappa-B activation
KLC4	HUMAN Kinesin light chain 4 (KLC 4) (Kinesin-like protein 8)	Unknown	Kinesin is a microtubule-associated force-producing protein that may play a role in organelle transport. The light chain may function in coupling of cargo to the heavy chain or in the modulation of its ATPase activity
NUCKS	HUMAN Nuclear ubiquitous casein and cyclin-dependent kinases substrate	Nucleus	Unknown
ANKS1	HUMAN Ankyrin repeat and SAM domain-containing protein 1A (Odin)	Cytoplasm	Signal transduction
ARVC	HUMAN Armadillo repeat protein deleted in velo-cardio-facial syndrome	Unknown	Involved in protein-protein interactions at adherent junctions
K0310	HUMAN Uncharacterized protein KIAA0310	Unknown	Unknown
SRC8	HUMAN Src substrate cortactin (Amplaxin) (Oncogene EMS1)	Cytoplasm	Cell cycle
RBM39	HUMAN RNA-binding protein 39 (RNA-binding motif protein 39)	Nucleus	RNA processing and Transcription regulation
CV009	HUMAN Uncharacterized protein C22orf9	Unknown	Unknown
BCLF1	HUMAN Bcl-2-associated transcription factor 1 (Btf)	Cytoplasm. Nucleus	Death-promoting transcriptional repressor

Table A-3 (continued).

Swissprot code	Protein name	Subcellular localization	Functional category
LAP2B	HUMAN Lamina-associated polypeptide 2, isoforms beta/gamma	Nucleus	DNA processing
UBP14	HUMAN Ubiquitin carboxyl-terminal hydrolase 14	Unknown	Unknown
PHC3	HUMAN Polyhomeotic-like protein 3 (hPH3) (Homolog of polyhomeotic 3)	Nucleus	RNA processing and Transcription regulation
SRRM1	HUMAN Serine/arginine repetitive matrix protein 1	Nucleus	Translation
KAP0	HUMAN cAMP-dependent protein kinase type I-alpha regulatory subunit	Unknown	Unknown
NPM	HUMAN Nucleophosmin (NPM) (Nucleolar phosphoprotein B23)	Nucleus	Associated with nucleolar ribonucleoprotein structures and bind single-stranded nucleic acids. It may function in the assembly and/or transport of ribosome
HNRH1	HUMAN Heterogeneous nuclear ribonucleoprotein H (hnRNP H)	Nucleus; nucleoplasm.	RNA processing and Transcription regulation
STMN1	HUMAN Stathmin (Phosphoprotein p19) (pp19) (Oncoprotein 18)	Cytoplasm	Involved in the regulation of the microtubule (MT)
UBP10	HUMAN Ubiquitin carboxyl-terminal hydrolase 10	Unknown	Ubiquitin specific protease
HN1	HUMAN Hematological and neurological expressed 1 protein	Nucleus	Unknown
TIF1B	HUMAN Transcription intermediary factor 1-beta (TIF1-beta)	Nucleus	Transcription factor
CBLL1	HUMAN Cordon-bleu protein-like 1	Unknown	Unknown
IF34	HUMAN Eukaryotic translation initiation factor 3 subunit 4 (eIF-3 delta)	Unknown	Translation
RCOR1	HUMAN REST corepressor 1	Nucleus	RNA processing and Transcription regulation

Table A-3 (continued).

Swissprot code	Protein name	Subcellular localization	Functional category
LARP1	HUMAN La-related protein 1	Unknown	Unknown
AAKB2	HUMAN 5'-AMP-activated protein kinase subunit beta-2 (AMPK beta-2 chain)	Unknown	AMPK is responsible for the regulation of fatty acid synthesis by phosphorylation of acetyl-CoA carboxylase
CHSP1	HUMAN Calcium-regulated heat stable protein 1	Cytoplasm	May play a role in acinar cell metabolism
ODBA	HUMAN 2-oxoisovalerate dehydrogenase subunit alpha, mitochondrial precursor	Mitochondrion; mitochondrial matrix	The branched-chain alpha-keto dehydrogenase complex
PPHLN	HUMAN Periphilin-1 (Gastric cancer antigen Ga50)	Nucleus. Cytoplasm	Involved in epithelial differentiation and contributes
K1802	HUMAN Zinc finger protein KIAA1802	Unknown	Unknown
SF3A1	HUMAN Splicing factor 3 subunit 1 (Spliceosome-associated protein 114)	Nucleus	Unknown
TAOK2	HUMAN Serine/threonine-protein kinase TAO2	Cytoplasm	Activates the JNK MAP kinase pathway through the specific activation of the upstream MKK3 and MKK6 kinases.
KPCD1	HUMAN Serine/threonine-protein kinase D1 (nPKC-D1) (Protein kinase D)	Unknown	Unknown
STK39	HUMAN STE20/SPS1-related proline-alanine-rich protein kinase	Cytoplasm (Probable). Nucleus (Probable).	Signal transduction
KLC2	HUMAN Kinesin light chain 2 (KLC 2)	Unknown	Kinesin is a microtubule-associated force-producing protein that may play a role in organelle transport. The light chain may function in coupling of cargo to the heavy chain or in the modulation of its ATPase activity
LRRF1	HUMAN Leucine-rich repeat flightless-interacting protein 1	Nucleus. Cytoplasm.	RNA processing and Transcription regulation

Table A-3 (continued).

Swissprot code	Protein name	Subcellular localization	Functional category
ARHG6	HUMAN Rho guanine nucleotide exchange factor 6	Unknown	Acts as a RAC1 guanine nucleotide exchange factor
CD2L1	HUMAN PITSLRE serine/threonine-protein kinase CDC2L1	Cytoplasm. Nucleus	Appears to play multiple roles in cell cycle progression, cytokinesis and apoptosis
PYRG1	HUMAN CTP synthase 1 (UTP--ammonia ligase 1)	Unknown	Catalyzes the ATP-dependent amination of UTP to CTP with either L-glutamine or ammonia as the source of nitrogen.
TYY1_	HUMAN Transcriptional repressor protein YY1 (Yin and yang 1) (YY-1)	Nucleus	Transcription factor
SMN	HUMAN Survival motor neuron protein (Component of gems 1) (Gemin-1)	Cytoplasm. Nucleus	The SMN complex plays an essential role in spliceosomal snRNP assembly in the cytoplasm and is required for pre-mRNA splicing in the nucleus. It may also play a role in the metabolism of snoRNPs.
PAK2	HUMAN Serine/threonine-protein kinase PAK 2 (p21-activated kinase 2)	Unknown	The activated kinase acts on a variety of targets. Phosphorylates ribosomal protein S6, histone H4 and myelin basic protein.
SSRP1	HUMAN FACT complex subunit SSRP1	Nucleus	Component of the FACT complex, a general chromatin factor that acts to reorganize nucleosomes.
CTNA1	HUMAN Catenin alpha-1 (Cadherin-associated protein)	Cell junction	May play a crucial role in cell differentiation
SFRS9	HUMAN Splicing factor, arginine/serine-rich 9	Nucleus	Translation
AGM1	HUMAN Phosphoacetylglucosamine mutase (PAGM)	Unknown	Interconvert GlcNAc-6-P and GlcNAc-1-P
MORC2	HUMAN MORC family CW-type zinc finger protein 2	Unknown	Unknown
BAD	HUMAN Bcl2 antagonist of cell death (BAD)	Mitochondrion; mitochondrial outer membrane	Cell cycle
TB182	HUMAN 182 kDa tankyrase 1-binding protein	Nucleus. Cytoplasm	Binds to the ANK repeat domain of TNKS1 and TNKS2
AKTS1	HUMAN Proline-rich AKT1 substrate 1 (40 kDa proline-rich AKT substrate)	Cytoplasm; cytosol	Signal transduction

Table A-3 (continued).

Swissprot code	Protein name	Subcellular localization	Functional category
PUM1	HUMAN Pumilio homolog 1 (Pumilio-1) (HsPUM)	Cytoplasm	RNA processing and Transcription regulation
ODPA	HUMAN Pyruvate dehydrogenase E1 component alpha subunit	Mitochondrion; mitochondrial matrix.	Metabolic pathway
SRRM2	HUMAN Serine/arginine repetitive matrix protein 2	Nucleus	Translation
RBM10	HUMAN RNA-binding protein 10 (RNA-binding motif protein 10)	Nucleus	Unknown
HIRP3	HUMAN HIRA-interacting protein 3	Nucleus	May play a role in chromatin function and histone metabolism via its interaction with HIRA and histones.
FA62A	HUMAN Protein FAM62A (Membrane-bound C2 domain-containing protein)	Membrane	Unknown
PACN3	HUMAN Protein kinase C and casein kinase substrate in neurons protein 3	Cytoplasm. Cell membrane; peripheral membrane protein; cytoplasmic side.	May play a role in vesicle formation and transport.
MLRN	HUMAN Myosin regulatory light chain 2, smooth muscle isoform	Unknown	Plays an important role in regulation of both smooth muscle and nonmuscle cell contractile activity
HSPB1	HUMAN Heat-shock protein beta-1 (HspB1) (Heat shock 27 kDa protein)	Cytoplasm, Nucleus	Involved in stress resistance and actin organization.
LA	HUMAN Lupus La protein (Sjoegren syndrome type B antigen)	Nucleus	RNA processing and Transcription regulation
IF2P	HUMAN Eukaryotic translation initiation factor 5B (eIF-5B)	Unknown	Translation
FXR1	HUMAN Fragile X mental retardation syndrome-related protein 1 (hFXR1p)	Cytoplasm.	RNA processing and Transcription regulation
HS90B	HUMAN Heat shock protein HSP 90-beta (HSP 84)	Cytoplasm	Molecular chaperone

Table A-3 (continued).

Swissprot code	Protein name	Subcellular localization	Functional category
CFDP1	HUMAN Craniofacial development protein 1 (Bucentaur)	Unknown	May play a role during embryogenesis (By similarity).
LC7L2	HUMAN Putative RNA-binding protein Luc7-like 2	Unknown	May bind to RNA via its Arg/Ser-rich domain
IF38	HUMAN Eukaryotic translation initiation factor 3 subunit 8 (eIF3 p110)	Unknown	Translation
MYPT1	HUMAN Protein phosphatase 1 regulatory subunit 12A	Cytoplasm	Regulates myosin phosphatase activity
ZN330	HUMAN Zinc finger protein 330 (Nucleolar cysteine-rich protein)	Nucleus	Unknown
HNRPK	HUMAN Heterogeneous nuclear ribonucleoprotein K	Cytoplasm. Nucleus; nucleoplasm.	One of the major pre-mRNA-binding proteins.
HDGF	HUMAN Hepatoma-derived growth factor (HDGF)	Cytoplasm	Heparin-binding protein, with mitogenic activity for fibroblasts.
OSBP1	HUMAN Oxysterol-binding protein 1	Cytoplasm	May play a role in the regulation of sterol metabolism
ABCF1	HUMAN ATP-binding cassette sub-family F member 1	Unknown	Translation
HNRH2	HUMAN Heterogeneous nuclear ribonucleoprotein H' (hnRNP H') (FTP-3)	Nucleus; nucleoplasm	Translation
MK67I	HUMAN MKI67 FHA domain-interacting nucleolar phosphoprotein	Nucleus; nucleolus	Unknown
LMNA	HUMAN Lamin-A/C (70 kDa lamin)	Nucleus.	Unknown
CDC2	HUMAN Cell division control protein 2 homolog (p34 protein kinase)	Nucleus	Cell cycle
PCY1A	HUMAN Choline-phosphate cytidylyltransferase A	Cytoplasm; cytosol. Membrane; peripheral membrane protein.	Controls phosphatidylcholine synthesis

Table A-3 (continued).

Swissprot code	Protein name	Subcellular localization	Functional category
CCDC6	HUMAN Coiled-coil domain-containing protein 6 (H4 protein)	Cytoplasm. Cytoplasm; cytoskeleton	Unknown
SMC4	HUMAN Structural maintenance of chromosomes protein 4	Nucleus. Cytoplasm	DNA processing
SMRC2	HUMAN SWI/SNF-related matrix-associated actin-dependent regulator of chromatin subfamily C member 2	Nucleus	transcriptional activation and repression
MDC1	HUMAN Mediator of DNA damage checkpoint protein 1	nucleus	Cell cycle
PPIL4	HUMAN Peptidyl-prolyl cis-trans isomerase-like 4	Nucleus	PPIases accelerate the folding of proteins
XRCC1	HUMAN DNA-repair protein XRCC1	Nucleus	Unknown
SYEP	HUMAN Bifunctional aminoacyl-tRNA synthetase	Unknown	Unknown
CALX	HUMAN Calnexin precursor	Endoplasmic reticulum	Translation
FUSIP	HUMAN FUS-interacting serine-arginine-rich protein 1	Nucleus; cytoplasm	Translation
MLF2	HUMAN Myeloid leukemia factor 2	Cytoplasm; nucleus	Unknown
PCBP2	HUMAN Poly(rC)-binding protein 2 (Alpha-CP2)	Nucleus; cytoplasm	Major cellular poly(rC)-binding protein
CLIP1	HUMAN Restin	cytoplasm	Unknown
MPRI	HUMAN Cation-independent mannose-6-phosphate receptor precursor	Lysosome; lysosomal membrane	Signal transduction
NOP56	HUMAN Nucleolar protein Nop56	Nucleus	Translation
RBM5	HUMAN RNA-binding protein 5	Nucleus	Tumor suppressor protein that reduces cell proliferation and promotes apoptosis and cell cycle arrest
LIPB2	HUMAN Liprin-beta-2	Unknown	May regulate the disassembly of focal adhesions. Did not bind receptor-like tyrosine phosphatases type 2A

Table A-3 (continued).

Swissprot code	Protein name	Subcellular localization	Functional category
TXLNA	HUMAN Alpha-taxilin	Unknown	Unknown
PHF6	HUMAN PHD finger protein 6 (PHD-like zinc finger protein)	Nucleus	Transcription regulation
TRA2A	HUMAN Transformer-2 protein homolog	Nucleus	Translation
BIRC3	HUMAN Baculoviral IAP repeat-containing protein 3	Unknown	Unknown
MCM2	HUMAN DNA replication licensing factor MCM2	Nucleus	Cell cycle
NFAC3	HUMAN Nuclear factor of activated T-cells, cytoplasmic 3 (NF-ATc3)	Cytoplasm, nucleus	Plays a role in the inducible expression of cytokine genes in T-cells, especially in the induction of the IL-2.
CT172	HUMAN Uncharacterized protein C20orf172	Nucleus	Cell cycle
PKCB1	HUMAN Protein kinase C-binding protein 1 (Rack7)	Unknown	Unknown
KAP1	HUMAN cAMP-dependent protein kinase type I-beta regulatory subunit	Unknown	Unknown
TAOK1	HUMAN Serine/threonine-protein kinase TAO1	Cytoplasm	Signal transduction
BRCA2	HUMAN Breast cancer type 2 susceptibility protein	Unknown	Cell cycle
LRC15	HUMAN Leucine-rich repeat-containing protein 15 precursor (hLib)	Membrane	Unknown
MRCKA	HUMAN Serine/threonine-protein kinase MRCK alpha	Cytoplasm	Cell cycle
NOL7	HUMAN Nucleolar protein 7	Nucleus	Unknown
GSTM2	HUMAN Glutathione S-transferase Mu 2	Cytoplasm	Unknown
MYH13	HUMAN Myosin-13 (Myosin heavy chain 13)	Unknown	Muscle contraction

Table A-3 (continued).

Swissprot code	Protein name	Subcellular localization	Functional category
ELL	HUMAN RNA polymerase II elongation factor ELL	Nucleus	Elongation factor
M10L1	HUMAN Putative helicase Mov10l1	Unknown	Putative RNA helicase. Isoform 1 may play a role in male germ cell development.
DPOA2	HUMAN DNA polymerase subunit alpha B	Nucleus.	RNA processing and transcription regulation
SNF5	HUMAN SWI/SNF-related matrix-associated actin-dependent regulator of chromatin subfamily B member 1	Nucleus	Cell cycle
UBR2	HUMAN E3 ubiquitin-protein ligase UBR2 (N-recognin-2)	nucleus	Signal transduction
MRP	HUMAN MARCKS-related protein (MARCKS-like protein 1)	Unknown	Signal transduction
NP1L4	HUMAN Nucleosome assembly protein 1-like 4	Nucleus	Unknown
4EBP1	HUMAN Eukaryotic translation initiation factor 4E-binding protein 1	Unknown	Translation
RANB3	HUMAN Ran-binding protein 3 (RanBP3)	Cytoplasm. Nucleus.	Acts as a cofactor for XPO1/CRM1-mediated nuclear export, perhaps as export complex scaffolding protein.
EP15	HUMAN Epidermal growth factor receptor substrate 15 (Protein Eps15)	Cytoplasm, cell membrane	Cell growth
1433E	HUMAN 14-3-3 protein epsilon (14-3-3E)	Cytoplasm	Signal transduction
RL1D1	HUMAN Ribosomal L1 domain-containing protein 1	Nucleus	Unknown
MARCS	HUMAN Myristoylated alanine-rich C-kinase substrate (MARCKS)	Unknown	MARCKS is the most prominent cellular substrate for protein kinase C
CD2B2	HUMAN CD2 antigen cytoplasmic tail-binding protein 2	Cytoplasm	Unknown
K1C18	HUMAN Keratin, type I cytoskeletal 18 (Cytokeratin-18) (CK-18)	Unknown	Unknown
PURB	HUMAN Transcriptional activator protein Pur-beta	Nucleus	Has capacity to bind repeated elements in single-stranded DNA such as the purine-rich single strand of the PUR element located upstream of the MYC gene.

Table A-3 (continued).

Swissprot code	Protein name	Subcellular localization	Functional category
ZN326	HUMAN Zinc finger protein 326	Nucleus	transcriptional activator
EF1D	HUMAN Elongation factor 1-delta (EF-1-delta) (Antigen NY-CO-4)	Unknown	Translation
NDRG3	HUMAN Protein NDRG3	Unknown	Unknown
SFR11	HUMAN Splicing factor arginine/serine-rich 11	Nucleus	RNA processing and Transcription regulation
PSA3	HUMAN Proteasome subunit alpha type 3 (Proteasome component C8)	Cytoplasm, nucleus	proteasome
FIP1	HUMAN Pre-mRNA 3'-end-processing factor FIP1 (FIP1-like 1)	Unknown	RNA processing and Transcription regulation
TE2IP	HUMAN Telomeric repeat-binding factor 2-interacting protein 1	Nucleus	May play a role in telomere length regulation.
MAP4	HUMAN Microtubule-associated protein 4 (MAP 4)	Unknown	Non-neuronal microtubule-associated protein. Promotes
K2C7	HUMAN Keratin, type II cytoskeletal 7	Unknown	Unknown
PININ	HUMAN Pinin (140 kDa nuclear and cell adhesion-related phosphoprotein)	Nucleus; nuclear speckle. Cell junction;	RNA processing and Transcription regulation
TBA6	HUMAN Tubulin alpha-6 chain (Alpha-tubulin 6)	Unknown	Tubulin is the major constituent of microtubules. It binds two moles of GTP, one at an exchangeable site on the beta chain and one at a non-exchangeable site on the alpha-chain.
UBP7	HUMAN Ubiquitin carboxyl-terminal hydrolase 7 (Ubiquitin thioesterase 7)	Nucleus	Cell cycle
HNRPF	HUMAN Heterogeneous nuclear ribonucleoprotein F (hnRNP F)	Nucleus; nucleoplasm	Component of the heterogeneous nuclear ribonucleoprotein (hnRNP) complexes which provide the substrate for the processing events that pre-mRNAs undergo before becoming functional, translatable mRNAs in the cytoplasm. Probably binds G-rich sequences in pre-mRNAs

Table A-3 (continued).

Swissprot code	Protein name	Subcellular localization	Functional category
CBX3	HUMAN Chromobox protein homolog 3	Nucleus (Probable).	RNA processing and Transcription regulation
SSH3	HUMAN Protein phosphatase Slingshot homolog 3 (SSH-3L)	Cytoplasm, nucleus	Protein phosphatase which may play a role in the regulation of actin filament dynamics
DDX21	HUMAN Nucleolar RNA helicase 2 (Nucleolar RNA helicase II)	Nucleus; nucleolus.	RNA processing and Transcription regulation
TACC2	HUMAN Transforming acidic coiled-coil-containing protein 2	Cytoplasm. Nucleus. Centrosome.	May play a role in organizing centrosomal microtubules. May act as a tumor suppressor protein. May represent a tumor progression marker
LIPB1	HUMAN Liprin-beta-1	Unknown	May regulate the disassembly of focal adhesions. Did not bind receptor-like tyrosine phosphatases type 2A.
IF4B	HUMAN Eukaryotic translation initiation factor 4B (eIF-4B)	Unknown	RNA processing and Transcription regulation
TIF1A	HUMAN Transcription intermediary factor 1-alpha (TIF1-alpha)	Nucleus	Interacts selectively in vitro with the AF2-activating domain of the estrogen receptors. Association with DNA-bound estrogen receptors requires the presence of estradiol.
MAP1B	HUMAN Microtubule-associated protein 1B (MAP 1B)	Unknown	The function of brain MAPS is essentially unknown. Phosphorylated MAP1B may play a role in the cytoskeletal changes that accompany neurite extension
EXOS9	HUMAN Exosome complex exonuclease RRP45 (Exosome component 9)	Cytoplasm. Nucleus; nucleolus.	RNA processing and Transcription regulation
BCL7C	HUMAN B-cell CLL/lymphoma 7 protein family member C	Unknown	May play an anti-apoptotic role
SNUT1	HUMAN U4/U6.U5 tri-snRNP-associated protein 1	Nucleus	Translation
WEE1	HUMAN Wee1-like protein kinase (Wee1A kinase) (WEE1hu)	Nucleus	Cell cycle

Table A-3 (continued).

Swissprot code	Protein name	Subcellular localization	Functional category
NCK1	HUMAN Cytoplasmic protein NCK1 (NCK adaptor protein 1)	Cytoplasm	Adapter protein which associates with tyrosine-phosphorylated growth factor receptors or their cellular substrates.
STUB1	HUMAN STIP1 homology and U box-containing protein 1	Cytoplasm	Unknown
DIDO1	HUMAN Death-inducer obliterator 1 (DIO-1)	Cytoplasm. Nucleus	RNA processing and Transcription regulation
SPF45	HUMAN Splicing factor 45 (45 kDa-splicing factor)	Nucleus.	RNA processing
PDCD4	HUMAN Programmed cell death protein 4 (Nuclear antigen H731-like)	Nucleus. Cytoplasm	Tumor suppressor. Inhibits tumor promoter-induced
IPYR2	HUMAN Inorganic pyrophosphatase 2, mitochondrial precursor (PPase 2)	Mitochondrion	Unknown
LS14A	HUMAN LSM14 protein homolog A (Protein SCD6 homolog)	Unknown	Unknown
SFRS6	HUMAN Splicing factor, arginine/serine-rich 6	Nucleus	Plays a role in constitutive splicing and can modulate the selection of alternative splice sites
SDS3	HUMAN Sin3 histone deacetylase corepressor complex component SDS3	Unknown	Regulatory protein which represses transcription and augments histone deacetylase activity of HDAC1. May have a potential role in tumor suppressor pathways. May function in the assembly and/or enzymatic activity of the mSin3A corepressor complex or in mediating interactions between the complex and other regulatory complexes
ARS2	HUMAN Arsenite-resistance protein 2	Unknown	Confers arsenite resistance
TBA1	HUMAN Tubulin alpha-1 chain (Alpha-tubulin 1)	Unknown	Tubulin is the major constituent of microtubules. It binds two moles of GTP, one at an exchangeable site on the beta chain and one at a non-exchangeable site on the alpha-chain
REPS1	HUMAN RalBP1-associated Eps domain-containing protein 1	Unknown	Unknown

Table A-3 (continued).

Swissprot code	Protein name	Subcellular localization	Functional category
UBXD7	HUMAN UBX domain-containing protein 7	Unknown	Unknown
YBOX1	HUMAN Nuclease sensitive element-binding protein 1	Cytoplasm. Nucleus	Translation
NDRG2	HUMAN Protein NDRG2 (Protein Syld709613)	Cytoplasm. Cytoplasm; perinuclear region	May be involved in dendritic cell and neuron differentiation. May have anti-tumor activity.
PGRC1	HUMAN Membrane-associated progesterone receptor component 1 (mPR)	Microsome; microsomal membrane;	Receptor for progesterone
EP15R	HUMAN Epidermal growth factor receptor substrate 15-like 1	Cell membrane	Seems to be a constitutive component of clathrin-coated pits that is required for receptor-mediated endocytosis
BIN1	HUMAN Myc box-dependent-interacting protein 1 (Bridging integrator 1)	Nucleus ; cytoplasm	Unknown
SGIP1	HUMAN SH3-containing GRB2-like protein 3-interacting protein 1	Unknown	Possible role in the regulation of energy homeostasis
MATN4	HUMAN Matrilin-4 precursor	Secreted protein	Unknown
YETS2	HUMAN YEATS domain-containing protein 2	Nucleus	Unknown
PDE10	HUMAN cAMP and cAMP-inhibited cGMP 3',5'-cyclic phosphodiesterase 10A	Soluble cellular fractions	Signal transduction
DPOD3	HUMAN DNA polymerase subunit delta 3 (DNA polymerase subunit delta p66)	Nucleus.	Unknown
NSF1C	HUMAN NSFL1 cofactor p47 (p97 cofactor p47)	Nucleus. Golgi apparatus;	Translation
WASF2	HUMAN Wiskott-Aldrich syndrome protein family member 2	Cytoplasm	Signal transduction
MEP50	HUMAN Methylosome protein 50 (MEP50 protein) (WD repeat protein 77)	Unknown	The methylosome may regulate an early step in the assembly of U snRNPs, possibly the transfer of Sm proteins to the SMN-complex

Table A-3 (continued).

Swissprot code	Protein name	Subcellular localization	Functional category
ARRB1	HUMAN Beta-arrestin-1 (Arrestin beta 1)	Unknown	Regulates beta-adrenergic receptor function. Beta-arrestins seem to bind phosphorylated beta-adrenergic receptors, thereby causing a significant impairment of their capacity to activate G(S) protein
CT2NL	HUMAN CTTNBP2 N-terminal-like protein	Unknown	Unknown
TJAP1	HUMAN Tight junction-associated protein 1 (Tight junction protein 4)	Golgi apparatus	Unknown
LAMA2	HUMAN Laminin subunit alpha-2 precursor (Laminin M chain)	Secreted protein; extracellular space; extracellular	Binding to cells via a high affinity receptor, laminin is thought to mediate the attachment, migration and organization of cells into tissues during embryonic development by interacting with other extracellular matrix components
PERQ2	HUMAN PERQ amino acid-rich with GYF domain-containing protein 2	Unknown	Signal transduction
NIPA	HUMAN Nuclear-interacting partner of ALK	Nucleus	Signal transduction
ANK3	HUMAN Ankyrin-3 (ANK-3) (Ankyrin-G)	Unknown	Unknown
CIP4	HUMAN Cdc42-interacting protein 4	Cytoplasm; lysosome; Golgi apparatus. Cell membrane	Signal transduction
PGRC2	HUMAN Membrane-associated progesterone receptor component 2	Unknown	Receptor for steroids
KKCC1	HUMAN Calcium/calmodulin-dependent protein kinase kinase 1	Cytoplasm, nucleus	Signal transduction Calcium/calmodulin-dependent protein kinase that belongs to a proposed calcium-triggered signaling cascade involved in a number of cellular processes
PEBP1	HUMAN Phosphatidylethanolamine-binding protein 1 (PEBP-1)	Cytoplasm	Unknown

Table A-3 (continued).

Swissprot code	Protein name	Subcellular localization	Functional category
BAIP2	HUMAN Brain-specific angiogenesis inhibitor 1-associated protein 2	Cytoplasm, membrane	Adapter protein that links membrane-bound small G-proteins to cytoplasmic effector proteins. Necessary for CDC42-mediated reorganization of the actin cytoskeleton and for RAC1-mediated membrane ruffling.
PDPK1	HUMAN 3-phosphoinositide-dependent protein kinase 1 (hPDK1)	Cytoplasm. membrane; peripheral membrane	Signal transduction
SH24A	HUMAN SH2 domain-containing protein 4A	Unknown	Unknown
NELFE	HUMAN Negative elongation factor E (NELF-E)	Nucleus	Transcription regulation
CN004	HUMAN Protein C14orf4	Nucleus	Unknown
NFIA	HUMAN Nuclear factor 1 A-type (Nuclear factor 1/A)	Nucleus	RNA processing and Transcription regulation
PI3R6	HUMAN Phosphoinositide 3-kinase regulatory subunit 6	Cytoplasm	Unknown
TAF1	HUMAN Transcription initiation factor TFIID subunit 1	Nucleus	Transcription regulation
CLC4F	HUMAN C-type lectin domain family 4 member F	Membrane	Receptor with an affinity for galactose and fucose. Could be involved in endocytosis
TLE3	HUMAN Transducin-like enhancer protein 3 (ESG3)	Unknown	Transcription regulation
ARHGG	HUMAN Rho guanine nucleotide exchange factor 16	Unknown	Unknown
ILF3	HUMAN Interleukin enhancer-binding factor 3	Nucleus	DNA processing
ZN496	HUMAN Zinc finger protein 496	Nucleus	Transcription regulation
G3BP2	HUMAN Ras GTPase-activating protein-binding protein 2 (G3BP-2)	Unknown	Scaffold protein

Table A-3 (continued).

Swissprot code	Protein name	Subcellular localization	Functional category
HNF3A	HUMAN Hepatocyte nuclear factor 3-alpha	Nucleus	Transcription activator
MYH9	HUMAN Myosin-9 (Myosin heavy chain 9)	Unknown	Cell cycle
RU17	HUMAN U1 small nuclear ribonucleoprotein 70 kDa (U1 snRNP 70 kDa)	Unknown	Unknown
ATM	HUMAN Serine-protein kinase ATM (Ataxia telangiectasia mutated)	Nucleus. Cytoplasmic vesicle	Signal transduction
RALY	HUMAN RNA-binding protein Raly	Nucleus	Translation
ZNF2	HUMAN Zinc finger protein 2 (Zinc finger 2.2) (Zinc finger protein 661)	Nucleus	Transcription regulation
STAC2	HUMAN SH3 and cysteine-rich domain-containing protein 2	Unknown	Unknown
FOXK1	HUMAN Forkhead box protein K1 (Myocyte nuclear factor) (MNF)	Unknown	Transcription regulation
ZBTB5	HUMAN Zinc finger and BTB domain-containing protein 5	Nucleus	Transcription regulation
RBGPR	HUMAN Rab3 GTPase-activating protein non-catalytic subunit	Cytoplasm	Regulatory subunit of a GTPase activating protein that has specificity for Rab3 subfamily (RAB3A, RAB3B, RAB3C and RAB3D). Rab3 proteins are involved in regulated exocytosis of neurotransmitters and hormones. Rab3 GTPase-activating complex specifically converts active Rab3-GTP to the inactive form Rab3-GDP. Required for normal eye and brain development.
ROA2	HUMAN Heterogeneous nuclear ribonucleoproteins A2/B1 (hnRNP A2 / hnRNP B1)	Nucleus	RNA processing and Transcription regulation

Table A-3 (continued).

Swissprot code	Protein name	Subcellular localization	Functional category
SEPT9	HUMAN Septin-9 (MLL septin-like fusion protein)	Cell membrane	Involved in cytokinesis. May function as an ovarian tumor suppressor
DTD1	HUMAN Probable D-tyrosyl-tRNA(Tyr) deacylase 1	Cytoplasm	Hydrolyzes D-tyrosyl-tRNA(Tyr) into D-tyrosine and free tRNA(Tyr). Could be a defense mechanism against a harmful effect of D-tyrosine
K0515	HUMAN Uncharacterized protein KIAA0515	Unknown	Unknown
MCM3	HUMAN DNA replication licensing factor MCM3	Nucleus	DNA processing
MTMR5	HUMAN SET-binding factor 1 (Sbf1) (Myotubularin-related protein 5)	Nucleus	Probable pseudophosphatase. Lacks several amino acids in the catalytic pocket which renders it catalytically inactive as a phosphatase. The pocket is however sufficiently preserved to bind phosphorylated substrates, and maybe protect them from phosphatases. Inhibits myoblast differentiation in vitro and induces oncogenic transformation in fibroblasts
ALKB5	HUMAN Alkylated repair protein alkB homolog 5	Unknown	Unknown
CHCH3	HUMAN Coiled-coil-helix-coiled-coil-helix domain-containing protein 3	Unknown	Unknown
VDAC1	HUMAN Voltage-dependent anion-selective channel protein 1 (VDAC-1)	Mitochondrion; mitochondrial outer membrane.	Unknown
B4GN4	HUMAN N-acetyl-beta-glucosaminyl-glycoprotein 4-beta-N-acetylgalactosaminyltransferase 1	Golgi apparatus	Transfers N-acetylgalactosamine (GalNAc) from UDP-GalNAc to N-acetylglucosamine-beta-benzyl with a beta-1,4-linkage to form N,N'-diacetyllactosediamine, GalNAc-beta-1,4-GlcNAc structures in N-linked glycans and probably O-linked glycans.
SNW1	HUMAN SNW domain-containing protein 1 (Nuclear protein SkiP)	Nucleus	RNA processing and Transcription regulation
PPA6	HUMAN Lysophosphatidic acid phosphatase type 6 precursor	Secreted protein	Hydrolyzes lysophosphatidic acid to monoacylglycerol

Table A-3 (continued).

Swissprot code	Protein name	Subcellular localization	Functional category
RFIP1	HUMAN Rab11 family-interacting protein 1 (Rab11-FIP1)	Endosome; recycling endosome. Isoform 2:	A Rab11 effector protein involved in the endosomal recycling process. Also involved in controlling membrane trafficking along the phagocytic pathway and in phagocytosis
TCEA1	HUMAN Transcription elongation factor A protein 1	Nucleus	Transcription regulation
SAP30	HUMAN Histone deacetylase complex subunit SAP30	Nucleus	Transcription regulation
SAM68	HUMAN KH domain-containing, RNA-binding, signal transduction-associated protein1	Nucleus. Membrane.	Signal transduction, transcription regulation and cell cycle
BI2L1	HUMAN Brain-specific angiogenesis inhibitor 1-associated protein 2-like protein1	Unknown	May function as adapter protein
ROA1	HUMAN Heterogeneous nuclear ribonucleoprotein A1	Nucleus, cytoplasm	Involved in the packaging of pre-mRNA into hnRNP particles, transport of poly(A) mRNA from the nucleus to the cytoplasm and may modulate splice site selection
PKP3	HUMAN Plakophilin-3	Nucleus. Cell junction; desmosome.	May play a role in junctional plaques.
SEBP2	HUMAN SECIS-binding protein 2	Nucleus	Binds to the SECIS element in the 3' UTR of some mRNAs encoding selenoproteins. Binding is stimulated by SELB.
NUP98	HUMAN Nuclear pore complex protein Nup98-Nup96 precursor	Nucleus	Nup98 and Nup96 play a role in the bidirectional transport across the nucleoporin complex (NPC). The repeat domain in Nup98 has a direct role in the transport
K1C9	HUMAN Keratin, type I cytoskeletal 9 (Cytokeratin-9)	Unknown	May serve an important special function either in the mature palmar and plantar skin tissue or in the morphogenic program of the formation of these tissues
ROA3	HUMAN Heterogeneous nuclear ribonucleoprotein A3 (hnRNP A3)	Nucleus	RNA processing and Transcription regulation
RL22L	HUMAN Ribosomal protein L22-like 1	Unknown	Unknown

Table A-3 (continued).

Swissprot code	Protein name	Subcellular localization	Functional category
RBM15	HUMAN Putative RNA-binding protein 15 (RNA-binding motif protein 15)	Nucleus	May be implicated in HOX gene regulation
JIP1	HUMAN C-jun-amino-terminal kinase-interacting protein 1	Cytoplasm; nucleus	Signal transduction
PAK4	HUMAN Serine/threonine-protein kinase PAK 4 (p21-activated kinase 4)	Unknown	Signal transduction
NONO	HUMAN Non-POU domain-containing octamer-binding protein (NonO protein)	Nucleus	RNA processing and Transcription regulation
RBM14	HUMAN RNA-binding protein 14 (RNA-binding motif protein 14)	Unknown	Transcription regulation
CSRP1	HUMAN Cysteine and glycine-rich protein 1 (Cysteine-rich protein 1)	Nucleus	Could play a role in neuronal development
MYEF2	HUMAN Myelin expression factor 2 (MyEF-2) (MST156)	Nucleus	Transcription repressor
KIRR1	HUMAN Kin of IRRE-like protein 1 precursor	Membrane	Signal transduction
DDX25	HUMAN ATP-dependent RNA helicase DDX25 (DEAD box protein 25)	Cytoplasm	ATP-dependent RNA helicase
RBM26	HUMAN RNA-binding protein 26 (RNA-binding motif protein 26)	Unknown	Unknown
HCN4	HUMAN Potassium/sodium hyperpolarization-activated cyclic nucleotide-gated channel 4	Membrane	Hyperpolarization-activated ion channel with very slow activation and inactivation exhibiting weak selectivity for potassium over sodium ions. May contribute to the native pacemaker currents in heart (If) and in neurons (Ih). Activated by cAMP. May mediate responses to sour stimuli.

Table A-3 (continued).

Swissprot code	Protein name	Subcellular localization	Functional category
PAR3L	HUMAN Partitioning-defective 3 homolog B (PAR3-beta)	Intracytoplasmic membrane. Cell junction	Putative adapter protein involved in asymmetrical cell division and cell polarization processes. May play a role in the formation of epithelial tight junctions
F262	HUMAN 6-phosphofructo-2-kinase/fructose-2,6-biphosphatase 2	Unknown	Synthesis and degradation of fructose 2,6-bisphosphate
EAF1	HUMAN ELL-associated factor 1	Nucleus	Transcription regulation
DENR	HUMAN Density-regulated protein (DRP) (Protein DRP1)	Unknown	Unknown
TB182	HUMAN 182 kDa tankyrase 1-binding protein	Nucleus, cytoplasm	Binds to the ANK repeat domain of TNKS1 and TNKS2
NHERF	HUMAN Ezrin-radixin-moesin-binding phosphoprotein 50 (EBP50)	Intracytoplasmic membrane; peripheral	Scaffold protein
HD	HUMAN Huntingtin (Huntington disease protein) (HD protein)	Cytoplasm, nucleus	May play a role in microtubule-mediated transport or vesicle function
NUDC	HUMAN Nuclear migration protein nudC	Cytoplasm. Nucleus	Plays a role in neurogenesis and neuronal migration
PGRC1	HUMAN Membrane-associated progesterone receptor component 1 (mPR)	Microsome; microsomal membrane; single-pass membrane protein	Receptor for progesterone
CX026	HUMAN UPF0368 protein Cxorf26	Unknown	Unknown
CLN3	HUMAN Battenin (Protein CLN3) (Batten disease protein)	Lysosome; lysosomal membrane	Unknown
TOIP1	HUMAN Torsin-1A-interacting protein 1	Nucleus	Unknown
SQSTM	HUMAN Sequestosome-1	Cytoplasm. Endosome; late endosome. Nucleus	Signal trasduction
LMNB1	HUMAN Lamin-B1	Nucleus	Unknown

Table A-3 (continued).

Swissprot code	Protein name	Subcellular localization	Functional category
RB12B	HUMAN RNA-binding protein 12B (RNA-binding motif protein 12B)	Unknown	Unknown
CTRO	HUMAN Citron Rho-interacting kinase (CRIK)	cytoplasm	Unknown
ATX2L	HUMAN Ataxin-2-like protein	Membrane	Unknown
TRA2B	HUMAN Arginine/serine-rich-splicing factor 10 (Transformer-2-beta)	Nucleus	Translation
UBP2L	HUMAN Ubiquitin-associated protein 2-like (Protein NICE-4)	Unknown	Unknown
AKT1	HUMAN RAC-alpha serine/threonine-protein kinase	Cytoplasm. Nucleus	Signal transduction
CHD1	HUMAN Chromodomain-helicase-DNA-binding protein 1	Nucleus	Gene Regulation
CBX4	HUMAN E3 SUMO-protein ligase CBX4	Nucleus.	Transcription regulation
BCKD	HUMAN [3-methyl-2-oxobutanoate dehydrogenase [lipoamide]] kinase	Mitochondrion; mitochondrial matrix.	Metabolic pathways
IF4H	HUMAN Eukaryotic translation initiation factor 4H (eIF-4H)	Cytoplasm	Translation regulation
PAIRB	HUMAN Plasminogen activator inhibitor 1 RNA-binding protein	Cytoplasm. Nucleus	RNA processing and transcription regulation
AAKB1	HUMAN 5'-AMP-activated protein kinase subunit beta-1	Cytoplasm	Metabolic pathways
MATR3	HUMAN Matrin-3	Nucleus	RNA processing and transcription regulation
PGAM1	HUMAN Phosphoglycerate mutase 1	Unknown	Unknown
K1143	HUMAN Uncharacterized protein KIAA1143	Unknown	Unknown
RGP2	HUMAN Rap1 GTPase-activating protein 1 (Rap1GAP)	Golgi apparatus; Golgi apparatus membrane	Signaling transduction

Table A-3 (continued).

Swissprot code	Protein name	Subcellular localization	Functional category
TRAF4	HUMAN TNF receptor-associated factor 4	Cytoplasm. Nucleus	Signal transduction
MINT	HUMAN Msx2-interacting protein (SPEN homolog)	Nucleus	Signal transduction
FA76B	HUMAN Protein FAM76B	Unknown	Unknown
PPIG	HUMAN Peptidyl-prolyl cis-trans isomerase G	Nucleus	RNA processing and transcription regulation
ZO2	HUMAN Tight junction protein ZO-2 (Zonula occludens 2 protein)	Cell junction	Cell structure
CBX8	HUMAN Chromobox protein homolog 8 (Polycomb 3 homolog)	Nucleus	RNA processing and transcription regulation

The information was compiled from Swiss-Prot annotations.

Table A-4 Details of characterized phosphoproteins.

Accession number	Protein	Peptide	Site	Phosphory-lation site	99-029	98-065	99-045	99-067	99-010
		Phosphoproteins found in all 5 specimens							
Q05682	Caldesmon	K.RGS*IGENQVEVMVEEK.T	S202 (b6）	Y	Y	Y	Y	Y	Y
		K.RGS*IGENQVEVM#VEEK.T	S202	Y	N	Y	N	N	N
P17661	Desmin	R.TFGGAPGFPLGSPLSS*PVFPR.A	S32 (y5, y6)	Y	N	Y	Y	N	N
		R.TFGGAPGFPLGS*PLSSPVFPR.A	S28 (y9,y10)	N	Y	Y	Y	Y	Y
		R.TFGGAPGFPLGS*PLSS*PVFPR.A	S32 (y5, y6)	Y	Y	N	Y	Y	N
P04792	Heat-shock protein beta-1 (Heat shock 27 kDa protein)	R.QLS*SGVSEIR.H	S82 (y7, y8)	Y	Y	Y	Y	Y	Y
		R.GPS*WDPFR.D	S15 (b2, b3)	Y	Y	Y	Y	N	N
		R.GPS*WDPFRDWYPHSR.L	S15	Y	N	N	N	Y	N
Q9UMS6	Synaptopodin-2	R.AQS*PTPSLPASWK.Y	S902 (y10, y11)	Y	Y	Y	Y	Y	Y
		R.AQS*PTPS*LPASWK.Y	S906 (y5, y7)	Y	Y	N	Y	N	N
		R.TAKPFPGSVNQPATPFS*PTR.N	S604 (y3, y6)	Y	N	Y	N	Y	N
		K.PFPGSVNQPATPFS*PTR.N	S604	Y	N	Y	N	Y	N
		R.GVSS*PIAGPAQPPPWPQPAPWSQPAFYDSSER.I	S638 (not)	Y	N	Y	N	N	N
		K.SKS*PDPDPNLSHDR.I	S226 (not)	N	N	N	N	Y	N
		Phosphoproteins found in 4 out of 5 specimens							
O14558	Heat-shock protein beta-6 (Heat-shock 20 kDa-like protein)	R.RAS*APLPGLSAPGR.L	S16 (y11, y12)	N	Y	Y	N	Y	Y
Q14315	Filamin-C	R.LGS*FGSITR.Q	S2233 (b2, b3)	N	Y	N	Y	Y	Y

Table A-4 (continued).

Accession number	Protein	Peptide	Site	Phosphory-lation site	99-029	98-065	99-045	99-067	99-010
Q9H3Z4	DnaJ homolog subfamily C member 5	R.S*LSTSGESLYHVLGLDK.N	S8 (not)	Y	Y	N	Y	Y	N
		R.SLSTS*GESLYHVLGLDK.N	S12 (not)	Y	N	Y	N	N	N
Q9HBL0	Tensin-1	R.RMS*VGDR.A	S1393 (y5, y6)	N	Y	N	N	Y	N
		R.WDS*YDNFSGHR.D	S338 (y8, y9)	Y	Y	N	N	N	N
		K.EAT*SDPSRTPEEEPLNLEGLVAHR.V	T854 (not)	N	N	Y	N	N	N
		R.T*PTQPLLESGFR.S	T1105 (not)	N	N	N	Y	N	N
		K.EATSDPSRT*PEEEPLNLEGLVAHR.V	T860 (not)	N	N	N	Y	Y	N
		R.SQS*FSEAEPQLPPAPVR.G	S621 (not)	N	N	N	Y	N	N
		Phosphoproteins found in 2 out of 5 specimens							
Q15019	Septin-2	K.IYHLPDAES*DEDEDFKEQTR.L	S218 (y11, y12)	Y	Y	N	Y	N	N
Q08554	Desmocollin-1 precursor	R.MKVQDQDLPNT*PHSK.A	T385 (not)	N	Y	N	N	N	Y
P21291	Cysteine and glycine-rich protein 1	K.GFGFGQGAGALVHS*E	S192 (y2, y3)	Y	Y	N	Y	N	N
Q8N283	Ankyrin repeat domain-containing protein 35	R.QS*VGLLT*NELAM#EK.E	S672; T677 (b3, b4/ not)	N,N	Y	N	Y	N	N
Q01995	Transgelin	K.HVIGLQMGS*NR.G	S181 (y2,y6)	Y	Y	Y	N	N	N
P08670	Vimentin	R.ISLPLPNFS*SLNLR.E	S419 (y5, y6)	Y	N	N	Y	Y	N
Q6P597	Kinesin light chain 3	K.APRTLSAST*QDLS*PH	T493; S497 (not/y2,y3)	N,N	N	N	Y	N	Y
O95425	Supervillin	R.S*LSDFTGPPQLQALK.Y	S547 (not)	N	N	N	Y	Y	N
Q15746	Myosin light chain kinase	R.KSS*TGSPTSPLNAEK.L	S1773 (y12, y13)	Y	N	N	Y	Y	N
Q63ZY3	Ankyrin repeat domain-containing protein 25	R.ALAMPGRPES*PPVFR.S	S375 (y5,y6)	Y	N	N	Y	Y	N
		K.KIS*ITER.S	S406 (not)	N	N	N	Y	N	N

Table A-4 (continued).

Accession number	Protein	Peptide	Site	Phosphory-lation site	99-029	98-065	99-045	99-067	99-010
		Phosphoproteins found in 1 out of 5 specimens							
Q92736	Ryanodine receptor 2	R.SSSENAKVTS*LDS*SSHR.I	S4546; S4549 (not/not)	N,N	Y	N	N	N	N
P13796	Plastin-2	R.GS*VSDEEMMELR.E	S5 (y10, y11)	Y	Y	N	N	N	N
Q15283	Ras GTPase-activating protein 2	K.S*SFKETFMCEFFK.M	S559 (not)	N	Y	N	N	N	N
P43353	Aldehyde dehydrogenase 3B1	R.FDY*IFFTGS*PR.V	Y183; S189 (b3/y2, y4)	N,N	Y	N	N	N	N
P17252	Protein kinase C alpha type	R.STLNPQWNES*FTFK.L	S226 (y4, y5)	Y	N	Y	N	N	N
Q8IYX7	Protein FAM154A	R.EY*QKGPIPMEGLTTSR.R	Y59 (not)	N	N	Y	N	N	N
O75069	Transmembrane and coiled-coil domains protein 2	R.GAS*LHS*SSGGGSS*GSSSRRTK.S	S166; S169 (not/not)	N,N	N	Y	N	N	N
P27216	Annexin A13	K.YQKS*LSDMVRSDTSGDFR.K	S294 (not)	N	N	Y	N	N	N
Q6PCE3	Phosphoglucomutase-2-like 1	K.AVAGVMITAS*HNR.K	S175 (y3, y4)	Y	N	Y	N	N	N
P01854	Ig epsilon chain C region	R.VAHTPS*STDWVDNK.T	S92 (y8, y9)	N	N	Y	N	N	N
Q8TCU4	Alstrom syndrome protein 1	R.SPLQEAES*KVSMALEETLR.Q	S2367 (y11, y14)	N	N	Y	N	N	N
P80421	Ig heavy chain V-I region DOT	R.DRLVMSSDTSANTVS*MQLR.N	S79 (b14, b15)	N	N	Y	N	N	N
Q8TAP8	Putative uncharacterized protein C7orf47	K.S*SLALGLELR.A	S108 (not)	N	N	Y	N	N	N
P36871	Phosphoglucomutase-1	K.AIGGIILTAS*HNPGGPNGDFGIK.F	S117 (b9, b12)	Y	N	Y	N	N	N
P60174	Triosephosphate isomerase	R.KQS*LGELIGTLNAAK.V	S21 (y12, y13)	Y	N	N	Y	N	N
Q9NZN4	EH domain-containing protein 2	R.GPDEAMEDGEEGS*DDEAEWVVTK.D	S438 (not)	Y	N	N	Y	N	N
P22059	Oxysterol-binding protein 1	K.GDMS*DEDDENEFFDAPEIITMPENLGHK.R	S351 (b4)	Y	N	N	Y	N	N

Table A-4 (continued).

Accession number	Protein	Peptide	Site	Phosphory-lation site	99-029	98-065	99-045	99-067	99-010
Q32MZ4	Leucine-rich repeat flightless-interacting protein 1	R.RGS*GDTSISIDTEASIR.E	S120 (b3)	N	N	N	Y	N	N
Q9UBT6	DNA polymerase kappa	K.CDS*YKDDLLLR.M	S10 (b3)	N	N	N	Y	N	N
Q86SQ6	Probable G-protein coupled receptor 123	K.QVT*KKAPLCLDTDQPPYPR.Q	T833 (b4,b5)	N	N	N	Y	N	N
Q9Y618	Nuclear receptor corepressor 2	K.REGTPPPPPPS*R.D	S1390 (y2,y3)	N	N	N	Y	N	N
Q9H2J4	Phosducin-like protein 3	K.LS*ES*GAIMTDLEENPK.K	S199; S201 (not/y12, y14)	N,N	N	N	Y	N	N
P09496	Clathrin light chain A	R.LQS*EPESIR.K	S105 (b3,b4)	N	N	N	Y	N	N
O43237	Cytoplasmic dynein 1 light intermediate chain 2	K.SGQKT*VLSNVQEELDR.M	T463 (y10, y12)	N	N	N	Y	N	N
P35558	Phosphoenolpyruvate carboxykinase	R.WM#S*EEDFEK.A	S118 (y6, y7)	Y	N	N	Y	N	N
P05386	60S acidic ribosomal protein P1	K.KEES*EES*DDDMGFGLFD	S101; S104 (b5, b6/y10, y11)	Y,Y	N	N	Y	N	N
P13861	cAMP-dependent protein kinase type II-alpha regulatory subunit	K.GDS*ES*EEDEDLEVPVPSR.F	S77; S79 (not/not)	Y,Y	N	N	Y	N	N
Q6P9B9	Integrator complex subunit 5	R.FQAPSPS*TLLR.Q	S1012 (not)	N	N	N	Y	N	N
Q14195	Dihydropyrimidinase-related protein 3	R.GSPT*RPNPPVR.N	T524 (y6, y9)	N	N	N	Y	N	N
Q13618	Cullin-3	R.FLLES*FNNDRLFK.Q	S359 (not)	N	N	N	Y	N	N
P48681	Nestin	R.S*LGEQDQMTLRPPEK.V	S767 (not)	Y	N	N	N	Y	N
Q9NSE4	Isoleucyl-tRNA synthetase	K.GLVYRS*Y*KPVFWSPSSR.T	S239; Y240 (b5, b6/b6, b7)	N,N	N	N	N	Y	N

Table A-4 (continued).

Accession number	Protein	Peptide	Site	Phosphory-lation site	99-029	98-065	99-045	99-067	99-010
O43432	Eukaryotic translation initiation factor 4 gamma 3	R.SS*ASSLNR.F	S1194 (not)	N	N	N	N	Y	N
P27824	Calnexin precursor	K.AEEDEILNRS*PR.N	S583 (y2, y3)	Y	N	N	N	Y	N
P20711	Aromatic-L-amino-acid decarboxylase	K.GLQAY*IR.K	Y377 (y2, y3)	N	N	N	N	Y	N
O76041	Nebulette	R.SMQHS*PNLR.T	S953 (y4, y5)	N	N	N	N	Y	N
P08238	Heat shock protein HSP 90-beta (HSP 90)	K.IEDVGS*DEEDDSGKDKK.K	S254 (b5, b8)	Y	N	N	N	Y	N
O75385	Serine/threonine-protein kinase ULK1	R.KM#S*LGGGR.P	S495 (y4, y6)	N	N	N	N	Y	N
Q9Y5C1	Angiopoietin-related protein 3 precursor	K.NMSLELNS*K.L	S122 (y2, y3)	N	N	N	N	Y	N
Q6KC79	Nipped-B-like protein	K.QNEST*IVEPK.Q	T667 (y3, y6)	N	N	N	N	Y	N
P58107	Epiplakin	R.QPLQAT*FRGLRKQVS*AR.D	T1495, S1504 (b5, b6/b14, b15)	N,N	N	N	N	N	Y
P02545	Lamin A/C	R.LRLS*PSPTSQR.S	S390 (y7, y8)	Y	N	N	N	N	Y
Q13242	Splicing factor, arginine/serine-rich 9	R.GS*PHYFSPFRPY	S211 (b2)	Y	N	N	N	N	Y
Q13263	Transcription intermediary factor 1-beta	R.SRS*GEGEVSGLMR.K	S473 (b2, b3)	Y	N	N	N	N	Y
P07197	Neurofilament triplet M protein	K.GKSPVPKS*PVEEK.G	S617 (y5, y6)	Y	N	N	N	N	Y
P15924	Desmoplakin	K.GLPSPYNMSSAPGS*R.S	S2825 (y2)	Y	N	N	N	N	Y
O00264	Membrane associated progesterone receptor component 1	K.LLKEGEEPTVYS*DEEEPKDESAR.K	S180 (b11, b12)	Y	N	N	N	N	Y

The assignments of exact sites of phosphorylation were validated manually through inspection of the corresponding product ions.

Table A-5 Scansite results for the characterized phosphorylation sites.

Accession number	Protein	Site	Scansite result Kinase/binding	Type
O14558	Heat-shock protein beta-6 (Heat-shock 20 kDa-like protein)	S16	14-3-3 Mode 1	pS/T binding group
Q14315	Filamin-C	S2233	Akt Kinase	Basophilic S/T kinase group
Q9H3Z4	DnaJ homolog subfamily C member 5	S8	Calmodulin dependent Kinase 2	Basophilic S/T kinase group
Q9HBL0	Tensin-1	S1393	Protein Kinase A	Basophilic S/T kinase group
		T1105	Erk1 Kinase	Kinase binding site group
		S621	Calmodulin dependent Kinase 2	Basophilic S/T kinase group
Q15019	Septin-2	S218	Casein Kinase 2	Acidophilic S/T kinase group
Q9NZN4	EH domain-containing protein 2	S438	Casein Kinase 2	Acidophilic S/T kinase group
Q9Y618	Nuclear receptor corepressor 2	S1390	GSK3 Kinase	Acidophilic S/T kinase group
P09496	Clathrin light chain A	S105	14-3-3 Mode 1	pS/T binding group
P05386	60S acidic ribosomal protein P1	S104	Casein Kinase 2	Acidophilic S/T kinase group
P13861	cAMP-dependent protein kinase type II-alpha regulatory subunit	S77	Casein Kinase 2	Acidophilic S/T kinase group
		S79	Casein Kinase 2	Acidophilic S/T kinase group
P48681	Nestin	S767	14-3-3 Mode 1; Protein Kinase A	pS/T binding group; Basophilic S/T kinase group
P08238	Heat shock protein HSP 90-beta (HSP 90)	S254	Casein Kinase 2	Acidophilic S/T kinase group
P58107	Epiplakin	S1504	PKC zeta	Basophilic S/T kinase group

VITA

Li Chen was born on May 17, 1971, in Xinjiang, China. She graduated with a B.S. in chemistry in 1992 and a M.S. in pharmaceutical analysis in 1998. She joined in the Pharmaceutical Sciences program in the University of Tennessee Health Science Center in Memphis for her Ph.D. studies in 2005. She completed her doctorate degree in December 2009.